



CMS Experiment at the LHC, CERN

Data recorded: 2012-May-13 20:08:14.621490 GMT

Run/Event: 194108 / 564224000

Instrumentation in HEP

Calorimetry

Calorimetry - Basic principles

- *Interaction of charged particles and photons*
- *Electromagnetic cascades*
- *Nuclear interactions*
- *Hadronic cascades*

Homogeneous calorimeters

Sampling calorimeters

Upgrade calorimeters for High Luminosity LHC

Summary

Ludwik Dobrzynski

Laboratoire Leprince Ringuet - Ecole polytechnique - CNRS - IN2P3

The British University in Egypt - 6 December 2016



IN2P3
Les deux infinis

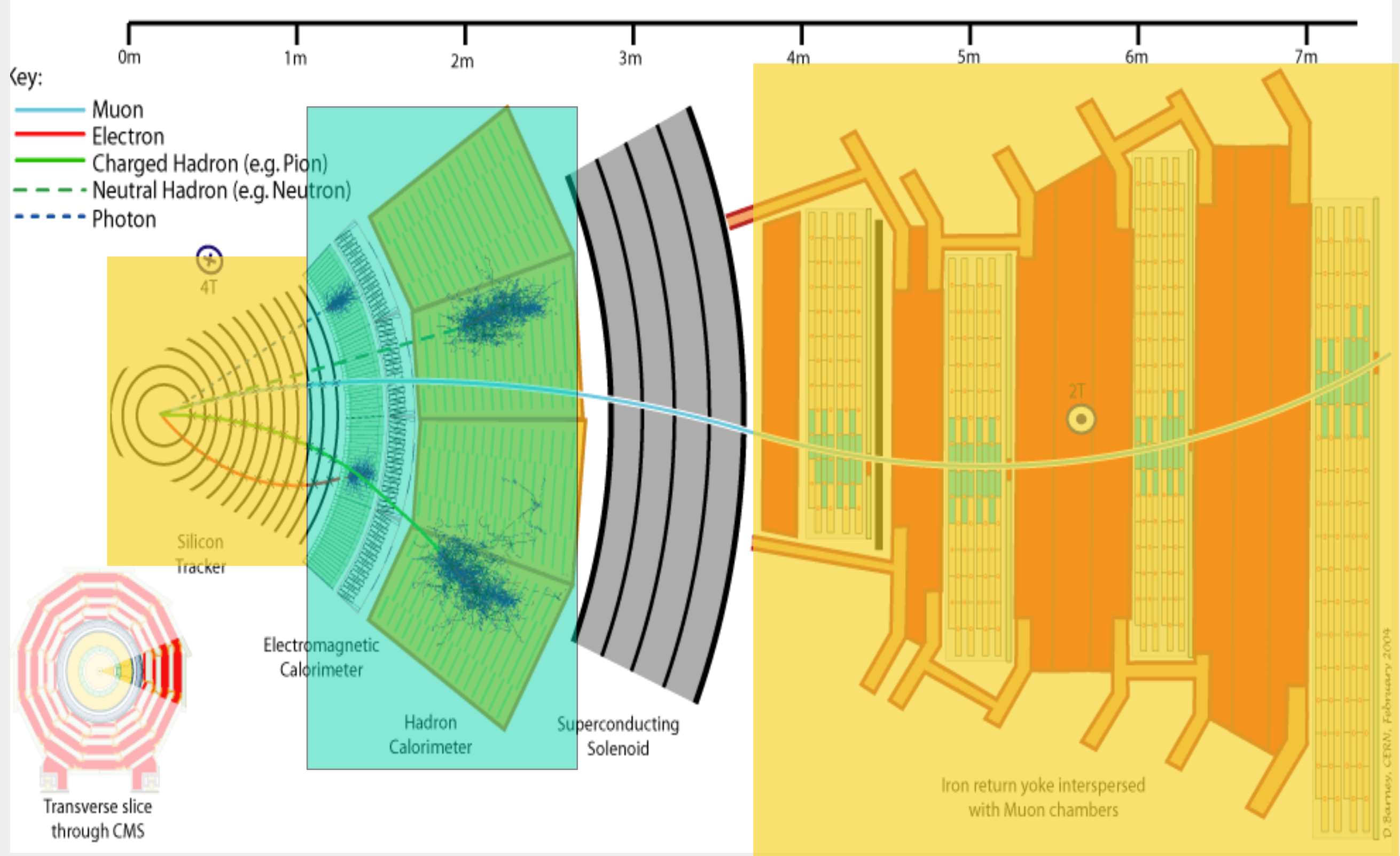


HOW ARE PARTICLES DETECTED ?

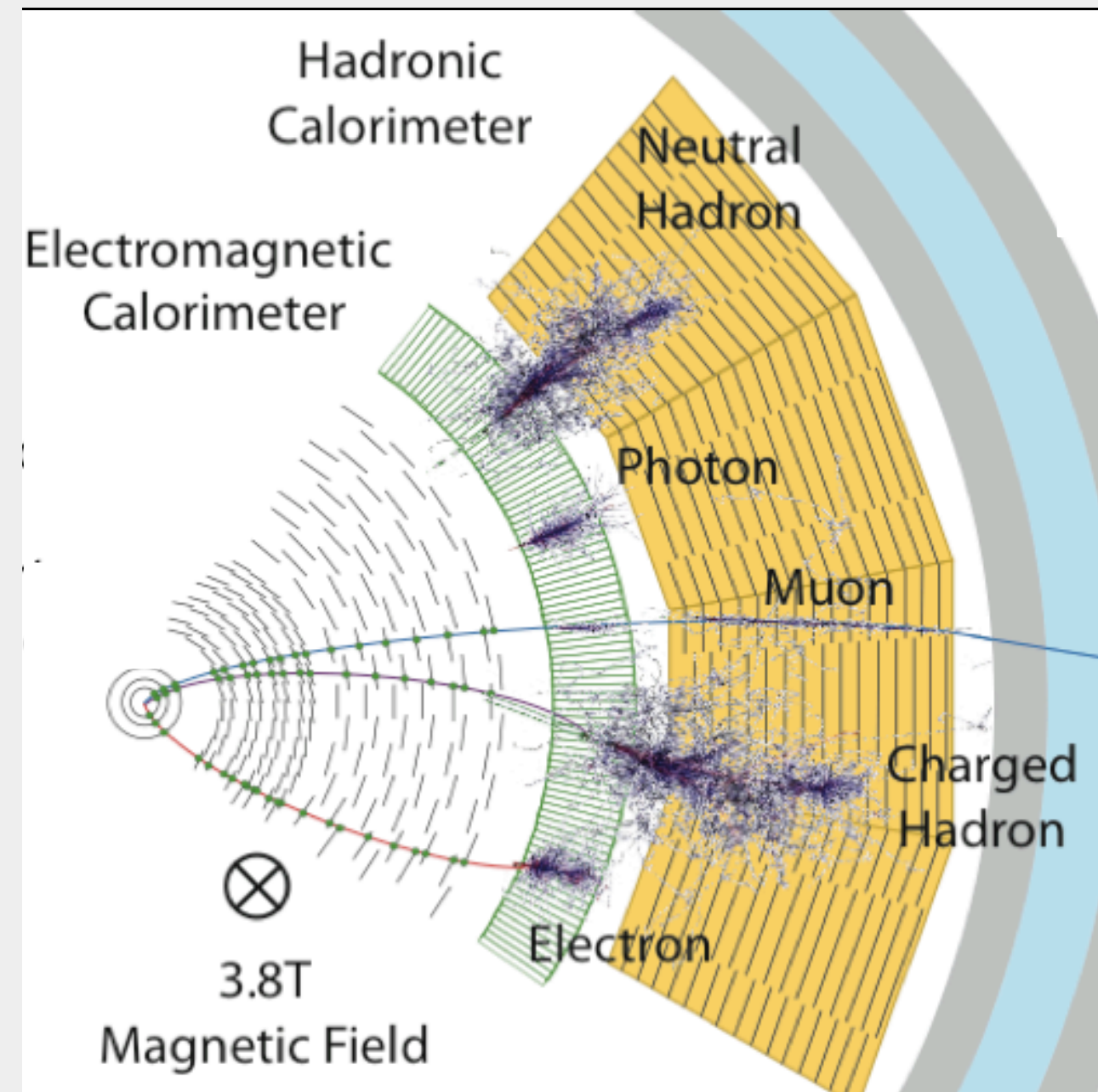
- In order to detect a particle it must
 - interact with the material of the detector
 - transfer energy in some recognisable way
 - and leave a signal.

Detection of particles happens via their energy loss in the material they traverse.

Charged particles	Ionization, Bremsstrahlung, Cherenkov, ...	multiple interactions
Photons	Photo/Compton effect, pair production	single interactions...
Hadrons	Nuclear interactions	multiple interactions
Neutrinos	Weak interactions	



- In nuclear and particle physics calorimetry refers to the detection of particles through total absorption in a block of matter
 - The measurement process is destructive for almost all particle
 - The exception are muons (and neutrinos) → identify muons easily since they penetrate a substantial amount of matter
- In the absorption, almost all particle's energy is eventually converted to heat → calorimeter
- Calorimeters are essential to measure neutral particles



Calorimetry: Basic Principle (1)

Calorimetry = Energy measurement by total absorption, usually combined with spatial reconstruction.

Basic mechanism for calorimetry in particle physics is the formation of

- electromagnetic showers
- and/or hadronic showers.

- Finally, the energy is converted into ionization or excitation of the matter.



- *Calorimetry is a “destructive” method.* The energy **and** the particle get absorbed!

- Detector response $\propto E$

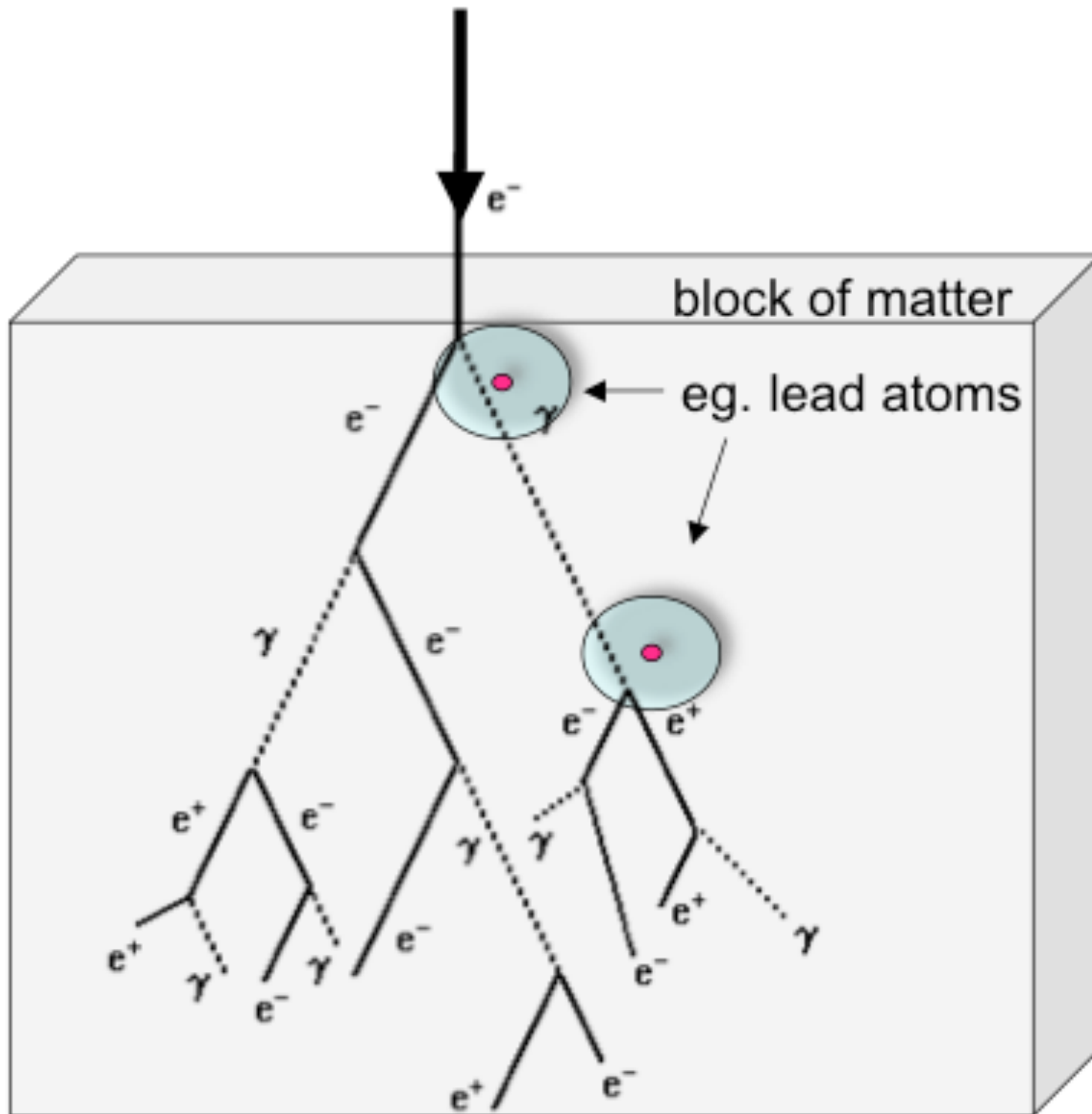
- Calorimetry works both for:

- charged particles (e^\pm and hadrons)

Complementary information to p (momentum) measurement

- and neutral particles (n, γ)

Only way to get direct kinematical information for neutral particles



Ionization, scintillation, Cherenkov light

Relevant quantities:

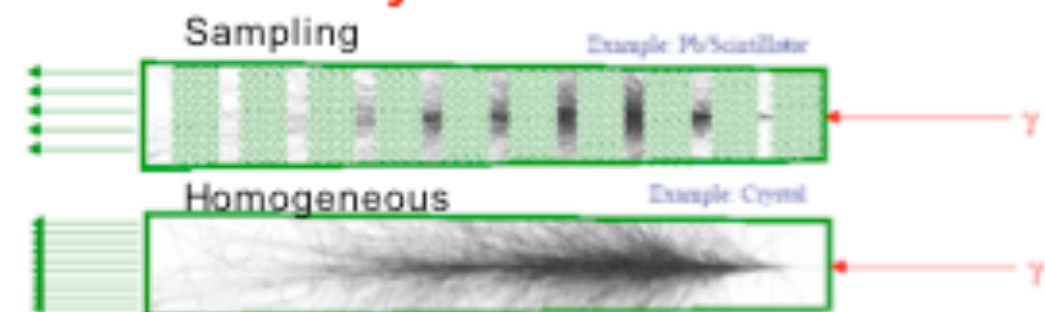
Radiation length X_0 :

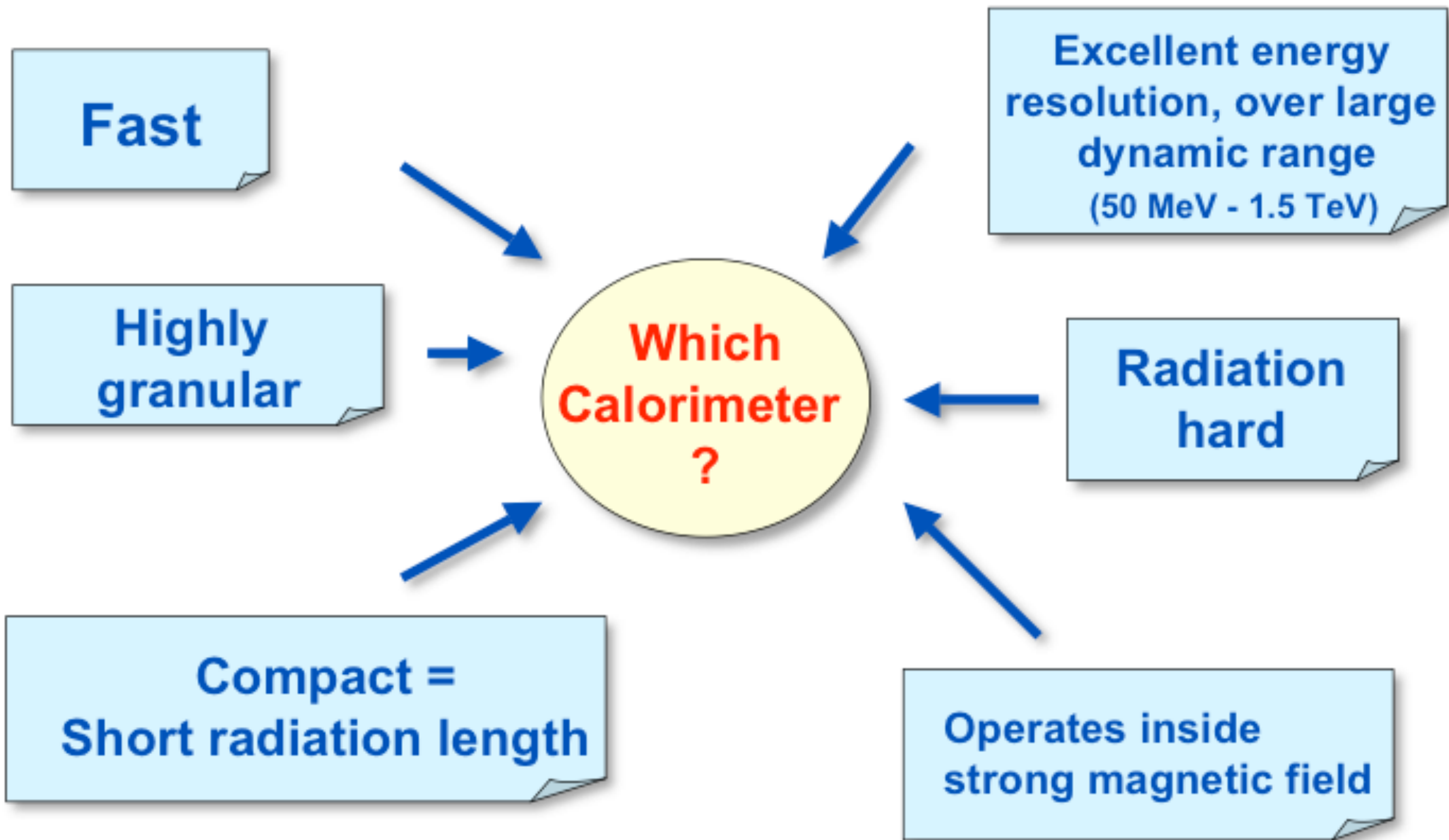
- e^- loses 63.2% of its energy via bremsstrahlung over distance X_0
- Mean free path of high-energetic photons = $9/7 X_0$

Moliere radius ρ_M :

- Measure for the lateral shower size
- On average, 90% of shower is contained within cylinder of radius ρ_M around the shower axis.

Detector layout





- Ideally, if all shower particles are counted:

$$E \propto N \quad \sigma_E \approx \sqrt{N} \approx \sqrt{E}$$

- In practice

$$\sigma_E = a\sqrt{E} \oplus bE \oplus c \quad \frac{\sigma_E}{E} = \frac{a}{\sqrt{E}} \oplus b \oplus \frac{c}{E}$$

a: stochastic term

- intrinsic statistical shower fluctuations
- sampling fluctuations
- signal quantum fluctuations (e.g. photo-electron statistics)

b: constant term

- inhomogeneities (hardware or calibration)
- imperfections in calorimeter construction (dimensional variations, etc.)
- non-linearity of readout electronics
- fluctuations in longitudinal energy containment (leakage can also be $\sim E^{-1/4}$)
- fluctuations in energy lost in dead material before or within the calorimeter

c: noise term

- readout electronic noise
- Radio-activity, pile-up fluctuations

Typical Calorimeter: two components ...

Electromagnetic (EM) +
Hadronic section (Had) ...

Different setups chosen for
optimal energy resolution ...

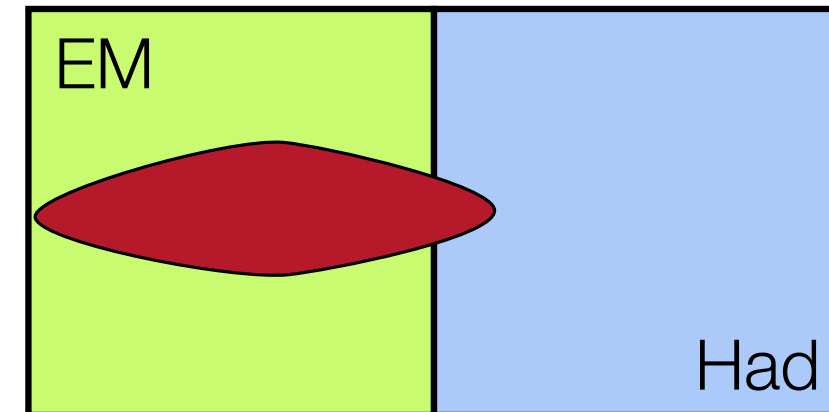
But:

Hadronic energy measured in
both parts of calorimeter ...

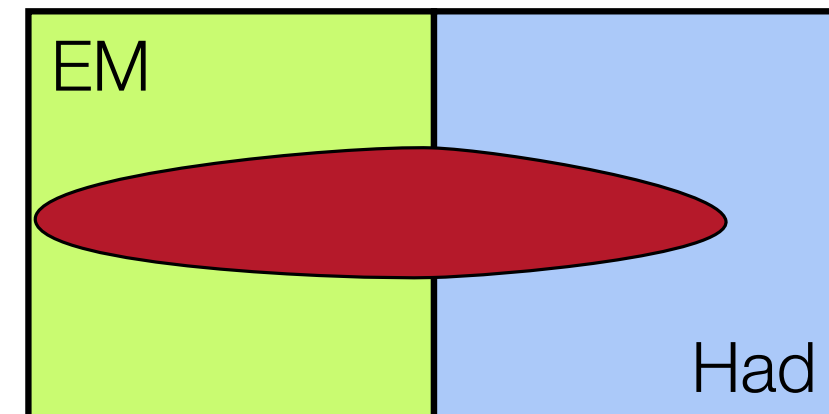
Needs careful consideration of
different response ...

Schematic of a
typical HEP calorimeter

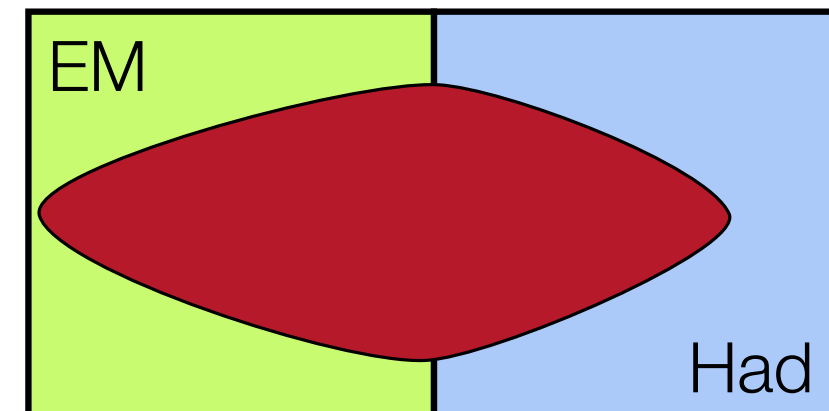
Electrons
Photons



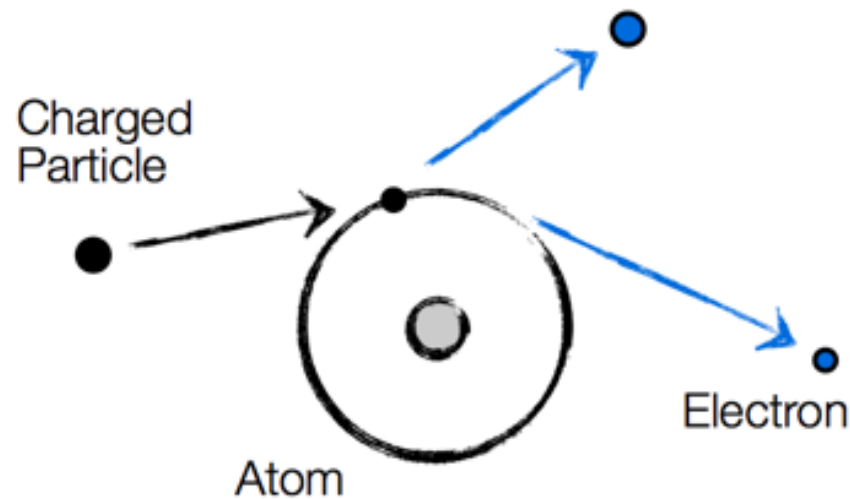
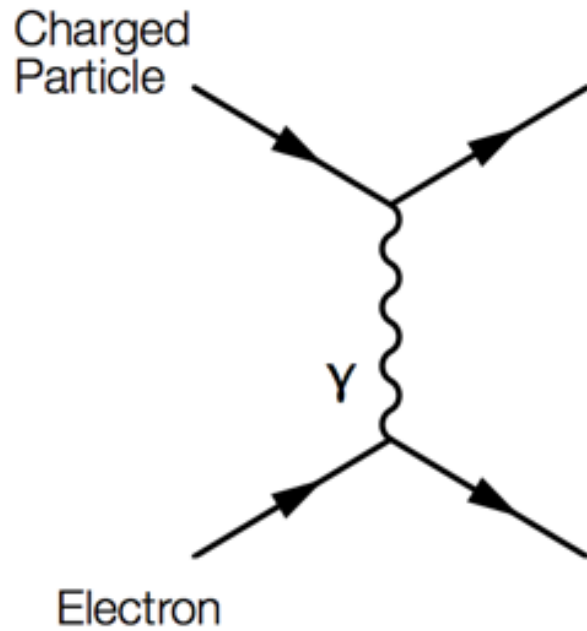
Taus
Hadrons



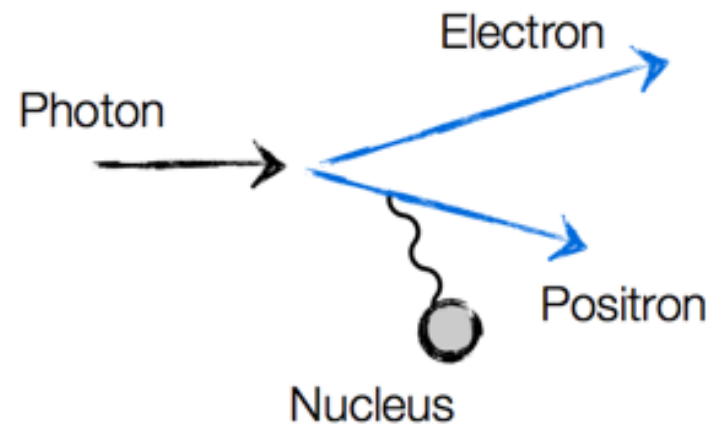
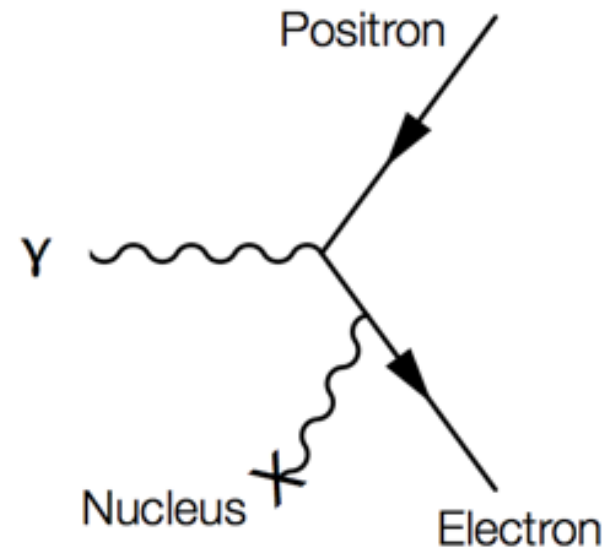
Jets



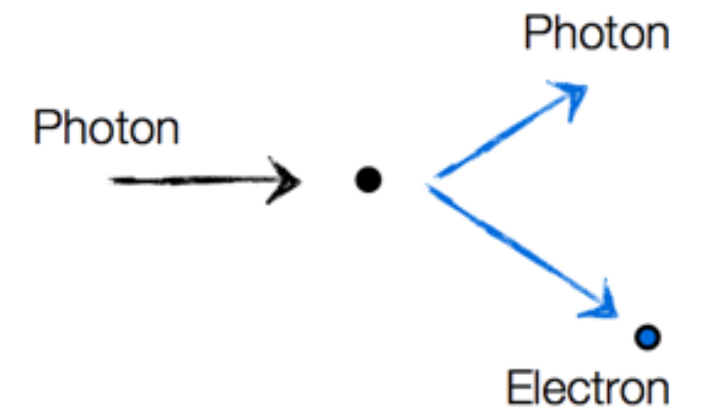
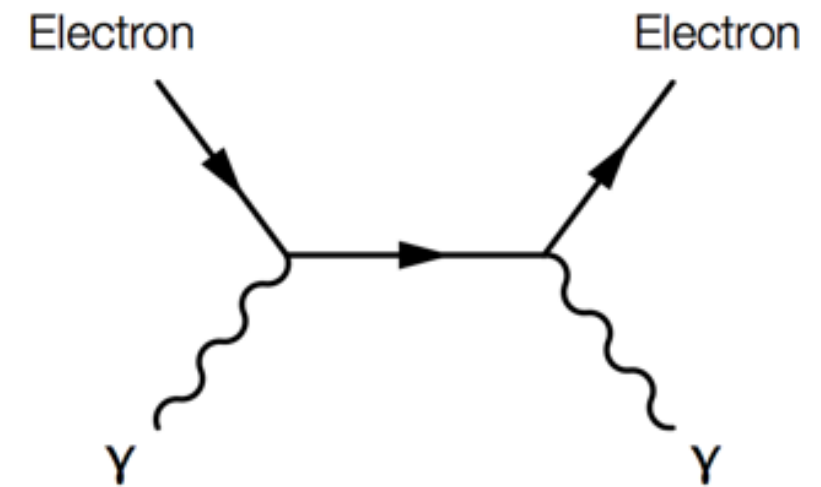
Ionisation



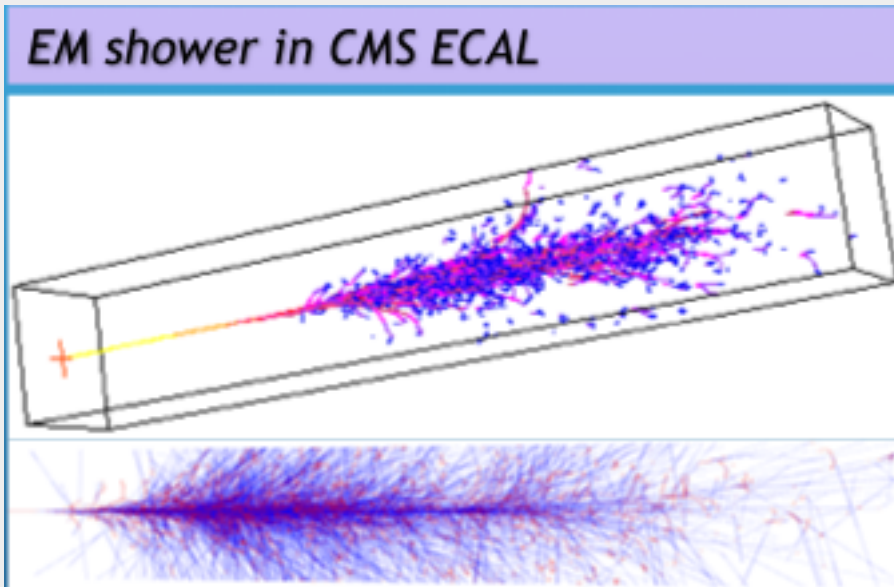
Production de paires e^+e^-



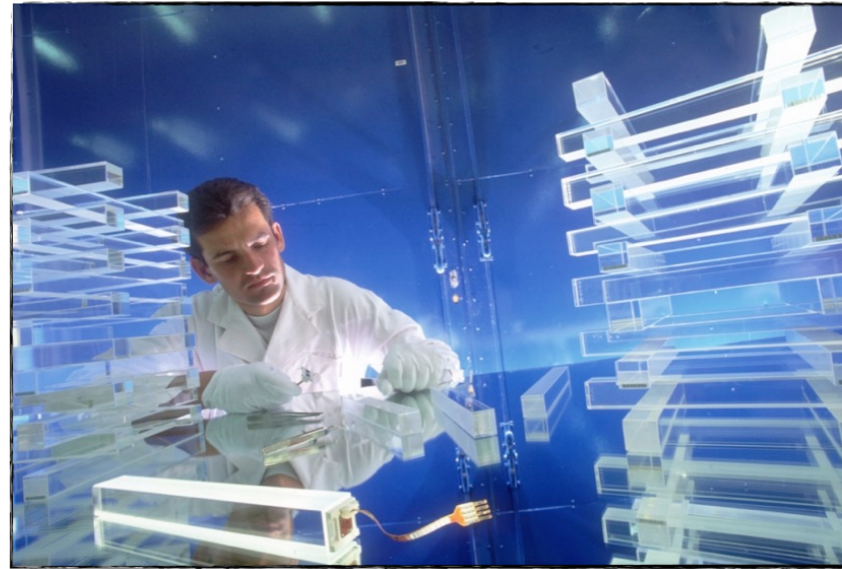
Diffusion Compton



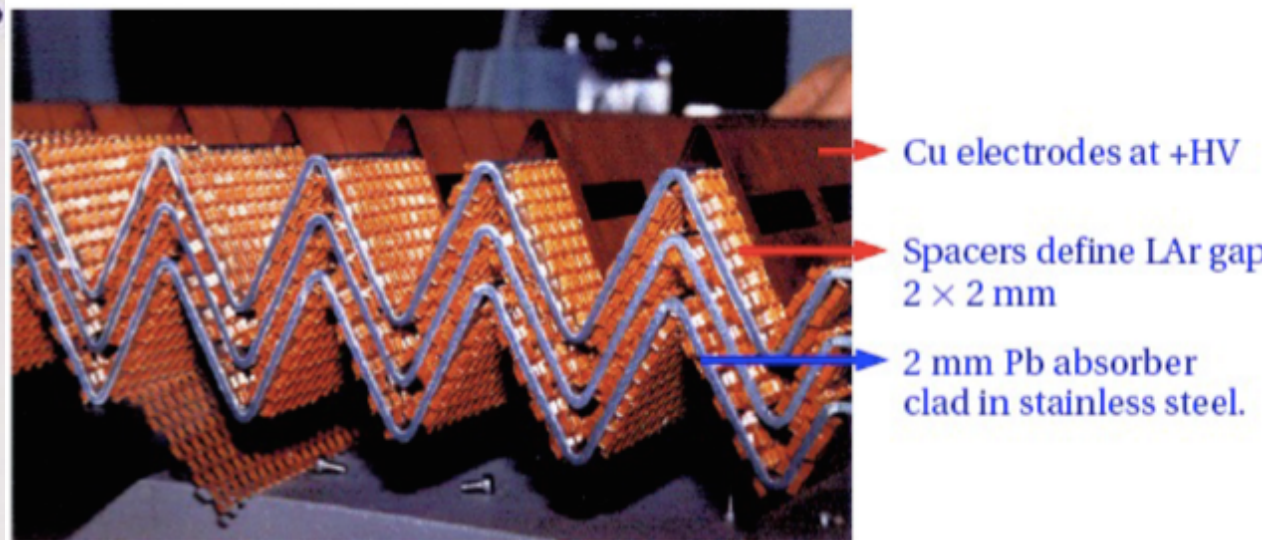
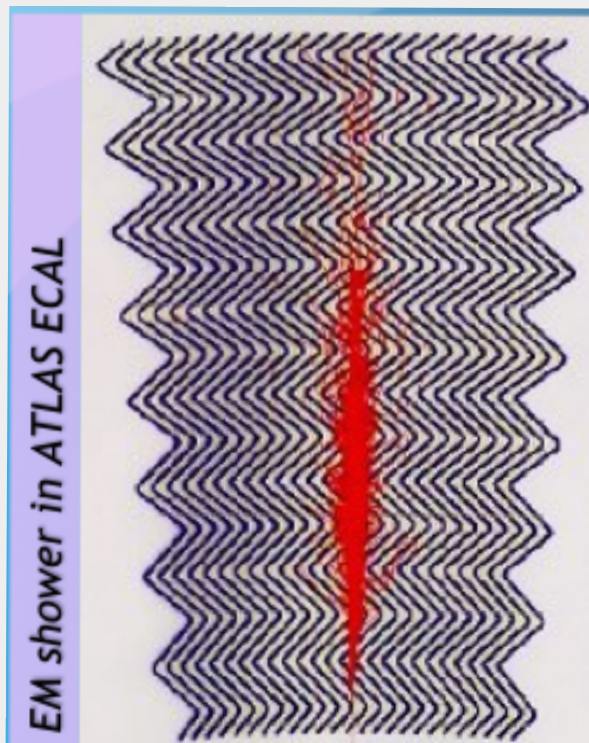
- Homogeneous



Homogeneous Calorimeters

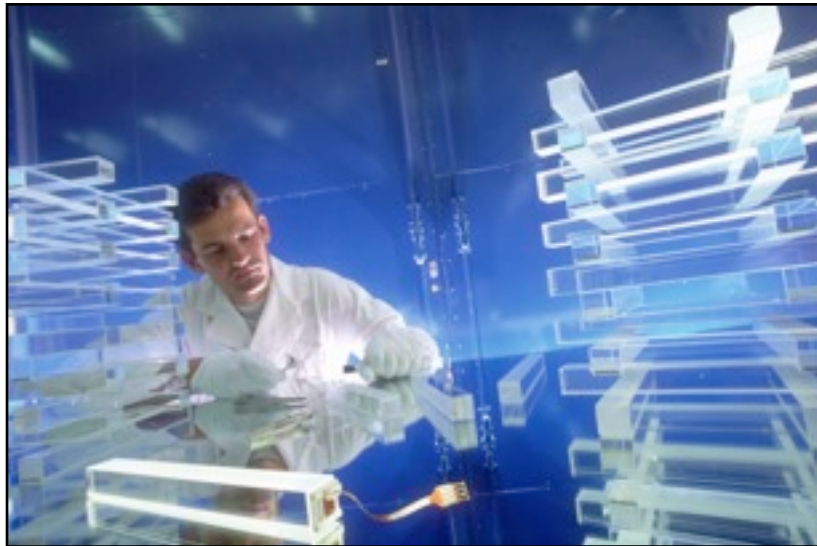


- Sampling



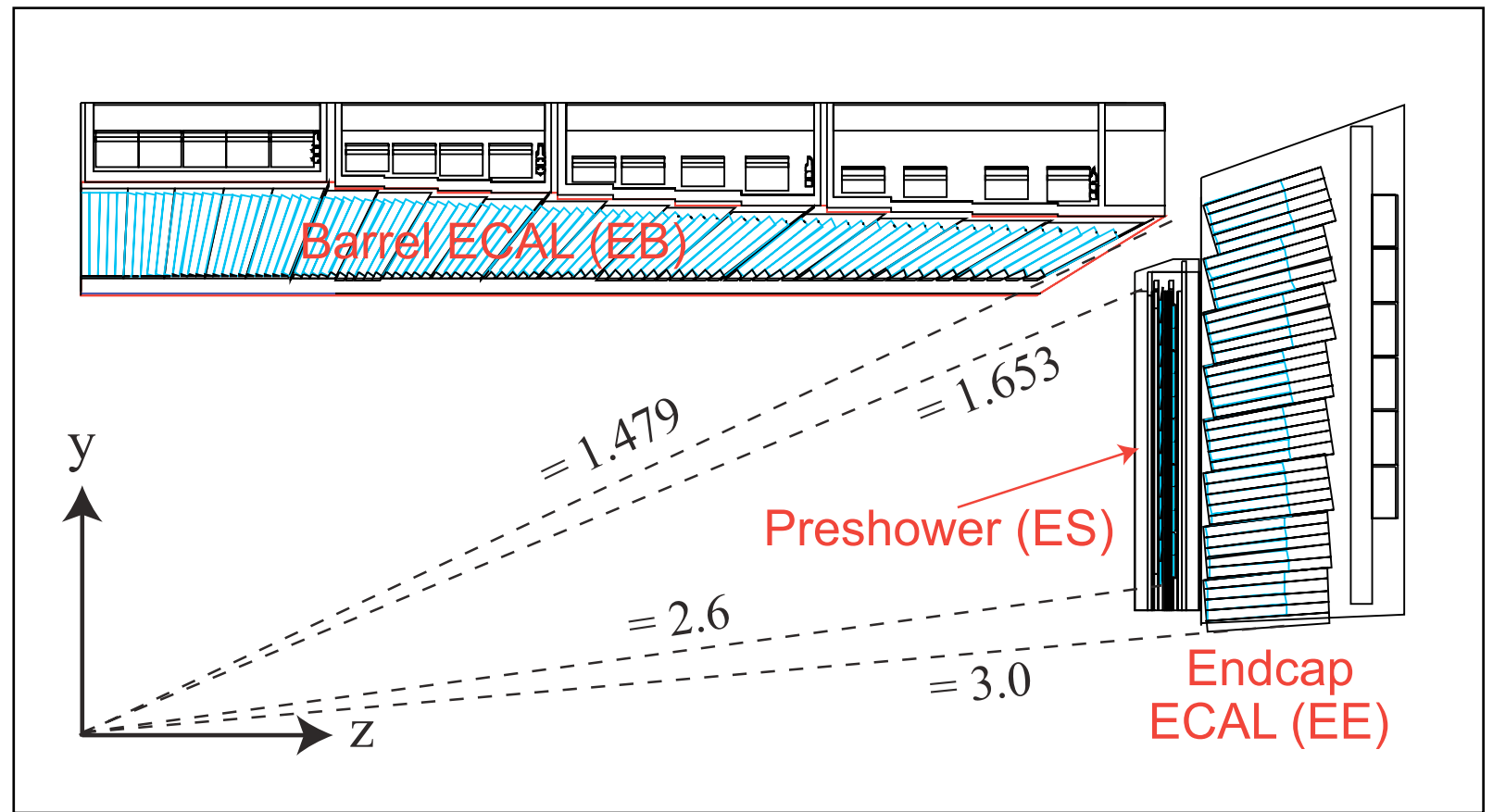
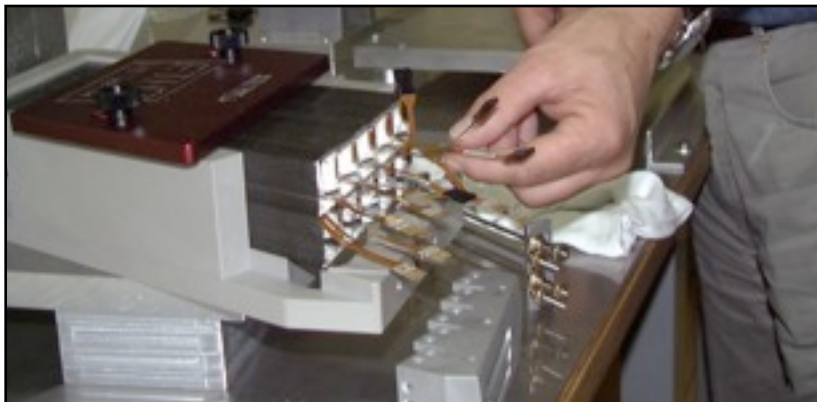
5 cm brass / 3.7 cm scint.
Embedded fibres, HPD readout

Homogeneous Calorimeters

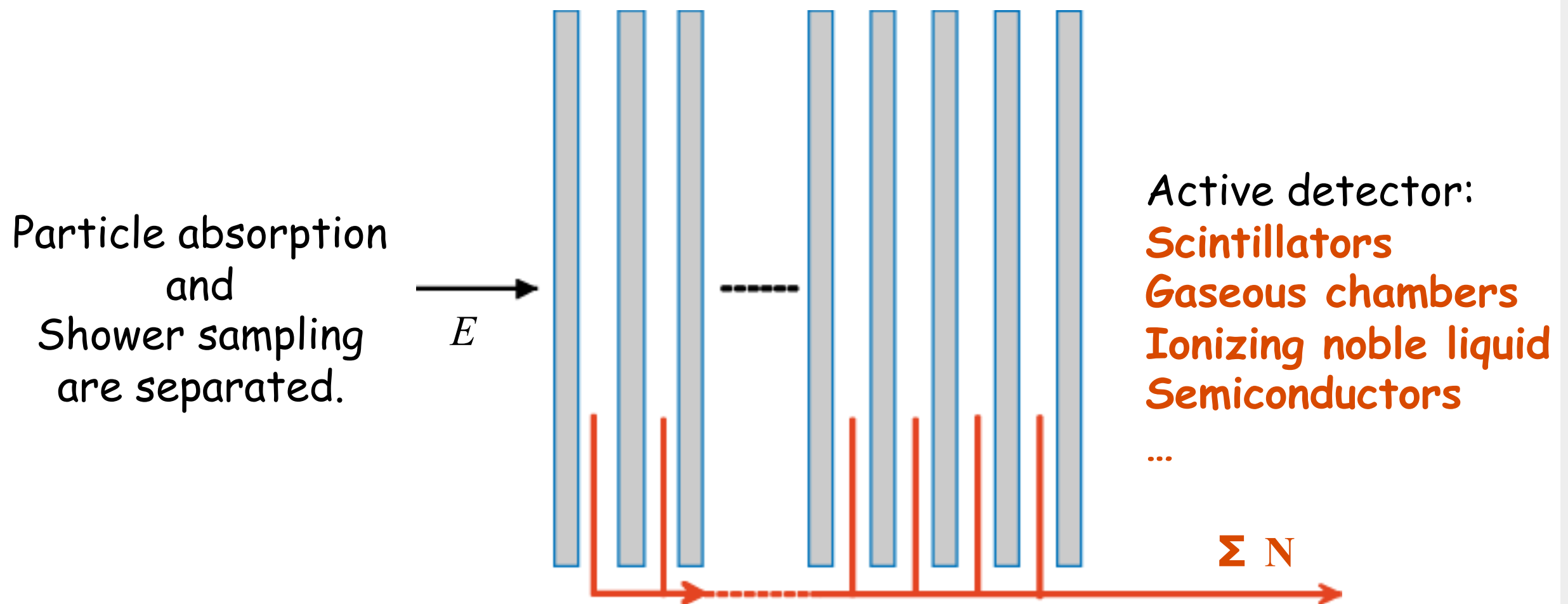


Scintillator : PbWO_4 [Lead Tungsten]
Photosensor : APDs [Avalanche Photodiodes]

Number of crystals: ~ 70000
Light output: 4.5 photons/MeV



Use a different medium to generate the shower and to detect signal : only a fraction of signal (f_s) is sampled in the active detector \rightarrow larger stochastic term



Intrinsic resolution goes from 1-3 % for crystal or homogeneous noble liquids to 8-12% for sampling calorimeters.

★ Advantages:

By separating passive and active layers the different layer materials can be optimally adapted to the corresponding requirements ...

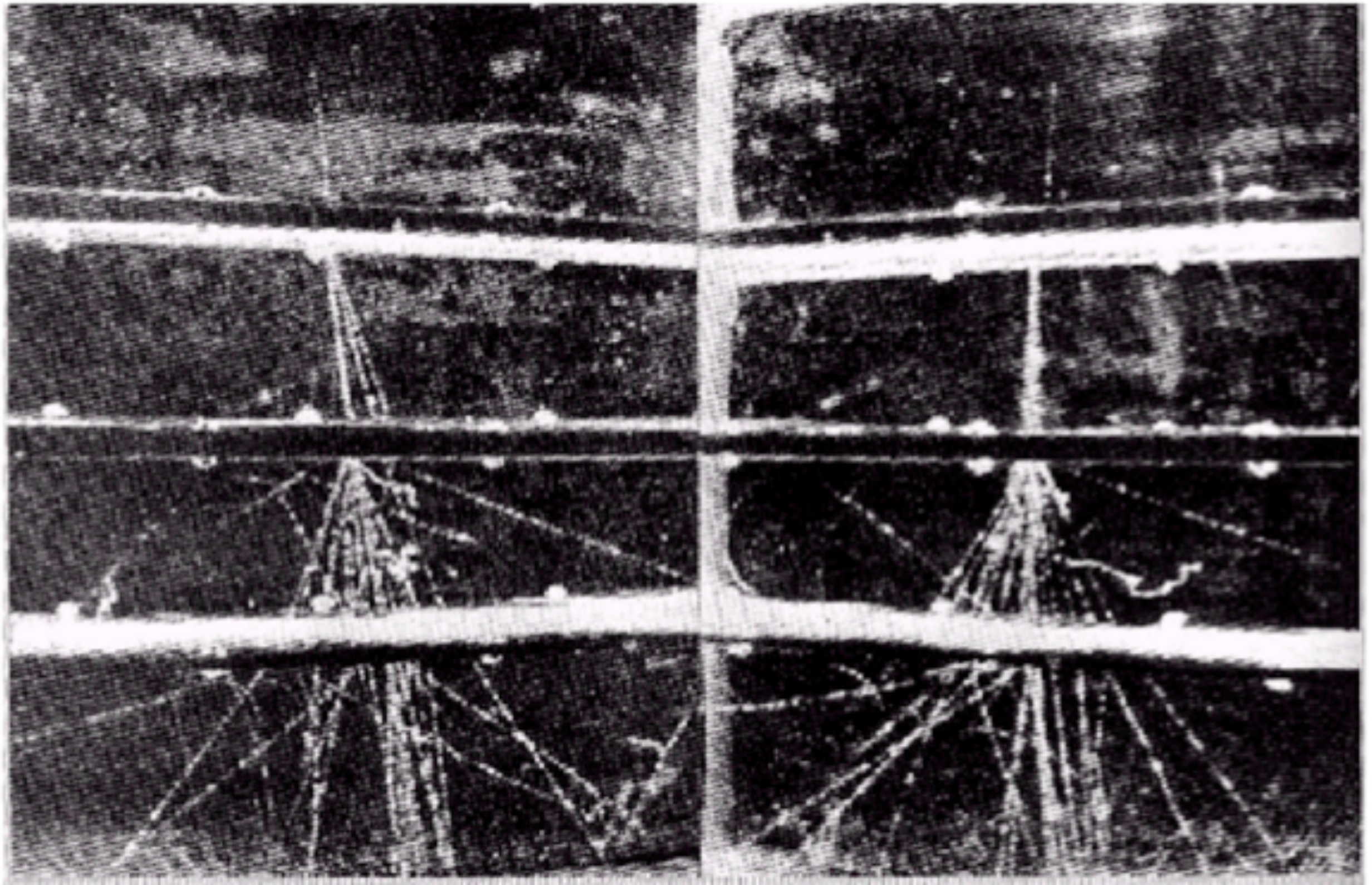
By freely choosing high-density material for the absorbers one can build very compact calorimeters ...

Sampling calorimeters are simpler with more passive material and thus cheaper than homogeneous calorimeters ...

★ Disadvantages:

Only part of the deposited particle energy is actually detected in the active layers; typically a few percent [for gas detectors even only $\sim 10^{-5}$] ...

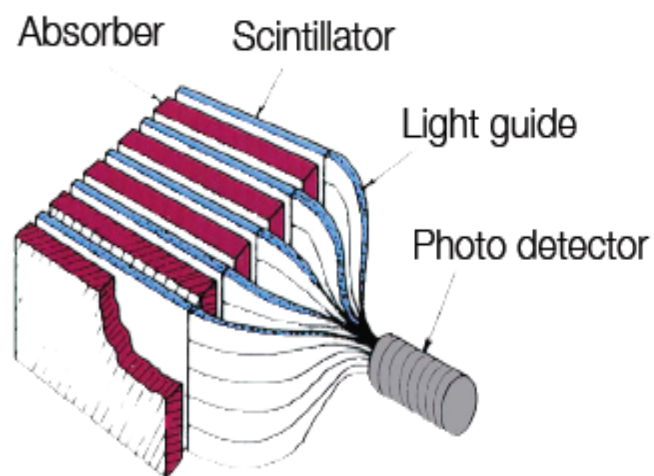
Due to this sampling-fluctuations typically result in a reduced energy resolution for sampling calorimeters ...



Cloud chamber photograph of e.m. shower developing in lead plates (thickness from top down 1.1, 1.1, 0.13 X_0) exposed to cosmic radiation

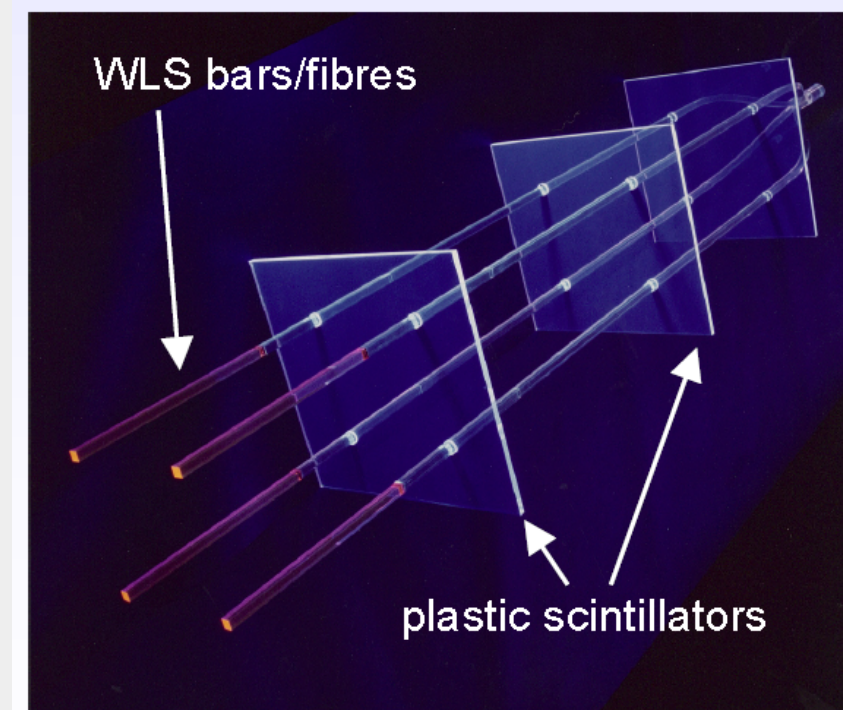
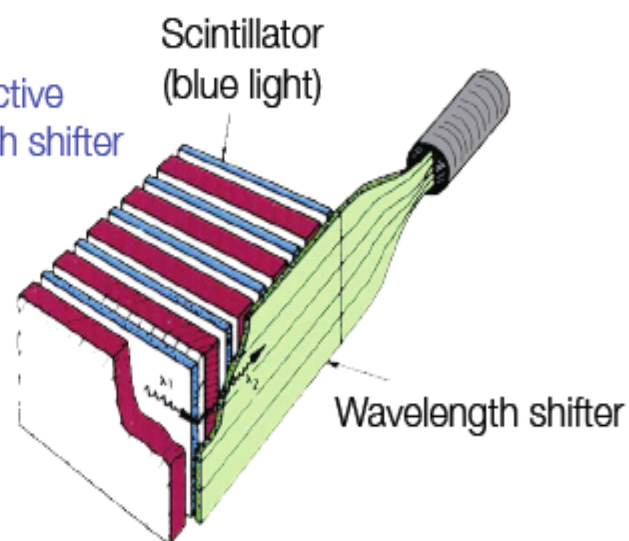
Sampling calorimeters = **Absorber + detector** (gaseous, liquid, solid)

Scintillators as active layer;
signal readout via photo multipliers



Possible setups

Scintillators as active layer; wave length shifter to convert light



'Shashlik' readout

Charge amplifier

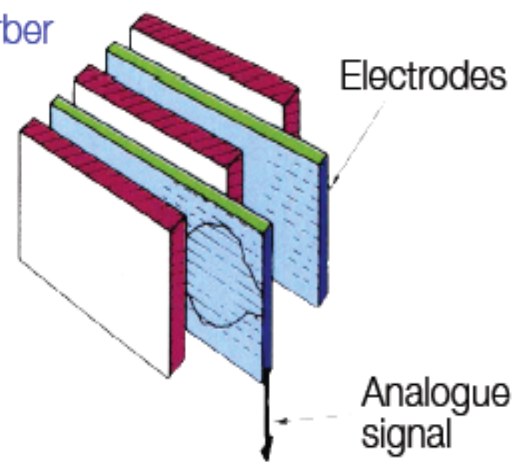
Absorber as electrodes

HV

Argon

Active medium: LAr; absorber embedded in liquid serve as electrods

Ionization chambers between absorber plates



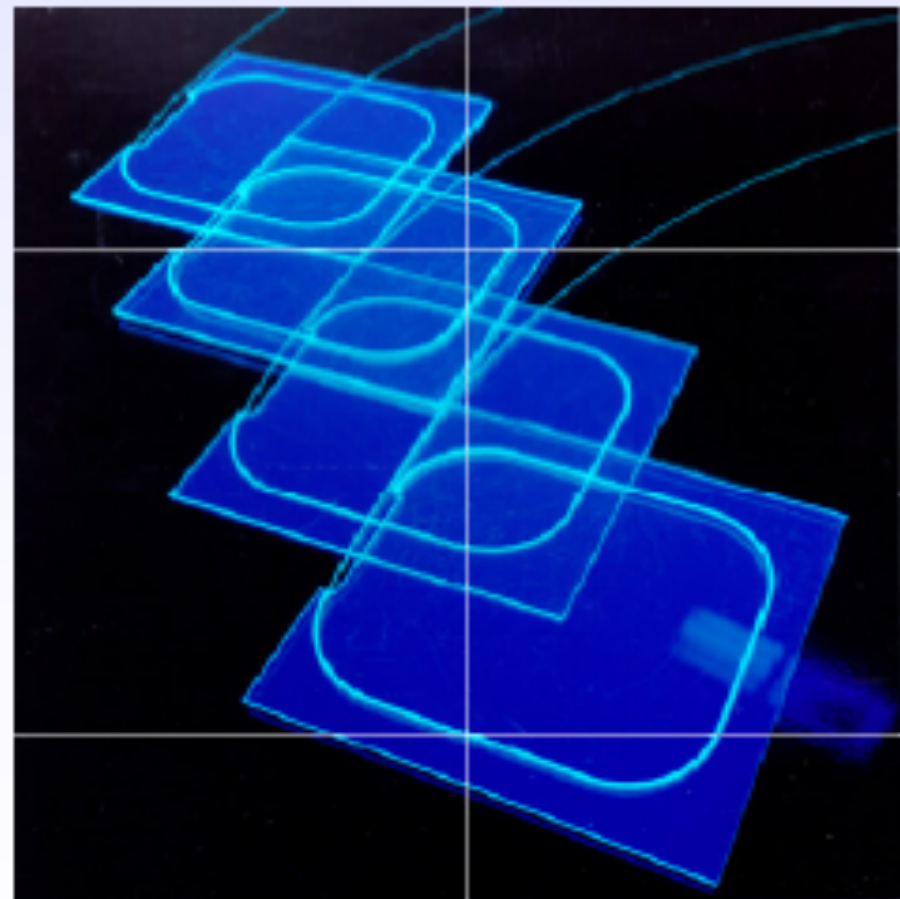
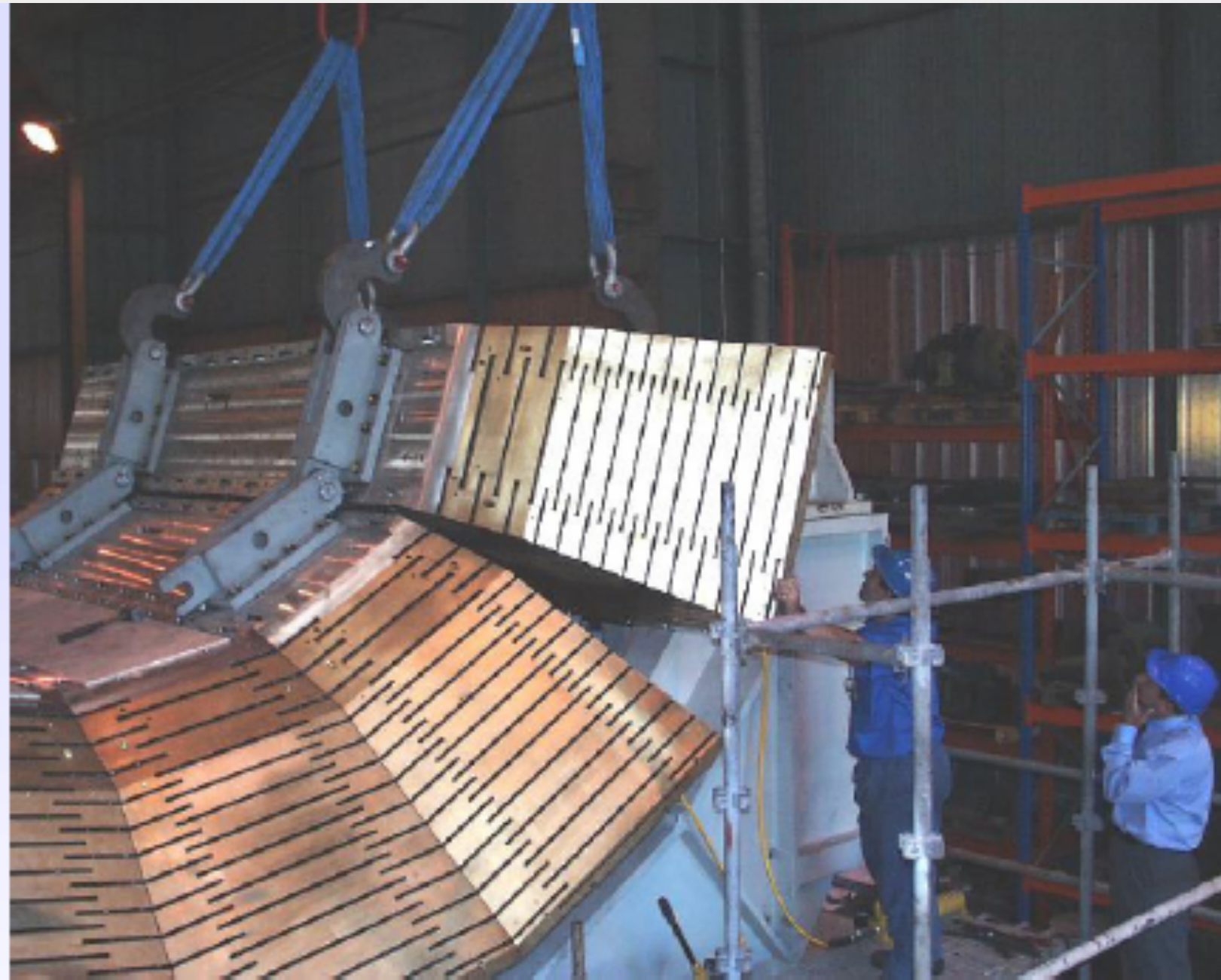
- MWPC, streamer tubes
- warm liquids (TMP = tetramethylpentane, TMS = tetramethylsilane)
- cryogenic noble gases: mainly LAr (LXe, LKr)
- scintillators, scintillation fibres, silicon detectors

CMS Hadron calorimeter

Brass absorber + plastic scintillators

- 2 x 18 wedges (barrel)
- + 2 x 18 wedges (endcap)
- ~ 1500 T absorber
- 5.8 λ_I at $\eta = 0$.

Scintillators fill slots and are read out via WLS fibres by HPDs (B = 4T!)



Test beam
resolution for
single hadrons

$$\frac{\sigma_E}{E} = \frac{65\%}{\sqrt{E}} \oplus 5\%$$

- The shower develops as a **cascade** by **energy transfer** from the incident particle to a **multitude of particles** (e^\pm and γ).
- The number of cascade particles is **proportional** to the energy deposited by the incident particle
- The role of the calorimeter is to **count** these cascade particles
The relative occurrence of the various processes briefly described is a function of the material (Z)
- The radiation length (X_0) allows to universally describe the shower development

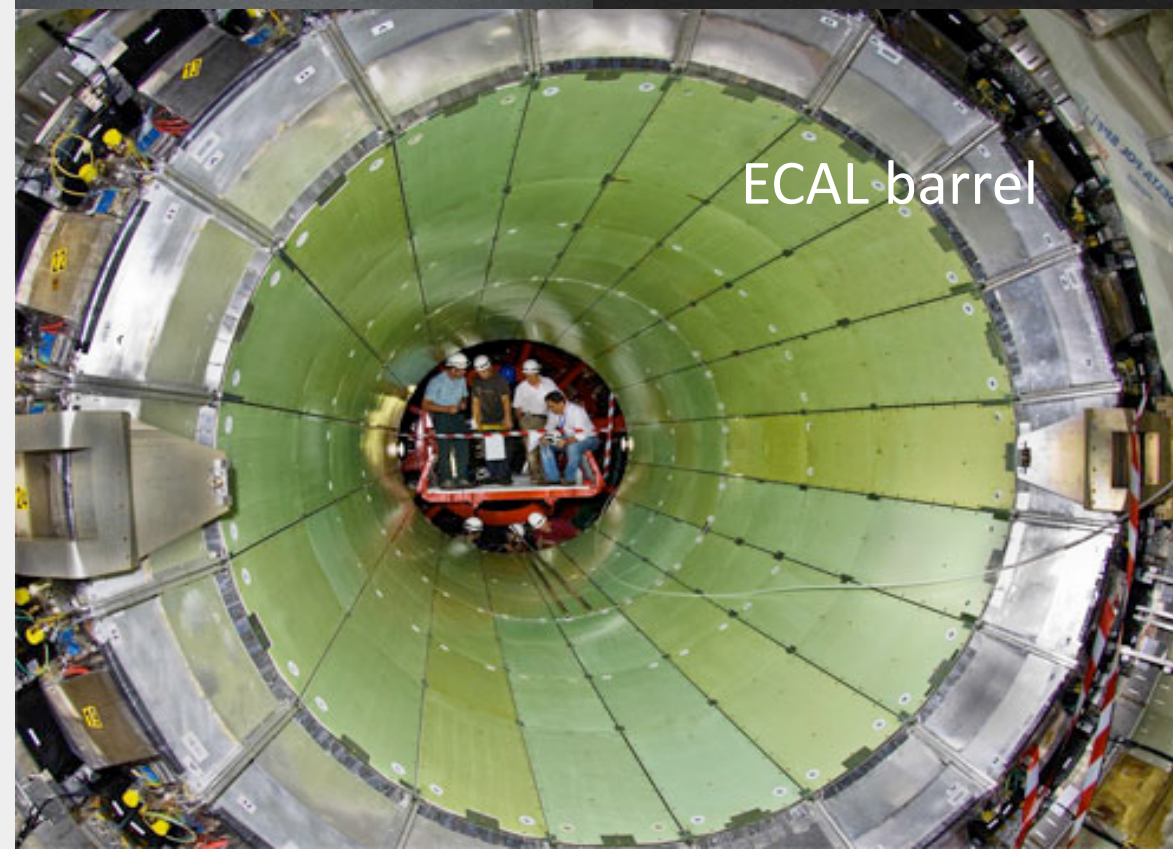
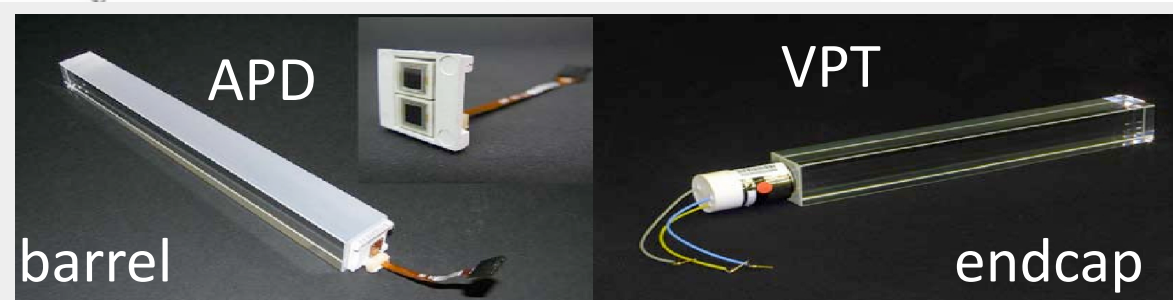
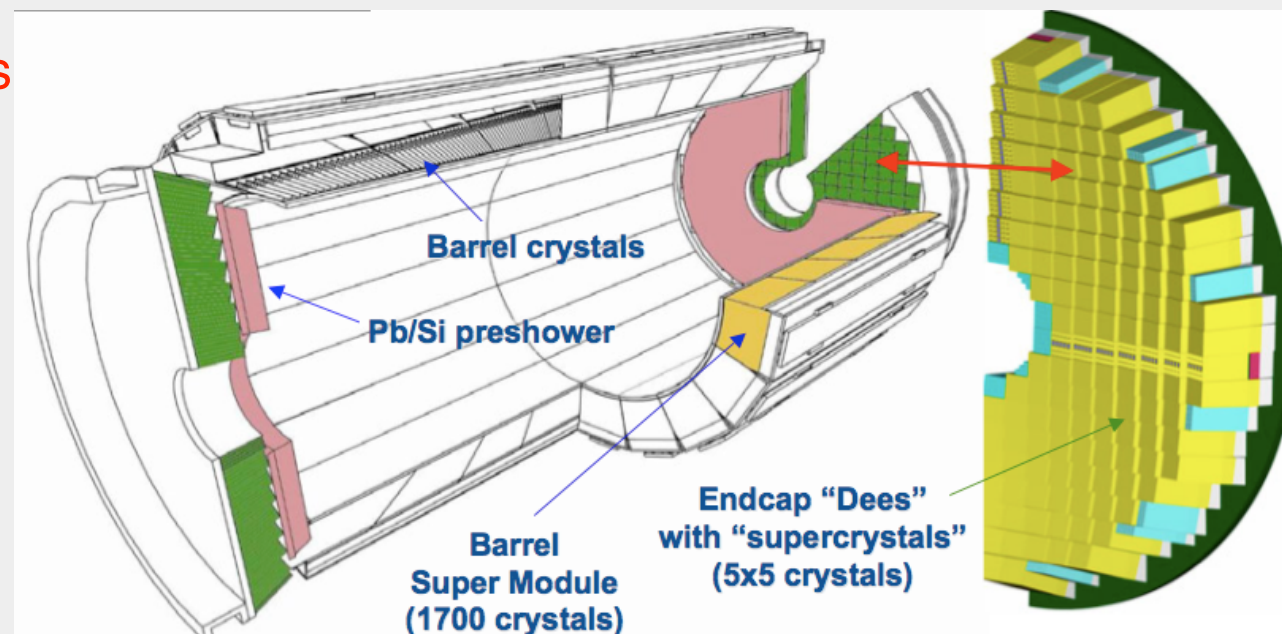
- Above 1 GeV the dominant processes become energy independent:
 - bremsstrahlung for e^+ and e^-
 - and pair production for photons
- Through a succession of these energy losses an e.m. cascade is propagated until the energy of the charged secondaries has been degraded to the regime dominated by ionization loss (below E_c)
- Below E_c a slow decrease in number of particles occurs as electrons are stopped and photons absorbed

Interaction with matter :

• *More of EM shower development : (for details clic*



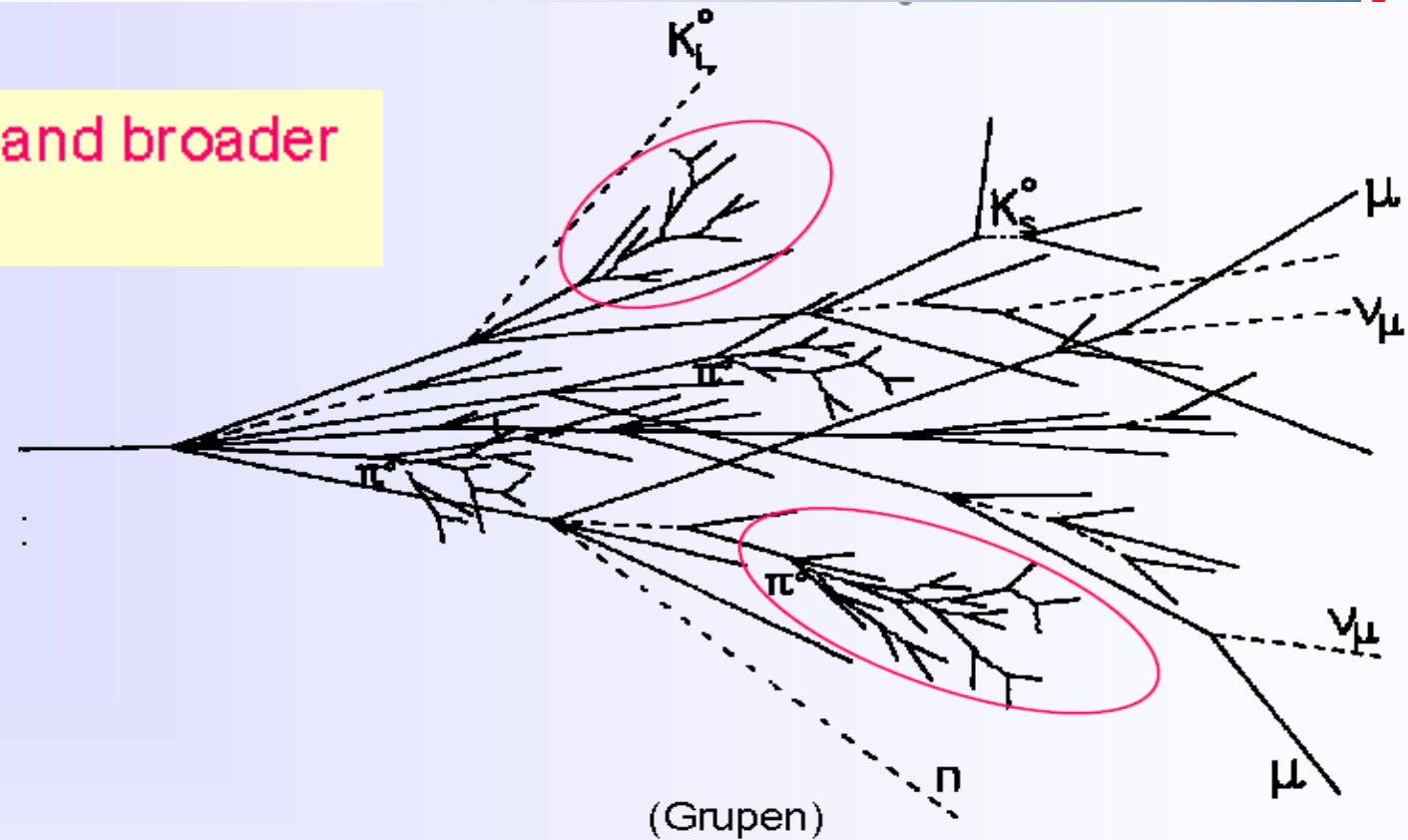
- Homogeneous Lead tungstate PbWO₄ crystals
- Fast scintillation response, excellent time resolution
 - about 80% of the light emitted in 25 ns
- Compact & high granularity
 - Molière radius 2.2 cm
 - Radiation length X₀ 0.89 cm
- Barrel $|\eta| < 1.48$:
 - ~61K crystals in 36 SuperModules (SM)
 - 2x2x23 cm³ covering 26 X₀
 - Photodetector: Avalanche Photo Diodes (APD)
- Endcap $1.48 < |\eta| < 3.0$
 - ~15k crystals in 4 Dees
 - 3x3x22 cm³ covering 24 X₀
 - Photodetector: Vacuum Photo Triodes (VPT)
- Preshower $1.65 < |\eta| < 2.6$
 - ~137k silicon strips in 2 planes per endcap
 - 3X₀ of lead radiator
- No longitudinal segmentation
- Energy resolution for electrons impinging on the center of a 3x3 barrel crystal matrix from Test Beam (no upstream material, no magnetic field, etc...)



$$\frac{\sigma_E}{E} = \frac{2.8\%}{\sqrt{E \text{ (GeV)}}} \oplus \frac{0.128}{E \text{ (GeV)}} \oplus 0.3\%$$

- Hadronic cascades develop in an analogous way to e.m. showers
- Strong interaction controls overall development
- High energy hadron interacts with material, leading to multi-particle production of more hadrons
- They interact with further nuclei
- Nuclear breakup and spallation neutrons
- Multiplication continues down to the pion production threshold ($E \sim 2m_{\pi} = 0.28 \text{ GeV}/c^2$)
- Neutral pions result in an electromagnetic component to the total énérgie(immediate decay: $\pi^0 \rightarrow \gamma\gamma$) and (also: $\eta \rightarrow \gamma\gamma$)

Hadronic showers are much longer and broader than electromagnetic ones !



A hadronic shower contains two components:

hadronic

+

electromagnetic



- charged hadrons p, π^\pm, K^\pm
- nuclear fragments
- breaking up of nuclei (binding energy)
- neutrons, neutrinos, soft γ 's, muons



neutral pions $\rightarrow 2\gamma$

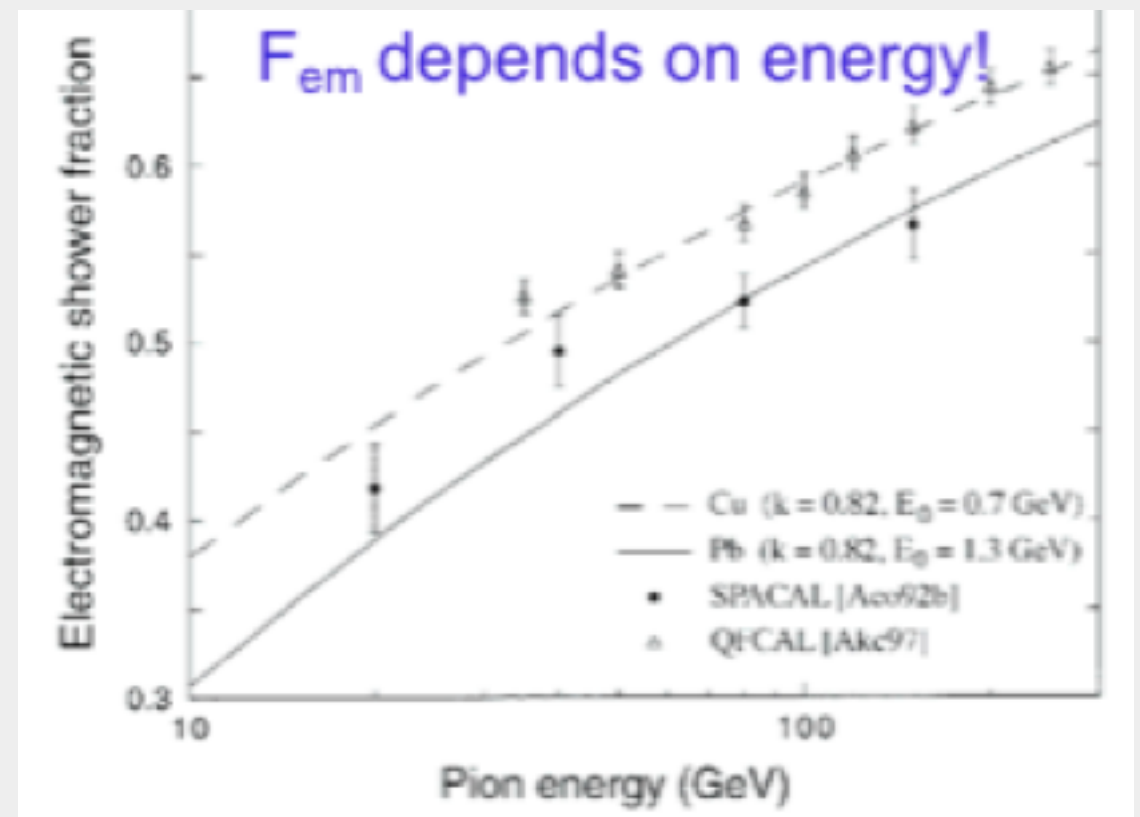
\rightarrow electromagnetic cascades

$$n(\pi^0) \approx \ln E(\text{GeV}) - 4.6$$

example $E = 100 \text{ GeV}$: $n(\pi^0) \approx 18$

invisible energy \rightarrow large energy fluctuations \rightarrow limited energy resolution

- A priori e and h give in a calorimeter a different response ($e/h > 1$)
- The fluctuation of the fraction of energy deposited by e and h limit the measured energy resolution.
- Moreover in average this fraction (e/h) is energy dependent inducing non linearity in detector response.
- **How to obtain $e/h=1$ (compensation)**
 - Suppress/reduce em component (use high Z absorber)
 - enhance n production through fission
 - enhance response to n using active materials hydrogen rich



• *More about compensation :*
for details clic →

Intrinsic hadronic resolution

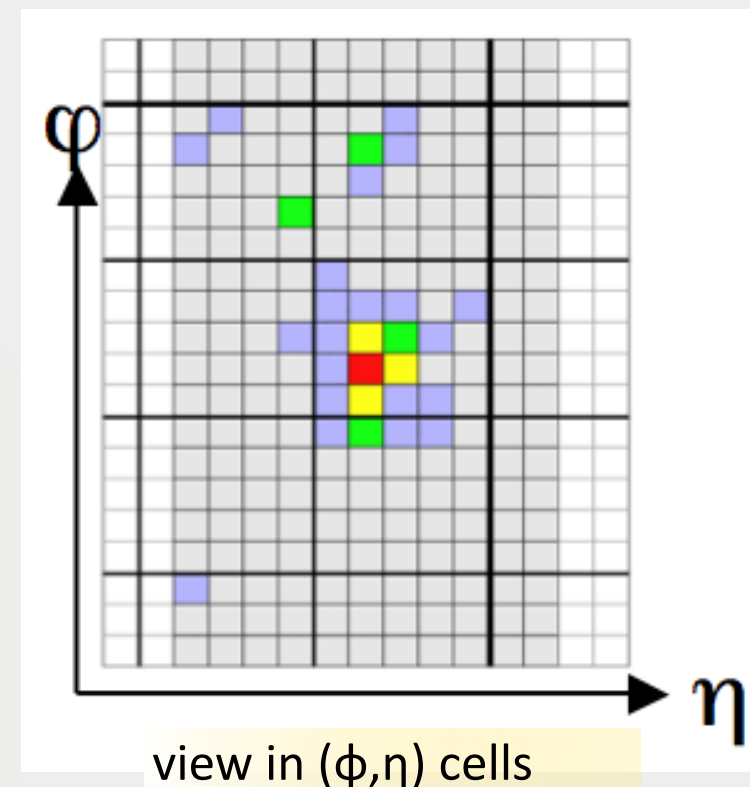
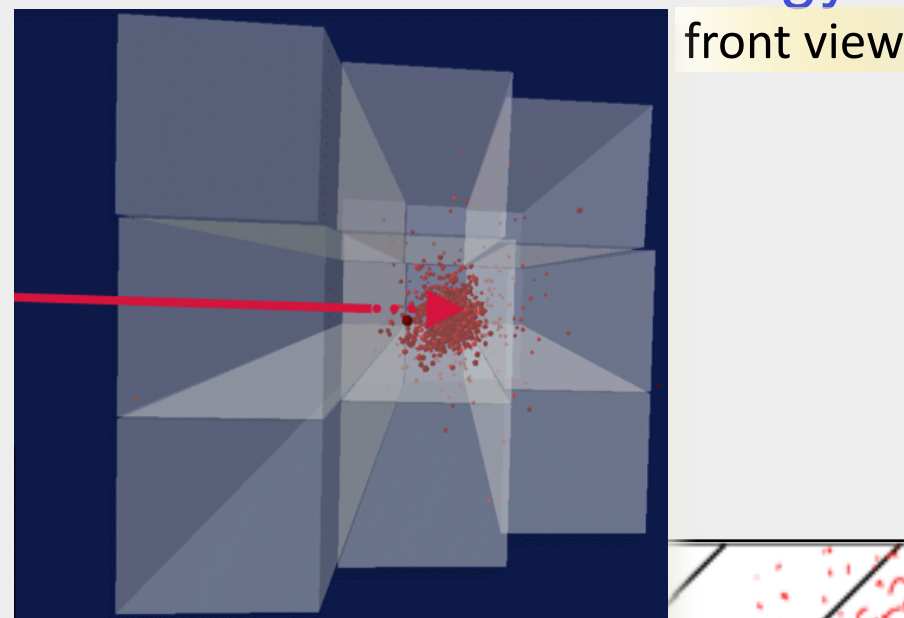
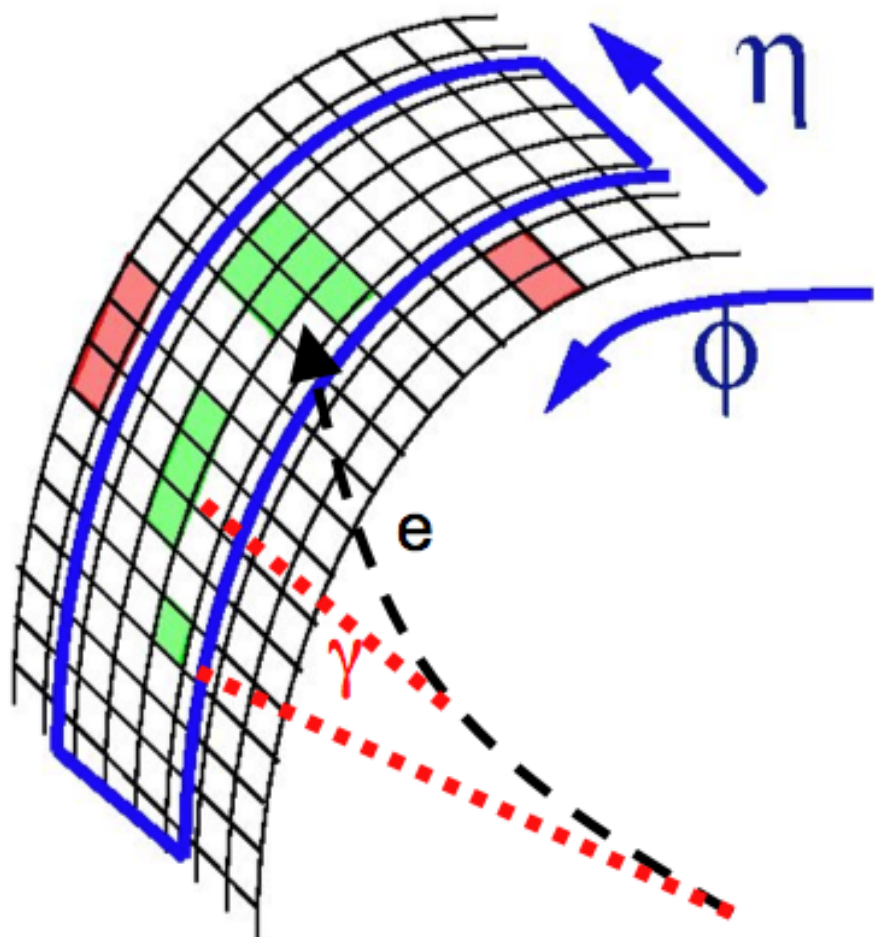
$$\sigma / E \sim (20 \div 40)\% / \sqrt{E(\text{GeV})}$$

+ sampling...+...

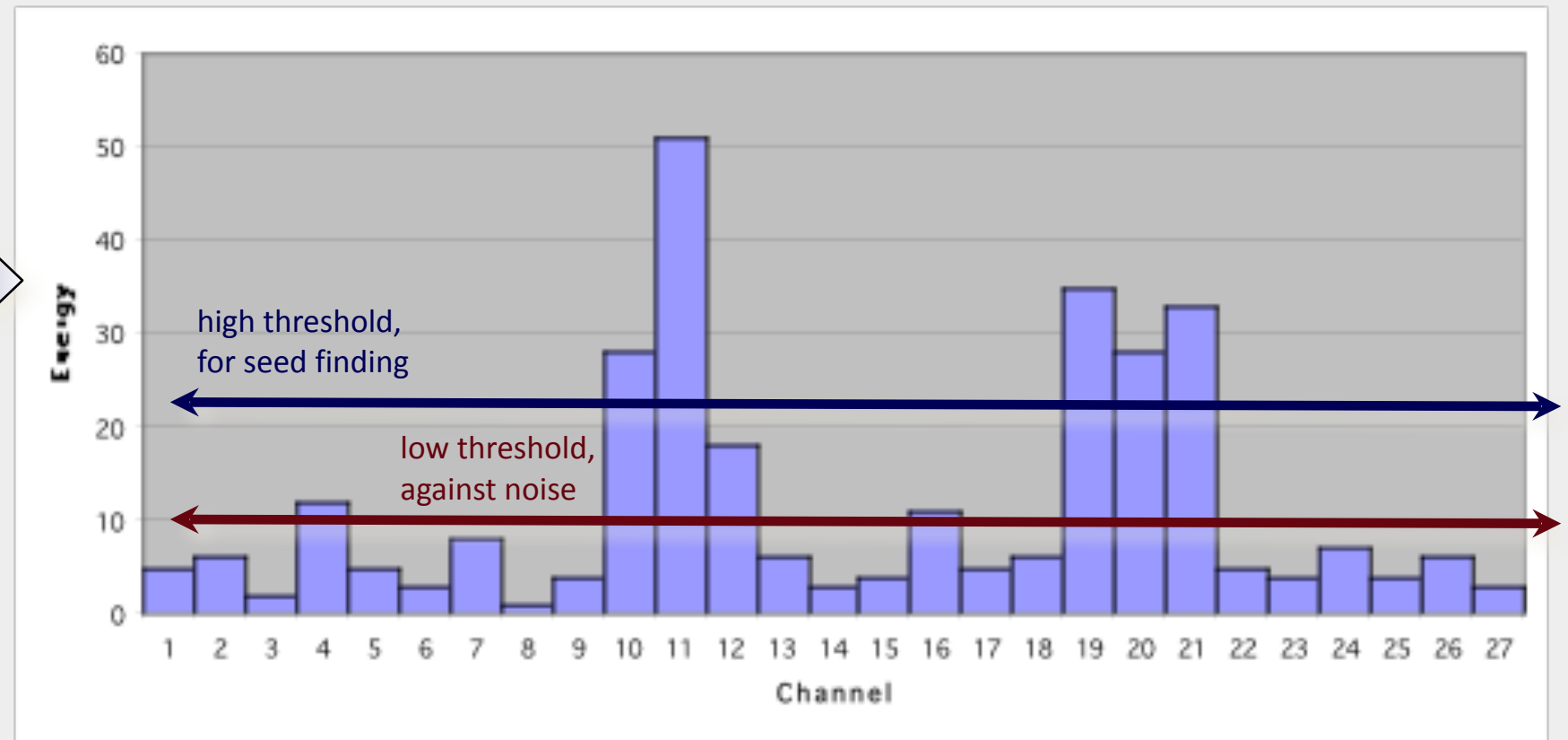
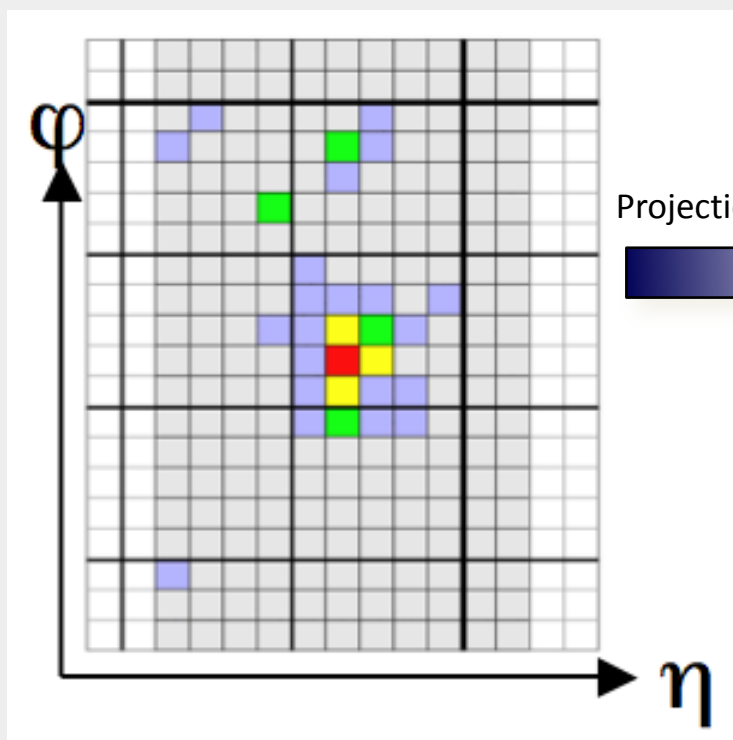
Hadrons interaction with matter :

• *More of Hadron shower development :* (for details clic) →

- Calorimeters are segmented in cells
- Typically a shower extends over several cells
 - Useful to reconstruct precisely the impact point from the “center-of-gravity” of the deposits in the various cells
- Example **CMS Crystal Calorimeter**:
 - electron energy in central crystal $\sim 80\%$, in 5×5 matrix around it $\sim 96\%$
- So the task is :
 - identify these clusters and reconstruct the energy they contain



- Clusters of energy in a calorimeter are due to the particles issued from the collision
 - Clustering algorithm groups individual channel energies
 - Don't want to miss any; don't want to pick up fakes

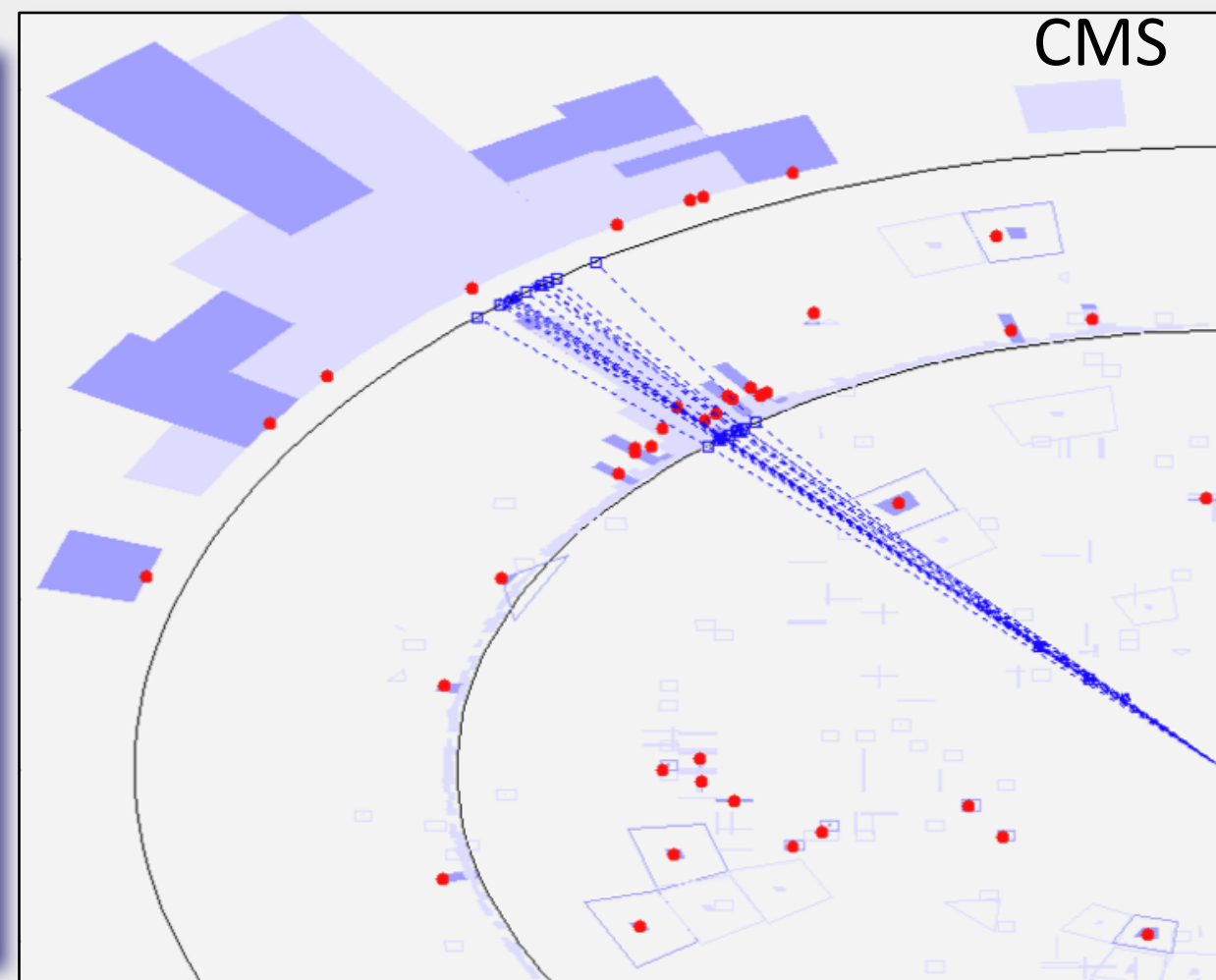
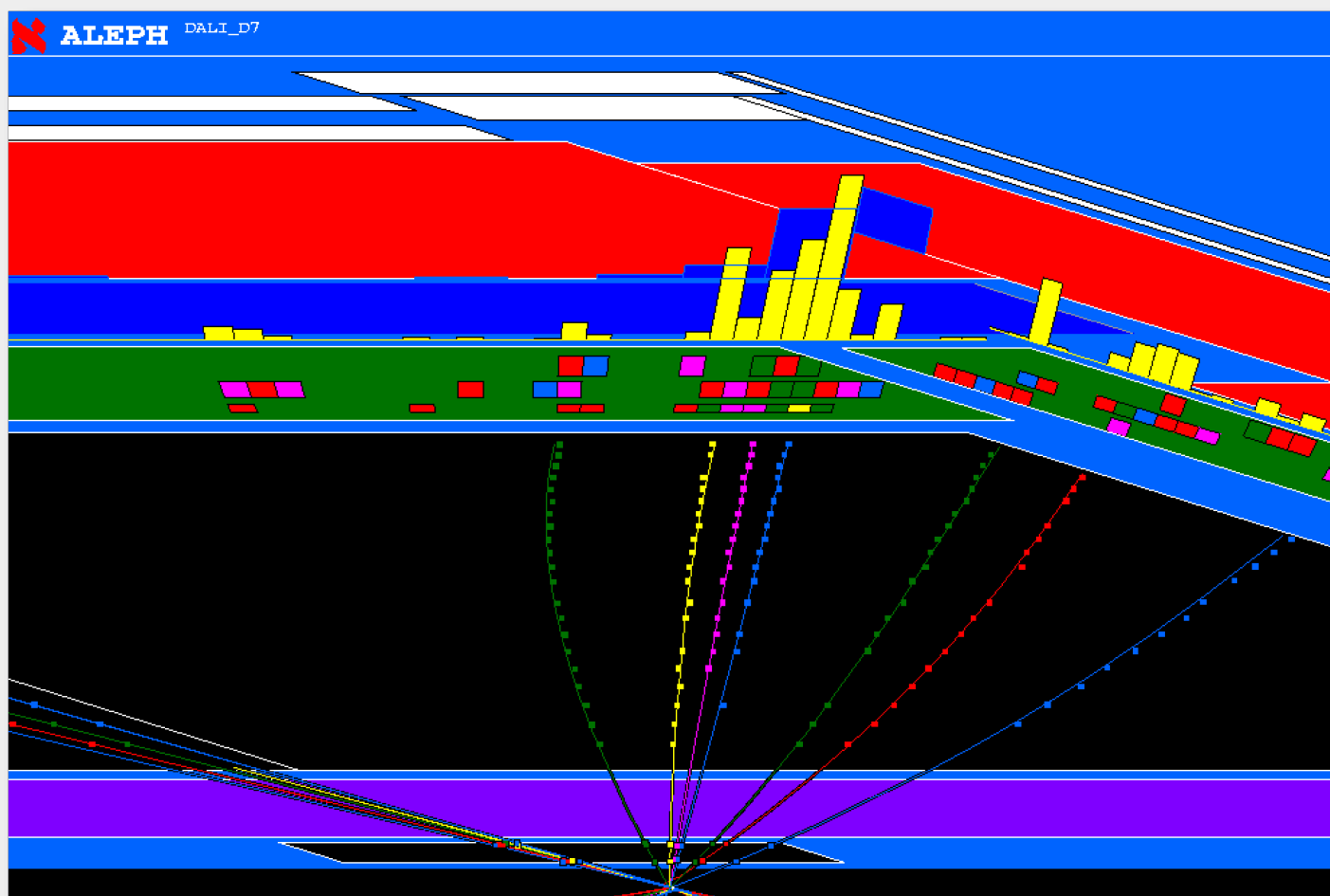


Simple algorithm example

- Scan for **seed** crystals = local energy maximum above a defined **seed threshold**
- Starting from the seed position, adjacent crystals are examined, scanning first in ϕ and then in η
- Along each scan line, crystals are **added to the cluster if**
 - The crystal's energy is above the **noise level (lower threshold)**
 - The crystal has not been assigned to another cluster already

Obtain energy cluster and the best possible resolution
Energy Flow technique

- Reconstruct energy deposited by charged and neutral particles in tracker and calorimeters
- Determine position of deposit, from direction of incident particles
- Be insensitive to noise and “un-wanted” (un-correlated) energy (pileup)



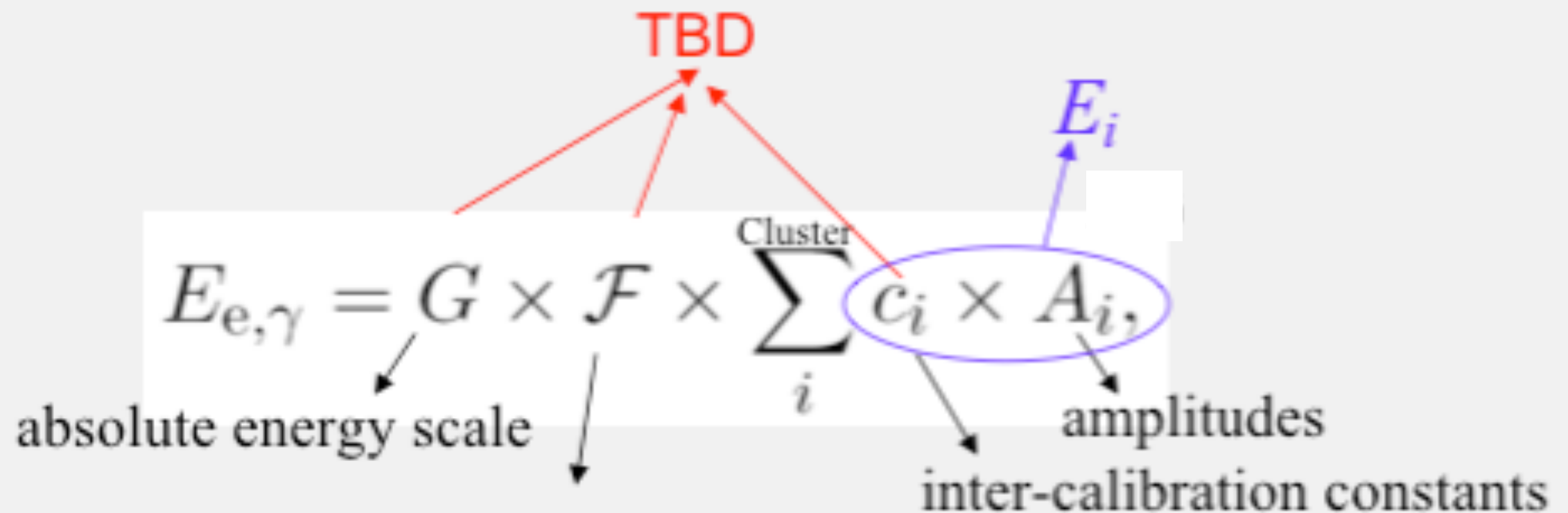
- Determine relationship between **signal** (pC, p.e.) and **energy** (GeV)
- **Fundamental problem in sampling calorimeters:**
 - Different shower components are sampled differently
 - Shower composition changes as shower develops
 - **Sampling fraction changes with the shower age** (also E dependent)
 - How to intercalibrate the sections of a longitudinally segmented calorimeter? (quite a challenge...)

Calibration Techniques:

- Test Beams
- Cosmic muons
- Laser/LED Monitoring
- Guided 60 Co sources
- Low-level, stable radioactive background
- Cell-weighting to optimize resolution, uniformity
- In situ physics:
 - **Electromagnetic particles :** $Z, J/\psi \text{ @ } e^+e^-; \pi^0, \eta \text{ @ } \gamma\gamma$
 - **Hadronic particles :** $W, Z \text{ @ } q\bar{q}; 'Z, \gamma - \text{jet balancing}'$

From single channel electrical signal to $E_{e,\gamma}$

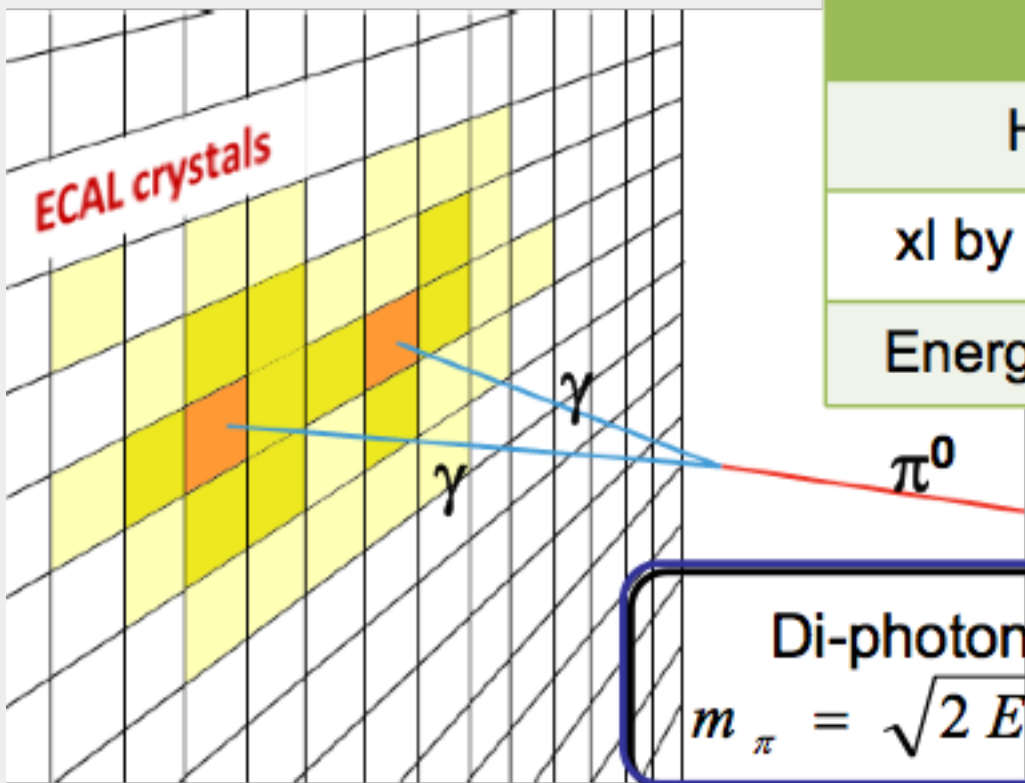
(The case of CMS)



(particle type, momentum, position & clustering algo)

Account for energy losses due to containment variations

π^0 calibration



Pros
High Statistics
x1 by x1 inter-calibration
Energy scale calibration

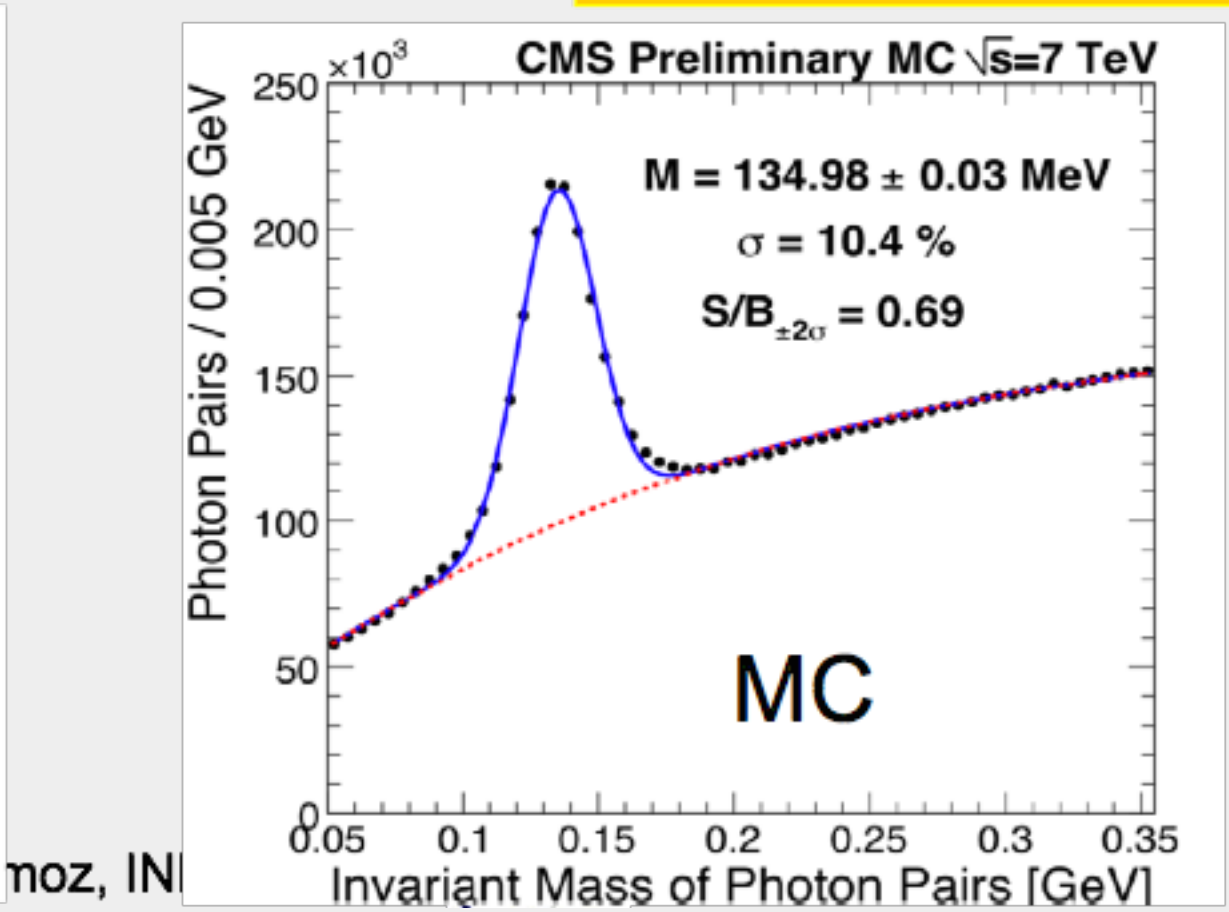
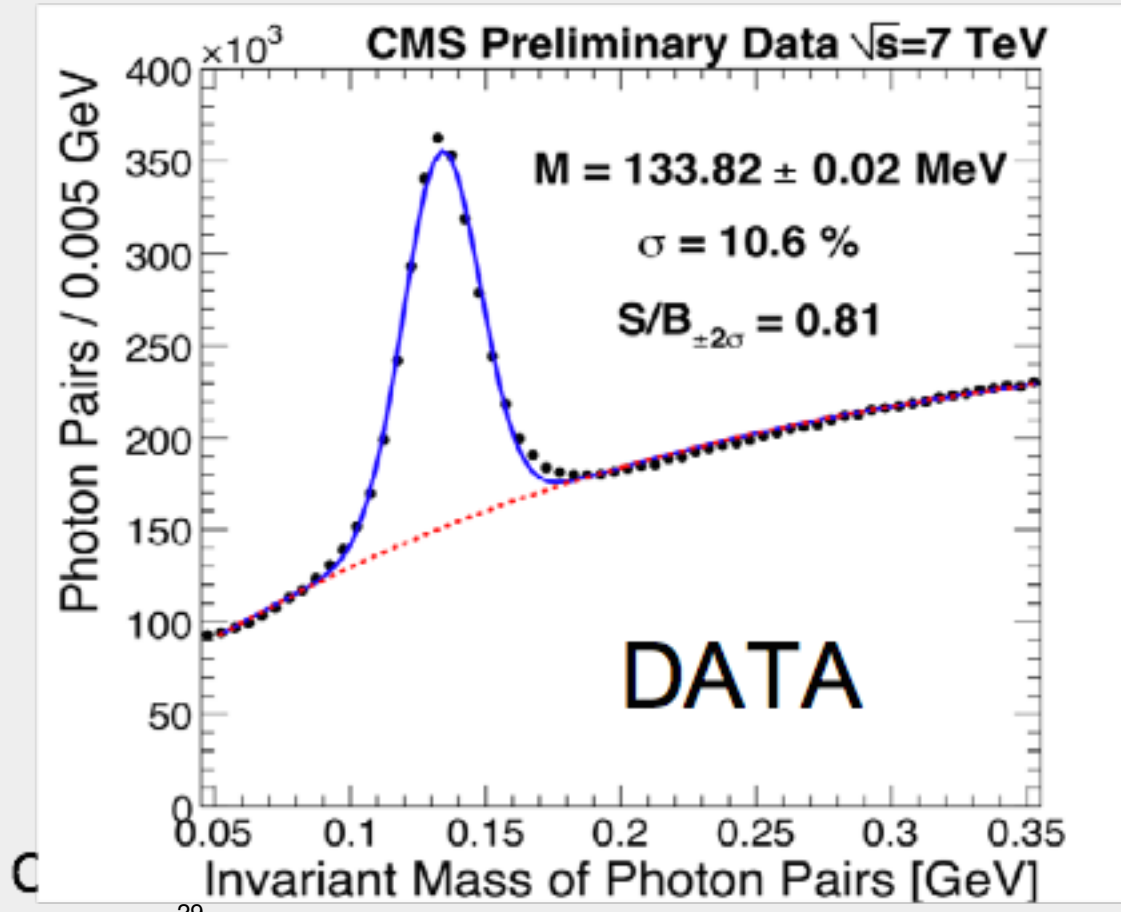
Cons
Reco of low energy γ
High energy γ overlap
Sizeable background

Di-photon invariant mass

$$m_{\pi} = \sqrt{2 E_1 E_2 (1 - \cos \vartheta)}$$

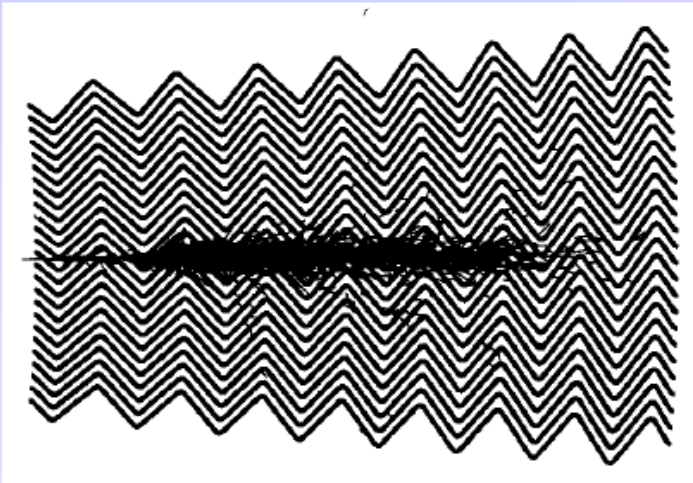
Calibrated photon energy

 π^0 mass peak at right position
 Minimum peak spread



ATLAS electromagnetic Calorimeter

Accordion geometry absorbers immersed in Liquid Argon

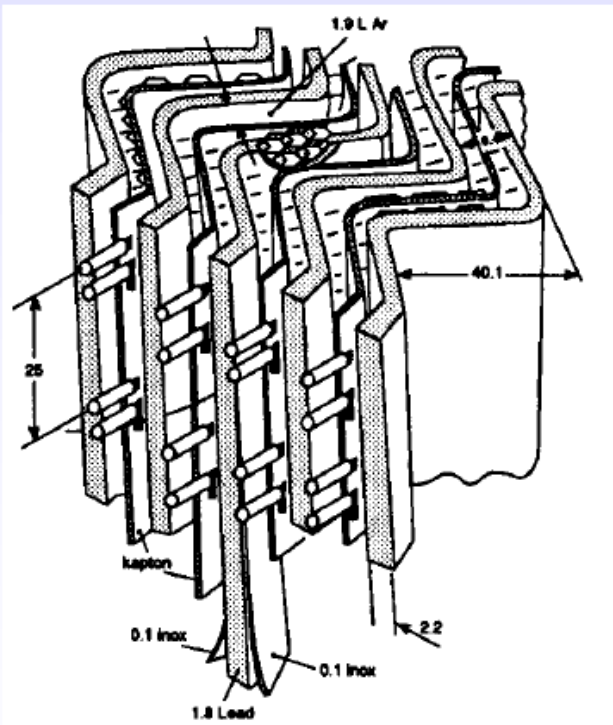


Liquid Argon (90K)

- + lead-steel absorbers (1-2 mm)
- + multilayer copper-polyimide readout boards

→ Ionization chamber.

1 GeV E-deposit → $5 \times 10^6 e^-$



- Accordion geometry minimizes dead zones.
- Liquid Ar is intrinsically radiation hard.
- Readout board allows fine segmentation (azimuth, pseudo-rapidity and longitudinal) acc. to physics needs



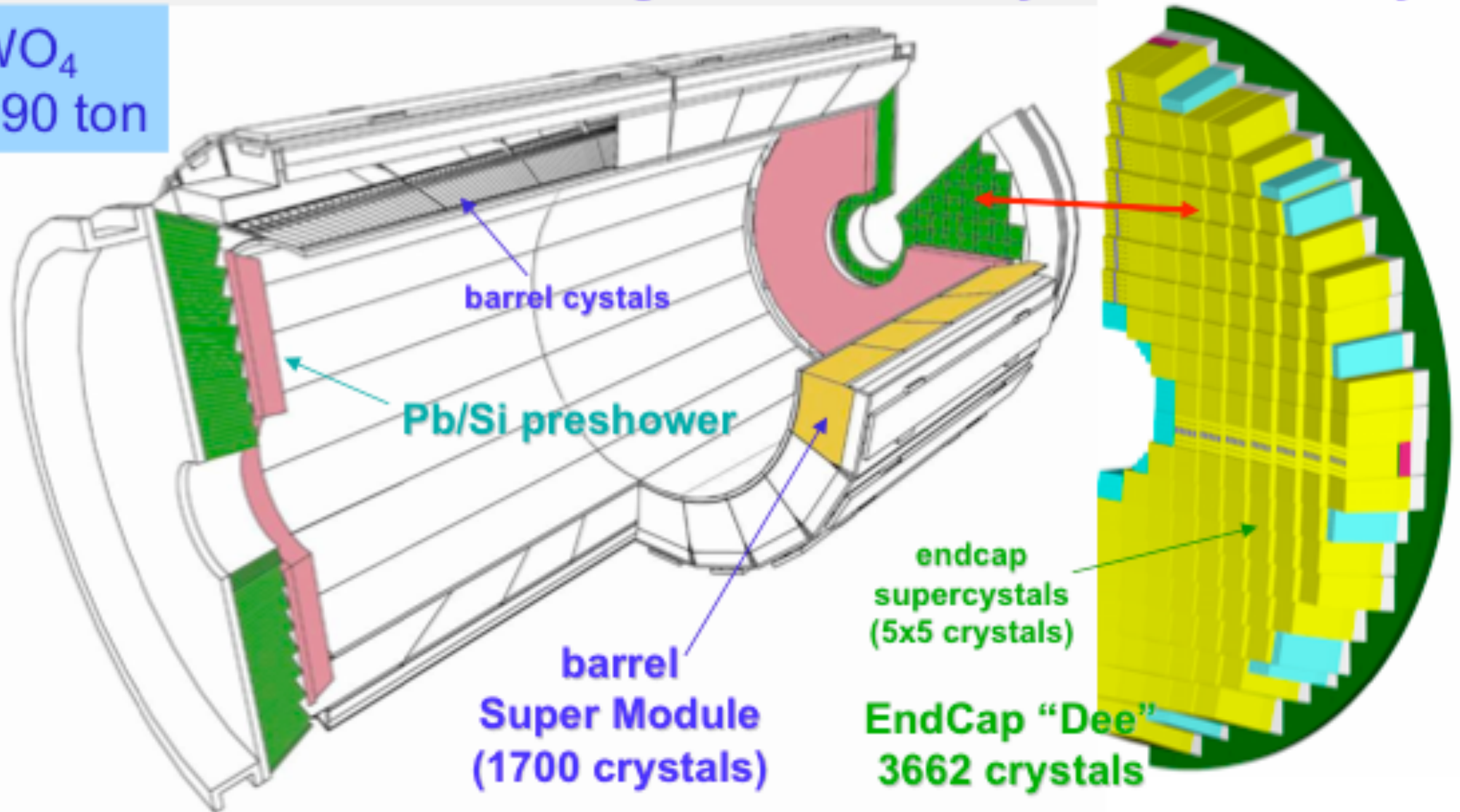
Test beam results $\sigma(E)/E = 9.24\%/\sqrt{E} \oplus 0.23\%$

Spatial resolution $\approx 5 \text{ mm} / \sqrt{E}$

Precision electromagnetic calorimetry: 75848 PWO crystals

PWO: PbWO_4
about 10 m^3 , 90 ton

Previous
Crystal
calorimeters:
max 1 m^3



Barrel: $|\eta| < 1.48$
36 Super Modules
61200 crystals ($2 \times 2 \times 23 \text{ cm}^3$)

EndCaps: $1.48 < |\eta| < 3.0$
4 Dees
14648 crystals ($3 \times 3 \times 22 \text{ cm}^3$)



CMS

- Compact
- Excellent energy resolution
- Fast
- High granularity
- Radiation resistance
- E range MIP \rightarrow TeV

- Homogeneous calorimeter made of 75000 PbWO_4 scintillating crystals + PS FW

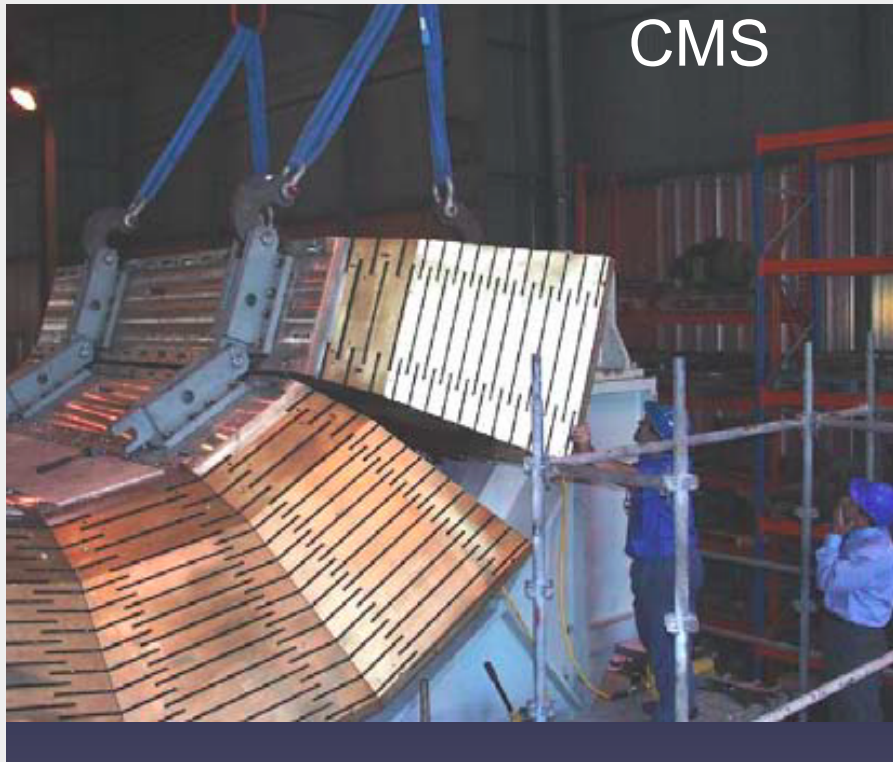
Atlas

- Good energy resolution
- Fast
- High granularity
- Longitudinally segmented
- Radiation resistance
- E range MIP \rightarrow TeV

- Sampling LAr-Pb, 3 Longitudinal layers + PS

ATLAS and CMS makes different choices:

sampling calorimeter allow to have redundant measurement of γ angle
homogenous calorimeter with very low stochastic term aims to excellent energy resolution, the measure of γ angle relies on vertex reconstruction from tracking.



CMS

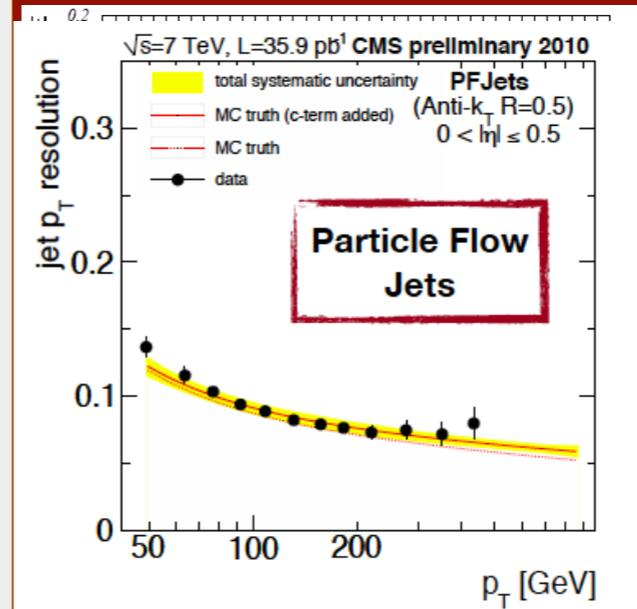
5 cm brass / 3.7 cm scint.
Embedded fibres, HPD readout



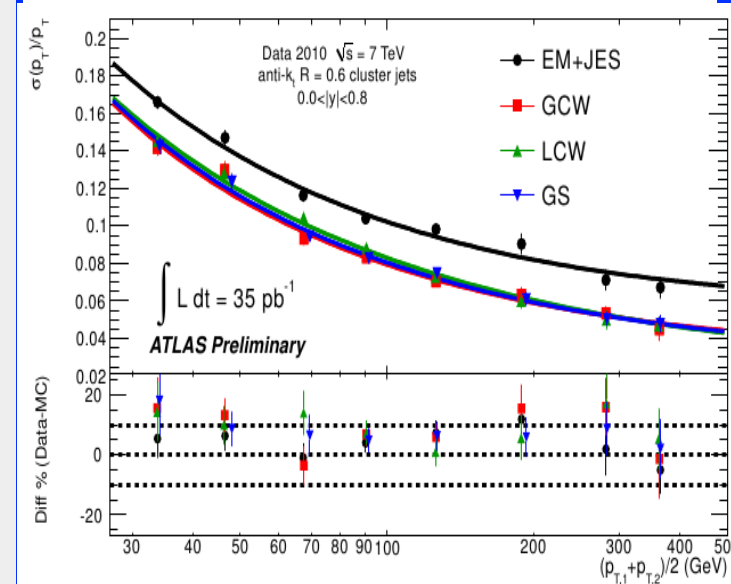
ATLAS

14 mm iron / 3 mm scint.
sci. fibres, read out by phototubes

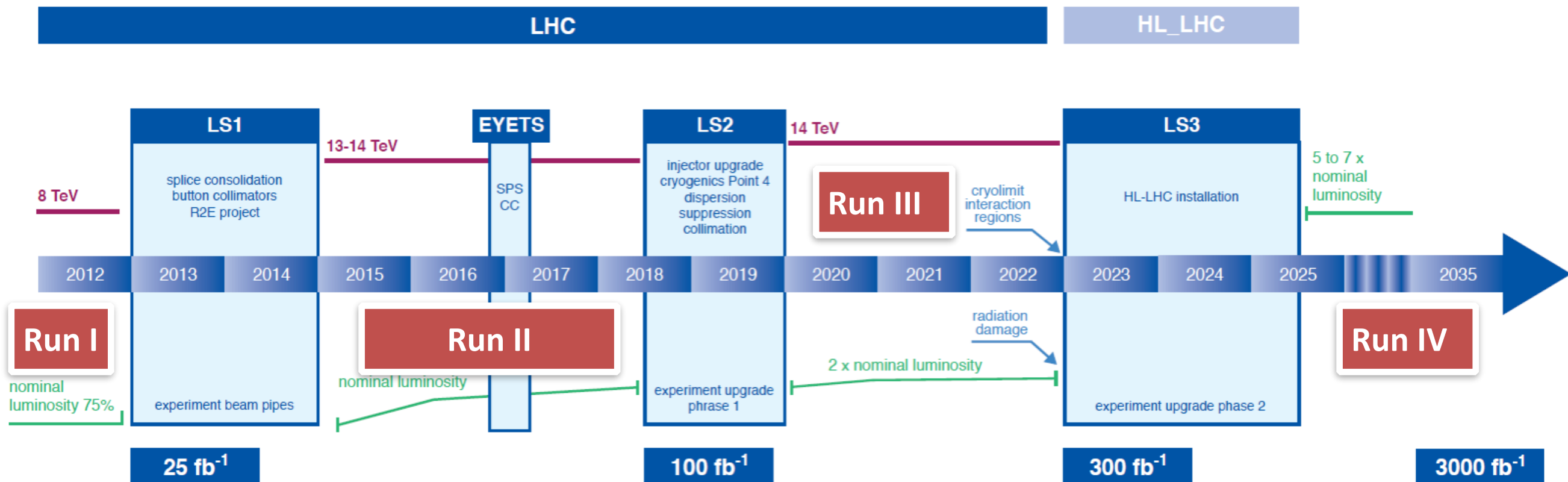
- CMS**
- HCAL only
 $\sigma/E = (93.8)\%/\sqrt{E} \oplus (7.4)\%$
 - ECAL+HCAL
 $\sigma/E = (82.6)\%/\sqrt{E} \oplus (4.5)\%$



- ATLAS**
- Standalone tile calorimeter
 $\sigma/E = (52.9)\%/\sqrt{E} \oplus (5.7)\%$
 - Improved resolution using full calorimetric system (ECAL+HCAL)
 $\sigma/E = (42)\%/\sqrt{E} \oplus (2)\%$



LHC / HL-LHC Plan



0.75 $10^{34} \text{ cm}^{-2}\text{s}^{-1}$
 50 ns bunch
 high pile up ~40

1.5 $10^{34} \text{ cm}^{-2}\text{s}^{-1}$
 25 ns bunch
 pile up ~40

1.7-2.2 $10^{34} \text{ cm}^{-2}\text{s}^{-1}$
 25 ns bunch
 pile up ~60

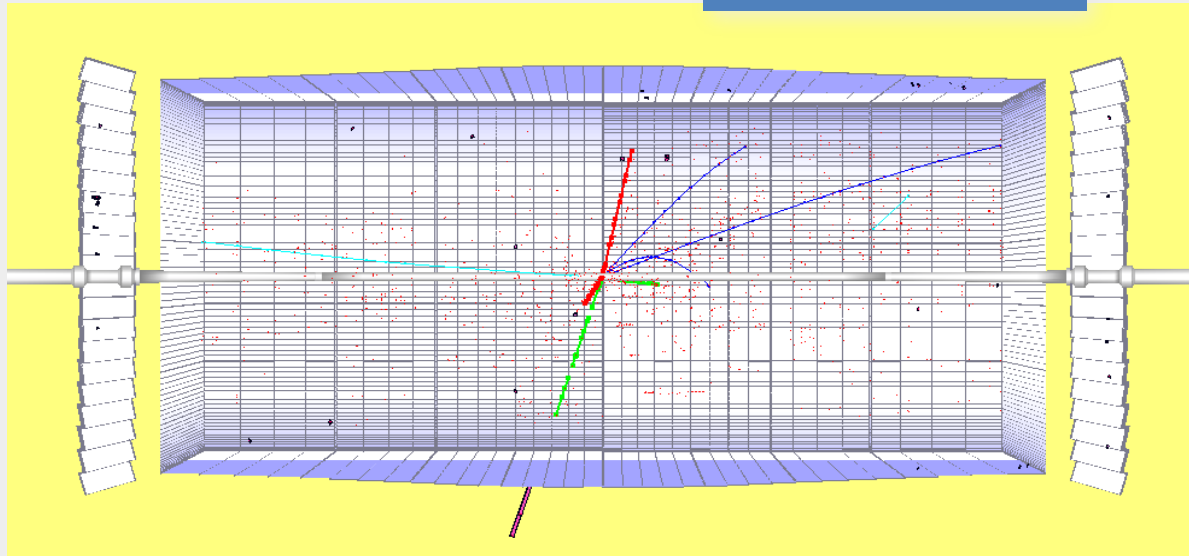
~5(7.5!) $10^{34} \text{ cm}^{-2}\text{s}^{-1}$
 25 ns bunch
 pile up ~140 - 200

50 \Rightarrow 25 ns

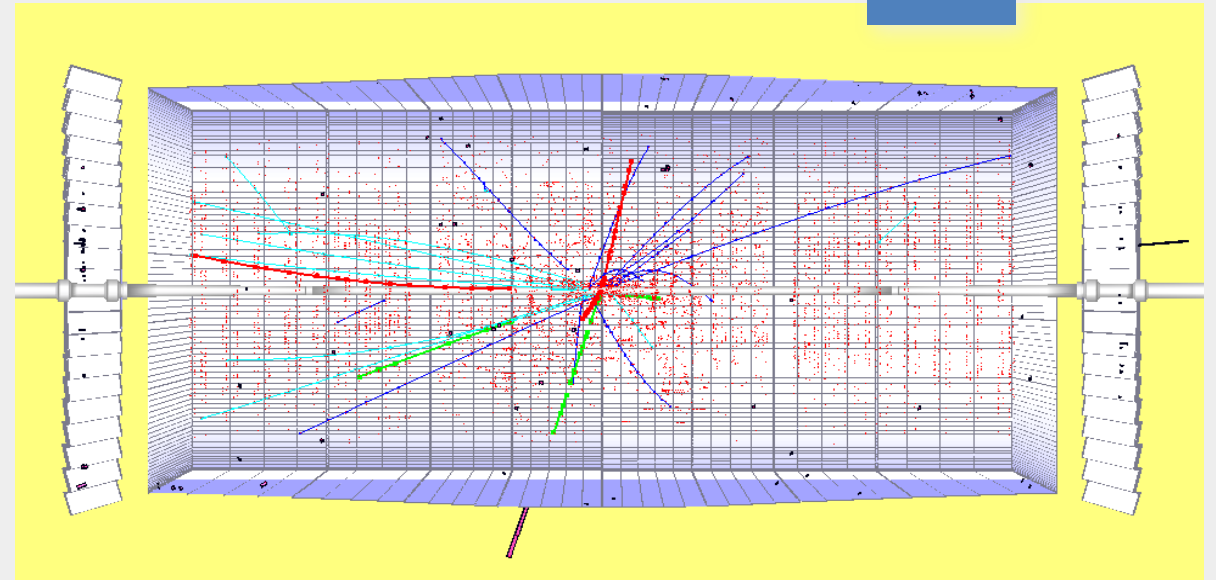
Detector occupancy

The challenge from simulation

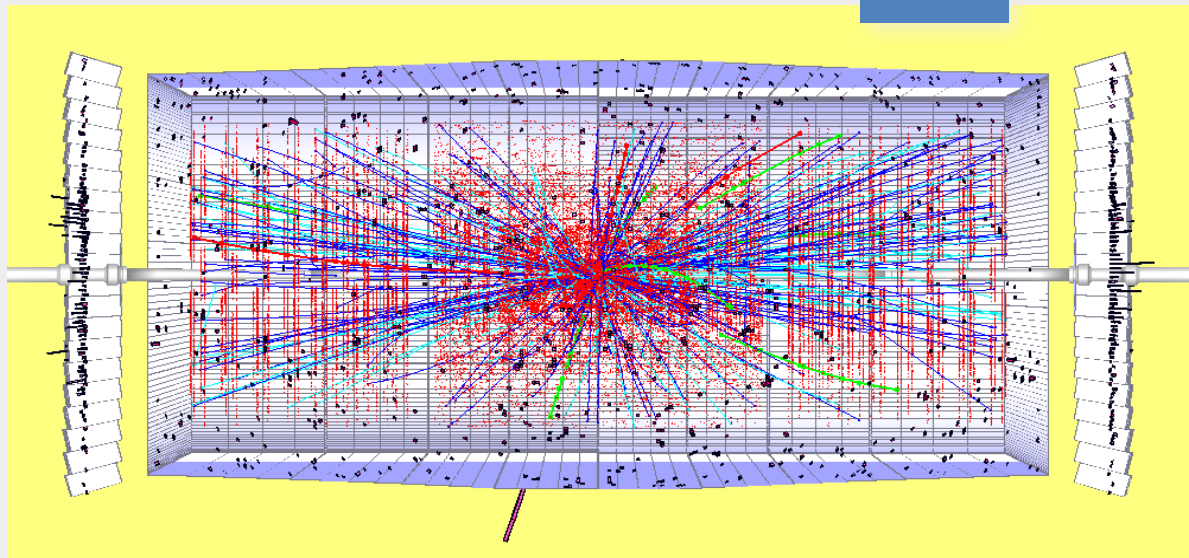
$10^{32} \text{ cm}^{-2} \text{ s}^{-1}$



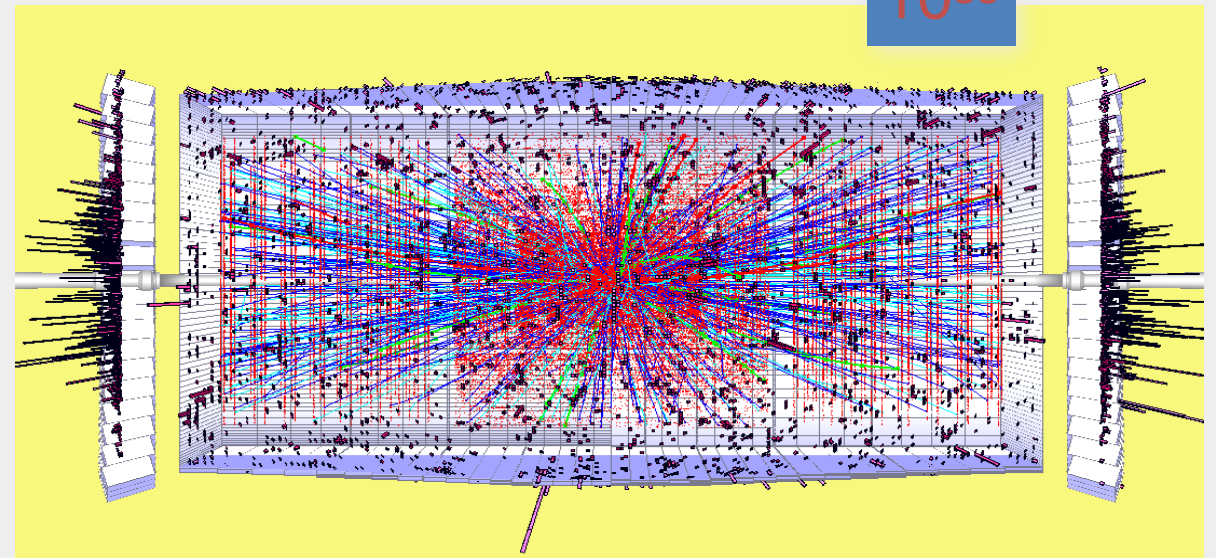
10^{33}

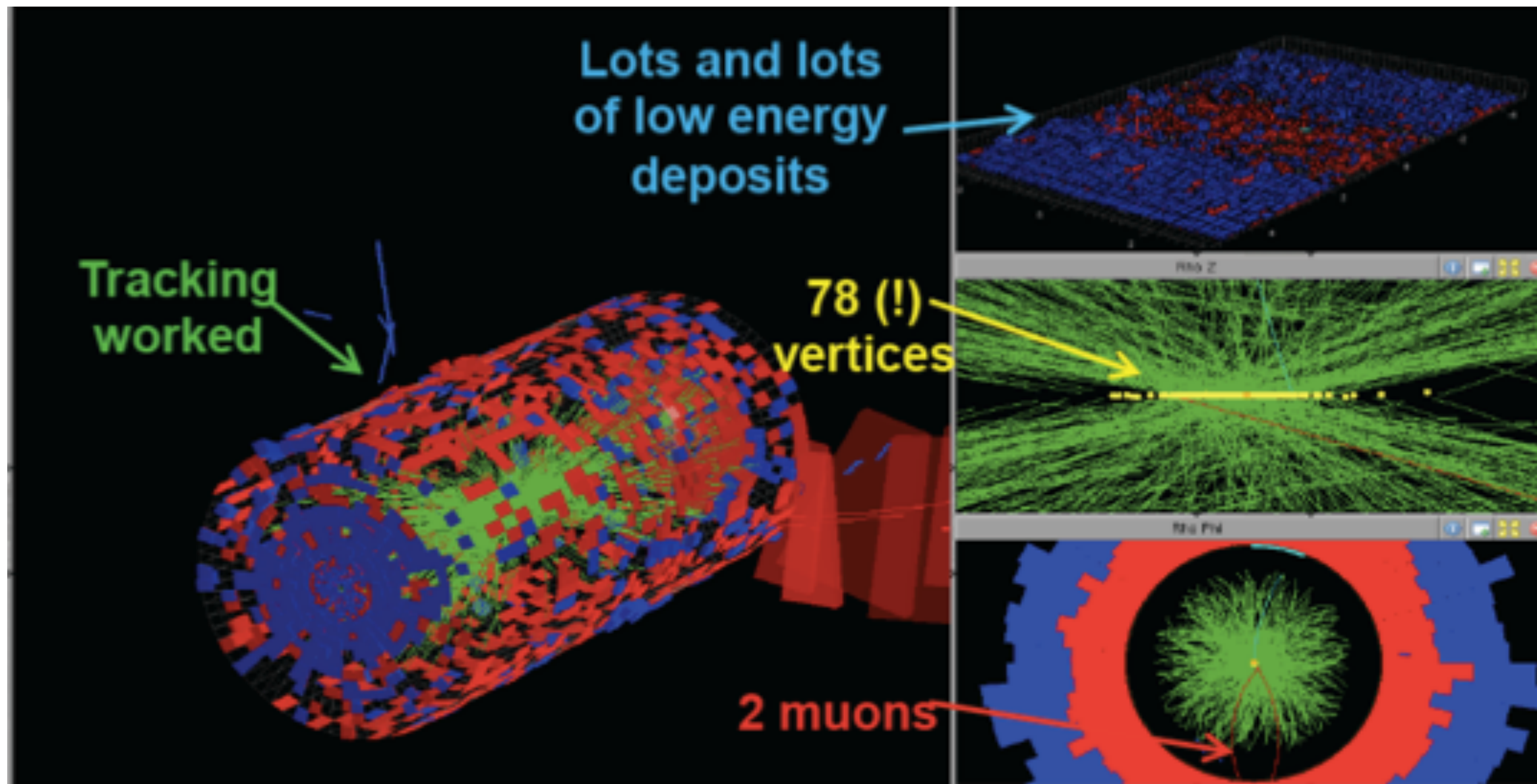


10^{34}



10^{35}





Extreme conditions for:

- radiation
- pileup
- Trigger / DAQ
- Data handling

Take advantage of all LHC downtimes to improve, upgrade and repair detector!

CMS Upgrades for HL-LHC

New Tracker

- Radiation tolerant - high granularity - less material
- Tracks in hardware trigger (L1)
- Coverage up to $\eta \sim 4$

New Endcap Calorimeters

- Radiation tolerant - high granularity
- Investigate coverage up to $\eta \sim 4$

Barrel ECAL

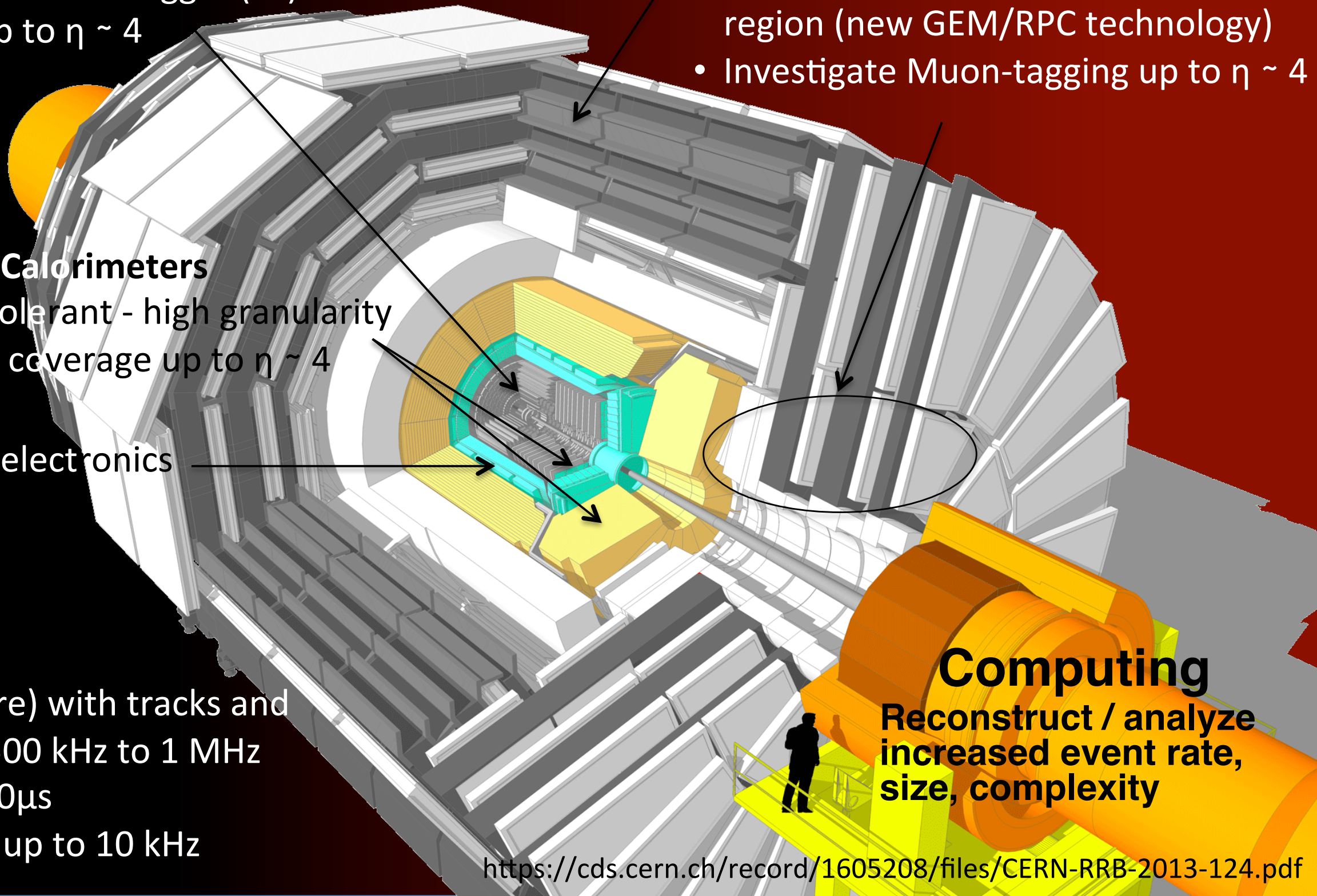
- Replace FE electronics

Trigger/DAQ

- L1 (hardware) with tracks and rate up ~ 500 kHz to 1 MHz
- Latency $\geq 10\mu\text{s}$
- HLT output up to 10 kHz

Muons

- Replace DT FE electronics
- Complete RPC coverage in forward region (new GEM/RPC technology)
- Investigate Muon-tagging up to $\eta \sim 4$



Computing
Reconstruct / analyze
increased event rate,
size, complexity

- Concentrate on improvement of jet energy resolution to match the requirement of the new physics expected in the next 10-30 years
- Two approaches:
 - minimize the influence of the calorimeter and measure jets using the combination of all detectors! ==> *Particle Flow technique*.
 - measure the hadronic shower components in each event & weight directly access to the source of fluctuations ! ==> *Dual (Triple) Readout*
- Also looking for more radiation hard crystals

- New developments:*
- *Shashlik*
 - *Crystals : LSO/LYSO*
 - *HGCAL*

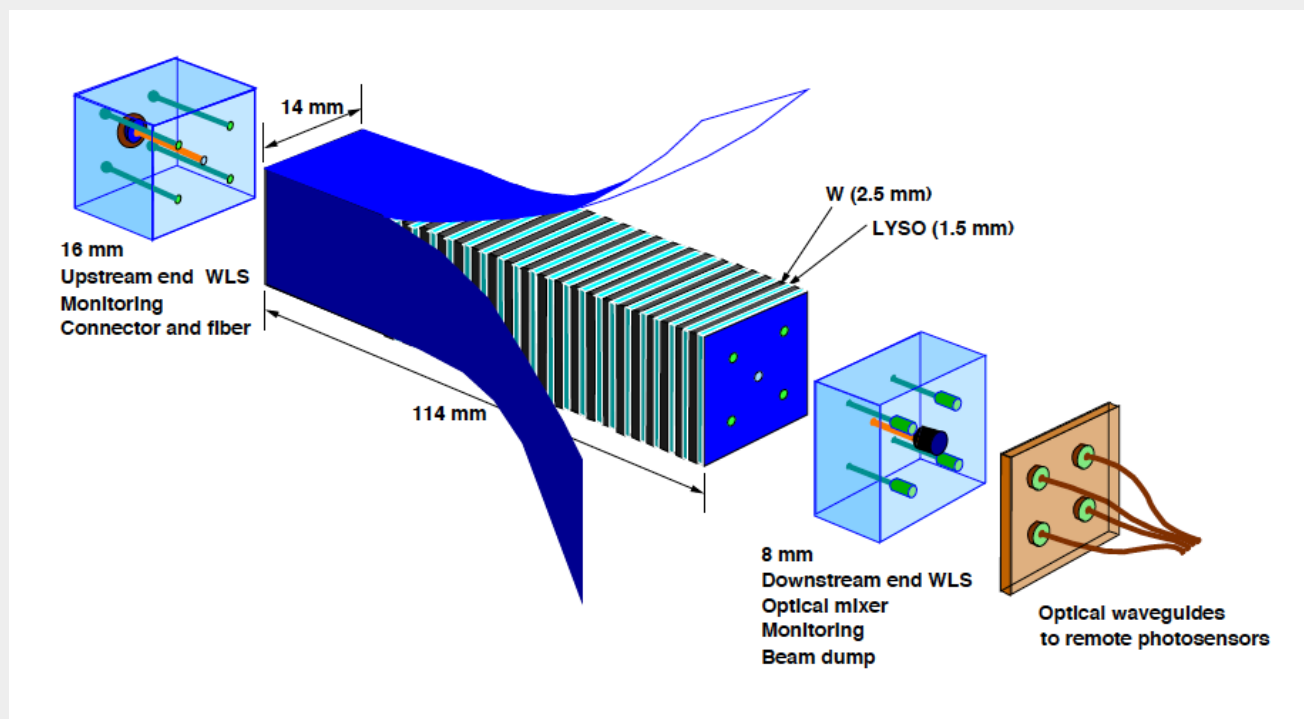
CMS Generic:

- Replace the forward calorimeter by a radiation hard detector capable of withstanding the very high luminosities expected at HL-LHC

HGCAL Specific:

- Aim for a dense and highly granular 3D sampling calorimeter inspired by CALICE (ILC), adapted to HL-LHC very high event rates
- Exploit topology of deposits and shower tracking capabilities in a particle flow reconstruction both for trigger and offline analysis

(Super modules are 5x5 Arrays of these Individual tiny modules)



Materials:

- Absorber: W
- Active Material: LYSO(Ce) (primary)
- Active material: CeF₃ also under study

Structure:

- 2.5 mm W plates (28 per module)
- 1.5 mm LYSO(Ce) plates (29 per module)

Module Dimensions:

- Transverse Size: Front Face 14 x 14 mm²
- Length 114 mm

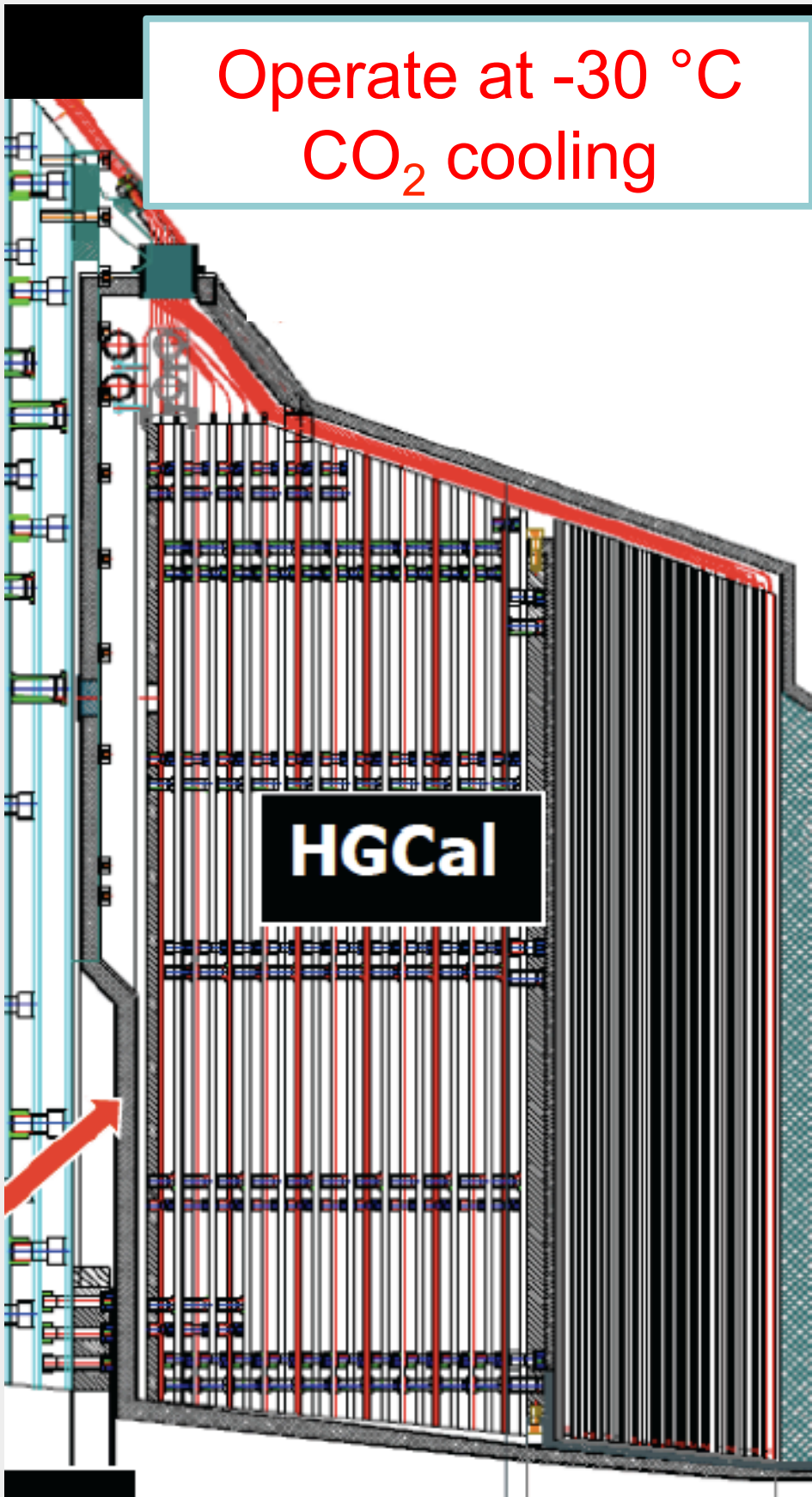
Readout:

- WLS Capillaries (4 per module)
- GaInP/SiPM Photosensors (4 per module)
- One QIE13 channel per module

Segmentation in depth: Unsegmented except for the possible extraction of a signal near shower max

Shashlik module cross section is very small, ~ Moliere radius, to minimize pileup.

Operate at $-30\text{ }^{\circ}\text{C}$
 CO_2 cooling



Si/W-ECAL Section ($\Sigma_{\text{depth}} > 25X_0, 1.5\lambda$)
 $10 \times 0.65X_0$
 $10 \times 0.88X_0$
 $8 \times 1.26X_0$

Si/Brass Front HCAL (FH) Section ($\Sigma_{\text{depth}} > 3.5\lambda$)
 $12 \times 0.3\lambda$

Scint/Brass Backing HCAL(BH)Section ($\Sigma_{\text{depth}} > 5\lambda$)
 $12 \times 0.45\lambda$

Total Depth $> 10\lambda$

Table 3.2: Parameters of the EE and FH.

	EE	FH	Total
Area of silicon (m^2)	380	209	589
Channels	4.3M	1.8M	6.1M
Detector modules	13.9k	7.6k	21.5k
Weight (one endcap) (tonnes)	16.2	36.5	52.7
Number of Si planes	28	12	40

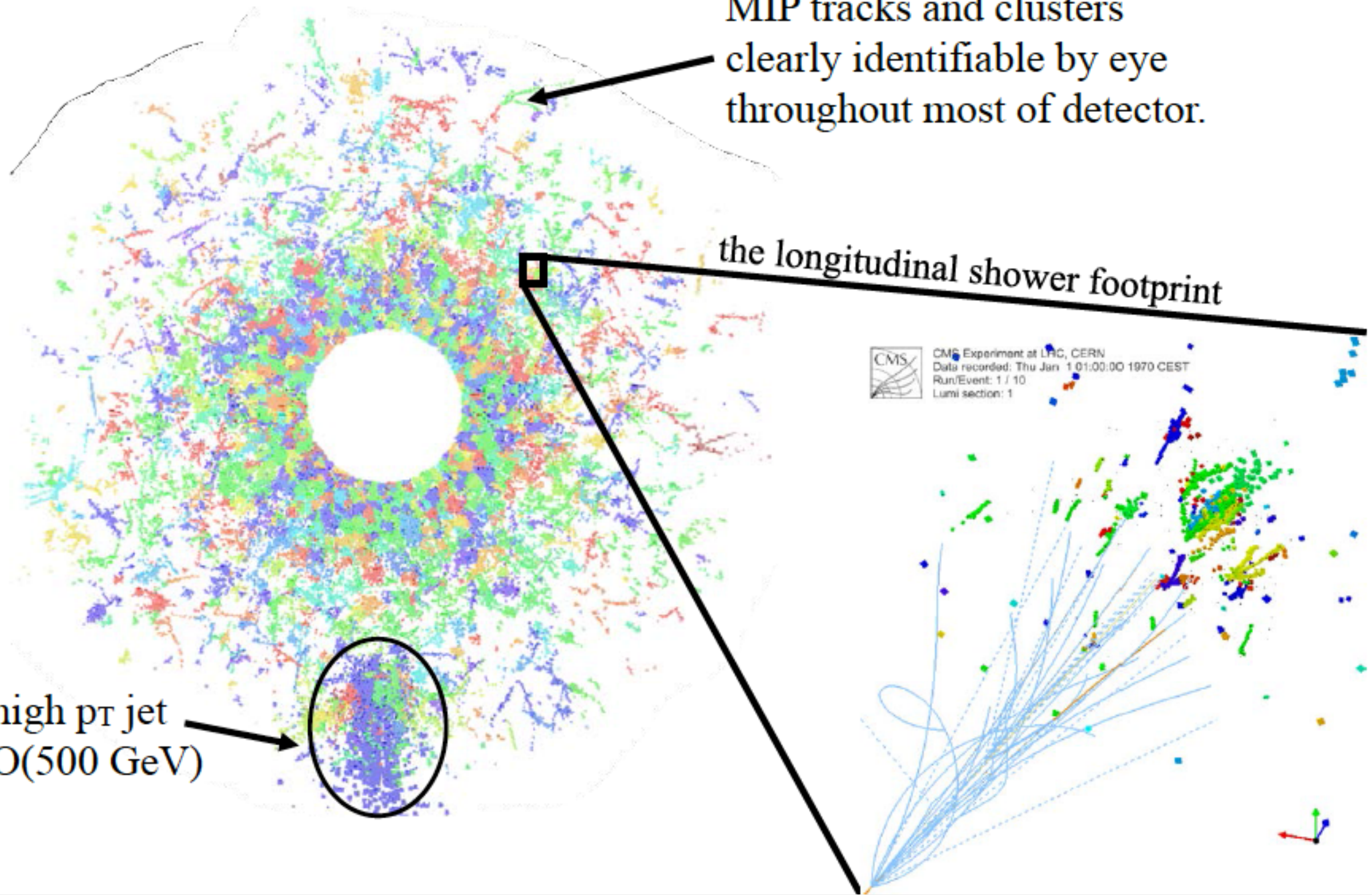
Imaging Showers with the HGCD

MIP tracks and clusters
clearly identifiable by eye
throughout most of detector.

the longitudinal shower footprint

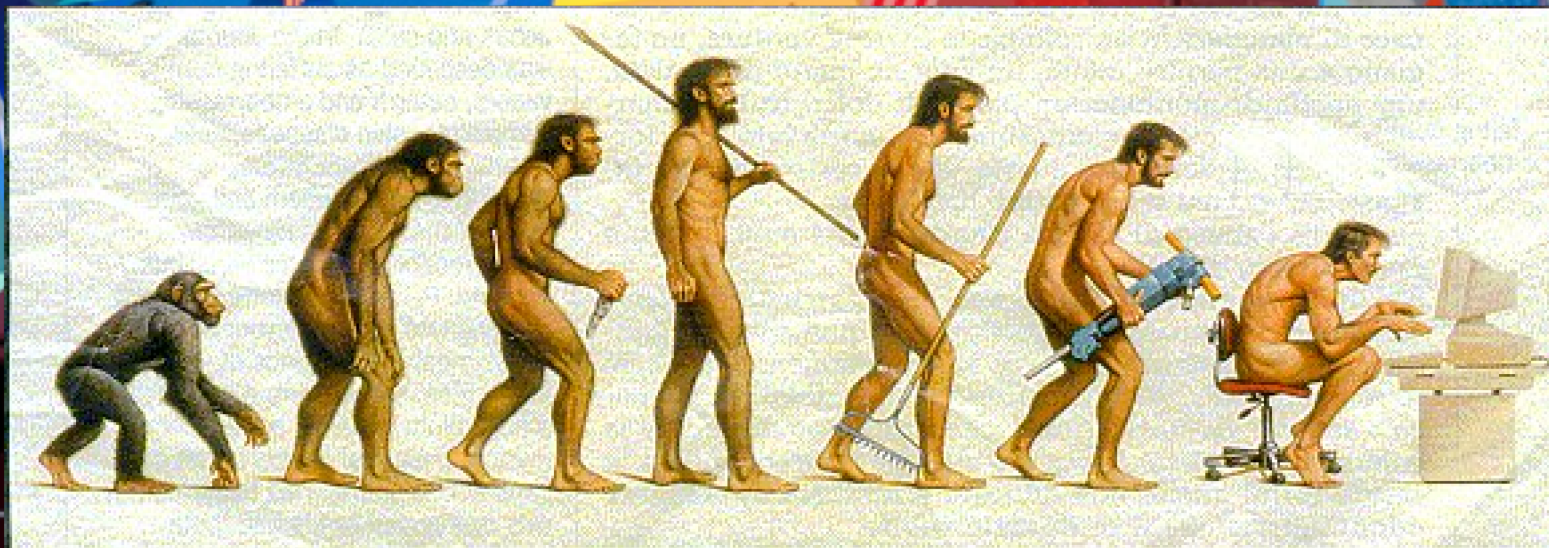
high pT jet
O(500 GeV)

CMS
CMS Experiment at LHC, CERN
Data recorded: Thu Jan 1 01:00:00 1970 CEST
Run/Event: 1 / 10
Lumi section: 1



- Detection of particle is based on quite simple mechanisms, most of them are very well known and simulated.
- Detectors R&D is a very rich domain in continuous evolution.
- Conception of an experiment is always a difficult enterprise : the best technology can be spoiled by the environment where it is used. One should define it with respect to the physics goals.
- This can take quite some time : ATLAS/CMS :
 - R&D started in 1990,
 - experiment general concept and approval (1994),
 - start of construction ~1998,
 - integration in pit from 2004, commissioned in 2008 and now operational.....
- Understanding the detector response correctly is an **absolutely needed step** before claiming any physics results !!!
- *Missing in my lecture : Photon detectors, scintillators, Cherenkov light detector (see in my Backup slides)*

Computing behind this all...



Somewhere, something went terribly wrong

Materials based upon:

This presentation is widely based on:

C. Joram, Particle detectors : principles and techniques, Part 4, Calorimetry, CERN Academic training lectures 2005, <http://indico.cern.ch/conferenceDisplay.py?confId=a042932>

J. Crittenden, Calorimetry in High-Energy Elementary-Particle Physics, Joint Dutch Belgian German Graduate School, Bad Honnef, 8-9 September 2006,

R. Wigmans, LHC luminosity upgrade: detector challenges (3/5), CERN Academic training programme 2006, <http://indico.cern.ch/conferenceDisplay.py?confId=a056410>

Bibliography

R. Wigmans, *Energy Measurement in Particle Physics (2000)*

**P.B. Cushman, *Electromagnetic and Hadronic Calorimeters,*
*in Instrumentation in High Energy Physics, ed. F.Sauli (1992)***

**C. Fabjan, *Calorimetry in High-Energy Physics,*
*in Experimental Techniques in High-Energy Physics, ed. T.Ferbel (1987)***

**U. Amaldi, *Calorimetry in High-Energy Physics,*
*in Experimental Techniques in High-Energy Physics, ed. T.Ferbel (1987)***

R. Fernow, *Introduction to Experimental Particle Physics (1986)*

C. Grupen, *Particle Detectors (1996)*

- Q1

Silicon detectors

→ Position resolution: $\sim 5 \mu\text{m}$

Gaseous detectors

→ Position resolution: $\sim 50 \mu\text{m}$

Calorimeters

→ Position resolution: few mm

Why (and whether) moderate position resolution of calorimeter can be used ?

Q2

What can be the problems for a) very low, b) very high shower energy measurement ?

Q3

Which background can you imagine to fake a muon reconstructed in a muon detector ?

Q1

Which part of the ECAL will degrade more from the irradiation in the experiment ?

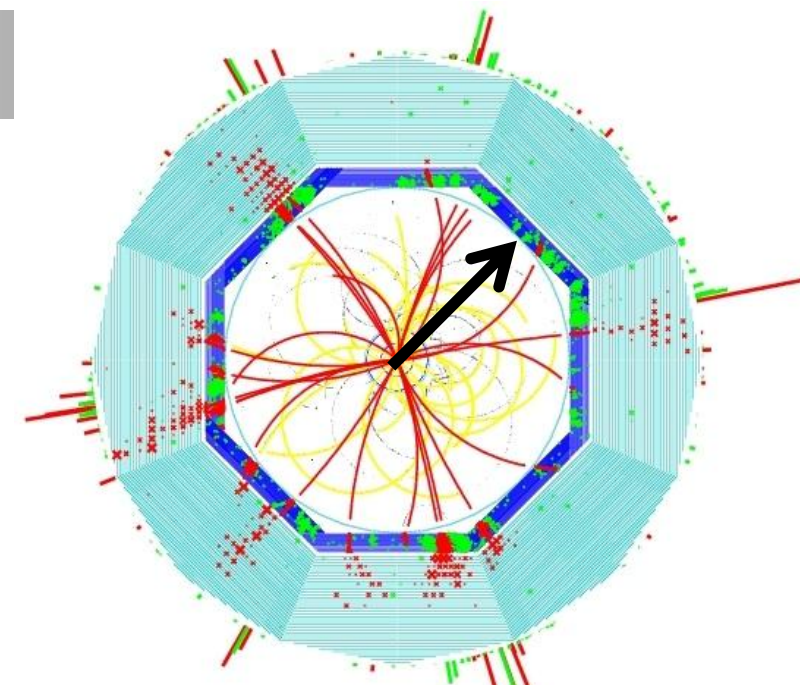
Q2

Reminder : EM Calorimeters: MANY (15-30) λ_0 deep
 H Calorimeters: many (5-8) λ_I deep

Why full shower containment is not always required ?

Q3

In order for the Particle Flow Analysis to perform better, would you position your calorimeter at a) 3m or b) 10m from the interaction point ? Resolution/granularity stays the same.



Backup

- ◆ *Photon Detection* [MORE](#)
- ◆ *Scintillators - General Characteristics* [MORE](#)
- ◆ *Energy loss by electron and photons* [MORE](#)
- ◆ *Interaction of charged particles:*
 - Multiple Scattering* [MORE](#)
 - Position resolution of EM shower* [MORE](#)
- ◆ *Nuclear Interactions* [MORE](#)
- ◆ *Hadronic Showers* [MORE](#)
- ◆ *Energy resolution* [MORE](#)
- ◆ *Particle Flow Calorimeter* [MORE](#)
- ◆ *CMS ECAL* [MORE](#)
- ◆ *Why HGCAL?* [MORE](#)
- ◆ *HGCAL Mechanical Design* [MORE](#)

Purpose : Convert light into a detectable electronic signal

Principle : Use **photo-electric effect** to convert photons to **photo-electrons (p.e.)**

Requirement :

High **Photon Detection Efficiency (PDE)** or **Quantum Efficiency**; $Q.E. = N_{p.e.}/N_{photons}$

TO BACKUP

Available devices [Examples]:

Photomultipliers [PMT]

Micro Channel Plates [MCP]

Photo Diodes [PD]

HybridPhoto Diodes [HPD]

Visible Light Photon Counters [VLPC]

Silicon Photomultipliers [SiPM]

Photomultipliers

Principle:

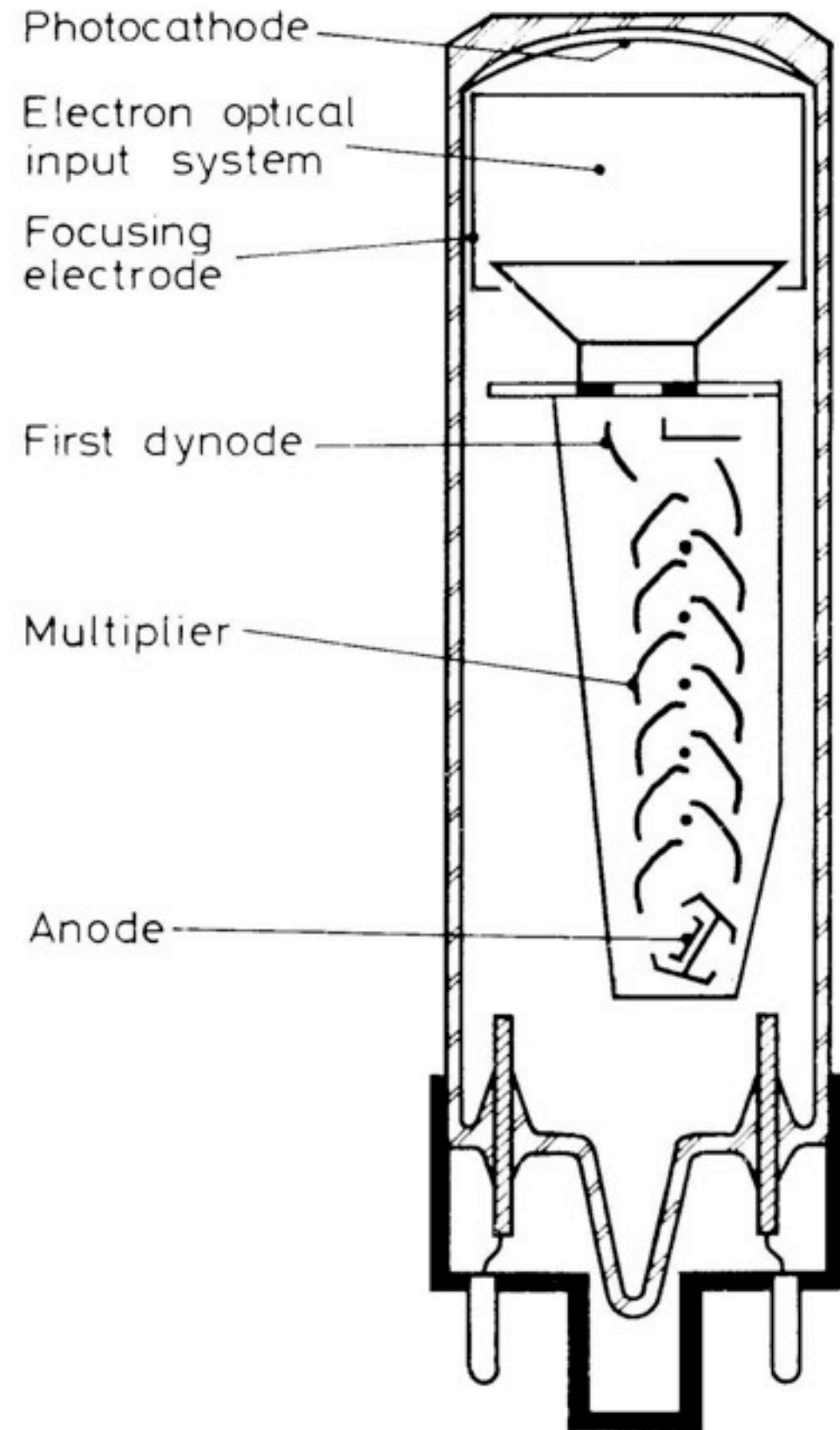
Electron emission
from photo cathode

Secondary emission
from dynodes; dynode gain: 3-50 [f(E)]

Typical PMT Gain: $> 10^6$
[PMT can see single photons ...]



PMT
Collection



Principle:

dE/dx converted into visible light

Detection via photosensor

[e.g. photomultiplier, human eye ...]

Main Features:

Sensitivity to energy

Fast time response

Pulse shape discrimination

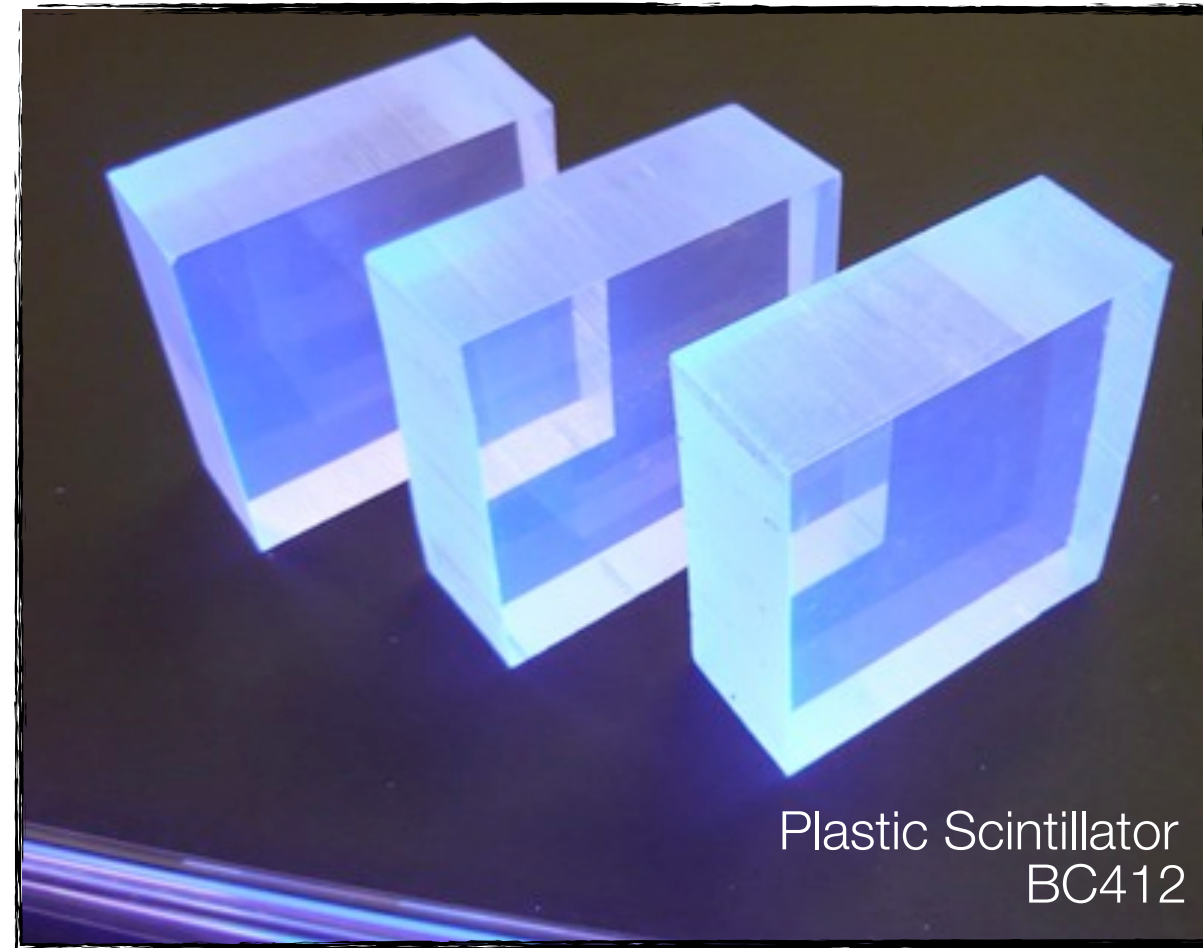
Requirements

High efficiency for conversion of excitation energy to fluorescent radiation

Transparency to its fluorescent radiation to allow transmission of light

Emission of light in a spectral range detectable for photosensors

Short decay time to allow fast response



Materials:

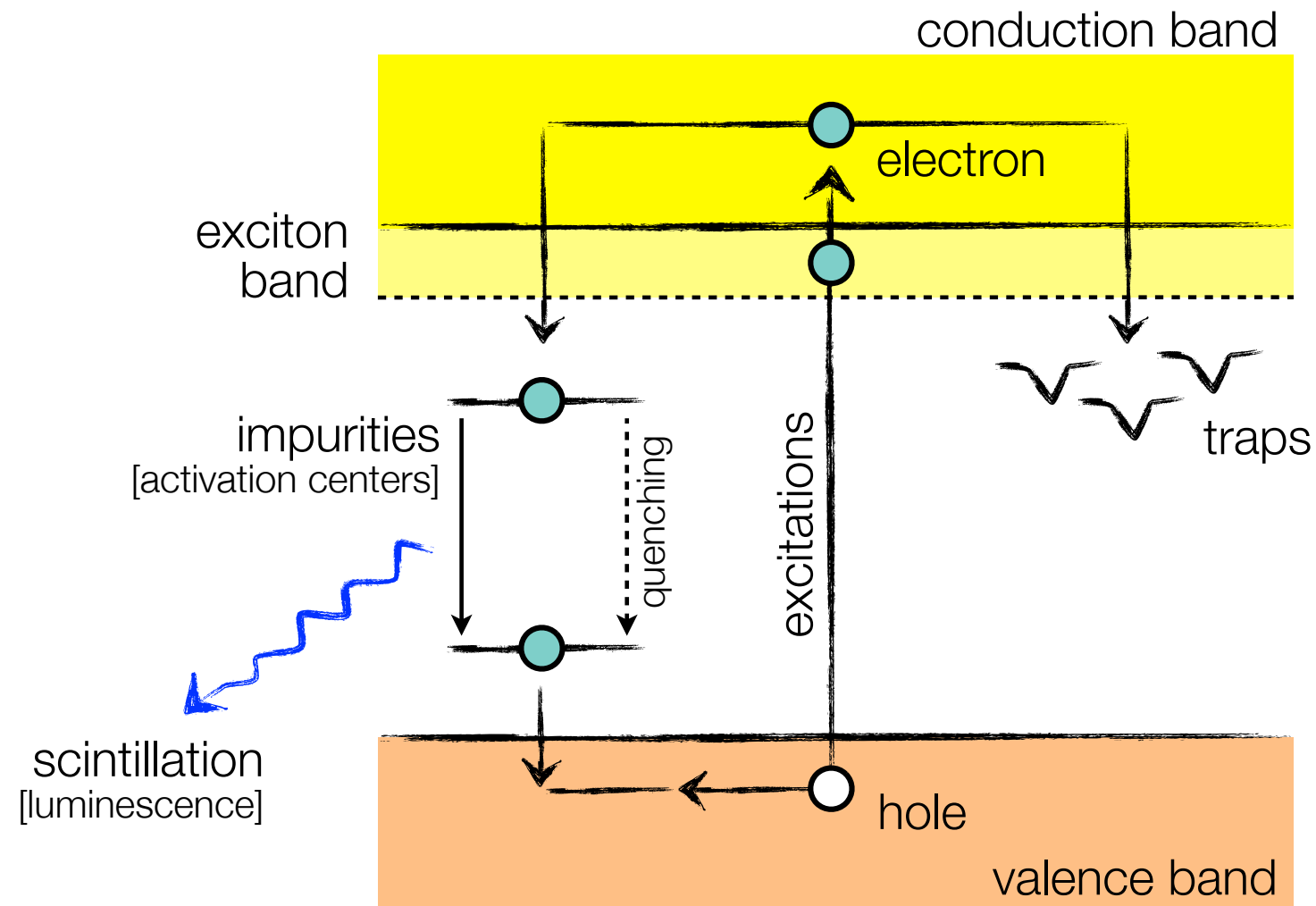
- Sodium iodide (NaI)
- Cesium iodide (CsI)
- Barium fluoride (BaF₂)
- ...

Mechanism:

- Energy deposition by ionization
- Energy transfer to impurities
- Radiation of scintillation photons

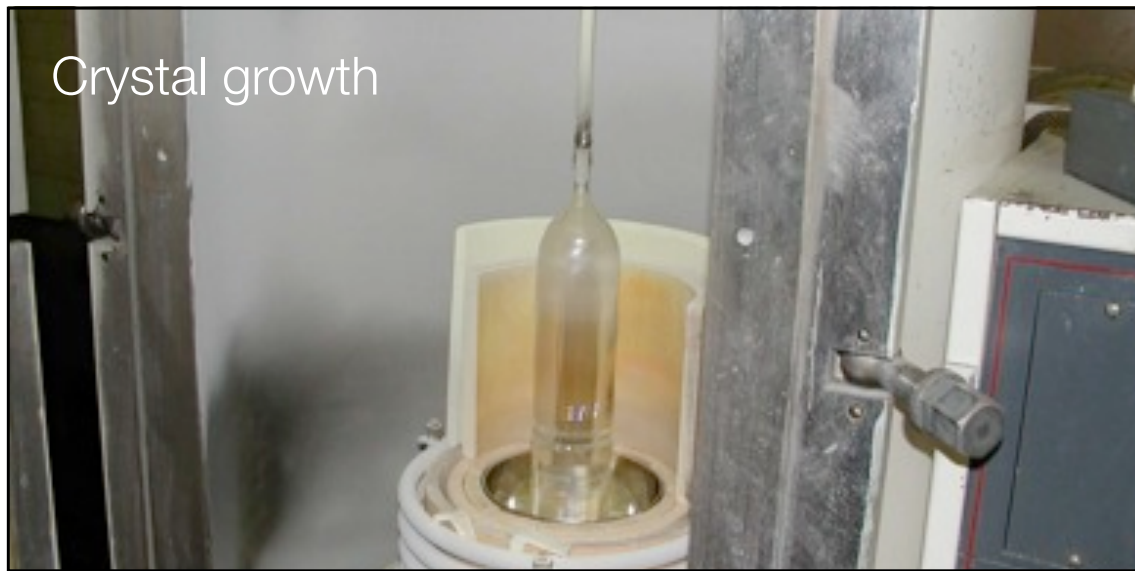
Time constants:

- Fast: recombination from activation centers [ns ... μs]
- Slow: recombination due to trapping [ms ... s]



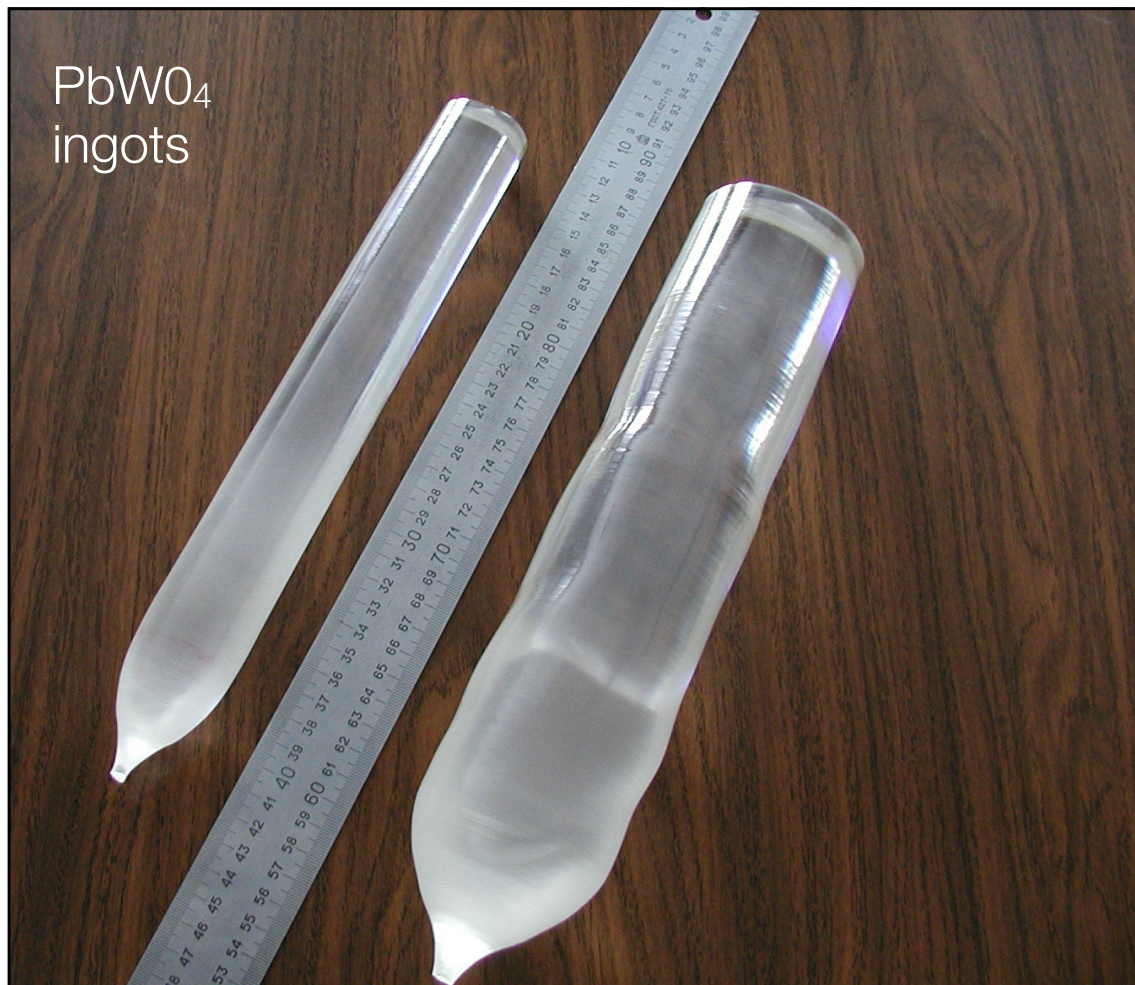
Energy bands in impurity activated crystal showing excitation, luminescence, quenching and trapping

Crystal growth

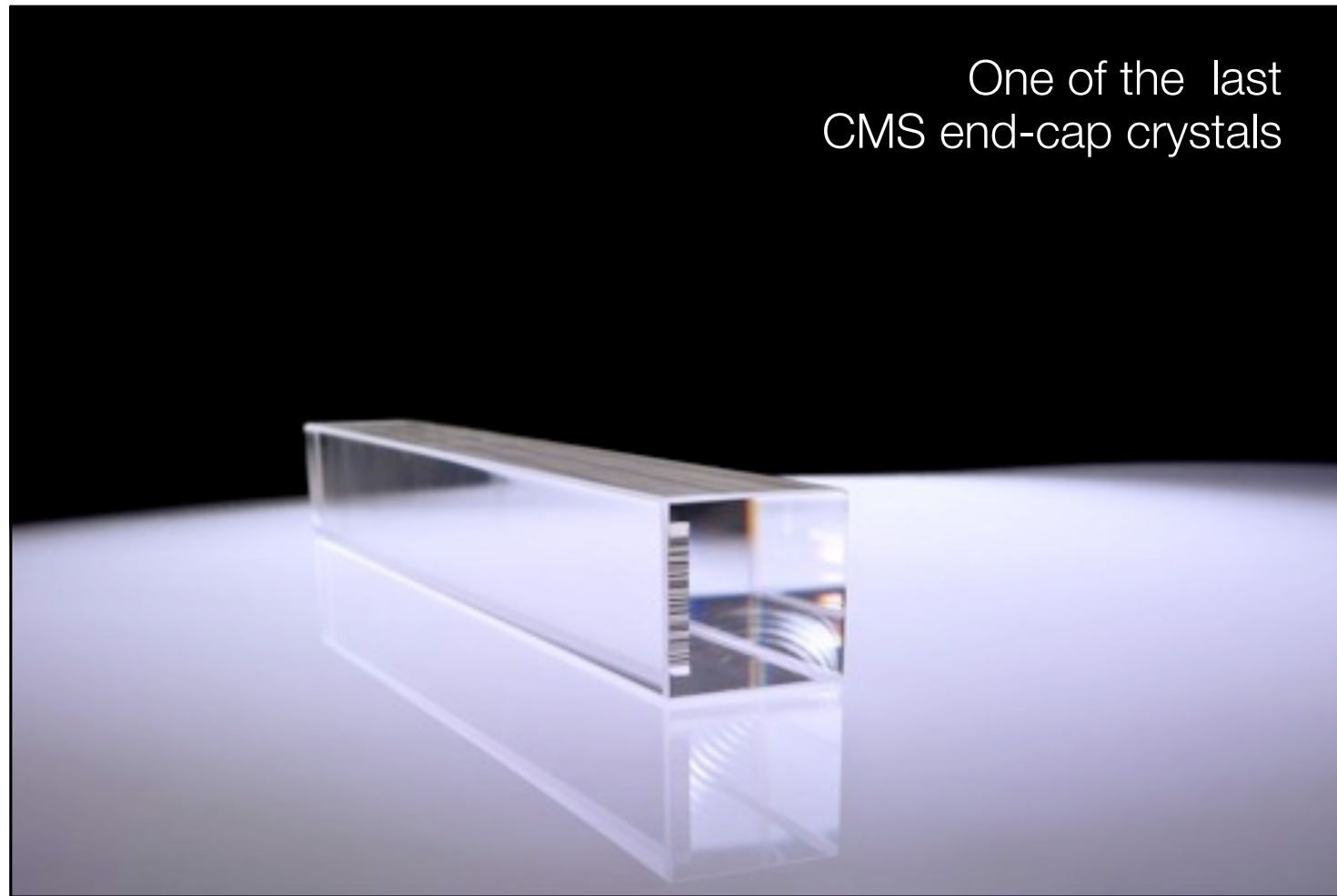


Example CMS
Electromagnetic Calorimeter

PbWO_4
ingots

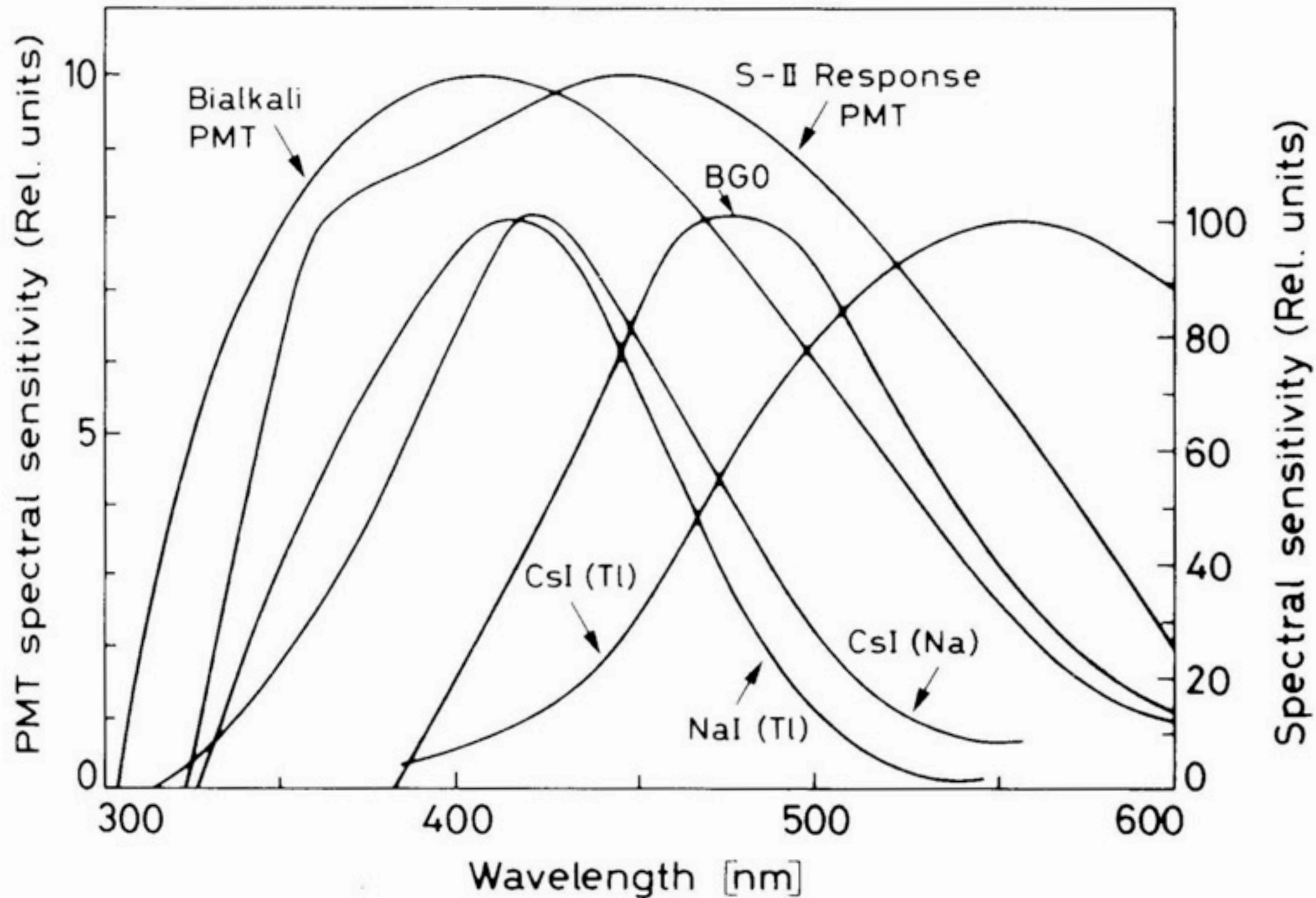


One of the last
CMS end-cap crystals



Light Output and PMT Sensitivity

Spectral sensitivity



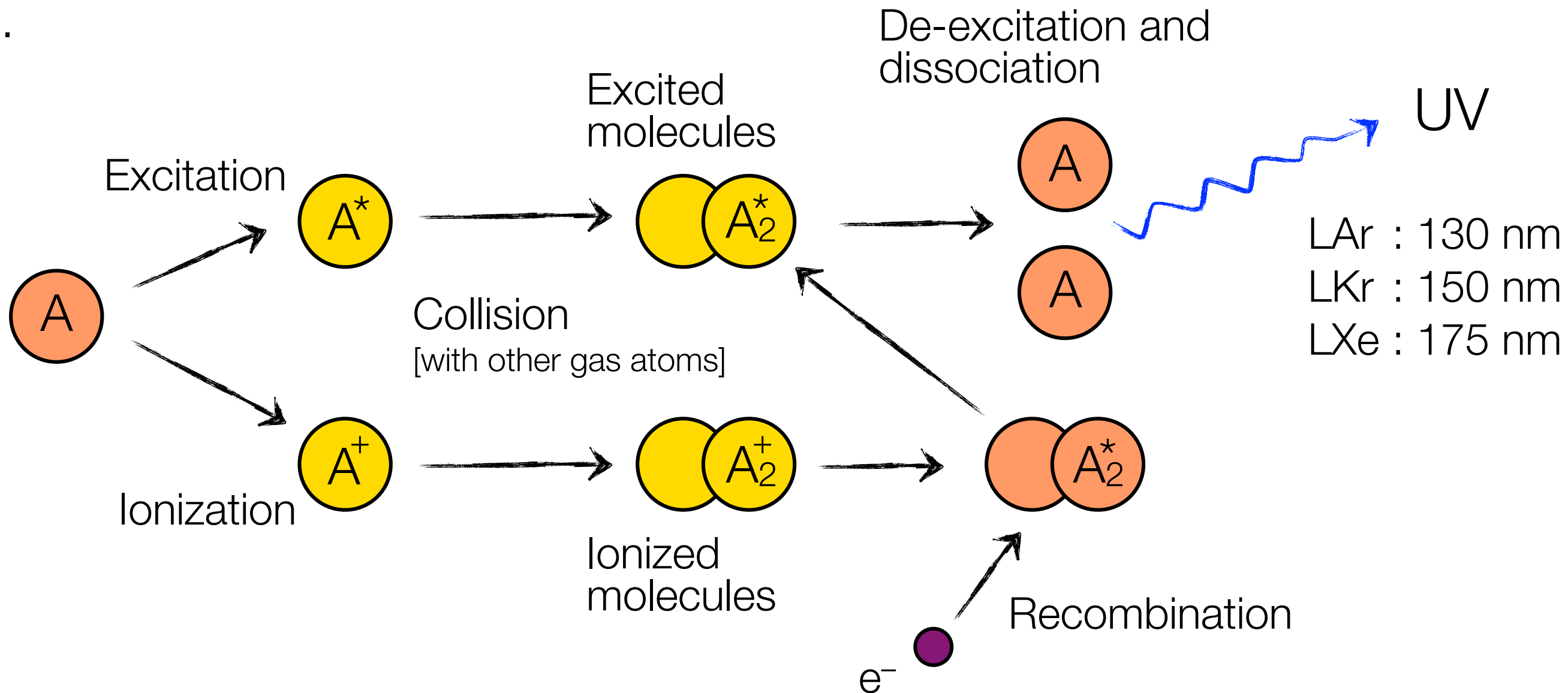
Materials:

- Helium (He)
- Liquid Argon (LAr)
- Liquid Xenon (LXe)
- ...

Decay time constants:

Helium : $\tau_1 = .02 \mu\text{s}$, $\tau_2 = 3 \mu\text{s}$

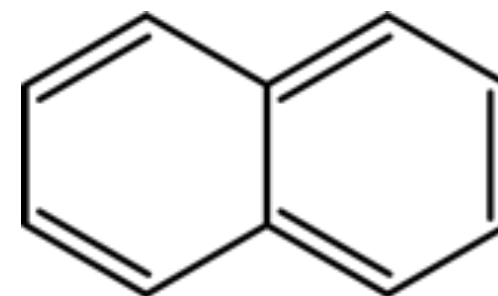
Argon : $\tau_1 \leq .02 \mu\text{s}$



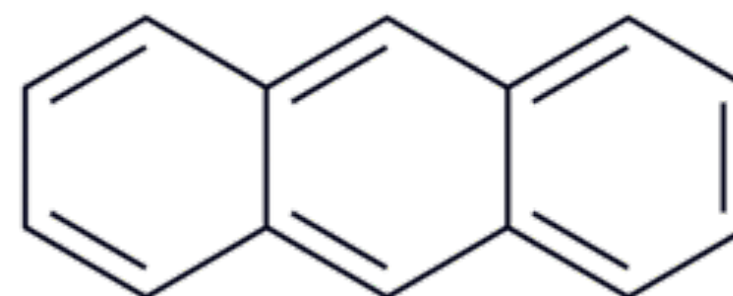
Aromatic hydrocarbon compounds:

e.g. Naphthalene [C₁₀H₈]
 Anthracene [C₁₄H₁₀]
 Stilbene [C₁₄H₁₂]
 ...

Naphthalene



Anthracene

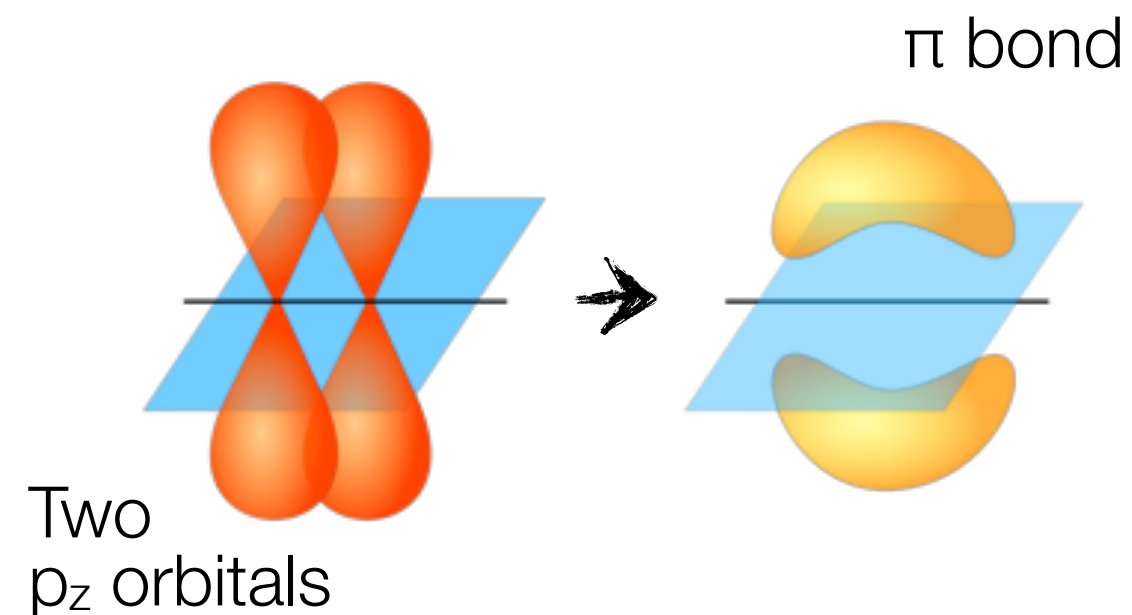


Very fast!
 [Decay times of O(ns)]

Scintillation light arises from delocalized electrons in π -orbitals ...

Transitions of 'free' electrons ...

Scintillation is based on electrons of the C=C bond ...



Inorganic Scintillators

Advantages

high light yield [typical; $\epsilon_{sc} \approx 0.13$]
high density [e.g. $PBWO_4$: 8.3 g/cm^3]
good energy resolution

Disadvantages

complicated crystal growth
large temperature dependence

Expensive

Organic Scintillators

Advantages

very fast
easily shaped
small temperature dependence
pulse shape discrimination possible

Disadvantages

lower light yield [typical; $\epsilon_{sc} \approx 0.03$]
radiation damage

Cheap

Scintillator light to be guided to photosensor

→ Light guide
[Plexiglas; optical fibers]

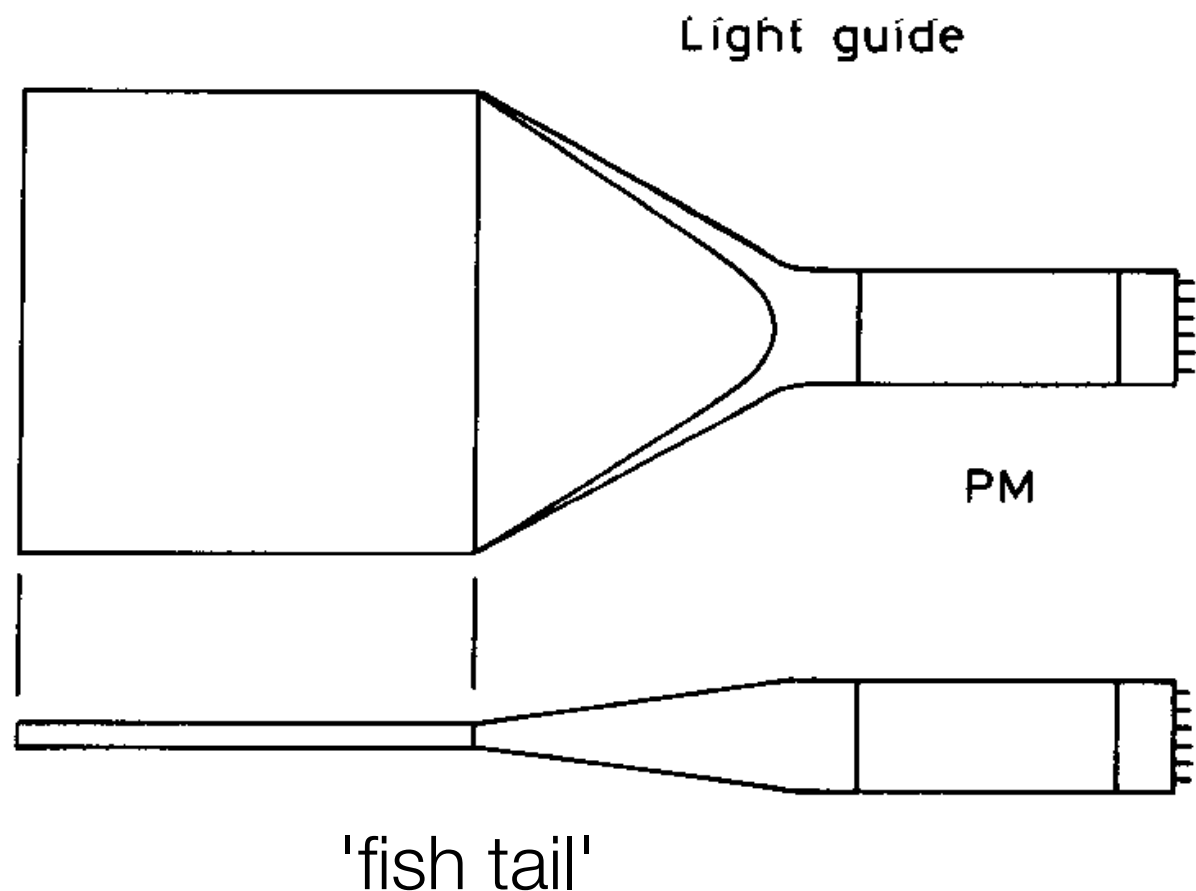
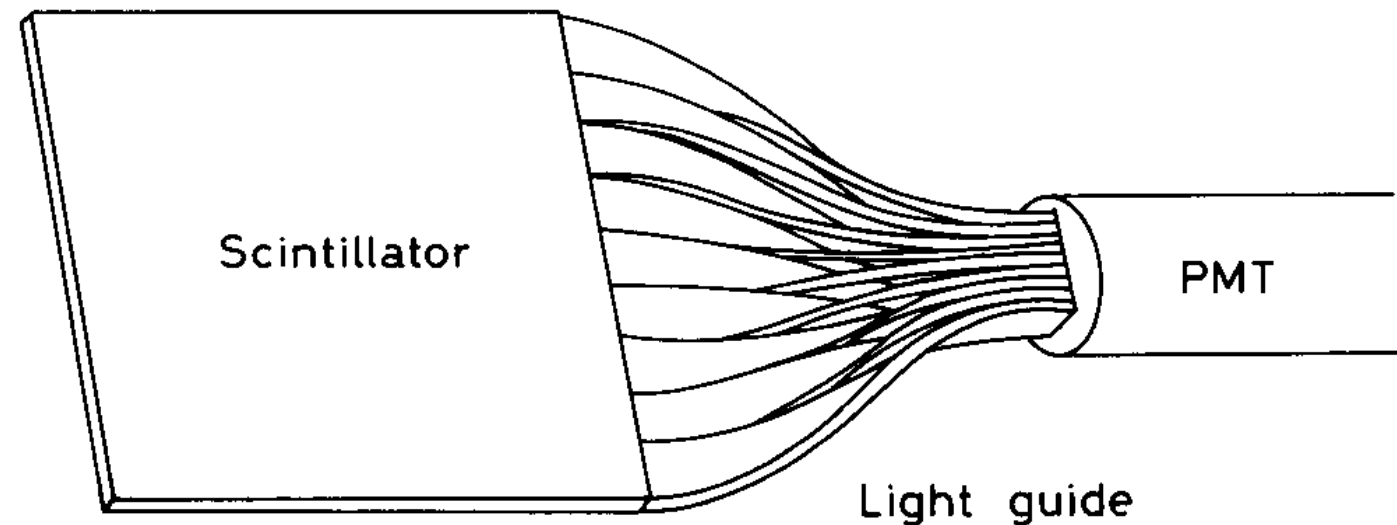
Light transfer by total internal reflection
[maybe combined with wavelength shifting]

Liouville's Theorem:

Complete light transfer impossible as $\Delta x \Delta \theta = \text{const.}$
[limits acceptance angle]

Use adiabatic light guide like 'fish tail';

→ appreciable energy loss



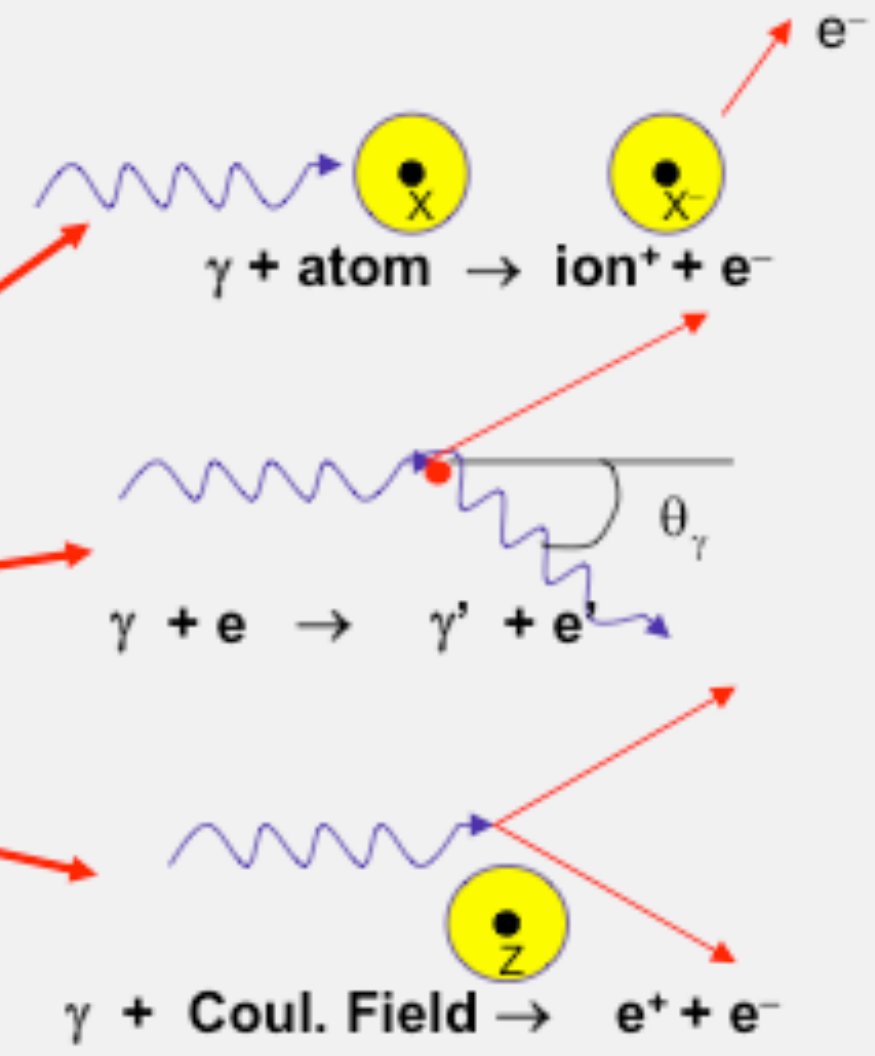
In matter electrons and photons lose energy interacting with nuclei and atomic electrons

Electrons

- ionization (atomic electrons)
- bremsstrahlung (nuclear)

Photons

- photoelectric effect (atomic electrons)
- Compton scattering (atomic electrons)
- pair production (nuclear)



Above 1 GeV radiative processes dominate energy loss by e/ γ



Reminder: basic electromagnetic interactions

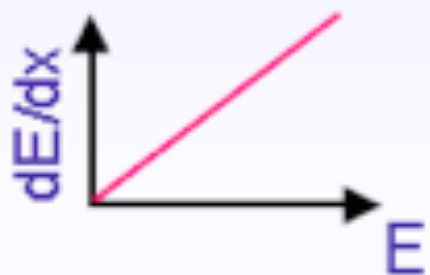


e^+ / e^-

■ Ionisation



■ Bremsstrahlung

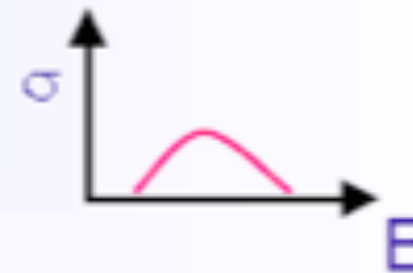


γ

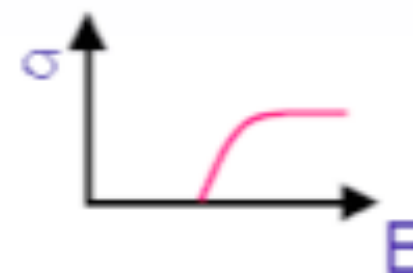
■ Photoelectric effect



■ Compton effect



■ Pair production



• Ionization

$$-\frac{dE}{dx}|_{ion} = N_A \frac{Z}{A} \frac{4\pi\alpha^2(\hbar c)^2}{m_e c^2} \frac{Z_i^2}{\beta^2} \left[\ln \frac{2m_e c^2 \gamma^2 \beta^2}{I} - \beta^2 - \frac{\delta}{2} \right]$$

➤ $\sigma \propto Z$; $\sigma \propto \ln E/m_e$

• Bremsstrahlung

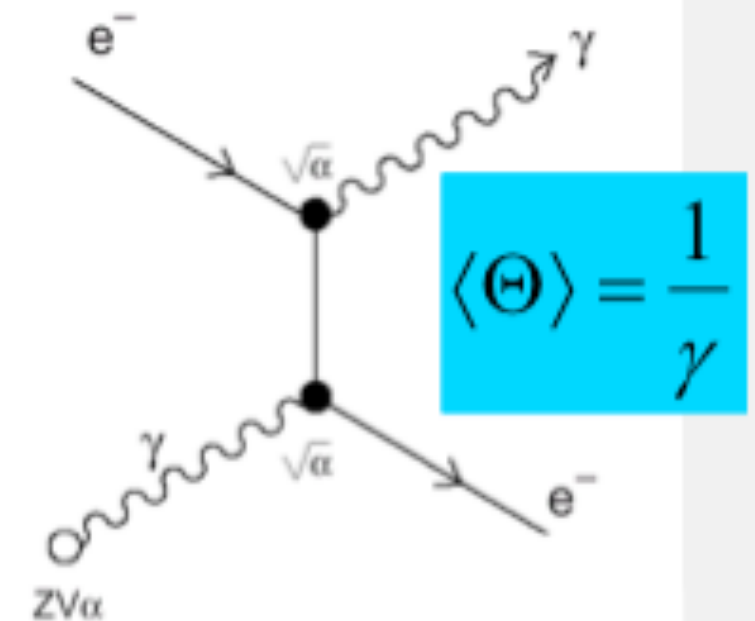
$$-\frac{dE}{dx}|_{rad} = \left[4n \frac{Z^2 \alpha^3 (\hbar c)^2}{m_e^2 c^4} \ln \frac{183}{Z^{1/3}} \right] E$$

$$-\frac{dE}{dx} \propto \frac{Z^2 E}{m^2}$$

$$X_0 = \left[4n \frac{Z^2 \alpha^3 (\hbar c)^2}{m_e^2 c^4} \ln \frac{183}{Z^{1/3}} \right]^{-1}$$

$$\frac{dE}{dx} = - \frac{E}{X_0}$$

$$X_0 \approx \frac{180 A}{Z^2} \text{ g.cm}^{-2}$$



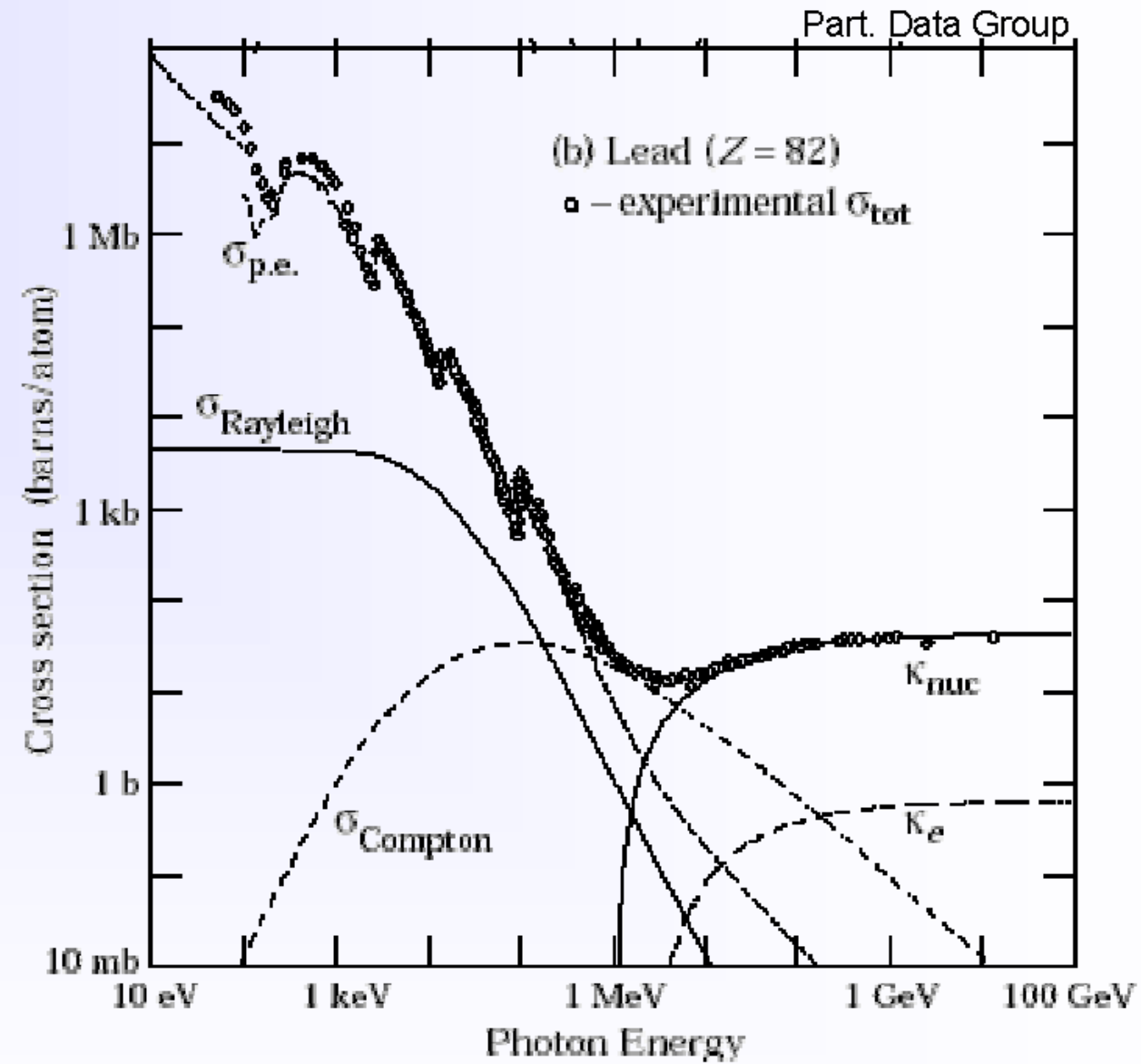
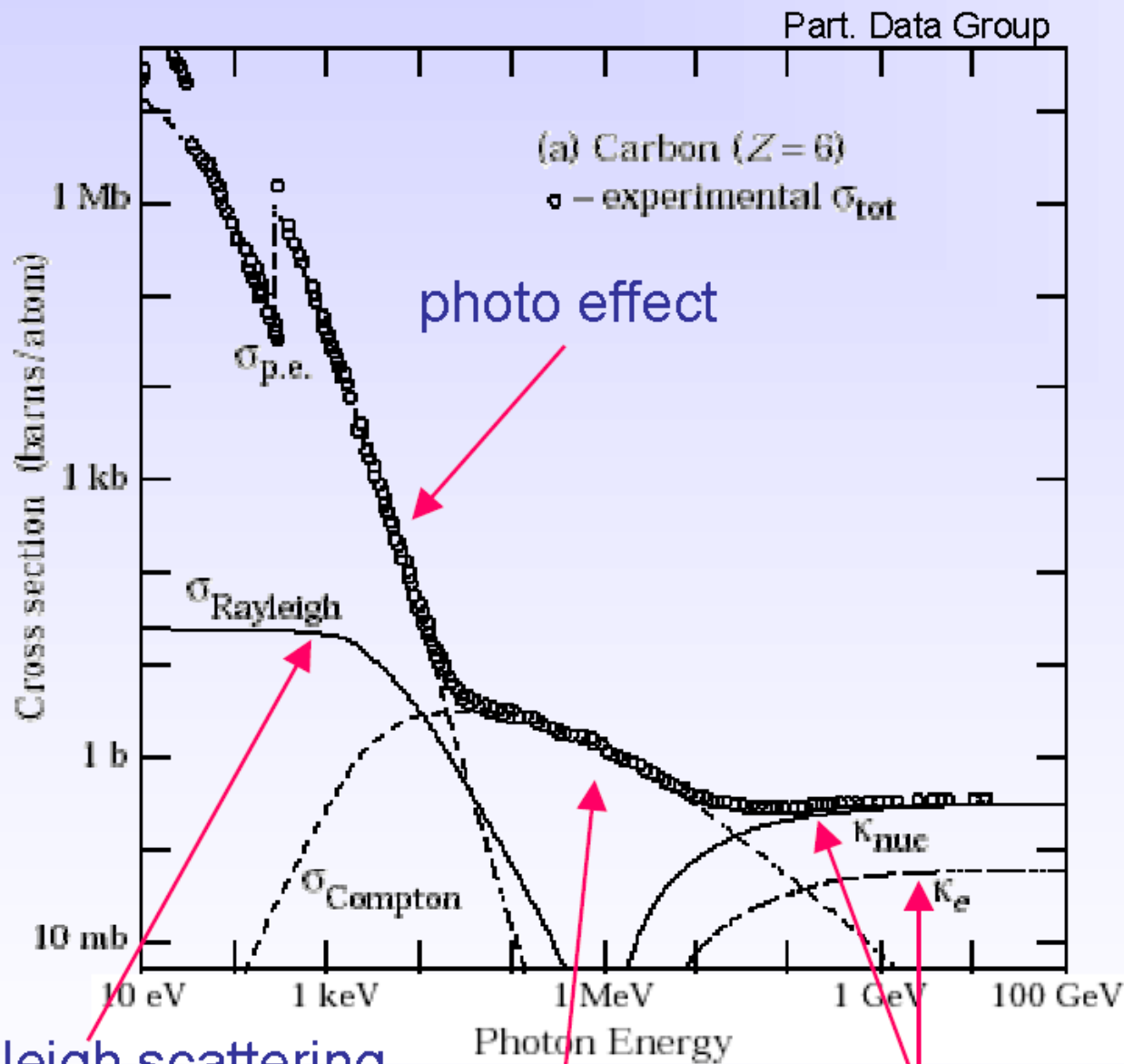
$$\langle \Theta \rangle = \frac{1}{\gamma}$$

➤ $\sigma \propto Z(Z+1)$; $\sigma \propto A/X_0$ $E > 1 \text{ GeV}$, $\sigma \propto \ln E/m_e$ $E < 1 \text{ GeV}$

Radiation length: thickness of material that reduces the mean energy of a beam of high energy electrons by a factor e. For dense materials $X_0 \sim 1 \text{ cm}$.

In summary: $I_\gamma = I_0 e^{-\mu x}$

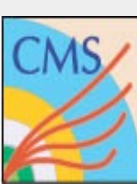
μ : mass attenuation coefficient $\mu_i = \frac{N_A}{A} \sigma_i \quad [cm^2 / g] \quad \mu = \mu_{photo} + \mu_{Compton} + \mu_{pair} + \dots$



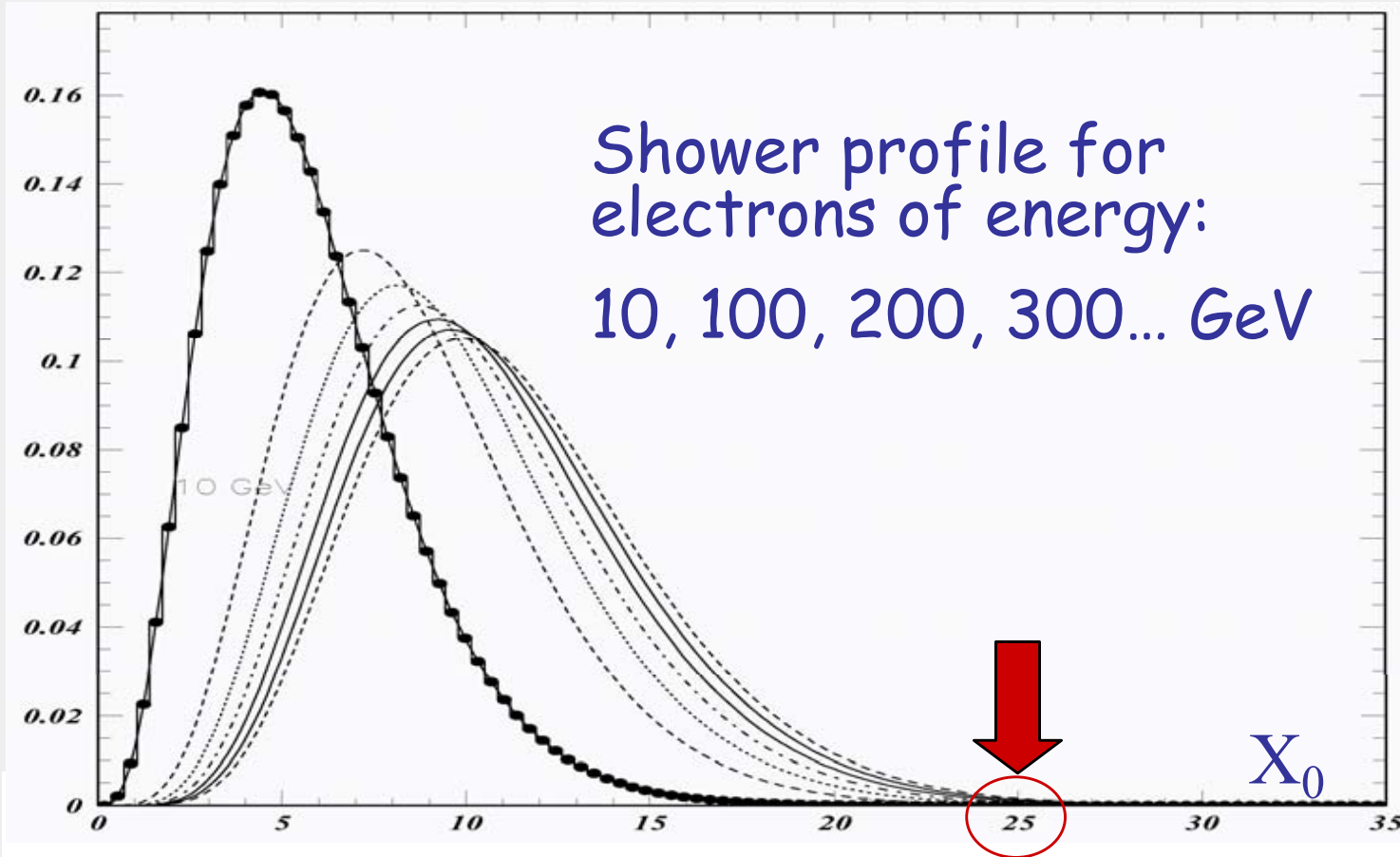
Rayleigh scattering
(no energy loss !)

Compton scattering

pair production



EM showers: longitudinal profile



Shower energy dep parametrization:

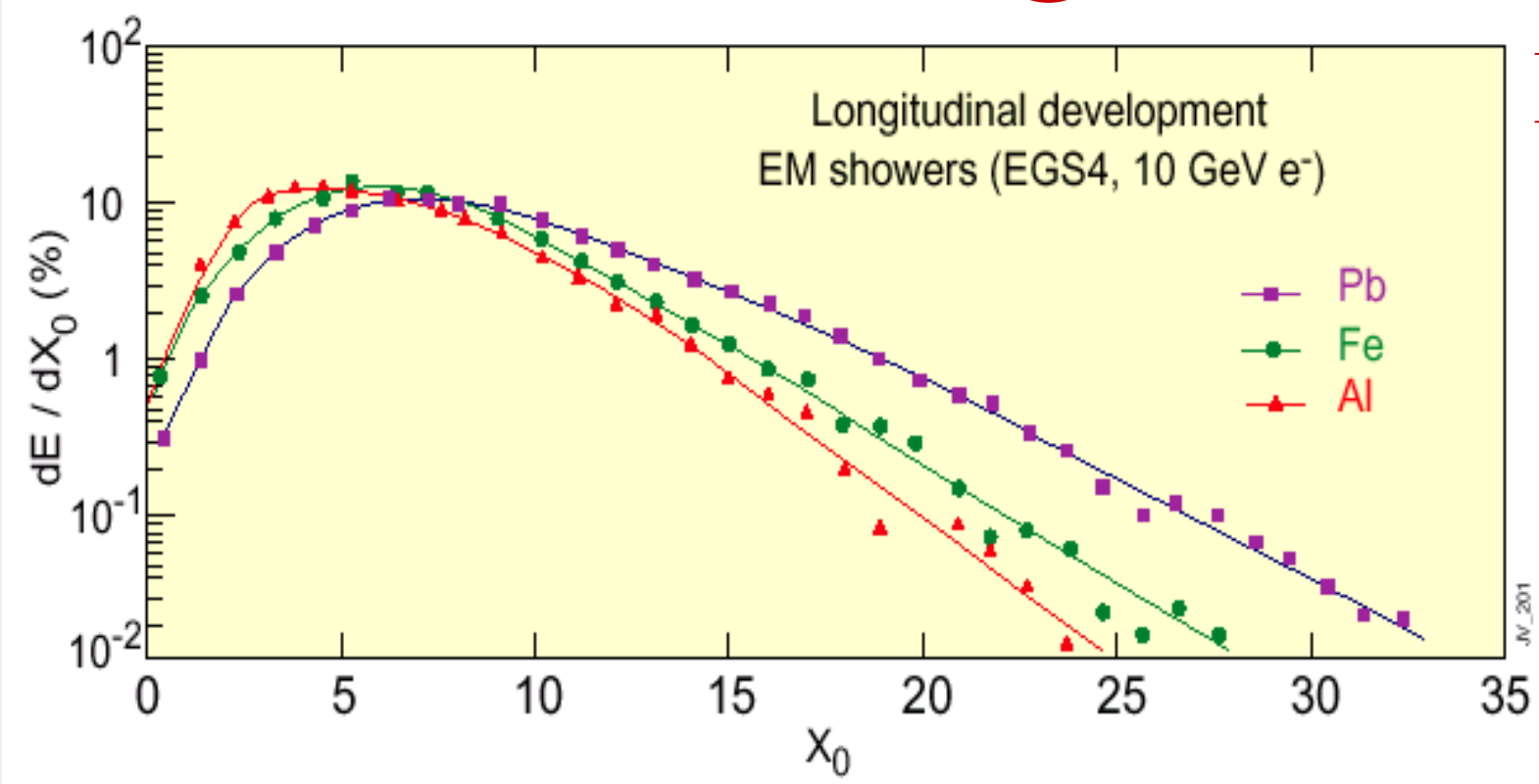
$$\frac{dE}{dt} \propto E_0 t^\alpha e^{\beta t}$$

E.Longo & I.Sestili
NIM 128 (1975)

β material dependent

$$t_{\max} = 1.4 \ln(E_0/E_c)$$

$$N_{\text{tot}} \propto E_0/E_c$$



$E_c \propto 1/Z$ \rightarrow

- shower max
- shower tail

Longitudinal containment:

$$t_{95\%} = t_{\max} + 0.08Z + 9.6$$



EM showers: transverse profile

Transverse shower profile

- Multiple scattering make electrons move away from shower axis
- Photons with energies in the region of minimal absorption can travel far away from shower axis

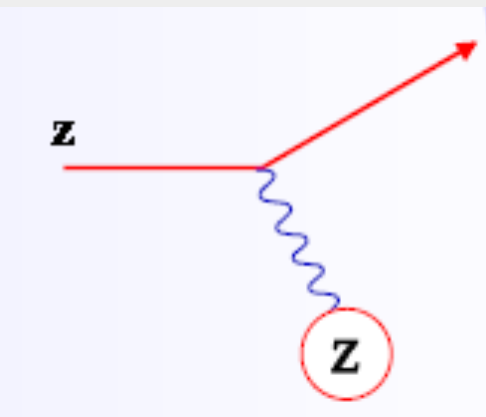
Molière radius sets transverse shower size, it gives the average lateral deflection of critical energy electrons after traversing $1X_0$

$$R_M = \frac{21\text{MeV}}{E_C} X_0$$

$$R_M \propto \frac{X_0}{E_C} \propto \frac{A}{Z} (Z \gg 1)$$

90% E_0 within $1R_M$, 95% within $2R_M$, 99% within $3.5R_M$

- This process will turn out to be closely related to the transverse profile of electromagnetic showers.
- Coulomb-scattering scales with the squared charges, so scattering in matter is dominated by scattering off nuclei (rather than off electrons), for $Z > 10$. Scattering of spin 0 (Rutherford) and spin 1/2 (Mott) particles are identical in a small-angle approximation.
- Result can be defined in terms of radiation length X_0 , to be defined later.



In a sufficiently thick material layer a particle will undergo ...

Multiple Scattering

$$\theta_0 = \theta_{plane}^{RMS} = \sqrt{\langle \theta_{plane}^2 \rangle}$$

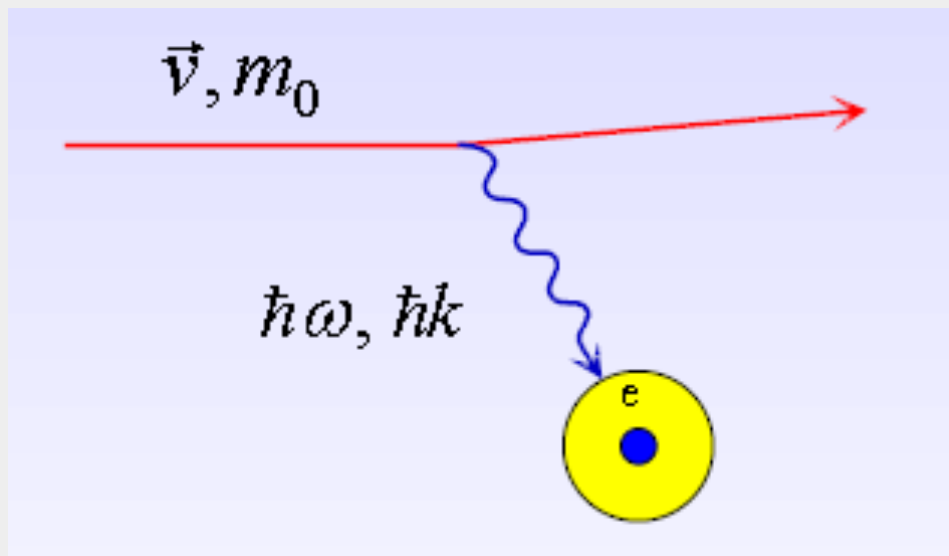
$$= \frac{1}{\sqrt{2}} \theta_{space}^{RMS}$$

Approximation $\theta_0 \propto \frac{1}{p} \sqrt{\frac{L}{X_0}}$ X_0 is radiation length of the medium (discuss later)

Detection of charged particles

Particles can only be detected if they deposit energy in matter.
How do they lose energy in matter ?

Discrete collisions with **the atomic electrons** of the absorber material.



$$\left\langle \frac{dE}{dx} \right\rangle = - \int_0^\infty N E \frac{d\sigma}{dE} \hbar d\omega$$

N : electron density

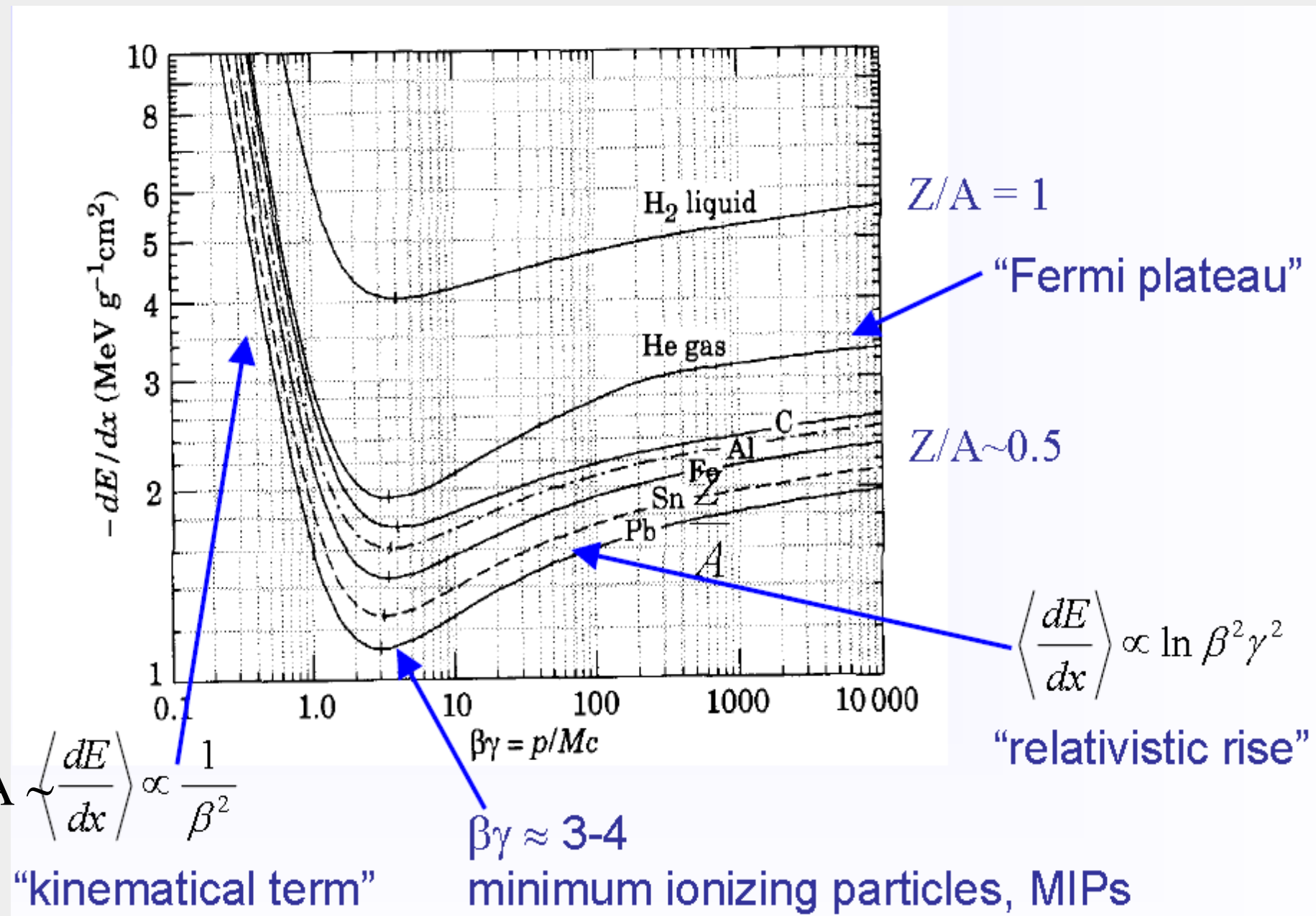
Collisions with nuclei not important ($m_e \ll m_N$) for energy loss.

If $\hbar\omega, \hbar k$ are in the right range \rightarrow **ionization**.

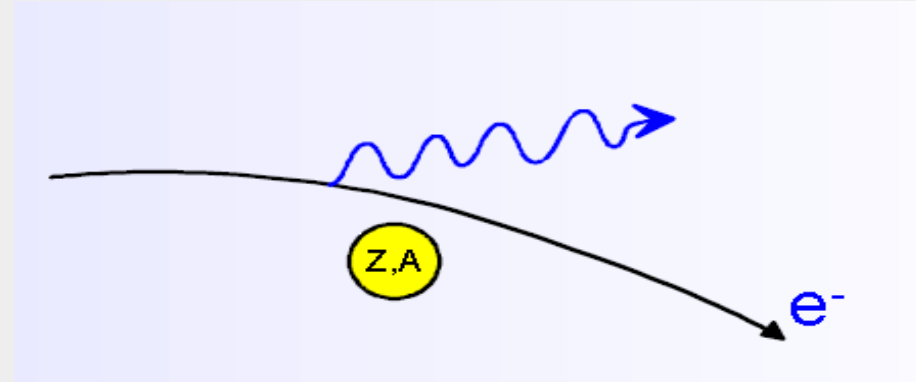
- Energy loss by ionization only: **Bethe-Bloch formula**

$$\left\langle \frac{dE}{dx} \right\rangle = -4\pi N_A r_e^2 m_e c^2 Z^2 \frac{Z}{A} \frac{1}{\beta^2} \left[\frac{1}{2} \ln \frac{2m_e c^2 \gamma^2 \beta^2}{I^2} T^{\max} - \beta^2 - \frac{\delta}{2} \right]$$

- dE/dx in $[\text{MeV g}^{-1} \text{cm}^2]$
- Valid for “heavy” particles ($m \geq m_\mu$).
- dE/dx depends only on β , independent of m !
- First approximation: medium simply characterized by Z/A electron density



- Energy loss by bremsstrahlung



Radiation of real photons in the Coulomb field

of the nuclei of the absorber medium:

$$-\frac{dE}{dx} = 4\alpha N_A \frac{Z^2}{A} z^2 \left(\frac{1}{4\pi\epsilon_0} \frac{e^2}{mc^2} \right)^2 E \ln \frac{183}{Z^{1/3}} \propto \frac{E}{m^2}$$

Effect plays a role only for e^\pm and ultra-relativistic μ (>1000 GeV)

For electrons:
$$-\frac{dE}{dx} = 4\alpha N_A \frac{Z^2}{A} r_e^2 E \ln \frac{183}{Z^{1/3}}$$

$$\boxed{-\frac{dE}{dx} = \frac{E}{X_0}} \quad \longrightarrow \quad E = E_0 e^{-x/X_0}$$

$$X_0 = \frac{A}{4\alpha N_A Z^2 r_e^2 \ln \frac{183}{Z^{1/3}}}$$

radiation length [g/cm²]

(divide by specific density to get X_0 in cm)

- Critical energy E_c

$$\left. \frac{dE}{dx}(E_c) \right|_{Brems} = \left. \frac{dE}{dx}(E_c) \right|_{ion}$$

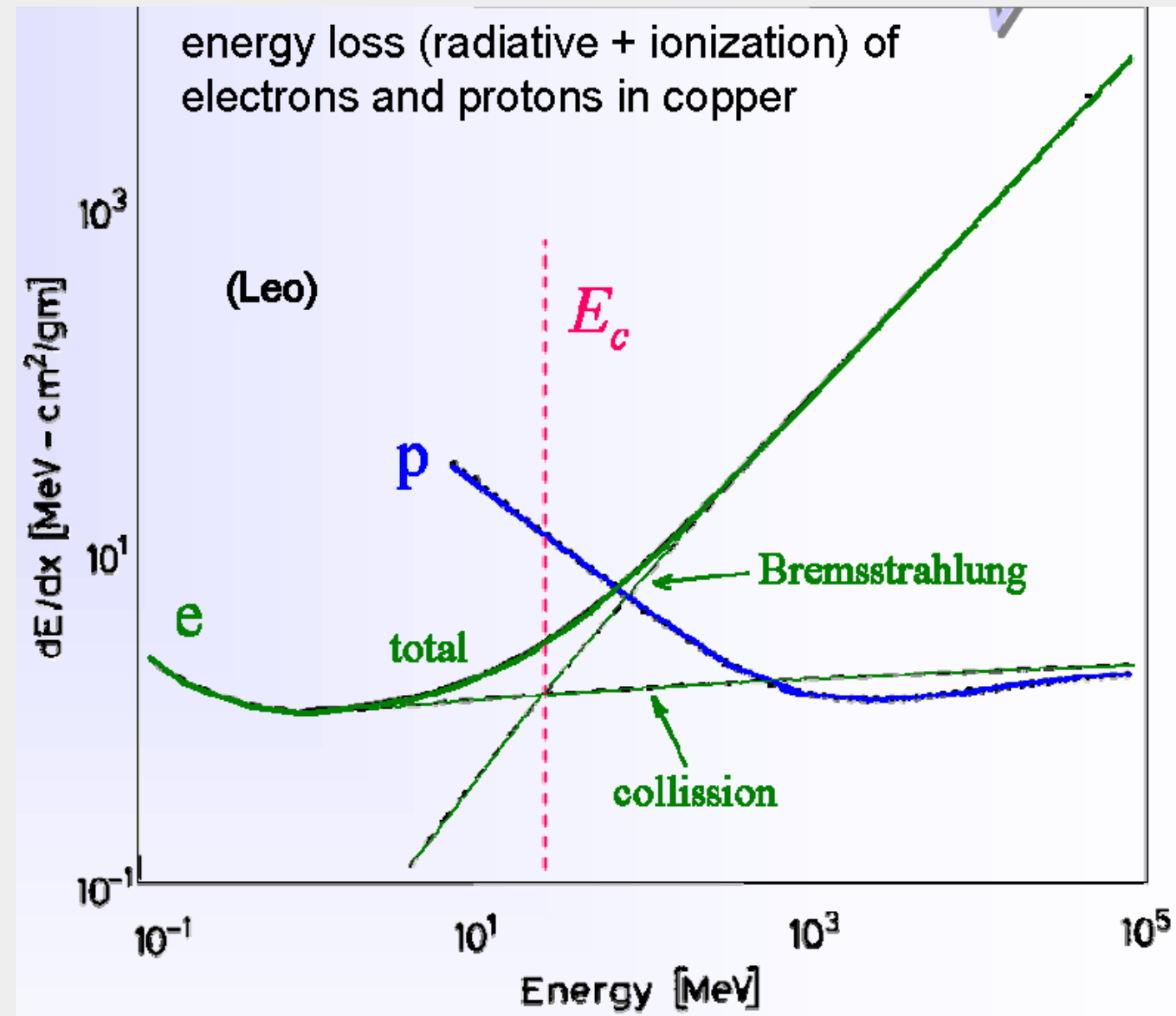
For electrons one finds approximately:

$$E_c^{solid+liq} = \frac{610MeV}{Z+1.24} \quad E_c^{gas} = \frac{710MeV}{Z+1.24}$$

$$E_c(e^-) \text{ in Cu}(Z=29) = 20 \text{ MeV}$$

$$\text{For muons } E_c \approx E_c^{elec} \left(\frac{m_\mu}{m_e} \right)^2$$

$$E_c(\mu) \text{ in Cu} \approx 1 \text{ TeV}$$



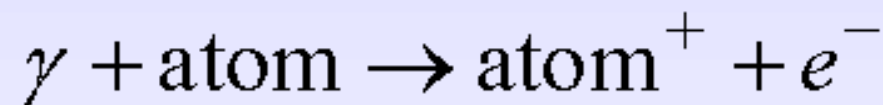
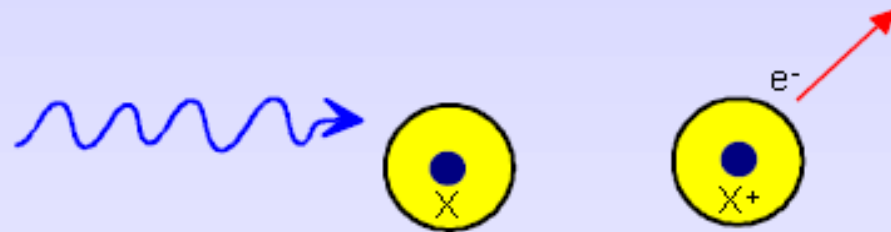
Unlike electrons, muons in multi-GeV range can traverse thick layers of dense matter.

Find charged particles traversing the calorimeter?

most likely a muon

In order to be detected, a photon has to create charged particles and/or transfer energy to charged particles

Photo-electric effect: (already met in photocathodes of photodetectors)



Only possible in the close neighborhood of a third collision partner \rightarrow photo effect releases mainly electrons from the K-shell.

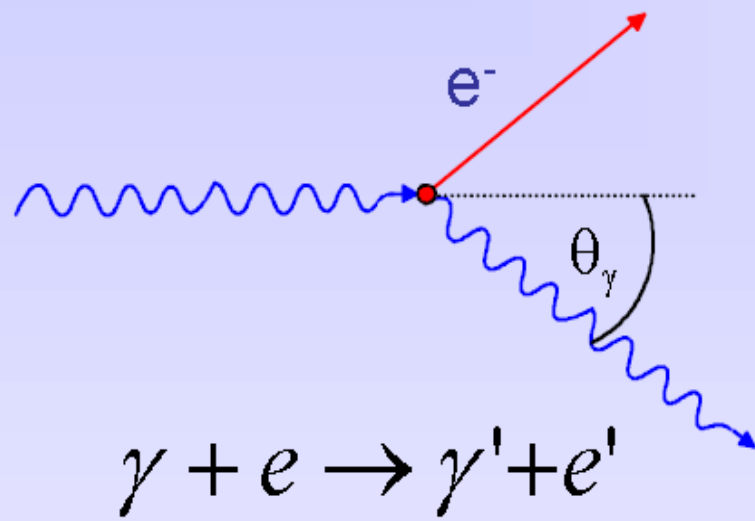
Cross section shows strong modulation if $E_\gamma \approx E_{shell}$

$$\sigma_{photo}^K = \left(\frac{32}{\epsilon^7}\right)^{\frac{1}{2}} \alpha^4 Z^5 \sigma_{Th}^e \quad \epsilon = \frac{E_\gamma}{m_e c^2} \quad \sigma_{Th}^e = \frac{8}{3} \pi r_e^2 \quad (\text{Thomson})$$

At high energies ($\epsilon \gg 1$)

$$\sigma_{photo}^K = 4\pi r_e^2 \alpha^4 Z^5 \frac{1}{\epsilon}$$

$$\sigma_{photo} \propto Z^5$$



$$E'_\gamma = E_\gamma \frac{1}{1 + \varepsilon(1 - \cos\theta_\gamma)}$$

$$E_e = E_\gamma - E'_\gamma$$

Assume electron as quasi-free.

Klein-Nishina $\frac{d\sigma}{d\Omega}(\theta, \varepsilon)$ \rightarrow

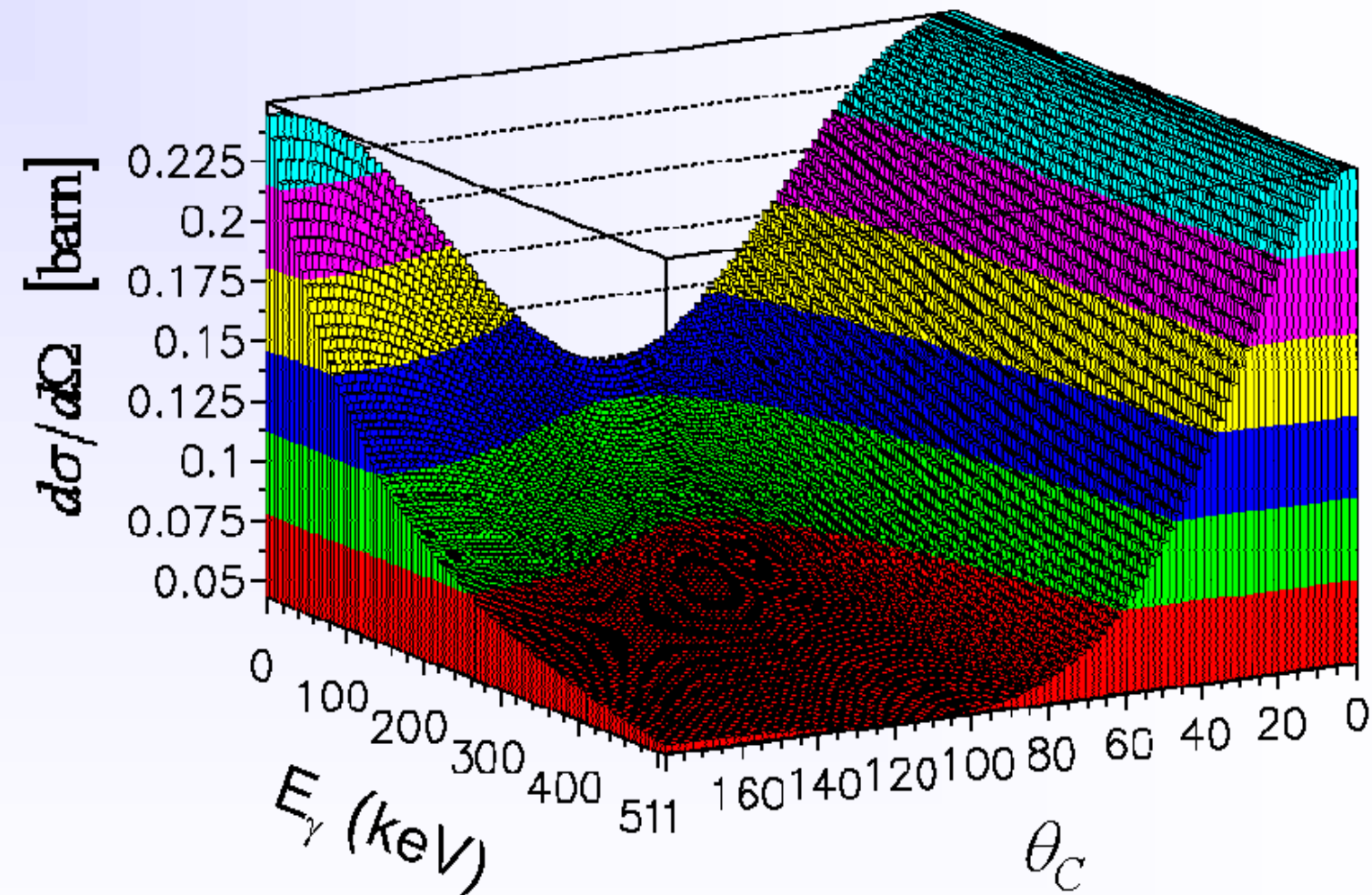
At high energies approximately

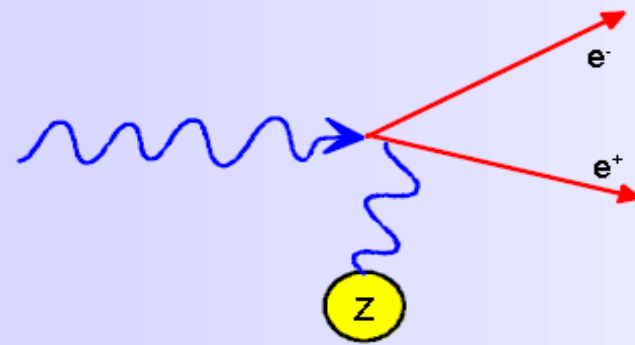
$$\sigma_c^e \propto \frac{\ln \varepsilon}{\varepsilon}$$

Atomic Compton cross-section:

$$\sigma_c^{atomic} = Z \cdot \sigma_c^e$$

Compton cross-section (Klein-Nishina)





Only possible in the Coulomb field of a nucleus (or an electron) if $E_\gamma \geq 2m_e c^2$

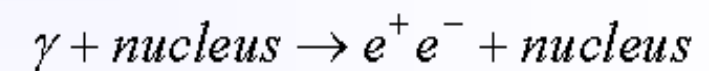
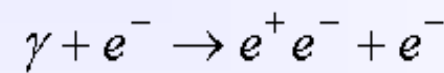
Cross-section (high energy approximation)

$$\sigma_{pair} \approx 4\alpha r_e^2 Z^2 \left(\frac{7}{9} \ln \frac{183}{Z^{1/3}} \right) \quad \text{independent of energy !}$$

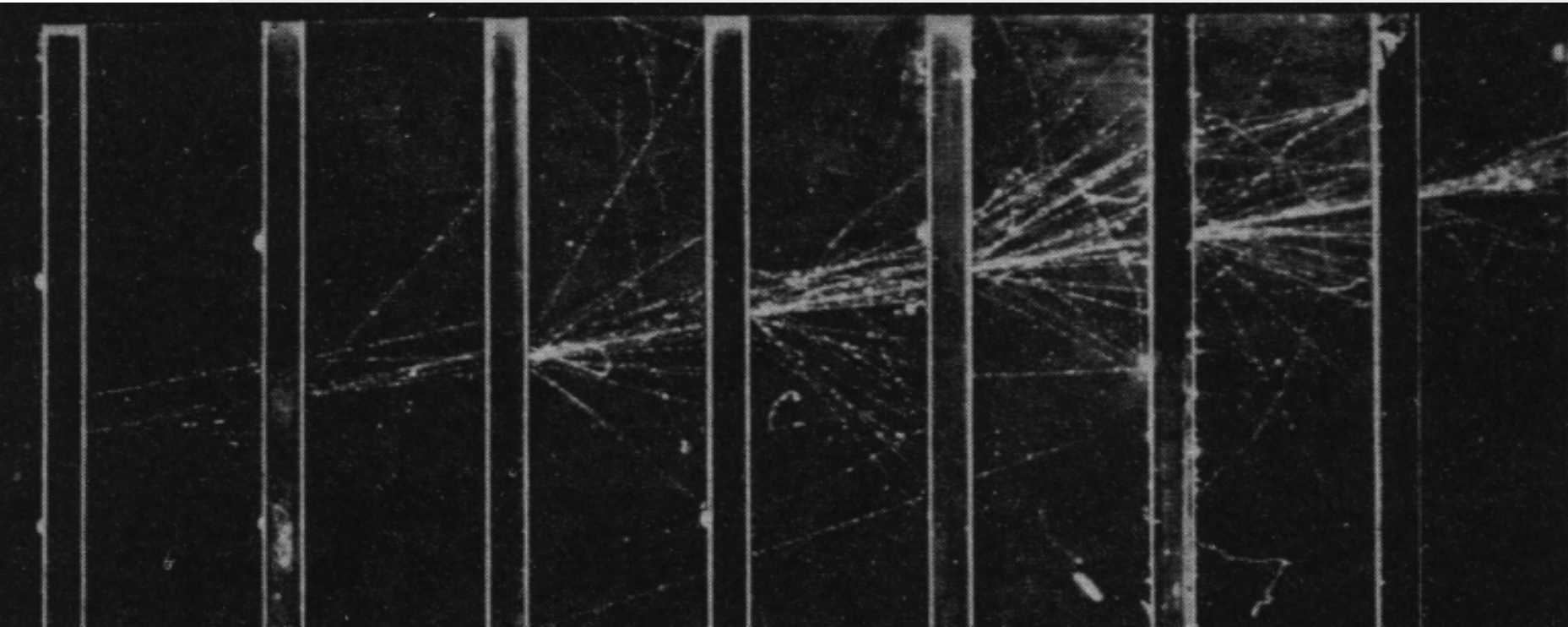
$$\approx \frac{7}{9} \frac{A}{N_A} \frac{1}{X_0}$$

$$\approx \frac{A}{N_A} \frac{1}{\lambda_{pair}}$$

$$\lambda_{pair} = \frac{9}{7} X_0$$



Electromagnetic cascades (showers)



Electromagnetic shower in a cloud chamber with lead absorbers

Simple qualitative model

- Consider only **Bremsstrahlung** and (symmetric) **pair production**.
- Assume: $X_0 \sim \lambda_{\text{pair}}$

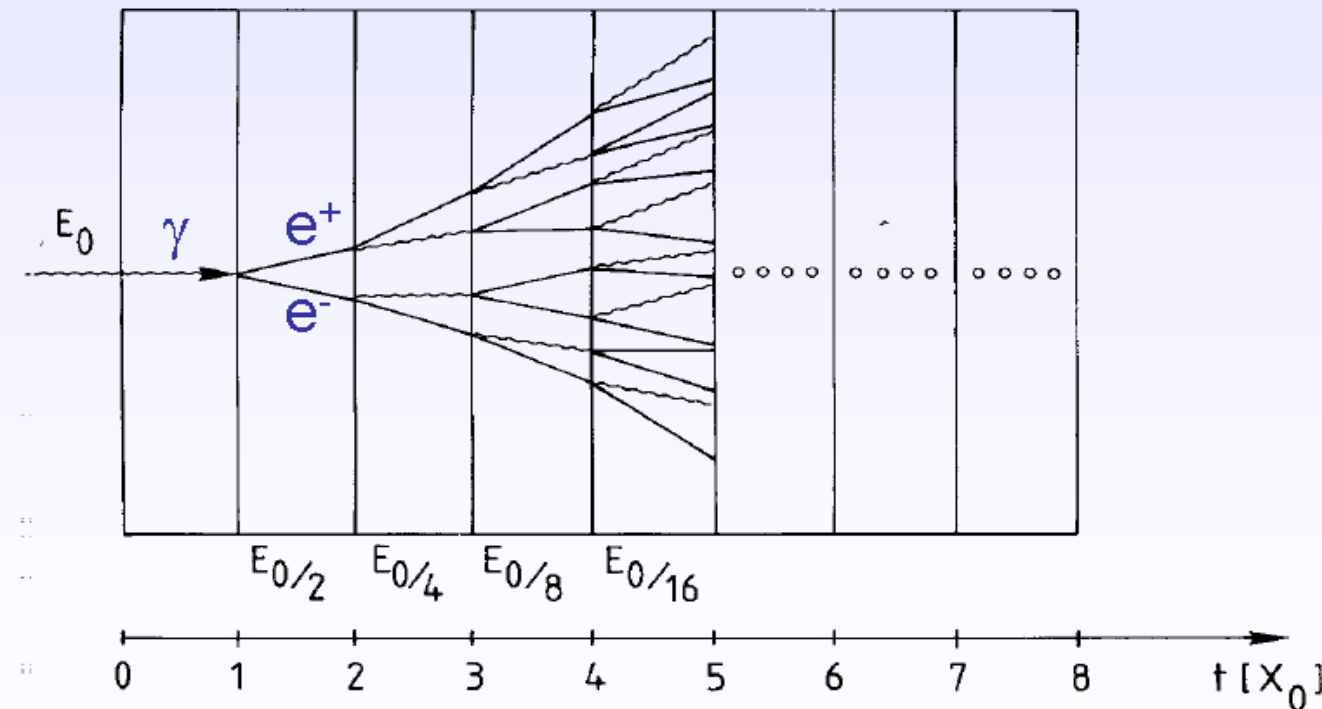
$$N(t) = 2^t \quad E(t) / \text{particle} = E_0 \cdot 2^{-t}$$

Process continues until $E(t) < E_c$

$$N^{\text{total}} = \sum_{t=0}^{t_{\text{max}}} 2^t = 2^{(t_{\text{max}}+1)} - 1 \approx 2 \cdot 2^{t_{\text{max}}} = 2 \frac{E_0}{E_c}$$

$$t_{\text{max}} = \frac{\ln E_0 / E_c}{\ln 2}$$

After $t = t_{\text{max}}$ the dominating processes are **ionization**, **Compton effect** and **photo effect** → **absorption of energy**.



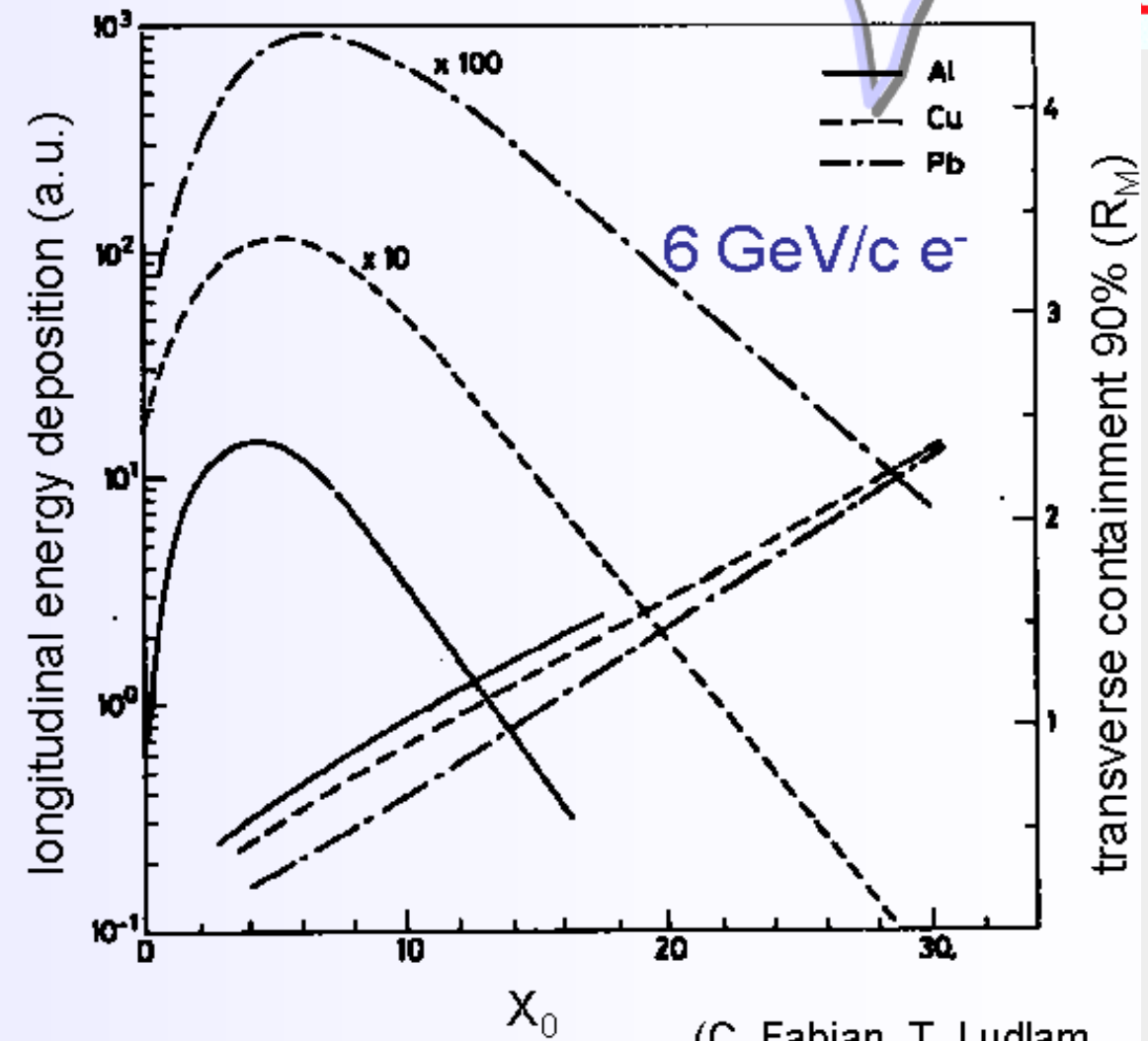
Longitudinal shower development

$$\frac{dE}{dt} \propto t^\alpha e^{-t}$$

Shower maximum at $t_{\max} = \ln \frac{E_0}{E_c} \frac{1}{\ln 2}$

95% containment $t_{95\%} \approx t_{\max} + 0.08Z + 9.6$

Size of a calorimeter grows only logarithmically with E_0 ,



Transverse shower development

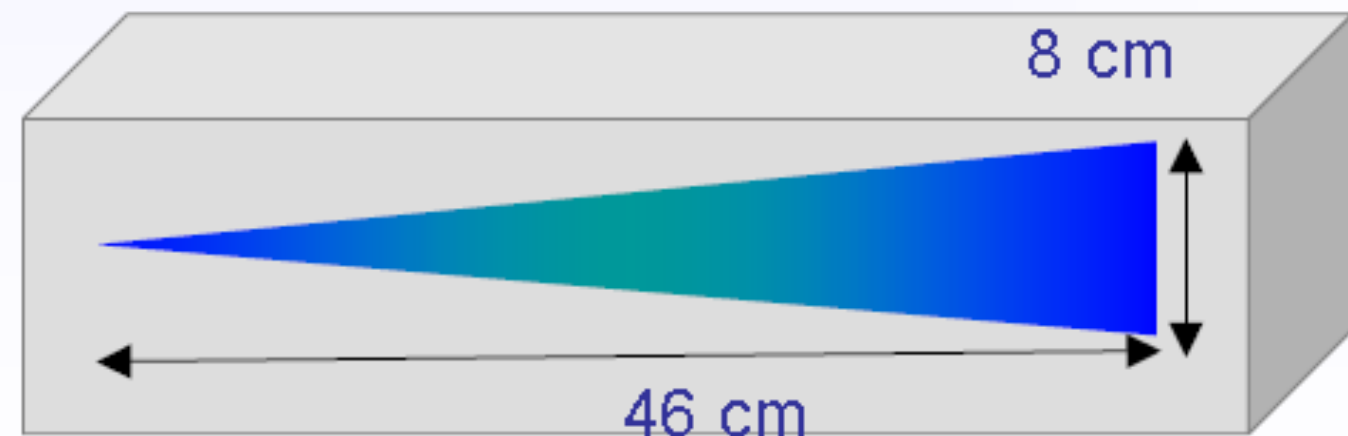
95% of the shower cone is located in a cylinder with radius $2 R_M$

Molière radius $R_M = \frac{21 \text{ MeV}}{X_0} \text{ [g/cm}^2\text{]}$

Example: $E_0 = 100 \text{ GeV}$ in lead glass

$E_c = 11.8 \text{ MeV} \rightarrow t_{\max} \approx 13, t_{95\%} \approx 23$

$X_0 \approx 2 \text{ cm}, R_M = 1.8 \cdot X_0 \approx 3.6 \text{ cm}$



Radiation length:

$$X_0 = \frac{180A}{Z^2} \frac{\text{g}}{\text{cm}^2}$$

Critical energy:

$$E_c = \frac{550 \text{ MeV}}{Z}$$

[Attention: Definition of Rossi used]

Shower maximum:

$$t_{\text{max}} = \ln \frac{E}{E_c} - \begin{cases} 1.0 & e^- \text{ induced shower} \\ 0.5 & \gamma \text{ induced shower} \end{cases}$$

Longitudinal energy containment:

$$L(95\%) = t_{\text{max}} + 0.08Z + 9.6 [X_0]$$

Transverse Energy containment:

$$R(90\%) = R_M$$

$$R(95\%) = 2R_M$$

Problem:

Calculate how much Pb, Fe or Cu is needed to stop a 10 GeV electron.

Pb : $Z=82$, $A=207$, $\rho=11.34 \text{ g/cm}^3$

Fe : $Z=26$, $A=56$, $\rho=7.87 \text{ g/cm}^3$

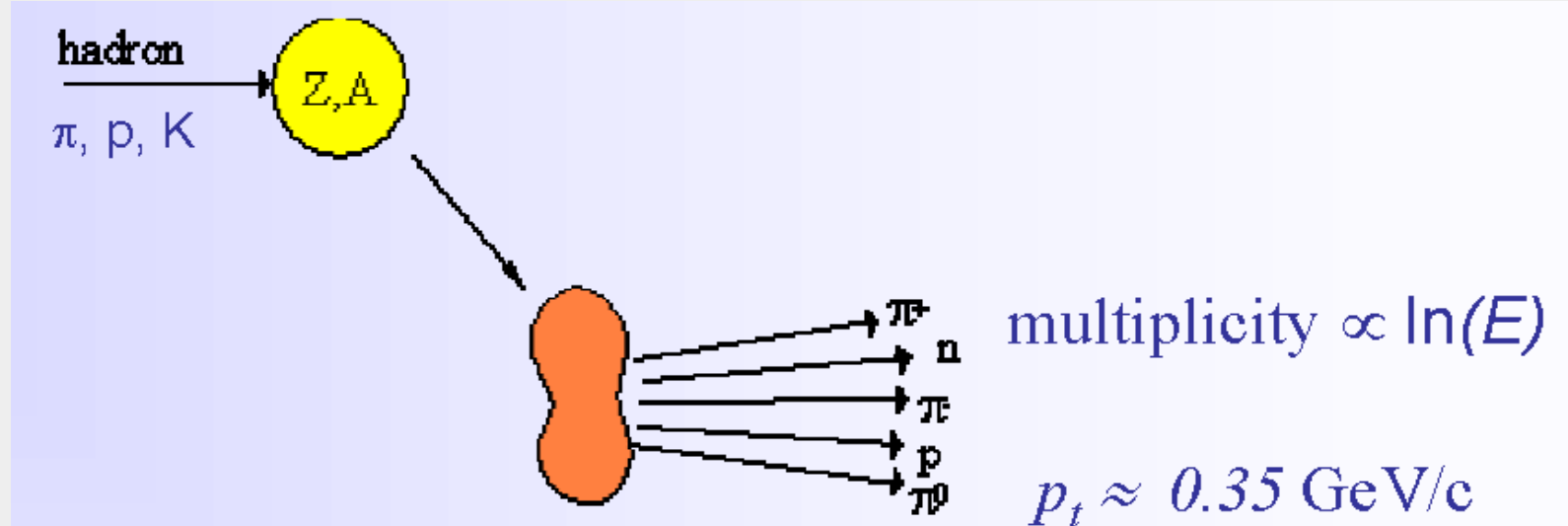
Cu : $Z=29$, $A=63$, $\rho=8.92 \text{ g/cm}^3$

Position resolution - EM

- Reconstruction of invariant masses of particles decaying into photons, electron identification using match with track measured in tracking devices
- Impact position of showers is determined using the transverse (and longitudinal) energy distribution in calorimeter cells
- Method based on center of gravity (COG) calculation
 - works for projective geometry and particles coming from the interaction vertex
 - calorimeter cell size $d \leq 1R_M$
- Typical resolutions: few mm/\sqrt{E}

The interaction of energetic hadrons (charged or neutral) with matter is determined by inelastic nuclear processes.

Excitation and finally
break-up of nucleus
→ nucleus fragments
+ production of
secondary particles.



For high energies (>1 GeV) the cross-sections depend only little on the energy and on the type of the incident particle (π , p , K ...).

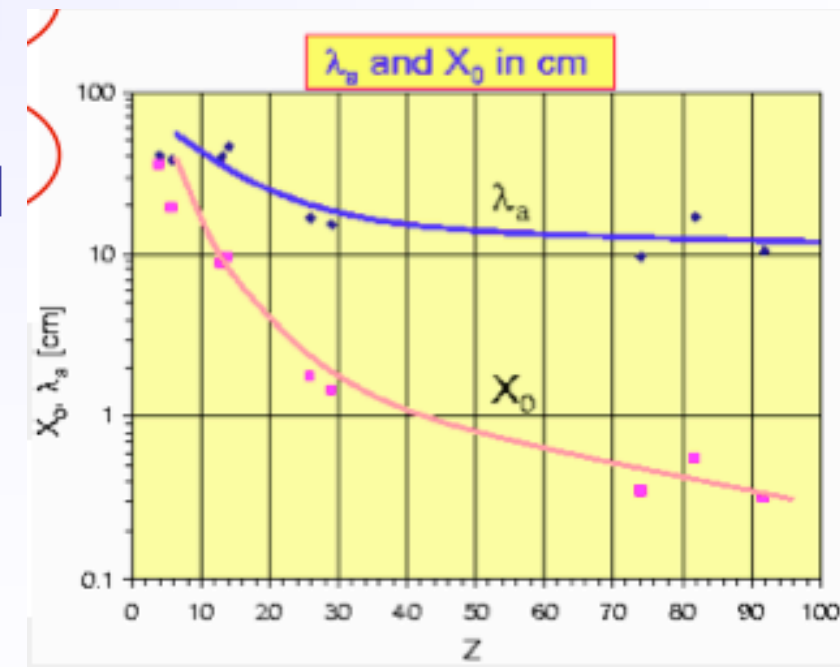
$$\sigma_{inel} \approx \sigma_0 A^{0.7} \quad \sigma_0 \approx 35 \text{ mb}$$

In analogy to X_0 a hadronic absorption length can be defined

$$\lambda_a = \frac{A}{N_A \sigma_{inel}} \propto A^{\frac{1}{4}} \quad \text{because } \sigma_{inel} \approx \sigma_0 A^{0.7}$$

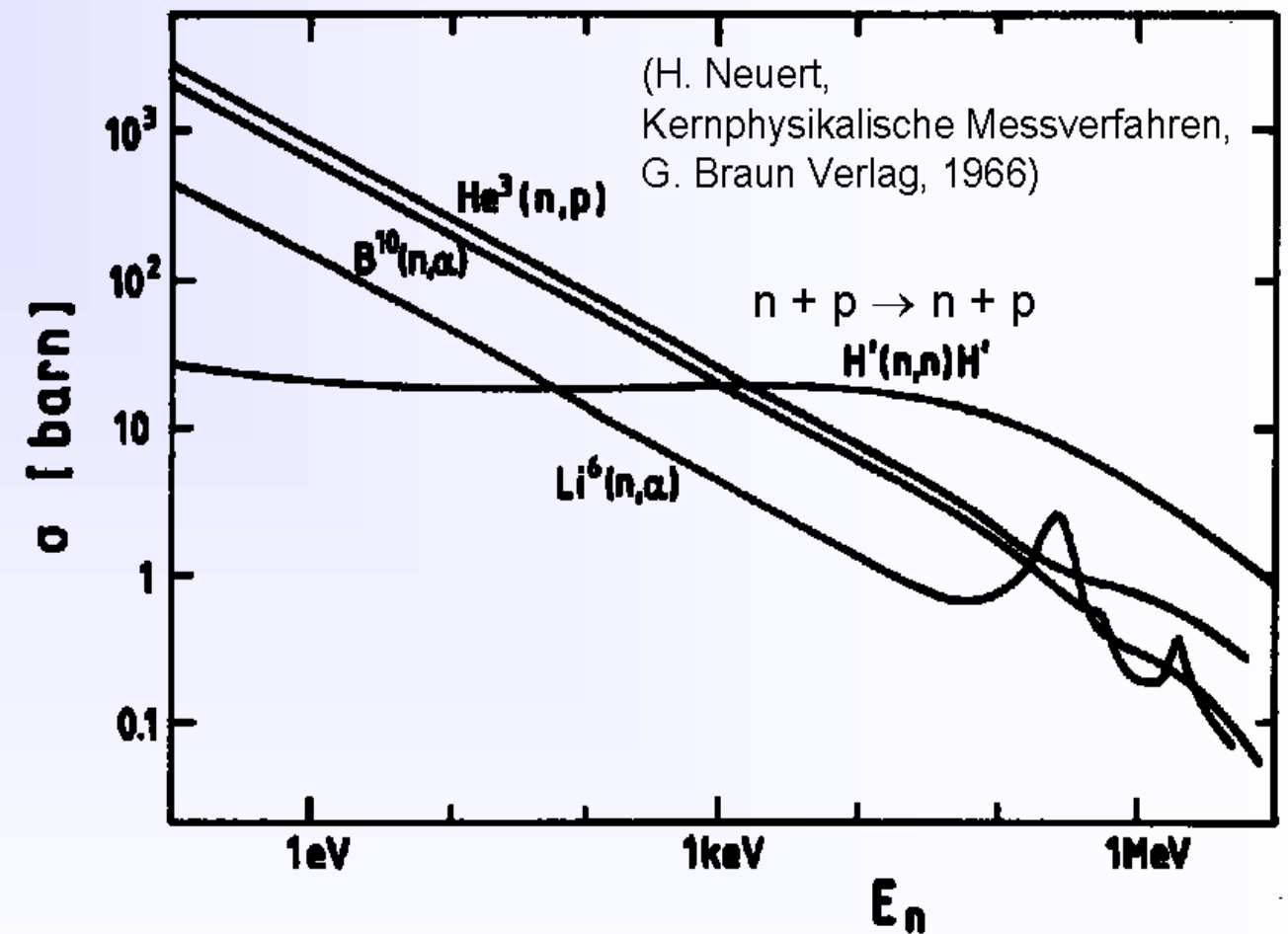
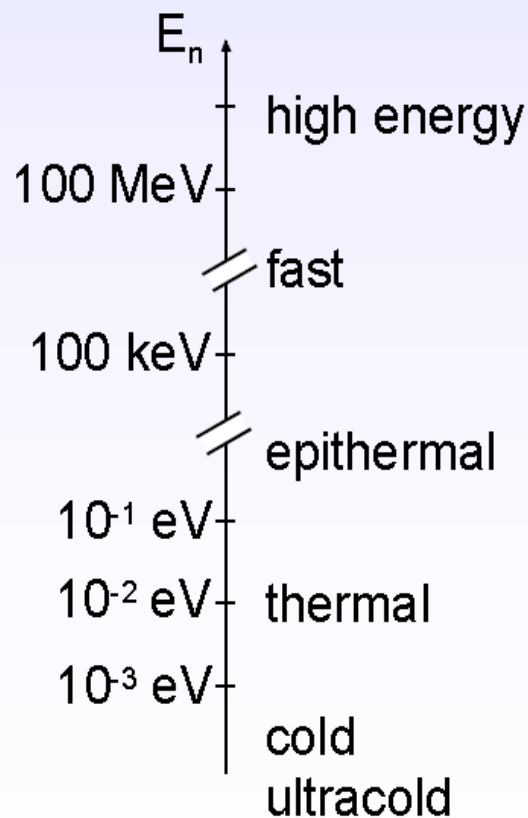
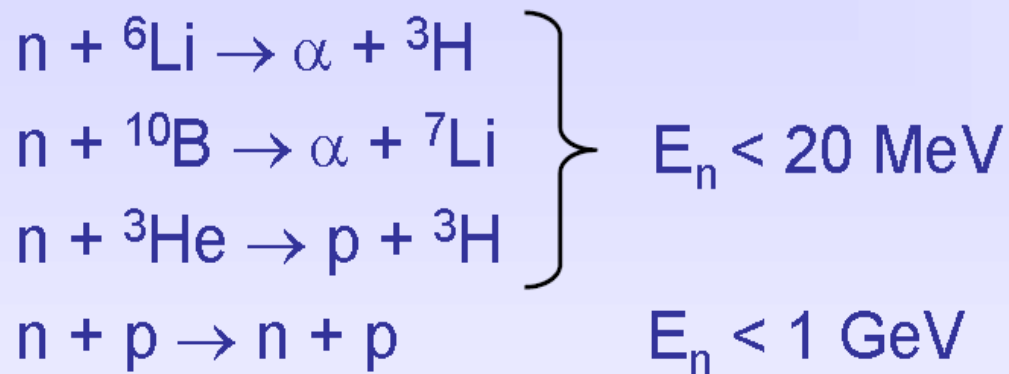
similarly a hadronic interaction length

$$\lambda_I = \frac{A}{N_A \sigma_{total}} \propto A^{\frac{1}{3}} \quad \lambda_I < \lambda_a$$



Neutrons have no charge, i.e. their interaction is based only on strong (and weak) nuclear force. To detect neutrons, we have to create charged particles.

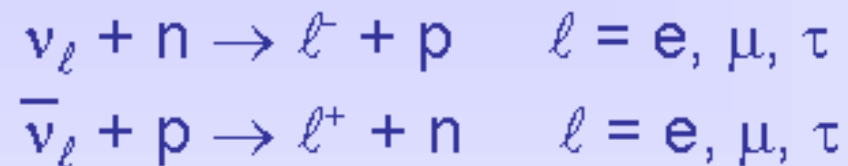
Possible neutron conversion and elastic reactions ...



In addition there are ...

- neutron induced fission $E_n \approx E_{th} \approx 1/40 \text{ eV}$
- inelastic reactions \rightarrow **hadronic cascades** (see below) $E_n > 1 \text{ GeV}$

Neutrinos interact only weakly \rightarrow tiny cross-sections. For their detection we need again first a charged particle. Possible detection reactions:



The cross-section for the reaction $\nu_e + n \rightarrow e^- + p$ is of the order of 10^{-43} cm^2 (per nucleon, $E_\nu \approx \text{few MeV}$).

\rightarrow detection efficiency

$$\varepsilon_{\text{det}} = \sigma \cdot N^{\text{surf}} = \sigma \cdot \rho \frac{N_A}{A} d$$

1 m Iron: $\varepsilon_{\text{det}} \approx 5 \cdot 10^{-17}$

1 km water: $\varepsilon_{\text{det}} \approx 6 \cdot 10^{-15}$

Neutrino detection requires big and massive detectors (ktons - Mtons) and very high neutrino fluxes (e.g. $10^{20} \nu / \text{yr}$).

In collider experiments fully **hermetic** detectors allow to detect neutrinos indirectly:

- sum up all visible energy and momentum.
- attribute missing energy and momentum to neutrino.

All the fluctuations described in em case plus more and more significant

- Breakdown of **non-em** energy deposit in **lead** absorber:
 - ***Ionizing particles*** **56%** (2/3 from spallation protons)
 - ***Neutrons*** **10%** (37 neutrons per GeV!)
 - ***Invisible*** **34%**

Spallation protons carry typically 100 MeV,
Evaporation neutrons 3 MeV

An important fraction of energy goes in nuclear binding: not detectable!

**FLUCTUATIONS OF E_{vis} :
INTRINSIC LIMIT
TO HADRONIC ENERGY
MEASUREMENT**

An important fraction of energy goes in em deposits and strongly varies

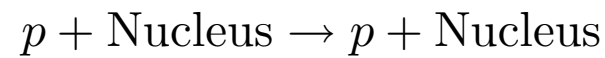
- Hadron showers contain em component (π^0 , η)
- Size of em component F_{em} is mainly determined by the first interaction
- On average 1/3 of mesons produced in the 1^o interaction will be a π^0 , this fraction fluctuates in a significant way
- The 2^o generation π^\pm will produce π^0 if enough energetic



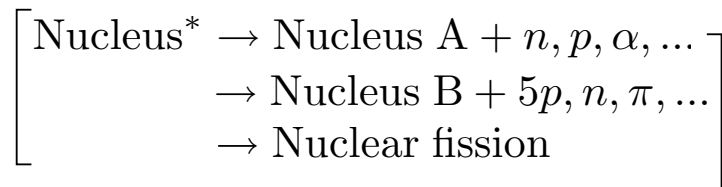
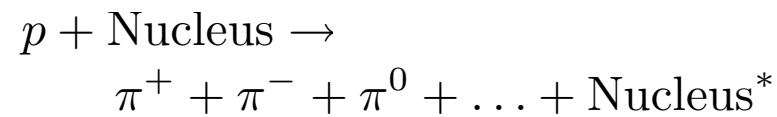
Hadronic Showers

Hadronic interaction:

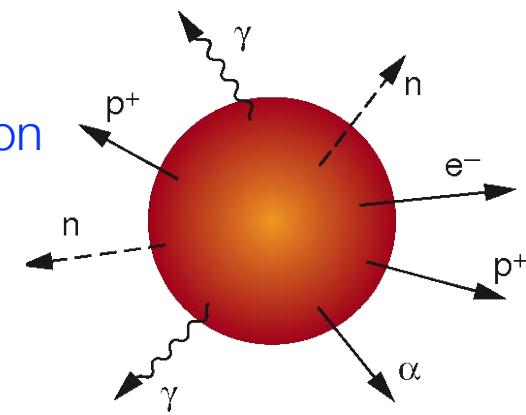
Elastic:



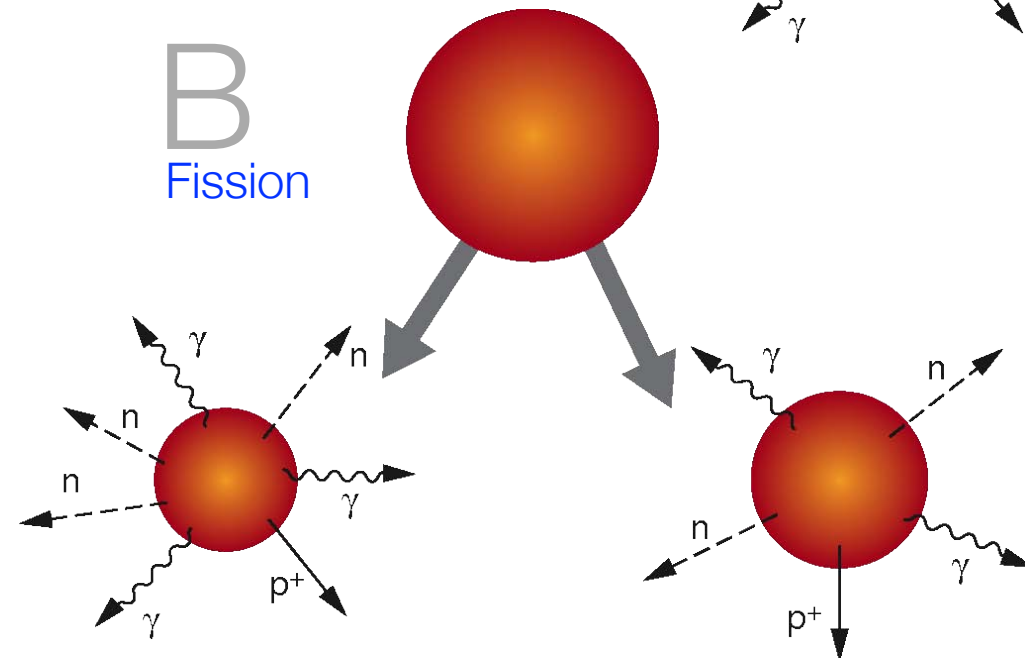
Inelastic:



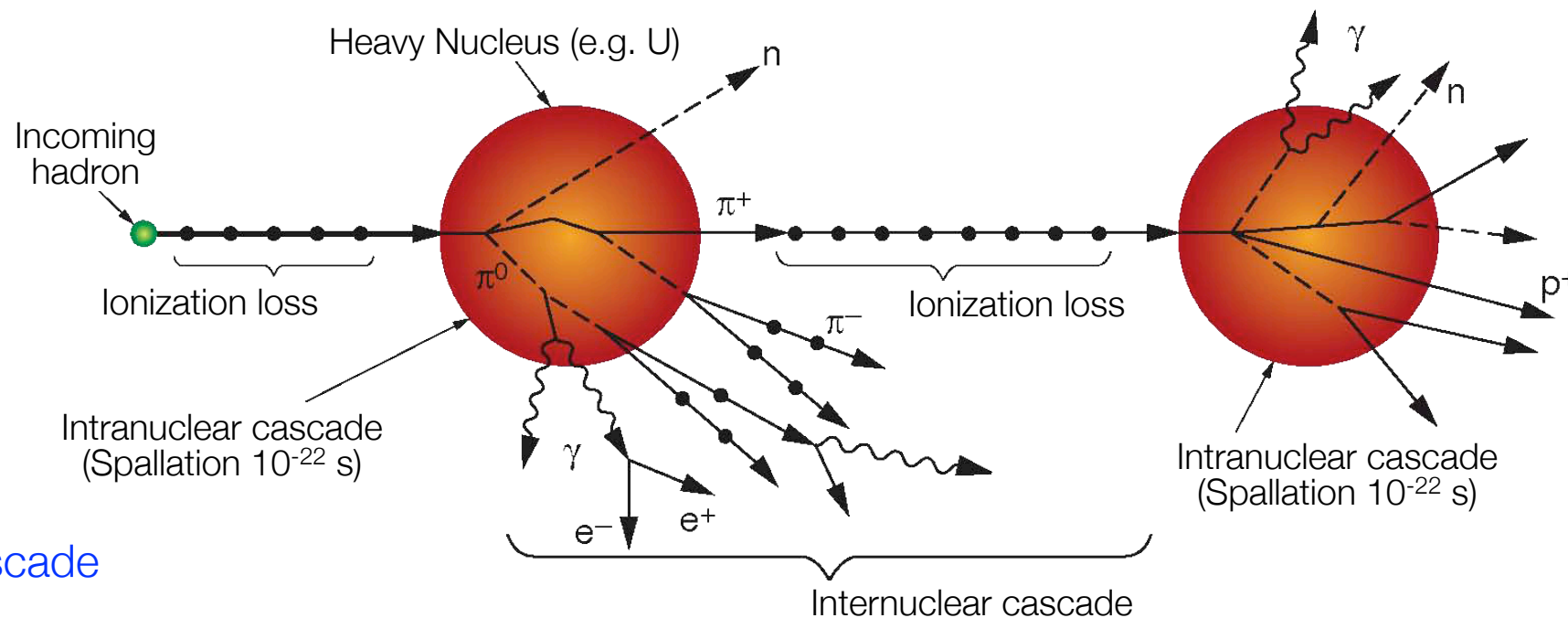
C Nuclear evaporation



B Fission



A Inter- and intranuclear cascade



TO BACKUP

Hadronic interaction:

Cross Section:

$$\sigma_{\text{tot}} = \sigma_{\text{el}} + \sigma_{\text{inel}}$$

For substantial energies
 σ_{inel} dominates:

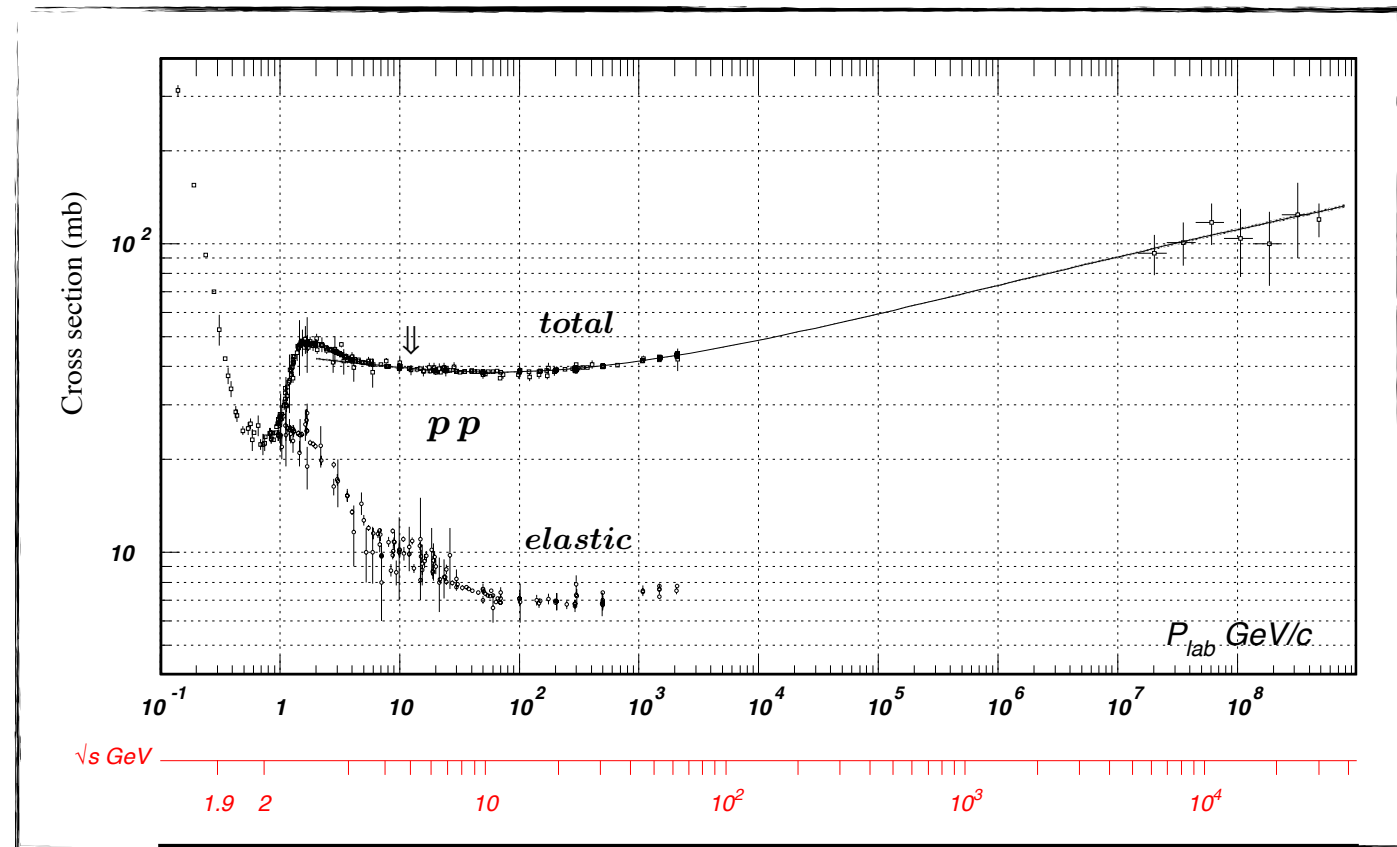
$$\sigma_{\text{el}} \approx 10 \text{ mb}$$

$$\sigma_{\text{inel}} \propto A^{2/3} \text{ [geometrical cross section]}$$

$$\therefore \sigma_{\text{tot}} = \sigma_{\text{tot}}(pA) \approx \sigma_{\text{tot}}(pp) \cdot A^{2/3}$$

[σ_{tot} slightly grows with \sqrt{s}]

at high energies
also diffractive contribution



Total proton-proton cross section
[similar for p+n in 1-100 GeV range]

Hadronic interaction length:

$$\lambda_{\text{int}} = \frac{1}{\sigma_{\text{tot}} \cdot n} = \frac{A}{\sigma_{pp} A^{2/3} \cdot N_A \rho} \sim A^{1/3} \text{ [for } \sqrt{s} \approx 1 - 100 \text{ GeV]}$$

$$\approx 35 \text{ g/cm}^2 \cdot A^{1/3}$$

which yields:

$$N(x) = N_0 \exp(-x/\lambda_{\text{int}})$$

Remark: In principle one should distinguish between collision length $\lambda_W \sim 1/\sigma_{\text{tot}}$ and interaction length $\lambda_{\text{int}} \sim 1/\sigma_{\text{inel}}$ where the latter considers inelastic processes only (absorption) ...

Interaction length characterizes both, longitudinal and transverse profile of hadronic showers ...

Hadronic vs. electromagnetic interaction length:

$$\left. \begin{aligned} X_0 &\sim \frac{A}{Z^2} \\ \lambda_{\text{int}} &\sim A^{1/3} \end{aligned} \right] \rightarrow \frac{\lambda_{\text{int}}}{X_0} \sim A^{4/3}$$

$$\lambda_{\text{int}} \gg X_0$$

[$\lambda_{\text{int}}/X_0 > 30$ possible; see below]

Typical
Longitudinal size: $6 \dots 9 \lambda_{\text{int}}$ [EM: 15-20 X_0]
[95% containment]

Typical
Transverse size: one λ_{int} [EM: 2 R_M ; compact]
[95% containment]

Some numerical values for materials typical used in hadron calorimeters

	λ_{int} [cm]	X_0 [cm]
Szint.	79.4	42.2
LAr	83.7	14.0
Fe	16.8	1.76
Pb	17.1	0.56
U	10.5	0.32
C	38.1	18.8

Hadronic calorimeter need more depth than electromagnetic calorimeter ...

Hadronic shower development:

[estimate similar to e.m. case]

Depth (in units of λ_{int}):

$$t = \frac{x}{\lambda_{\text{int}}}$$

Energy in depth t :

$$E(t) = \frac{E}{\langle n \rangle^t} \quad \& \quad E(t_{\text{max}}) = E_{\text{thr}}$$

[with $E_{\text{thr}} \approx 290 \text{ MeV}$]

$$E_{\text{thr}} = \frac{E}{\langle n \rangle^{t_{\text{max}}}}$$

Shower maximum:

$$\langle n \rangle^{t_{\text{max}}} = \frac{E}{E_{\text{thr}}}$$

Number of particles lower by factor E_{thr}/E_c compared to e.m. shower ...

Intrinsic resolution: worse by factor $\sqrt{E_{\text{thr}}/E_c}$

$$t_{\text{max}} = \frac{\ln(E/E_{\text{thr}})}{\ln \langle n \rangle}$$

But:

Only rough estimate as ...

energy sharing between shower particles fluctuates strongly ...

part of the energy is not detectable (neutrinos, binding energy); partial compensation possible (n-capture & fission)

spatial distribution varies strongly; different range of e.g. π^\pm and π^0 ...

electromagnetic fraction, i.e. fraction of energy deposited by $\pi^0 \rightarrow \gamma\gamma$ increases with energy ...

$$f_{\text{em}} \approx f_{\pi^0} \sim \ln E / (1 \text{ GeV})$$

Explanation: charged hadron contribute to electromagnetic fraction via $\pi^\pm \rightarrow \pi^0 n$; the opposite happens only rarely as π^0 travel only $0.2 \mu\text{m}$ before its decay ('one-way street') ...

At energies below 1 GeV hadrons lose their energy via ionization only ...

Thus: need Monte Carlo (GEISHA, CALOR, ...) to describe shower development correctly ...

Hadronic Showers

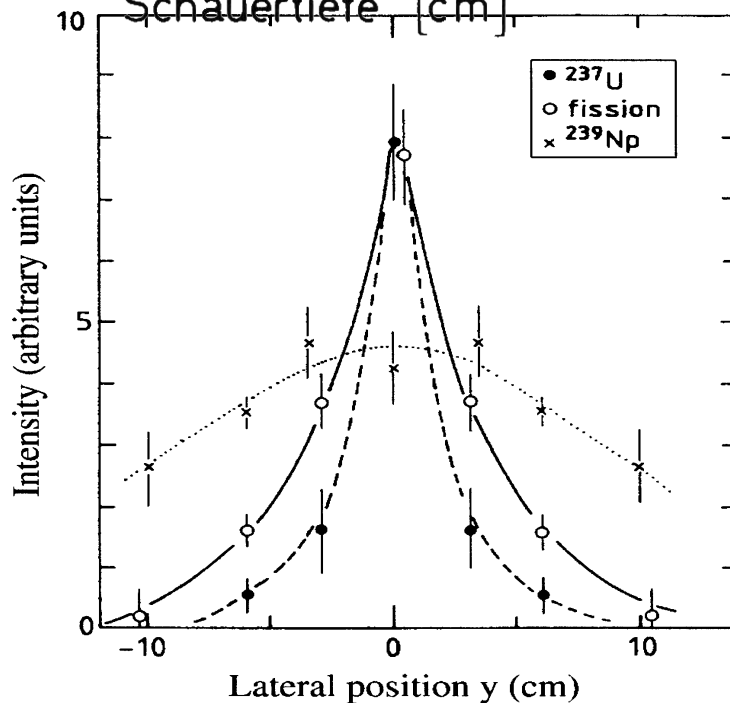
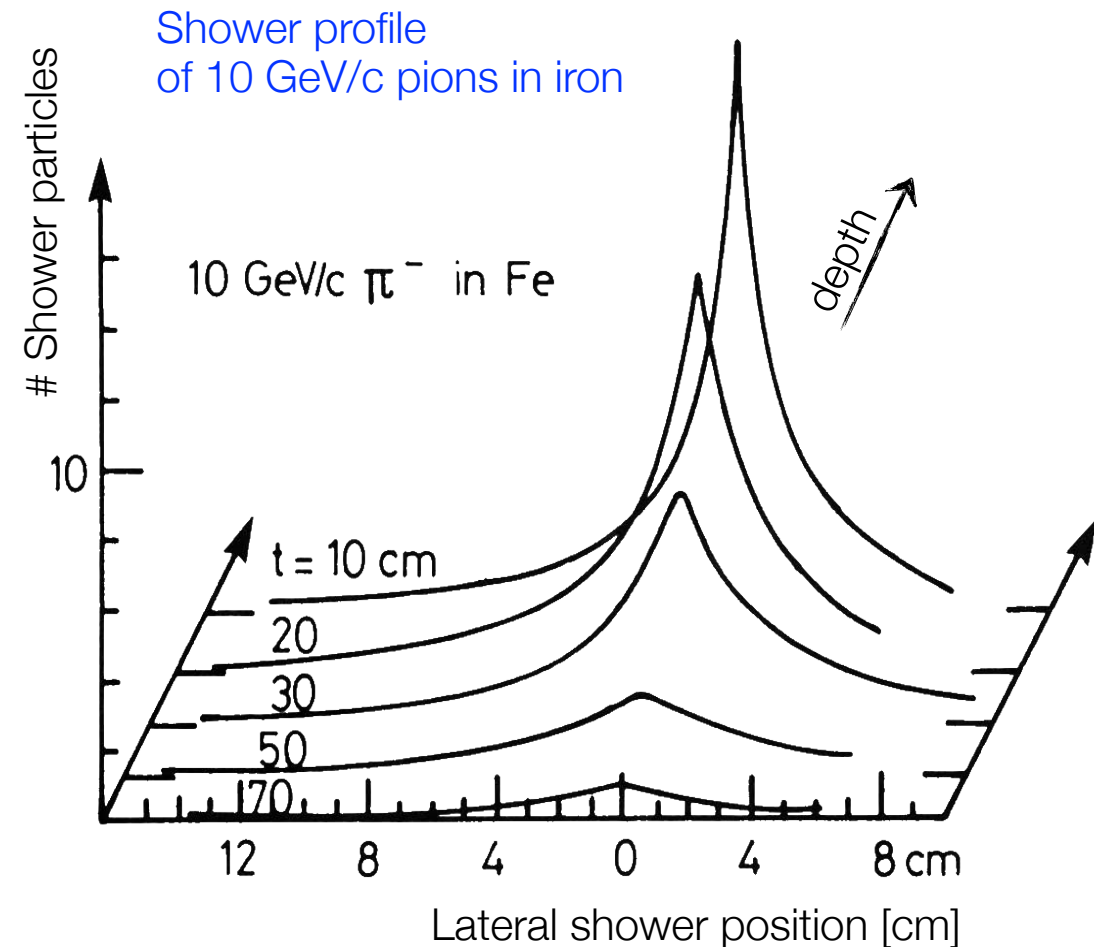
Transverse shower profile

Typical transverse momenta of secondaries: $\langle p_t \rangle \simeq 350 \text{ MeV}/c \dots$

Lateral extend at shower maximum: $R_{95\%} \simeq \lambda_{\text{int}} \dots$

Electromagnetic component leads to relatively well-defined core: $R \simeq R_M \dots$

Exponential decay after shower maximum ...



Lateral profile for 300 GeV π^-

[target material ^{238}U]
[measured at depth $4 \lambda_{\text{int}}$]

More π^0 's and γ in core
Energetic neutrons and charged pions form a wider core
Thermal neutrons generate broad tail

Measurement from induced radioactivity:

^{99}Mo (fission): neutron induced ...
[energetic neutron component]

^{237}U : mainly produced via $^{238}\text{U}(\gamma, n)^{237}\text{U} \dots$
[electromagnetic component]

^{239}Np : from ^{239}U decay ...
[thermal neutrons]

Ordinate indicates decay rate of different radioactive nuclides ...

Energy resolution:

e.g. inhomogeneities
shower leakage

e.g. electronic noise
sampling fraction variations

$$\frac{\sigma_E}{E} = \frac{A}{\sqrt{E}} \oplus B \oplus \frac{C}{E}$$

Fluctuations:

Sampling fluctuations

Leakage fluctuations

Fluctuations of electromagnetic fraction

Nuclear excitations, fission, binding energy fluctuations ...

Heavily ionizing particles

Typical:

A: 0.5 – 1.0 [Record:0.35]

B: 0.03 – 0.05

C: few %

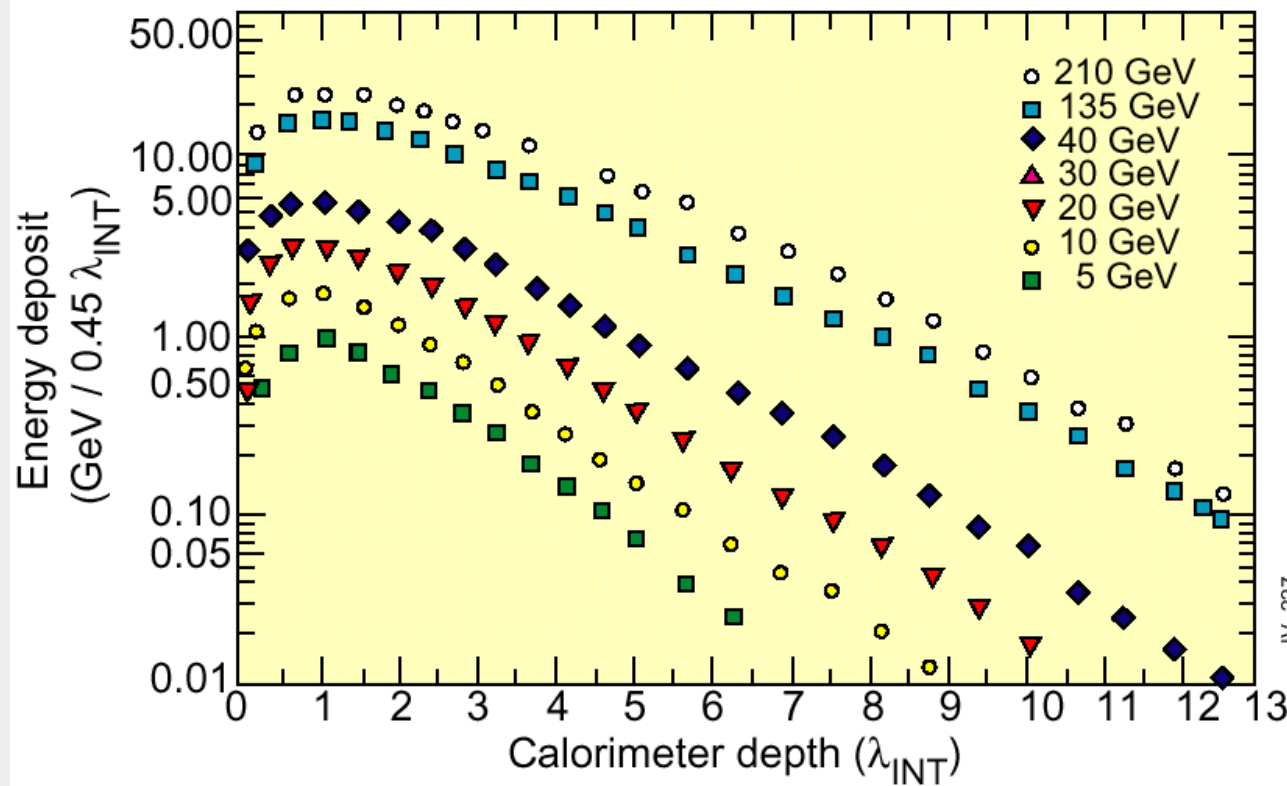
Hadron shower profile



LONGITUDINAL

- Sharp peak from π^0 from the 1^o interaction
- Gradual extinction with typical scale λ_{int}

WA78 : 5.4 λ of 10mm U / 5mm Scint + 8 λ of 25mm Fe / 5mm Scint

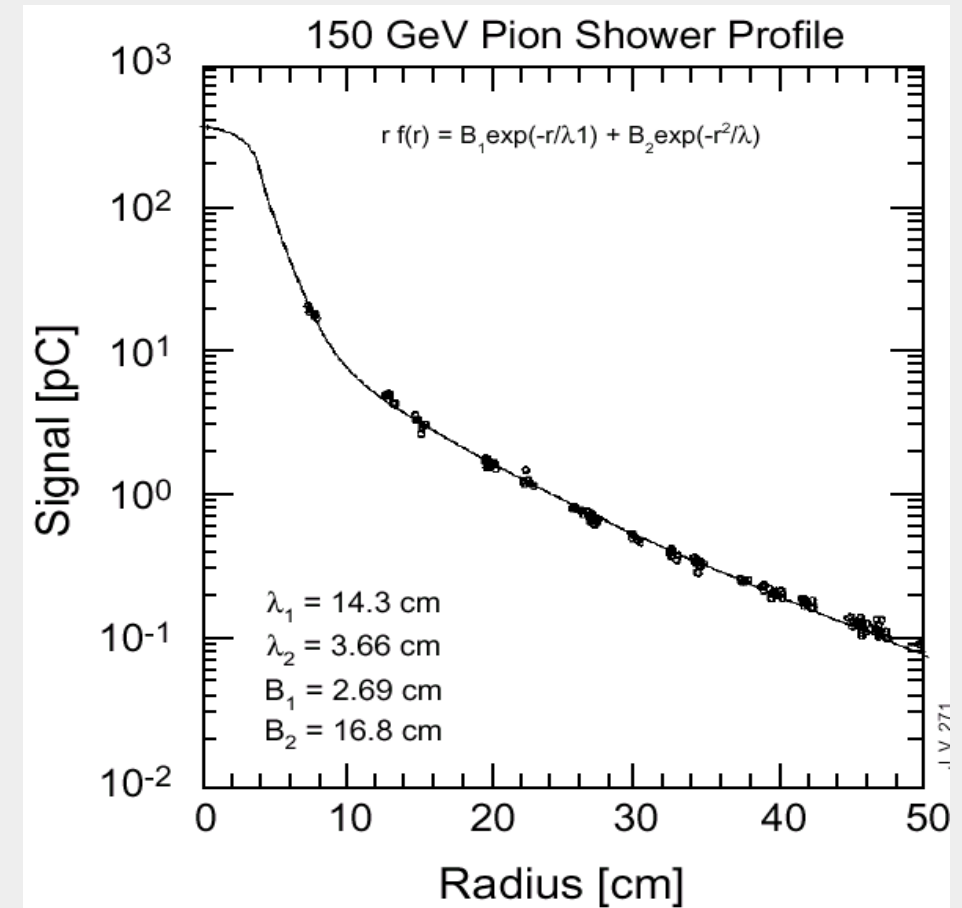


~10 λ needed to contain 99% E of 200 GeV π
(about 1 – 2 m of heavy absorber)

Need to sample

LATERAL

- Average p_t secondaries ~ 300 MeV
- Typical transverse scale λ_{int}
- Dense core due to π^0



Transverse radius for 95% E containment $\sim 1\lambda$

Calorimeter energy resolution determined by fluctuations ...

Homogeneous calorimeters:

- | | | |
|---|---|----------------------|
| Shower fluctuations | } | Quantum fluctuations |
| Photo-electron statistics | | |
| Shower leakage | | |
| Instrumental effects (noise, light attenuation, non-uniformity) | | |

In addition for

Sampling calorimeters:

- Sampling fluctuations
- Landau fluctuations
- Track length fluctuations

$$\frac{\sigma_E}{E} = \frac{a}{\sqrt{E}} \oplus \frac{b}{E} \oplus c$$

Quantum fluctuations	$\sim 1/\sqrt{E}$
Electronic noise	$\sim 1/E$
Shower leakage*	$\approx \text{const}$
Sampling fluctuations	$\sim 1/\sqrt{E}$
Landau fluctuations	$\sim 1/\sqrt{E}$
Track length fluctuations	$\sim 1/\sqrt{E}$

* Different for longitudinal and lateral leakage ...
Complicated; small energy dependence ...

Shower fluctuations: [intrinsic resolution]

Ideal (homogeneous) calorimeter without leakage: energy resolution limited only by statistical fluctuations of the number N of shower particles ...

i.e.:

$$\frac{\sigma_E}{E} \propto \frac{\sigma_N}{N} \approx \frac{\sqrt{N}}{N} = \frac{1}{\sqrt{N}} \quad \text{with } N = \frac{E}{W}$$

$$\frac{\sigma_E}{E} \propto \sqrt{\frac{W}{E}}$$

E : energy of primary particle
 W : mean energy required to produce 'signal quantum'

Examples:

Silicon detectors : $W \approx 3.6$ eV
 Gas detectors : $W \approx 30$ eV
 Plastic scintillator : $W \approx 100$ eV

Resolution improves due to correlations between fluctuations (Fano factor; see above) ...

$$\frac{\sigma_E}{E} \propto \sqrt{\frac{FW}{E}} \quad [\text{F: Fano factor}]$$

Photo-electron statistics:

For detectors for which the deposited energy is measured via light detection inefficiencies converting photons into a detectable electrical signal (e.g. photo electrons) contribute to the measurement uncertainty ...

i.e.:

$$\frac{\sigma_E}{E} \propto \frac{\sigma_{N_{pe}}}{N_{pe}} \approx \frac{1}{\sqrt{N_{pe}}} \quad N_{pe}: \text{number of photo electrons}$$

This contribution is present for calorimeters based on detecting scintillation or Cherenkov light; important in this context are quantum efficiency and gain of the used photo detectors (e.g. Photomultiplier, Avalanche Photodiodes ...)

Also important: losses in light guides and wavelength shifters

Marmor Calorimeter
[CHARM Collaboration]

Shower leakage:

Fluctuations due to finite size of calorimeter; shower not fully contained ...

Lateral leakage: limited influence

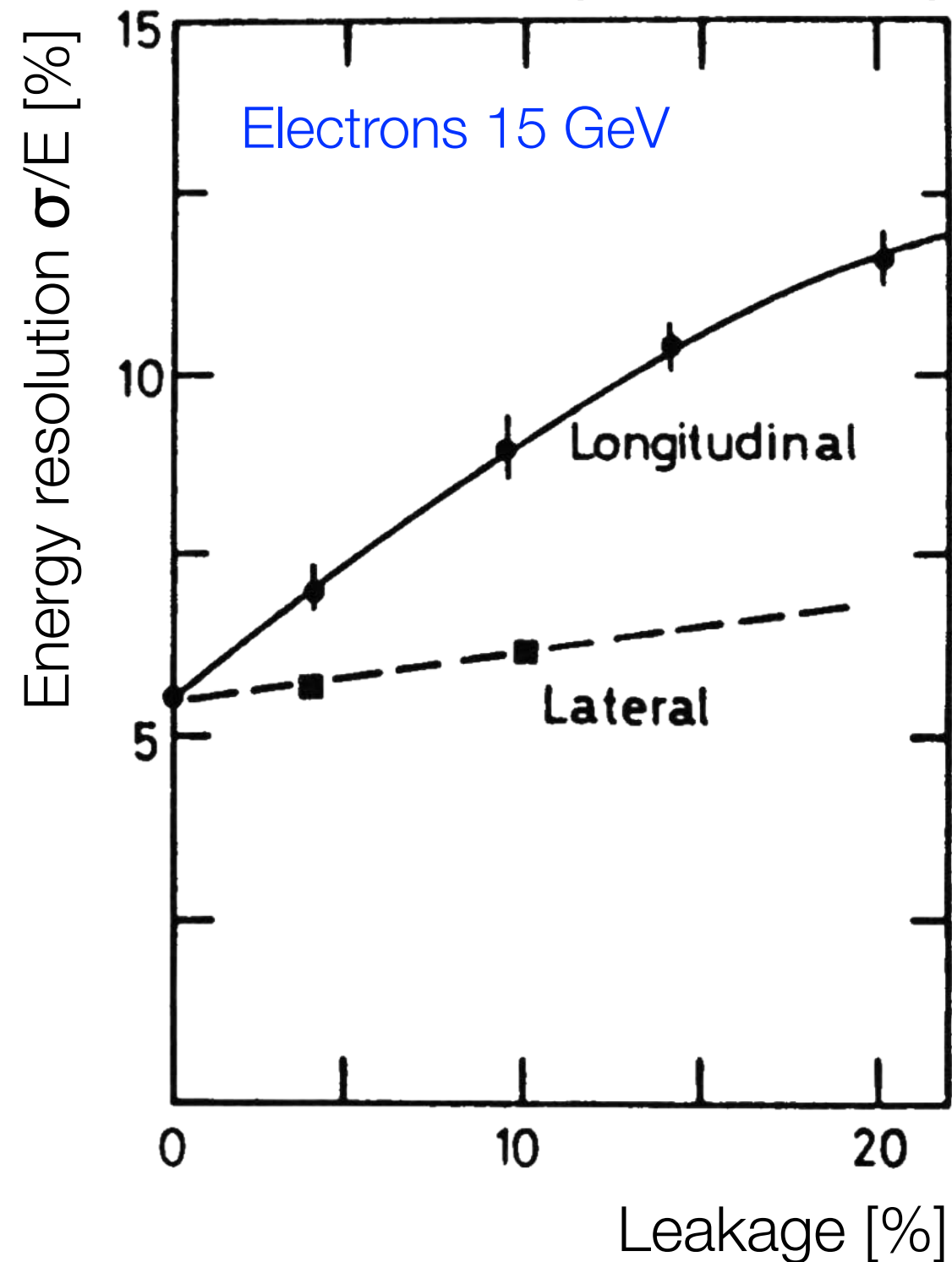
Longitudinal leakage: strong influence

Typical expression when including leakage effects:

$$\frac{\sigma_E}{E} \propto \left(\frac{\sigma_E}{E} \right)_{f=0} \cdot \left[1 + 2f\sqrt{E} \right]$$

[f : average fraction of shower leakage]

Remark: other parameterizations exist ...



Sampling fluctuations:

Additional contribution to energy resolution in sampling calorimeters due to fluctuations of the number of (low-energy) electrons crossing active layer ...

Increases linearly with energy of incident particle and fineness of the sampling ...

$$N_{\text{ch}} \propto \frac{E}{E_c t_{\text{abs}}}$$

N_{ch} : charged particles reaching active layer

N_{max} : total number of particles = E/E_c

t_{abs} : absorber thickness in X_0

Reasoning: Energy deposition dominantly due to low energy electrons; range of these electrons smaller than absorber thickness t_{abs} ; only few electrons reach active layer ...

Fraction $f \sim 1/t_{\text{abs}}$ reaches the active medium ...

Resulting energy resolution:

$$\frac{\sigma_E}{E} \propto \frac{\sigma_{N_{\text{ch}}}}{N_{\text{ch}}} \propto \sqrt{\frac{E_c t_{\text{abs}}}{E}}$$

Semi-empirical:

$$\frac{\sigma_E}{E} = 3.2\% \sqrt{\frac{E_c [\text{MeV}] \cdot t_{\text{abs}}}{F \cdot E [\text{GeV}]}}$$

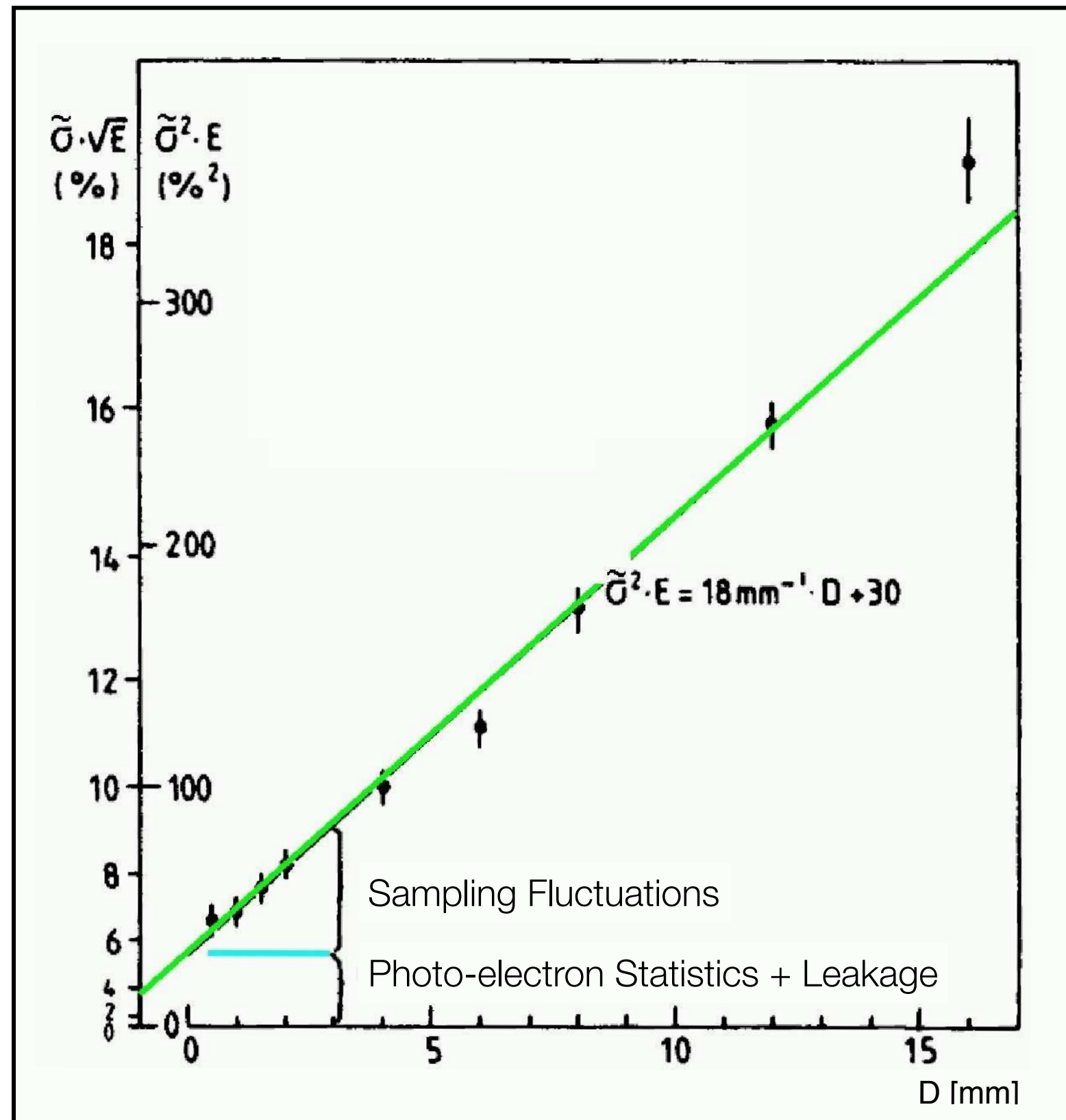
Choose: E_c small (large Z)
 t_{abs} small (fine sampling)

where F takes detector threshold effects into account ...

Measure energy resolution of a sampling calorimeter for different absorber thicknesses

Sampling contribution:

$$\frac{\sigma_E}{E} = 3.2\% \sqrt{\frac{E_c [\text{MeV}] \cdot t_{\text{abs}}}{F \cdot E [\text{GeV}]}}$$



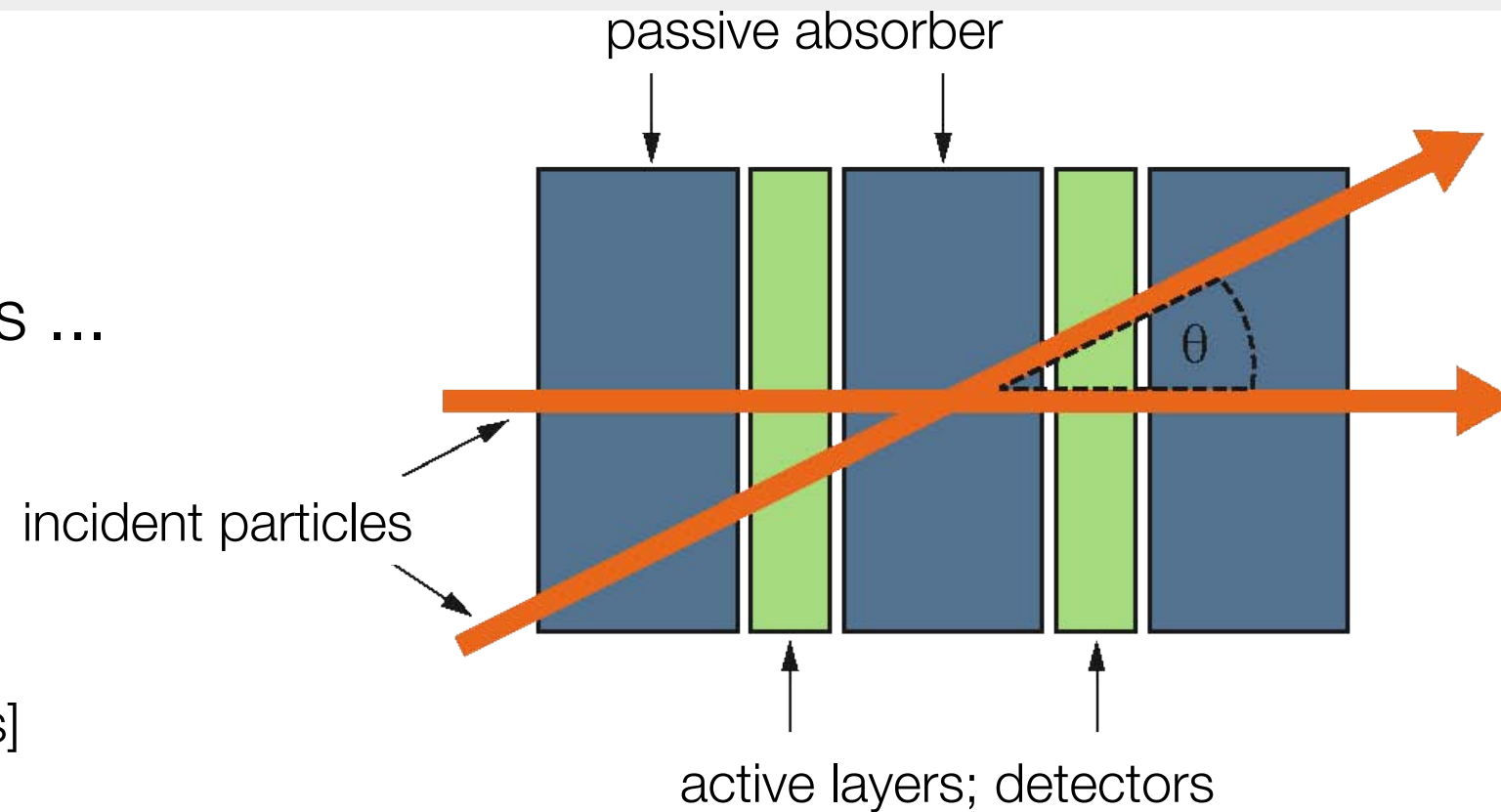
Track length fluctuations:

Due to multiple scattering particles traverse absorber at different angles ...

→ Different effective absorber thickness:

$$t_{\text{abs}} \rightarrow t_{\text{abs}} / \cos \theta$$

[Enters sampling (and Landau) fluctuations]



Landau fluctuations:

Asymmetric distribution of energy deposits in thin active layers yields correction [Landau instead of Gaussian distribution]:

$$\frac{\sigma_E}{E} = \frac{1}{\sqrt{N_{\text{ch}}}} \cdot \frac{3}{\ln(k \cdot \delta)}$$

[semi-empirical]

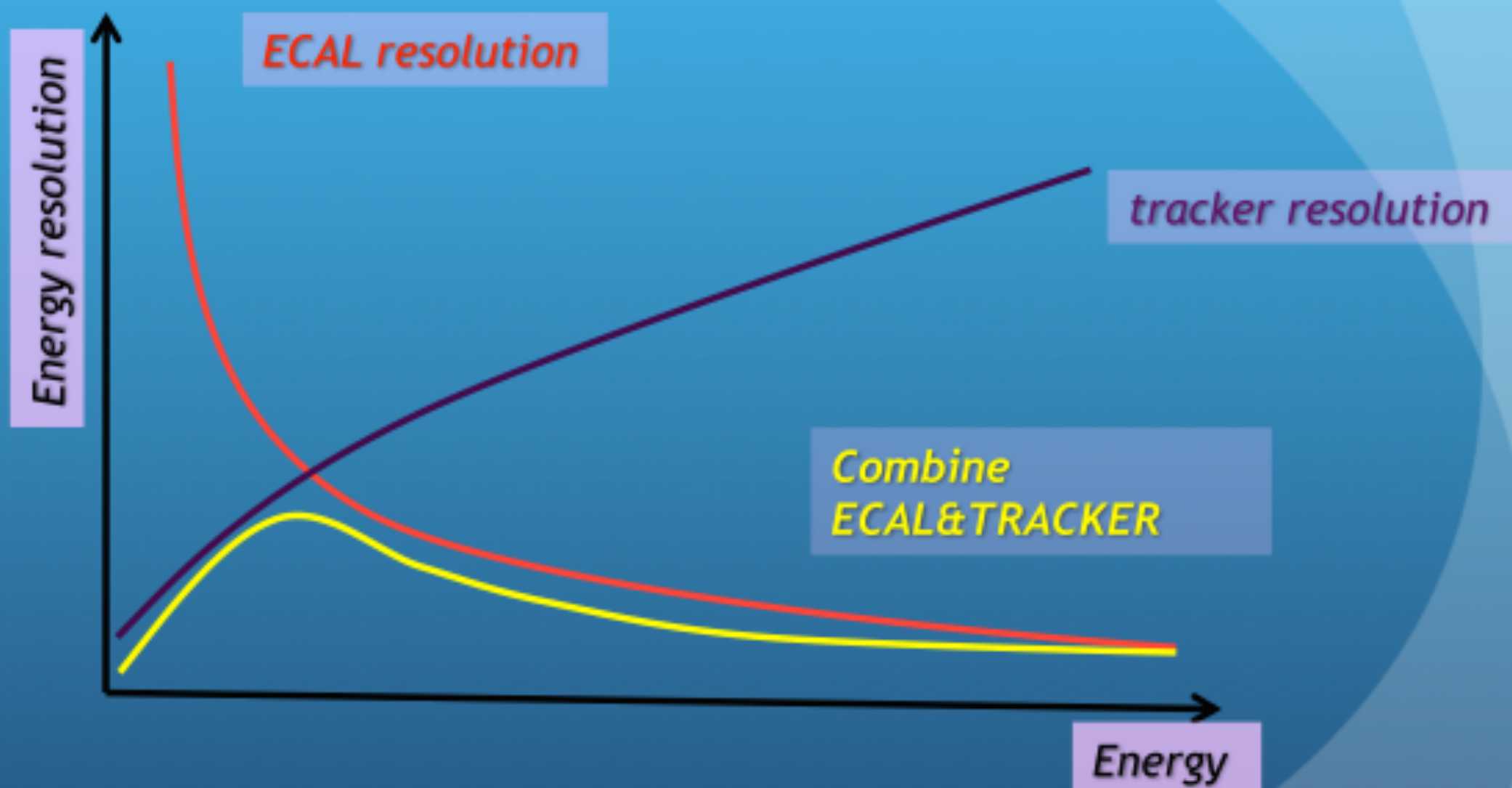
with:

- k : constant; $k = 1.3 \cdot 10^4$ if δ measured in MeV
- δ : average energy loss in active layer ('thickness')

Particle Flow Calorimeter

Particle flow principle: being able to reconstruct every individual particle in a collision event (or else) by combining efficiently subdetectors information

Requirements: good tracking ability, ECAL segmented, HCAL for ID..

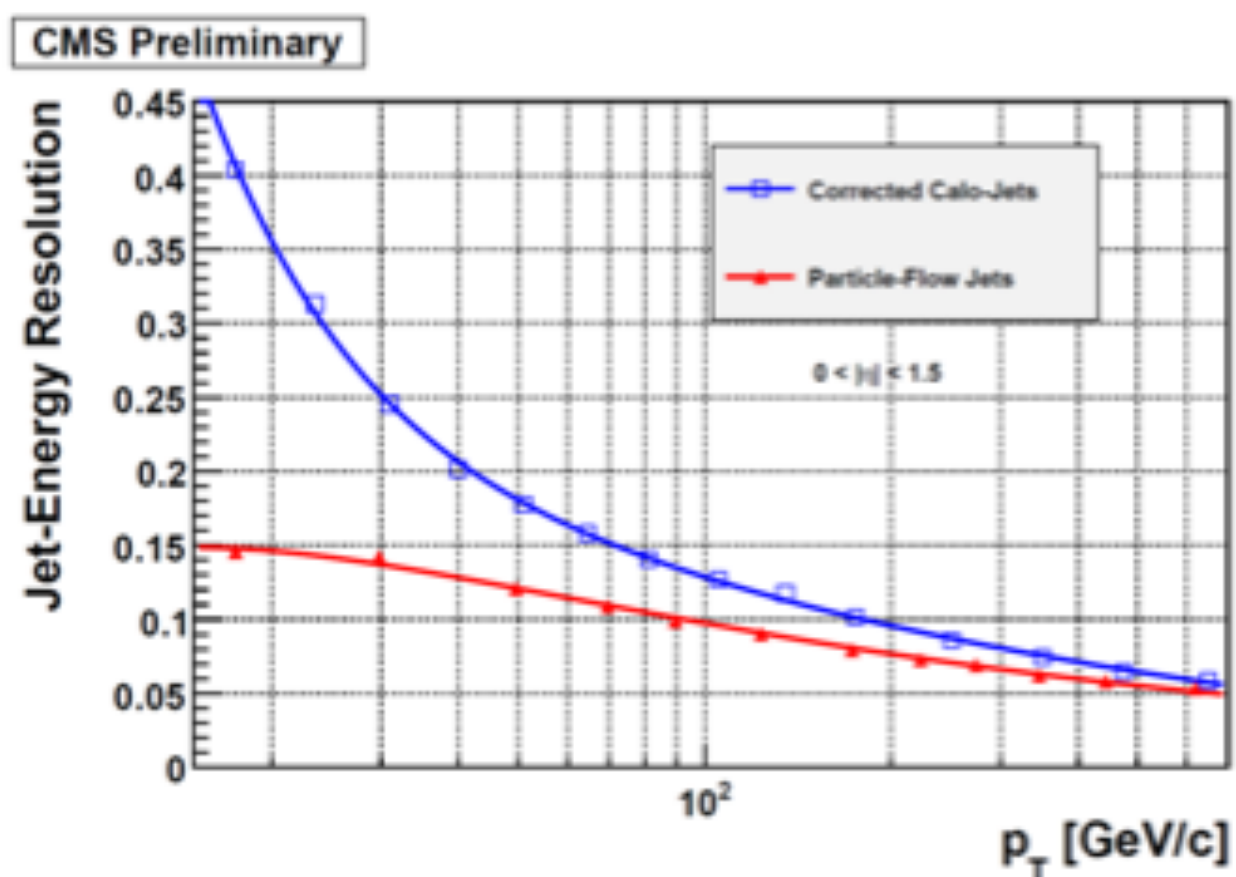


Combining subdetectors info: get a much better resolution on single object

Particle Flow Calorimeter

Particle flow algorithm: with an access to single particle 4-vectors

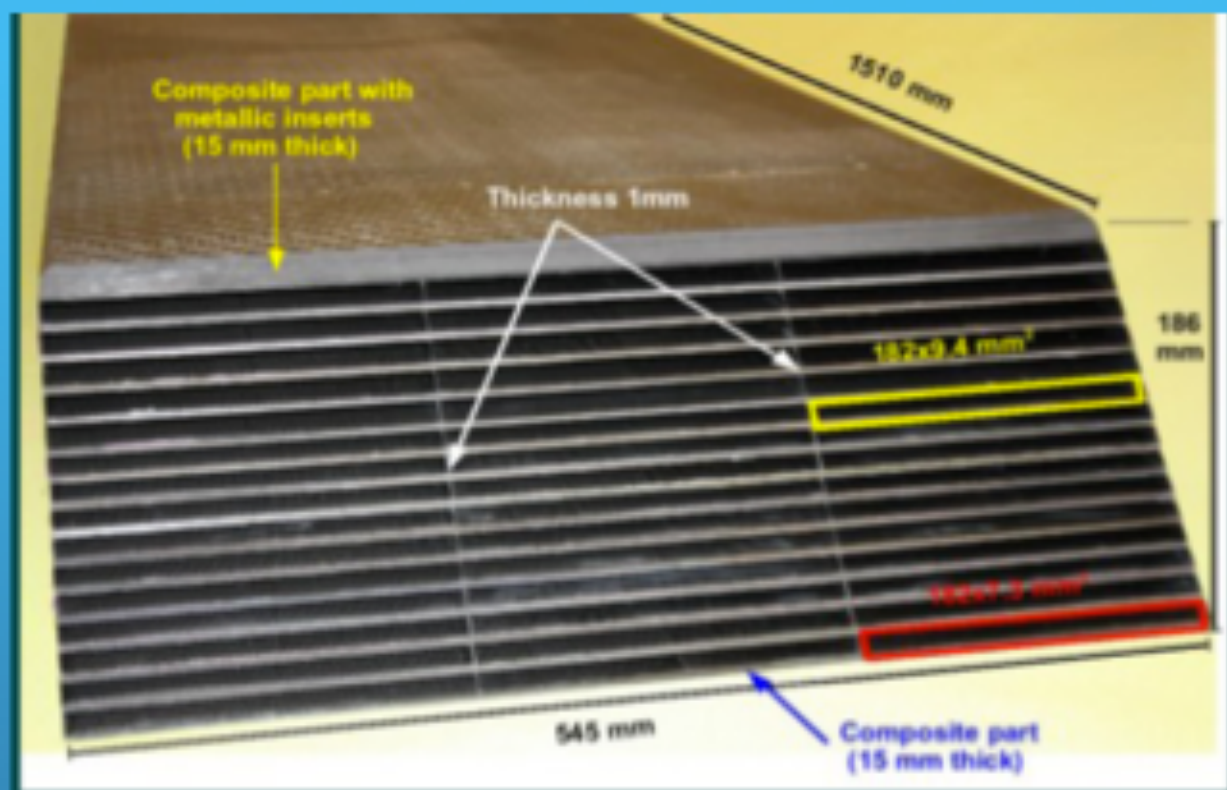
- Use **adapted calibration** for each objects electrons/photons/jets (avoid bias in energy response)
- Get the **best resolution from track** on charged particles (65% of a jet!)
- EM part measured **precisely by the ECAL** (neutral pions = 25% of jet)
- **Deduce neutral energy** from previous info (neutrals = 10% of a jet)
- Significant improvement **angular resolution**
- Correct **evaluation of missing ET** by including spiraling low energy particles



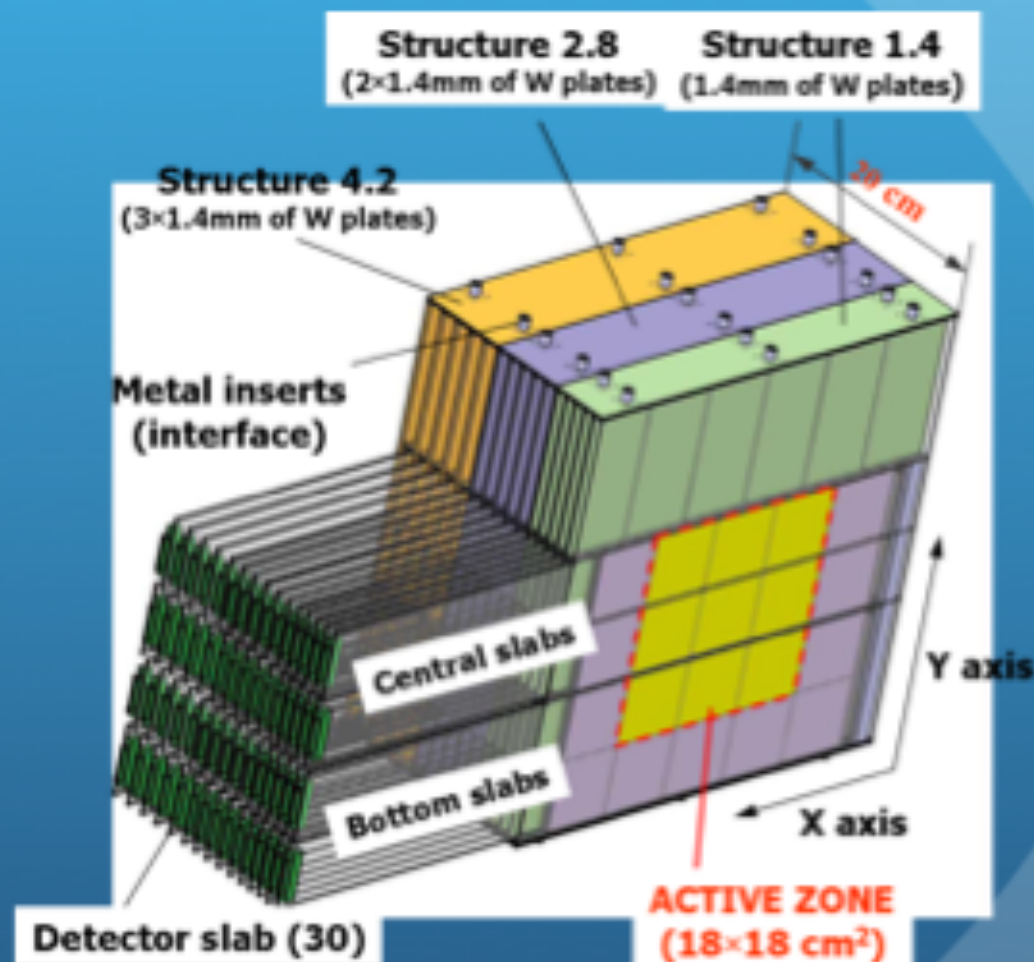
Example of performance on CMS jet energy resolution

*Can you make a PF detector?
Can you import tracking techniques into calorimetry?*

Particle Flow Calorimeter: ILC



SiW Silicon Tungstate calorimeter
 Single cell 1x1cm²
 20 cm depth for 24 X₀



Carbon-fibre/tungsten mechanical structure

Active Sensor Unit (1024 readout channels)

18x18 cm² PCB

16 readout ASICs

4 silicon sensors

(each with 256 5x5mm² pads)

Dynamic range: single MIP to

EM shower core @ 100s GeV

A hadron calorimeter shows in general different efficiencies for the detection of the hadronic and electromagnetic components ϵ_h and ϵ_e .

$$R_h = \epsilon_h E_h + \epsilon_e E_e$$

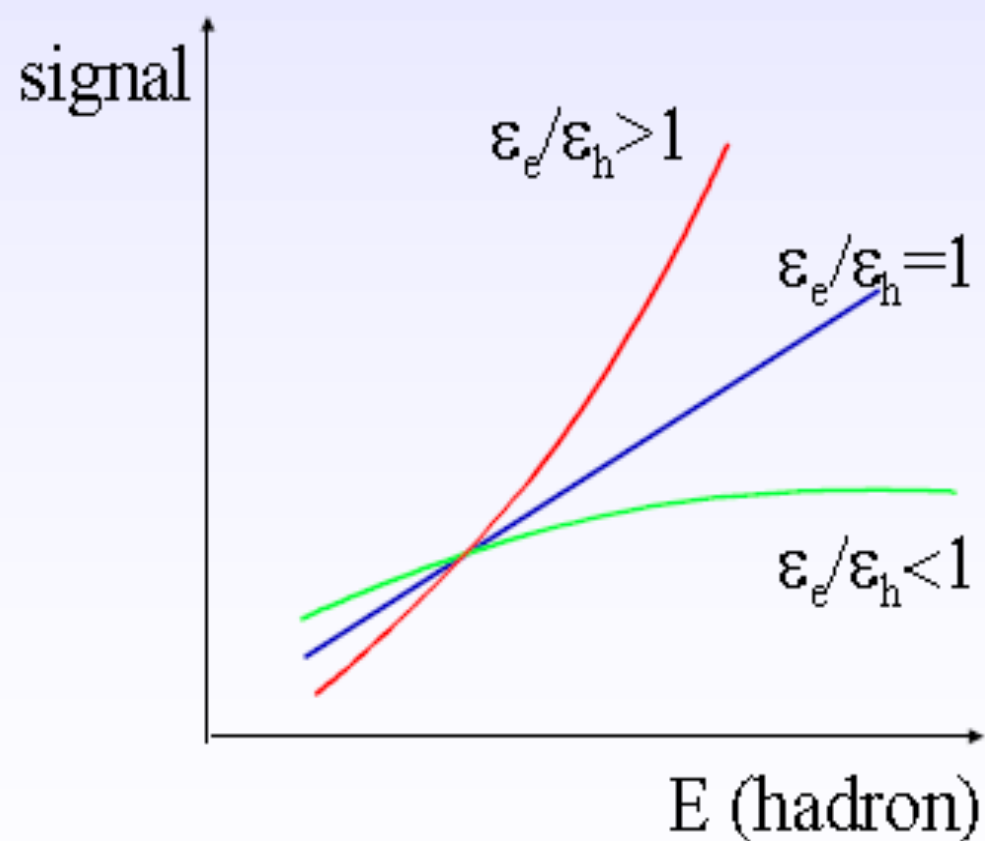
ϵ_h : hadron efficiency

ϵ_e : electron efficiency

The fraction of the energy deposited hadronically depends on the energy (remember $n(\pi^0)$)

$$\frac{E_h}{E} = 1 - f_{\pi^0} = 1 - k \ln E \text{ (GeV)} \quad k \approx 0.1$$

→ Response of calorimeter to hadron shower becomes non-linear



Energy resolution degraded !

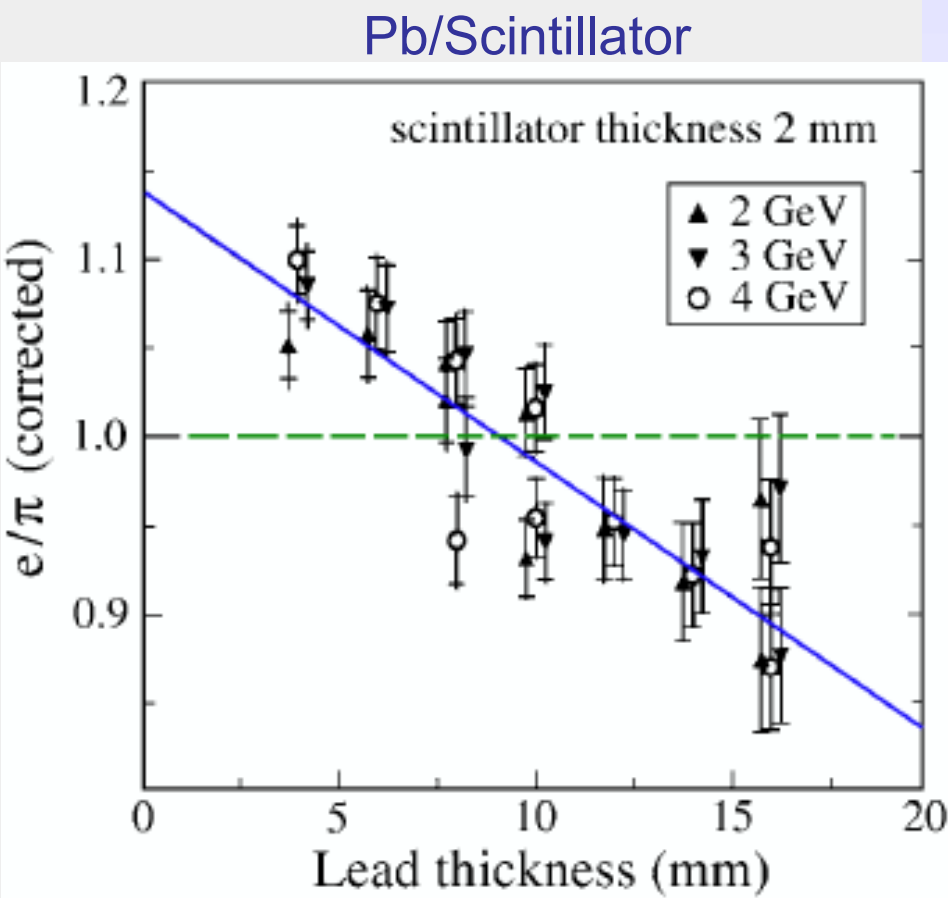
$$\frac{\sigma(E)}{E} = \frac{a}{\sqrt{E}} + b \cdot \left| \frac{\epsilon_e}{\epsilon_h} - 1 \right|$$

TO BACKUP

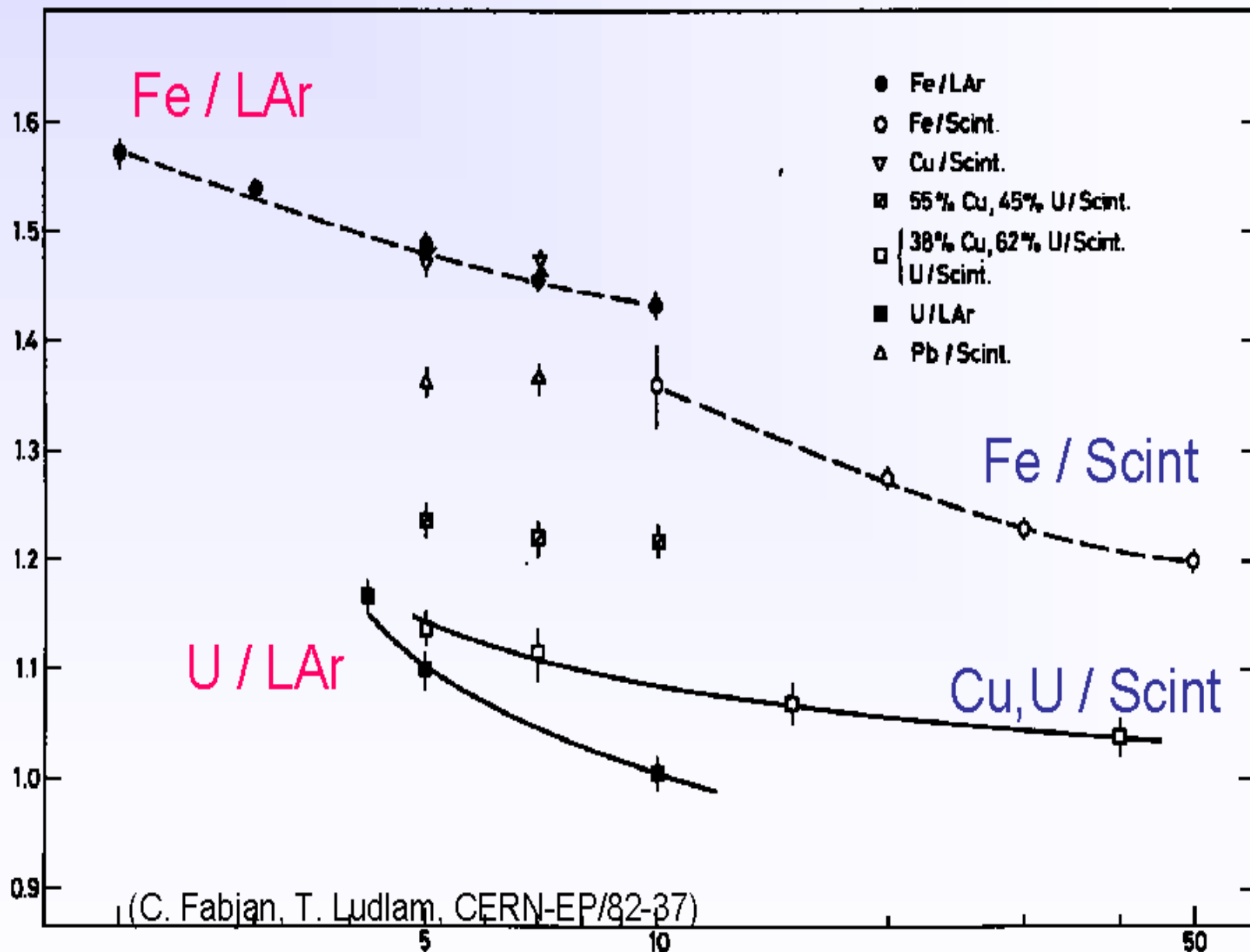
increase ε_h : use Uranium absorber \rightarrow amplify neutron and soft γ component by fission + use hydrogeneous detector \rightarrow high neutron detection efficiency

decrease ε_e : combine high Z absorber with low Z detectors. Suppressed low energy γ detection ($\sigma_{\text{photo}} \propto Z^5$)

offline compensation : requires detailed fine segmented shower data \rightarrow event by event correction.



signal ratio electrons / hadrons



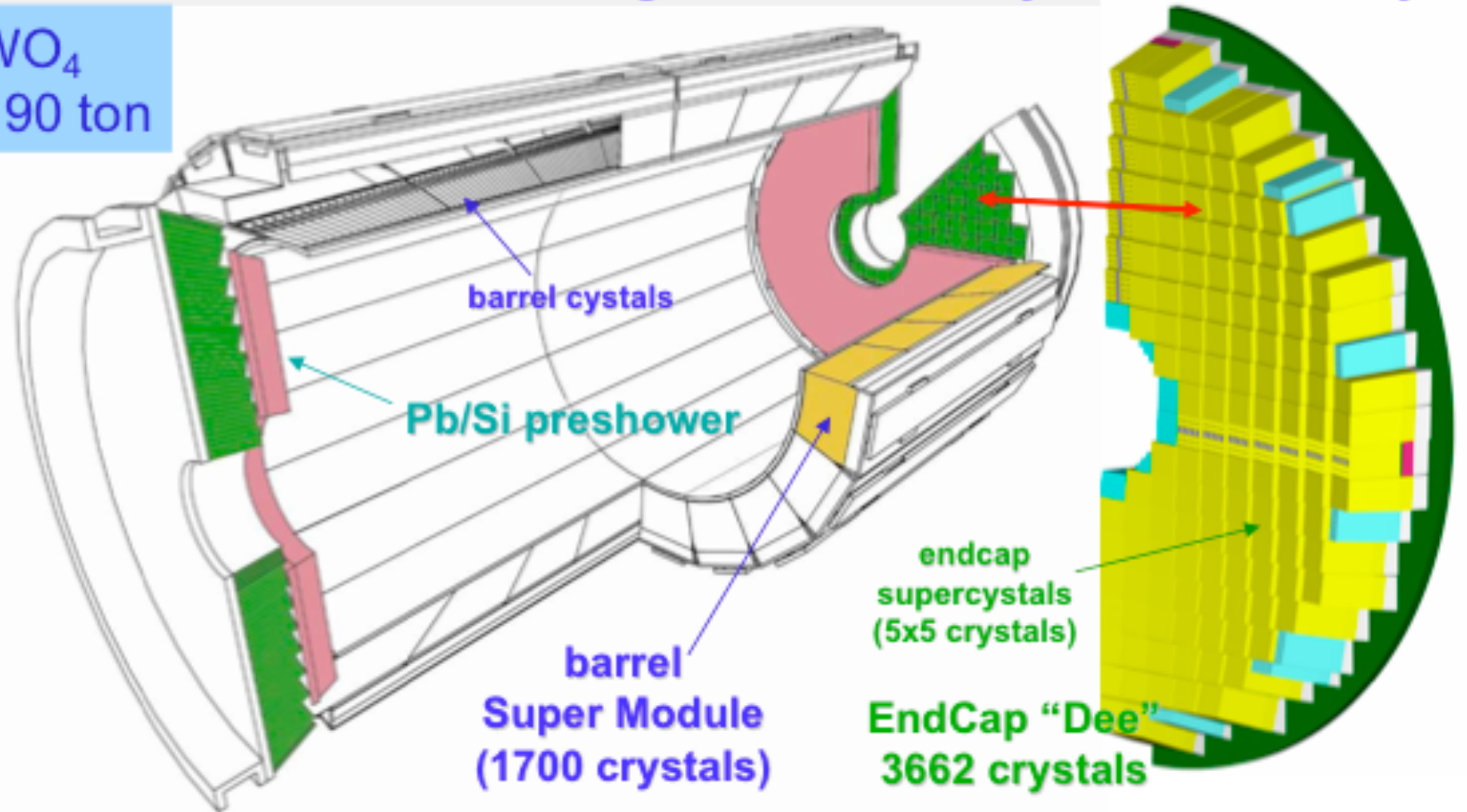
(C. Fabjan, T. Ludlam, CERN-EP/82-37)

Sampling fraction can be tuned to achieve compensation

Precision electromagnetic calorimetry: 75848 PWO crystals

PWO: PbWO_4
about 10 m^3 , 90 ton

Previous
Crystal
calorimeters:
max 1 m^3

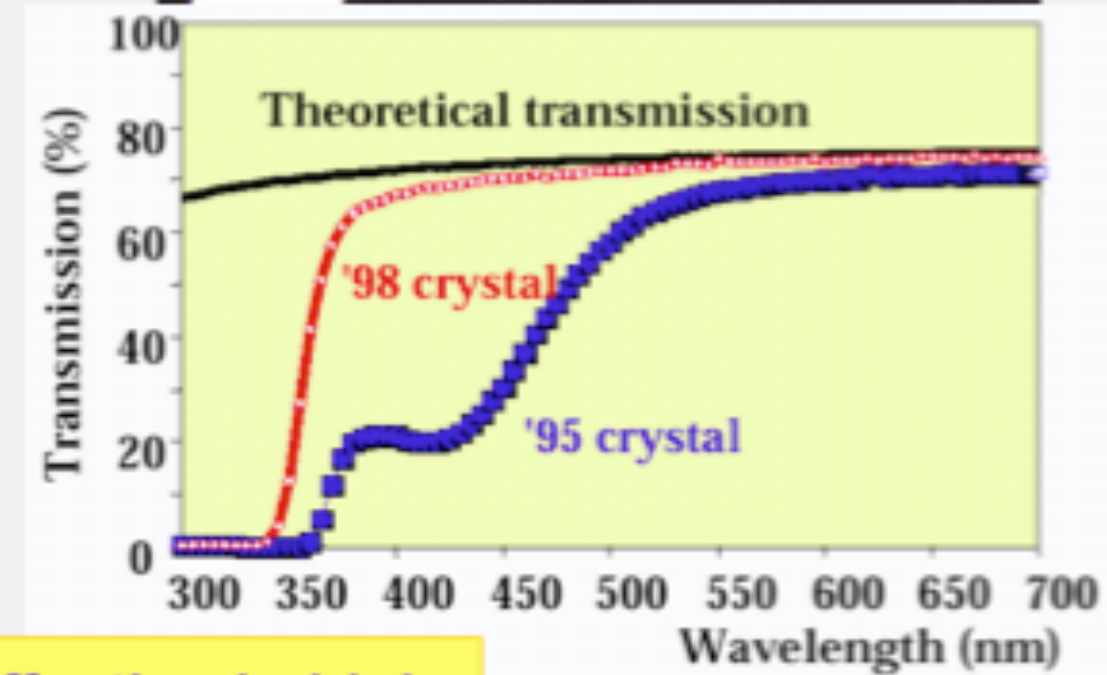
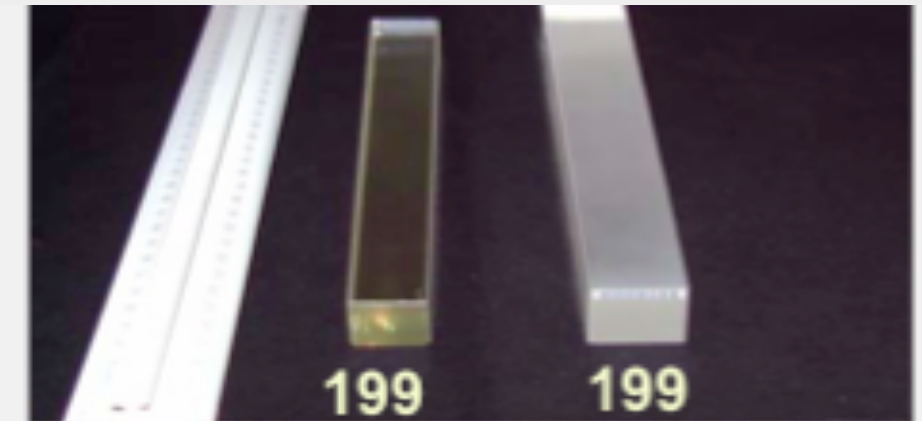


Barrel: $|\eta| < 1.48$
36 Super Modules
61200 crystals ($2 \times 2 \times 23 \text{ cm}^3$)

EndCaps: $1.48 < |\eta| < 3.0$
4 Dees
14648 crystals ($3 \times 3 \times 22 \text{ cm}^3$)

Lead Tungstate Crystals (PWO) for CMS

Parameter		Value
Radiation length	cm	0.89
Moliere radius	cm	2.2
Hardness	Moh	4
Refractive index		2.3
Peak emission	nm	440
% of light in 25 ns		80%
Light yield (23 cm)	γ/MeV	100

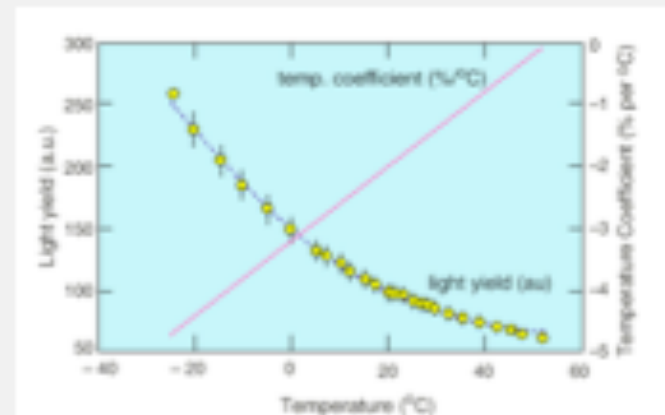


Very low light output

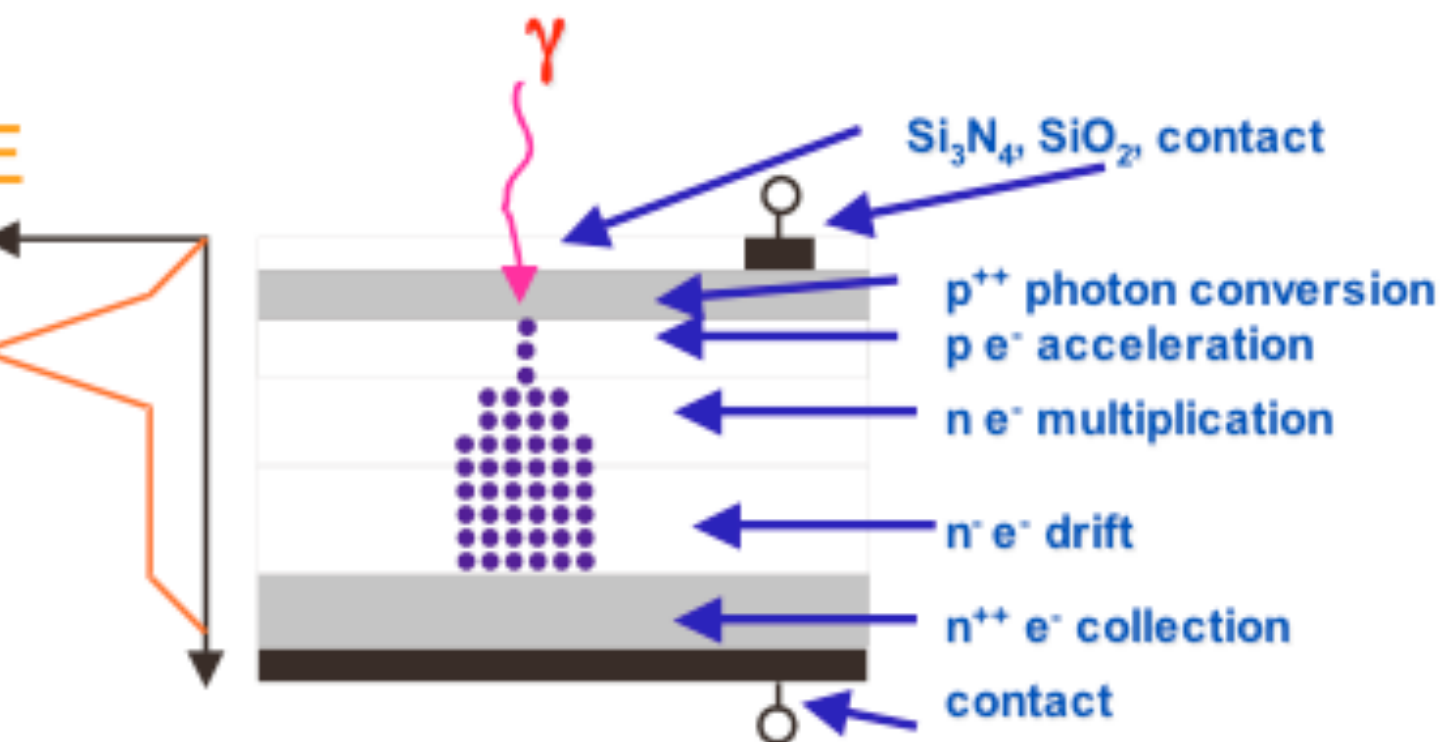
Hard light extraction

Very effective in high energy γ containment

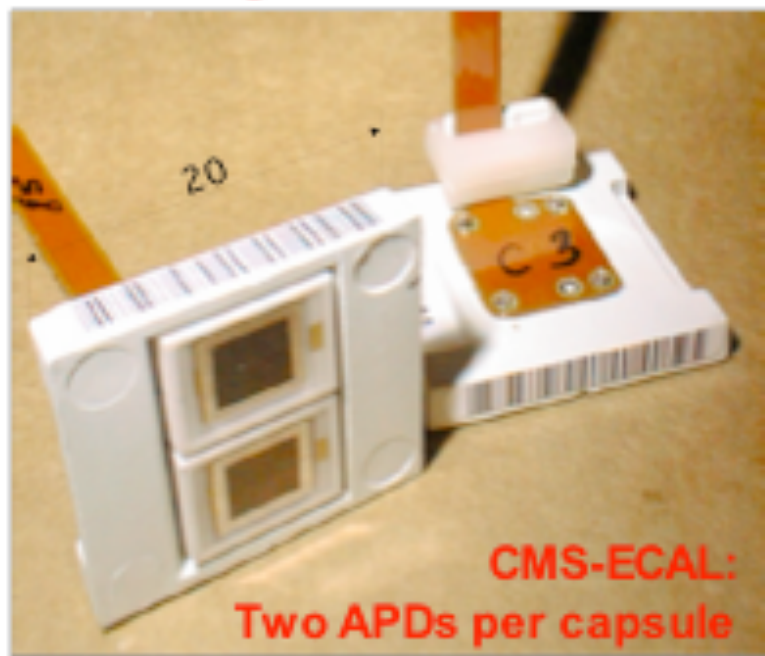
T dependent: $-2\%/^{\circ}\text{C}$



23 cm to contain em showers!



Internal gain=50 for $V=380 \text{ V}$



$$N_{\text{photons}}/\text{MeV} \times \text{Light-collection-efficiency (2 APDs)} \times \text{QE} \approx 5 \text{ photo-electrons/MeV (in CMS-ECAL)}$$

Drawback of PbWO_4 : Low light yield

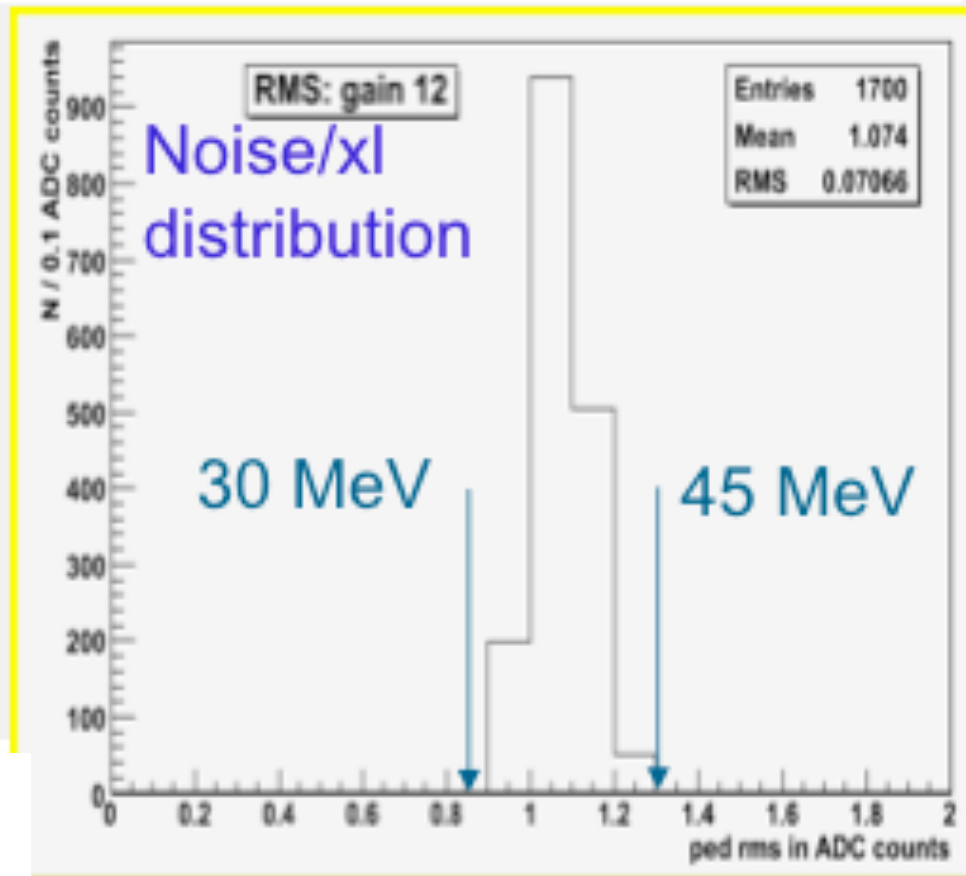
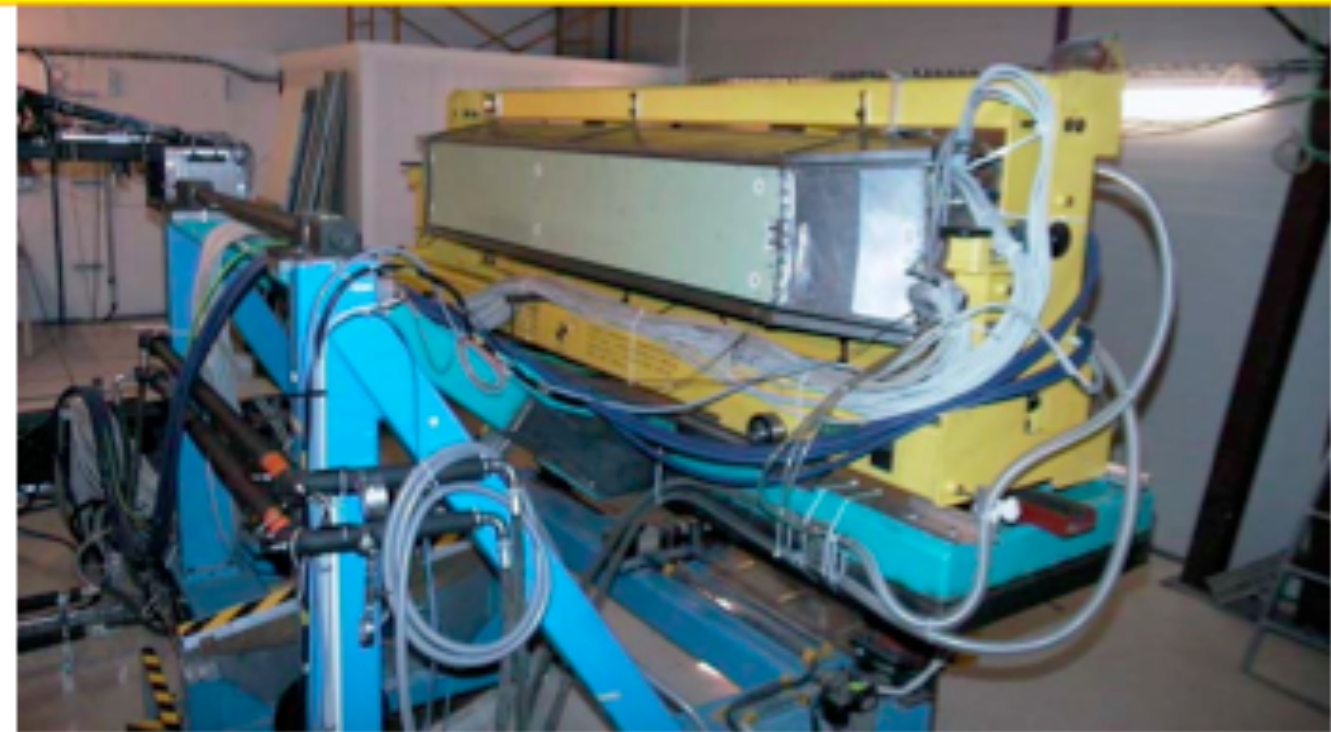
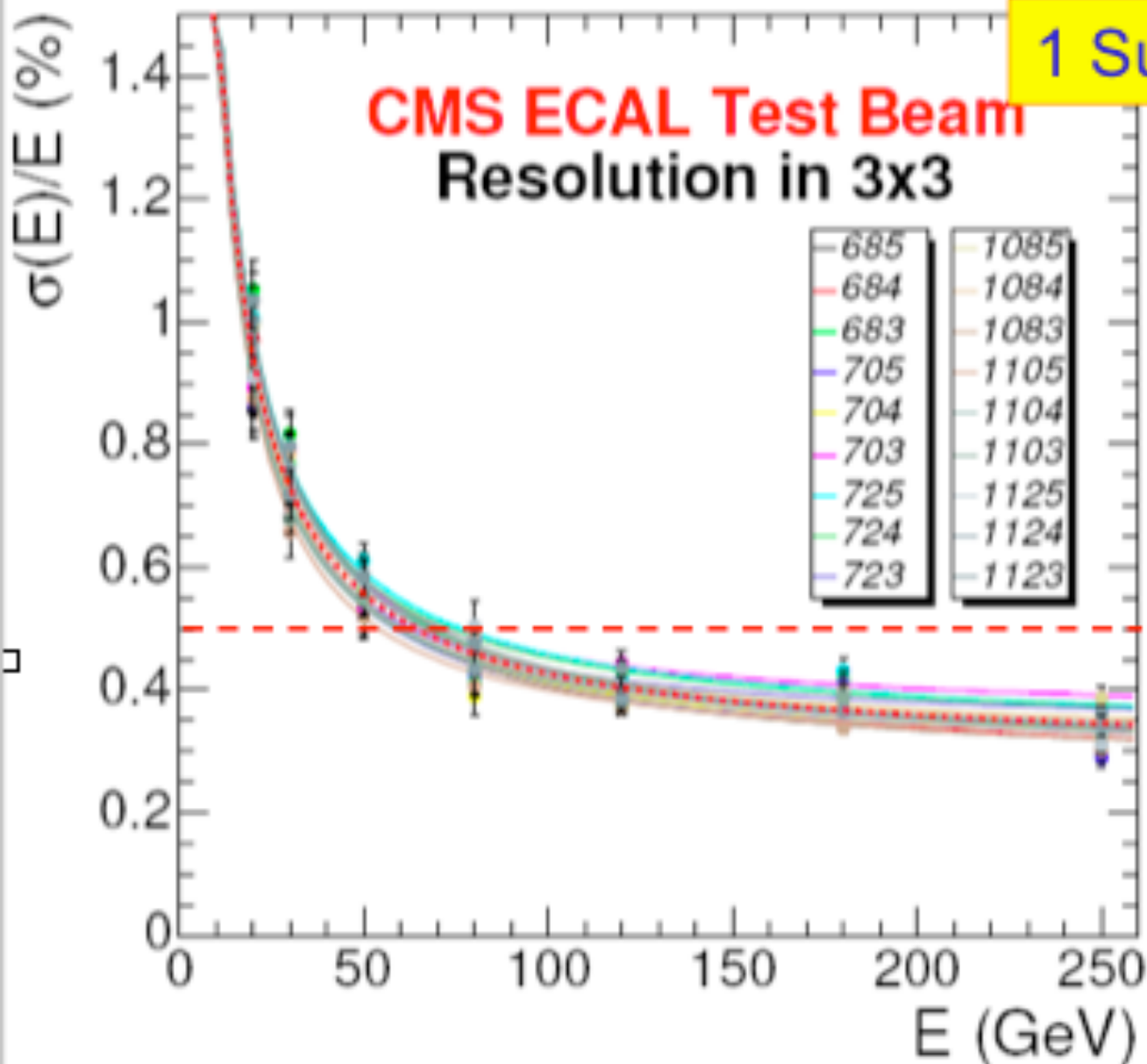
→ Need photodetectors with intrinsic gain (+radiation hard, +insensitive to magnetic field)

Choice for CMS-ECAL Barrel and ALICE PHOS: Avalanche Photo Diodes (APD)

- rad. hard, fast (few ns)
- Quantum efficiency (QE, photon conversion into electrons) : $\sim 75\%$ at 430 nm
- Active Area : 25 mm^2
- Excess noise factor $F \approx 2$
- **But :**
strong sensitivity of gain to voltage and temperature variations!

→ Good stability needed!

1 Super Module 1700 xl on test beam in 2004



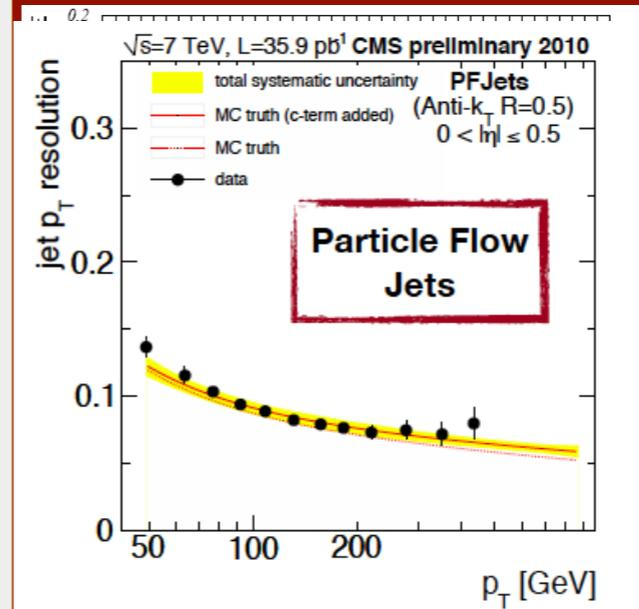
$$\frac{\sigma}{E} = \frac{2.8\%}{\sqrt{E(\text{GeV})}} \oplus \frac{125}{E(\text{MeV})} \oplus 0.3\%$$



CMS

5 cm brass / 3.7 cm scint.
Embedded fibres, HPD readout

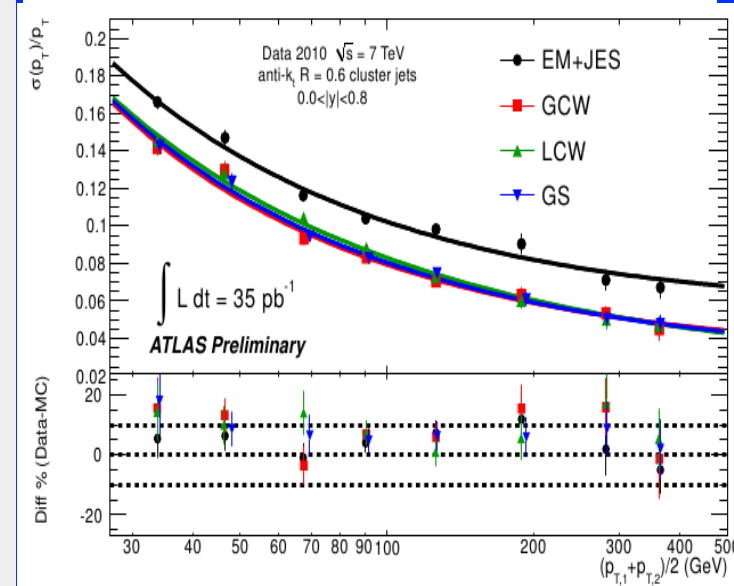
- CMS**
- HCAL only
 $\sigma/E = (93.8)\%/\sqrt{E} \oplus (7.4)\%$
 - ECAL+HCAL
 $\sigma/E = (82.6)\%/\sqrt{E} \oplus (4.5)\%$



ATLAS

14 mm iron / 3 mm scint.
sci. fibres, read out by phototubes

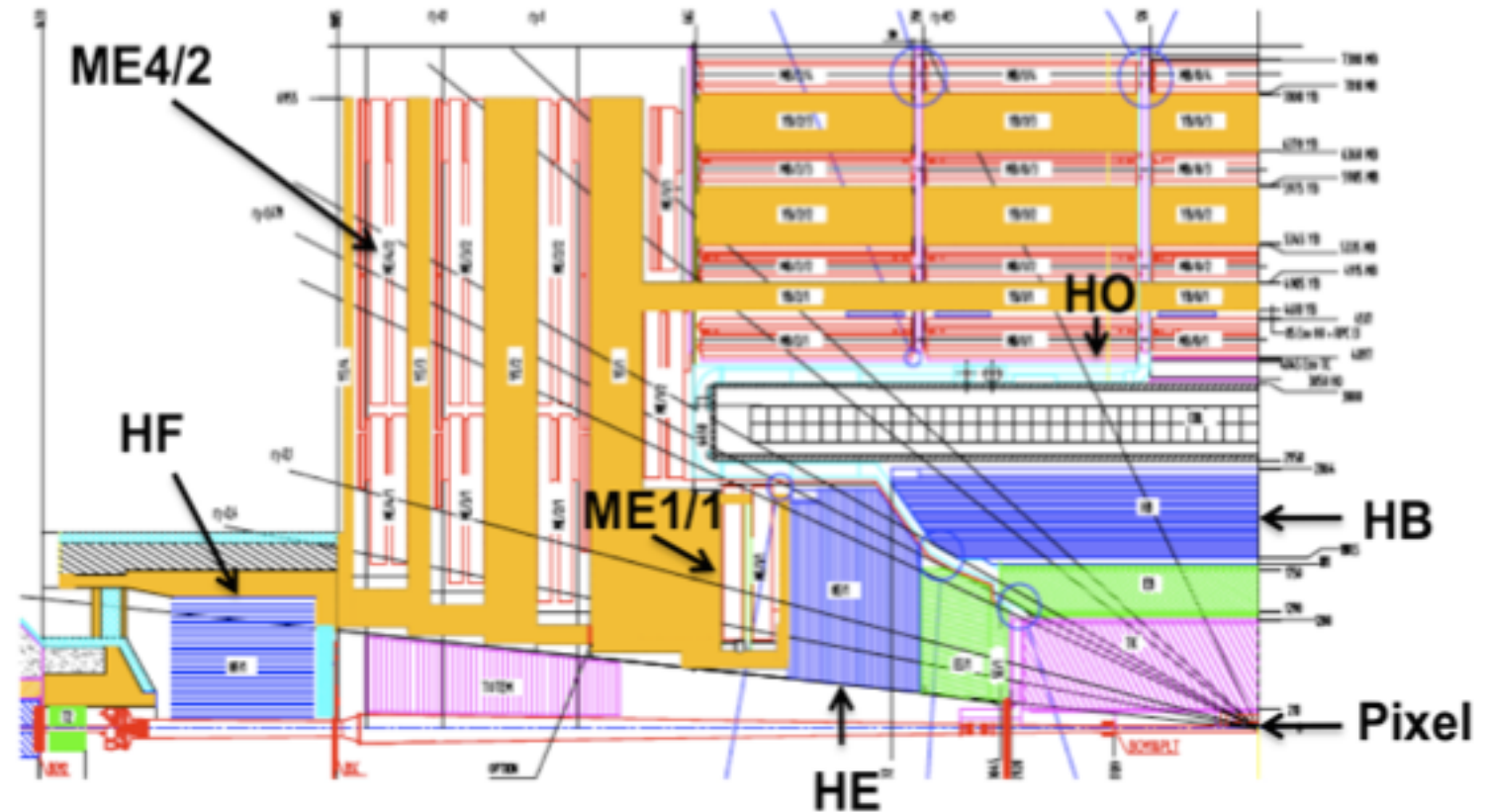
- ATLAS**
- Standalone tile calorimeter
 $\sigma/E = (52.9)\%/\sqrt{E} \oplus (5.7)\%$
 - Improved resolution using full calorimetric system (ECAL+HCAL)
 $\sigma/E = (42)\%/\sqrt{E} \oplus (2)\%$



LS1 Projects: in production

- Completes muon coverage (ME4)
- Improve muon operation (ME1), DT electronics
- Replace HCAL photo-detectors in Forward (new PMTs) and Outer (HPD → SiPM)
- DAQ1 → DAQ2

Now



Phase 1 Upgrades (TDRs)

LS2 - 2019

- New Pixels, HCAL electronics and L1-Trigger
- GEM under cost review
- Preparatory work during LS1
 - New beam pipe
 - Install test slices (*Pixel (cooling), HCAL, L1-trigger*)
 - Install ECAL optical splitters
 - *L1-trigger upgrade, transition to operations*

Phase 2: HL-LHC

LS3 - 2023

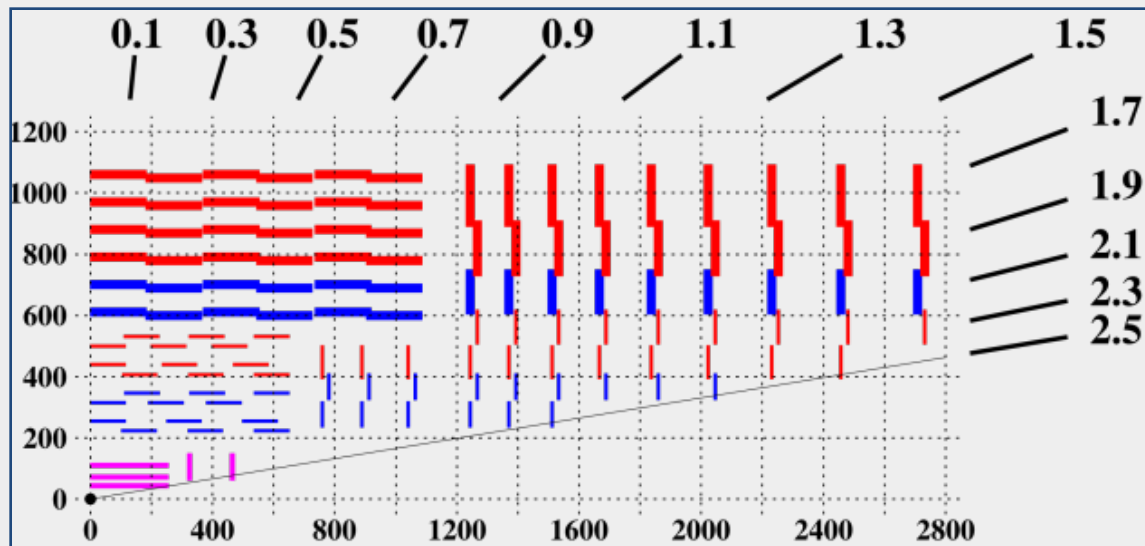
- Tracker Replacement, Track Trigger
- Forward : Calorimetry and Muons and tracking
- Further Trigger upgrade
- Further DAQ upgrade
- Shielding/beampipe for higher aperture

LS1

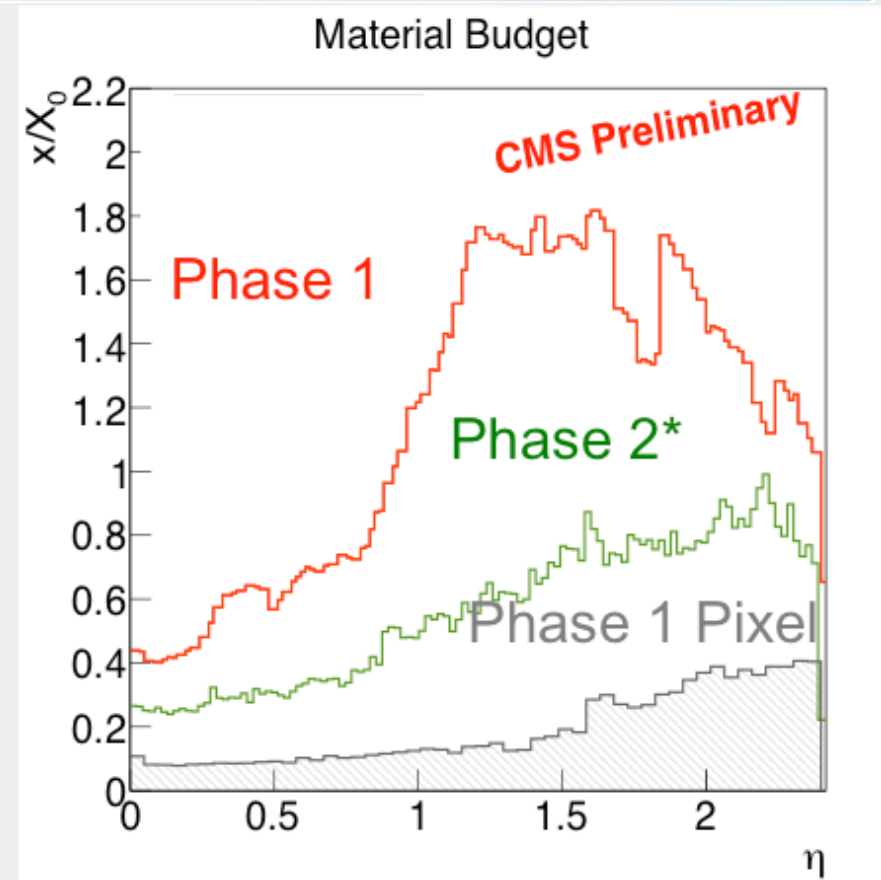
LS2

LS3





Current CMS Silicon Tracker



Proposed CMS Phase 2 tracker for 2015

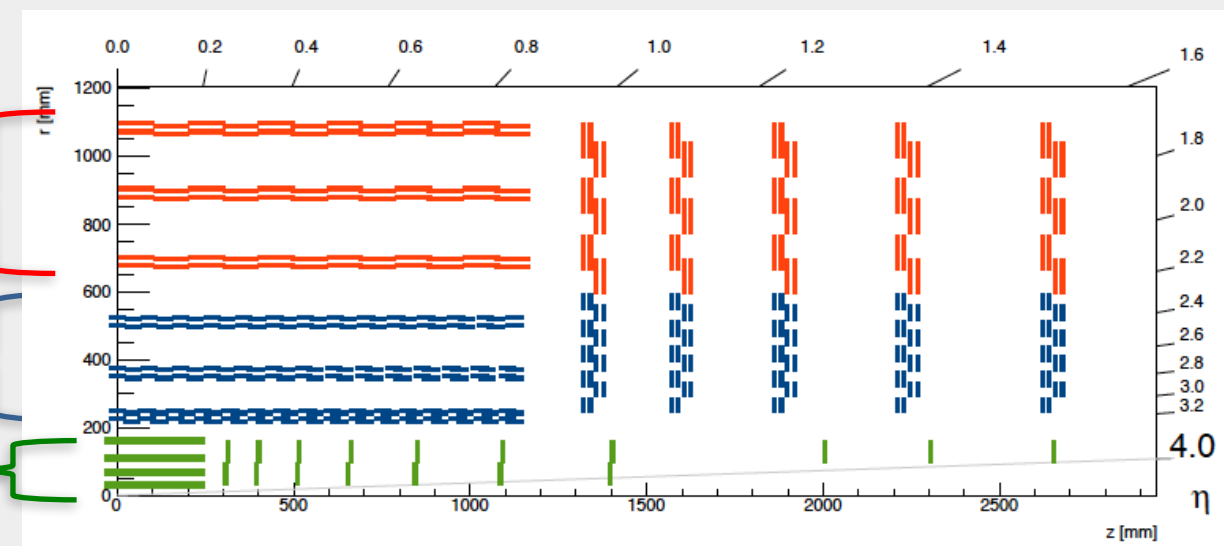
Requirements

- Radiation tolerance
- Increased granularity
- Improved 2-track separation
- Reduced material
- Robust pattern recognition
- Support for L1 trigger upgrade
- Extended tracking acceptance

Strip/Strip modules SS (pairs of strip sensors)

Strip/Pixel modules PS

Pixel modules



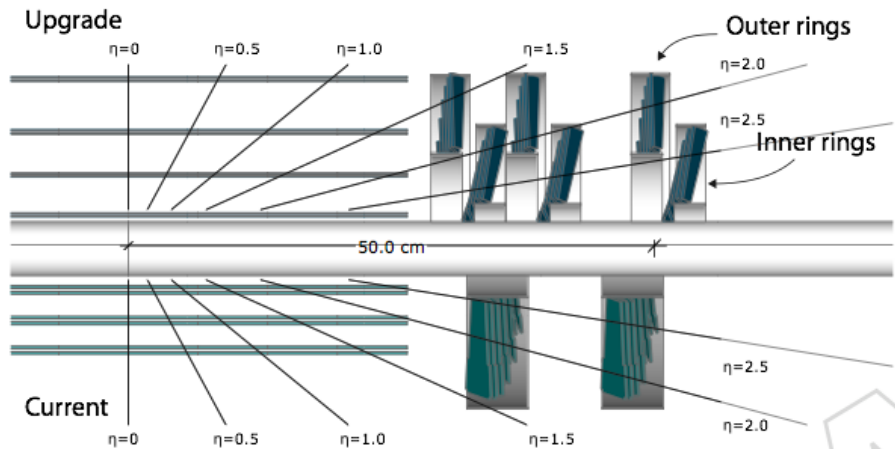
Inner Tracker, new Disks to $\eta=4$



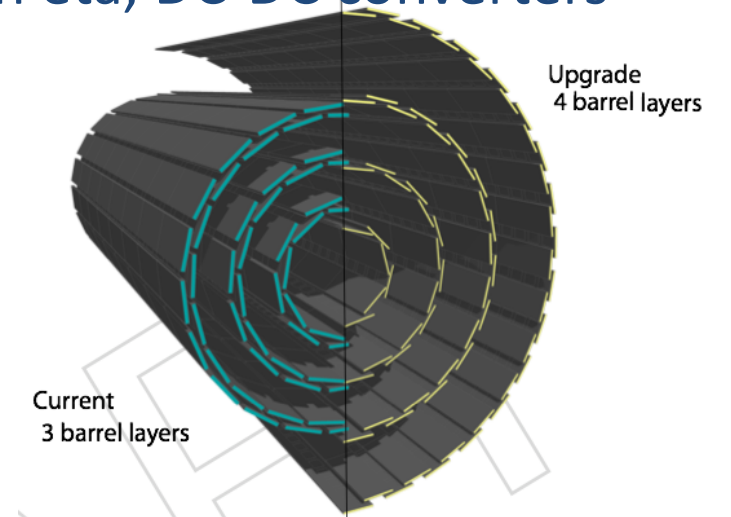
New pixel detector (EYETS)

Features of New Design

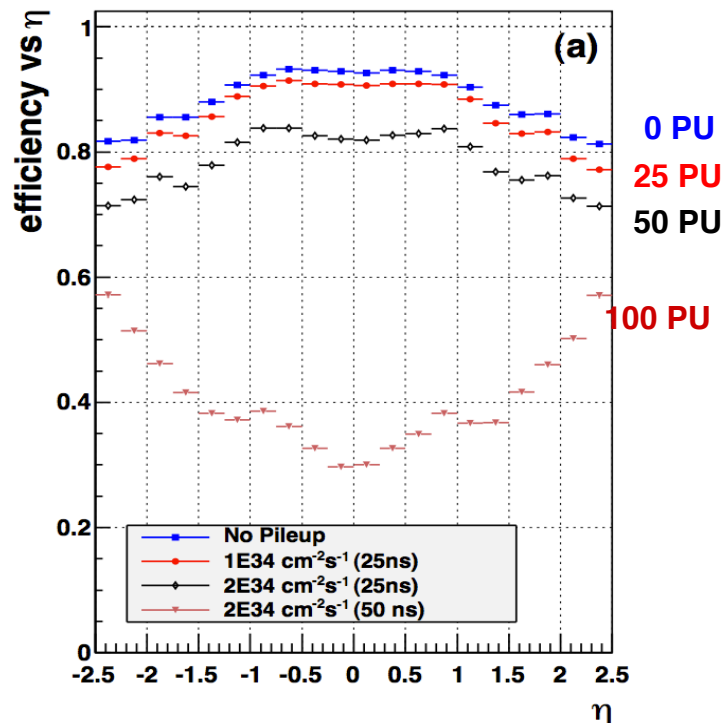
- Robust design: 4 barrel layers and 3 endcap disks at each end
- Smaller inner radius (new beampipe), large outer
- New readout chip with expanded buffers, embedded digitization and high speed data link
- Reduced mass with 2-phase CO₂ cooling, electronics moved to high eta, DC-DC converters



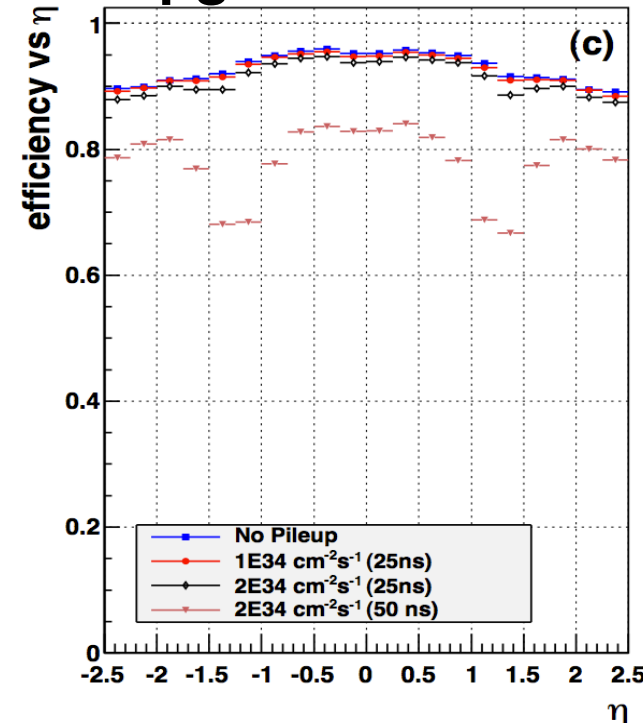
Will be installed
(2016-2017)



current detector



upgrade detector



Using same Higgs selections as 2012

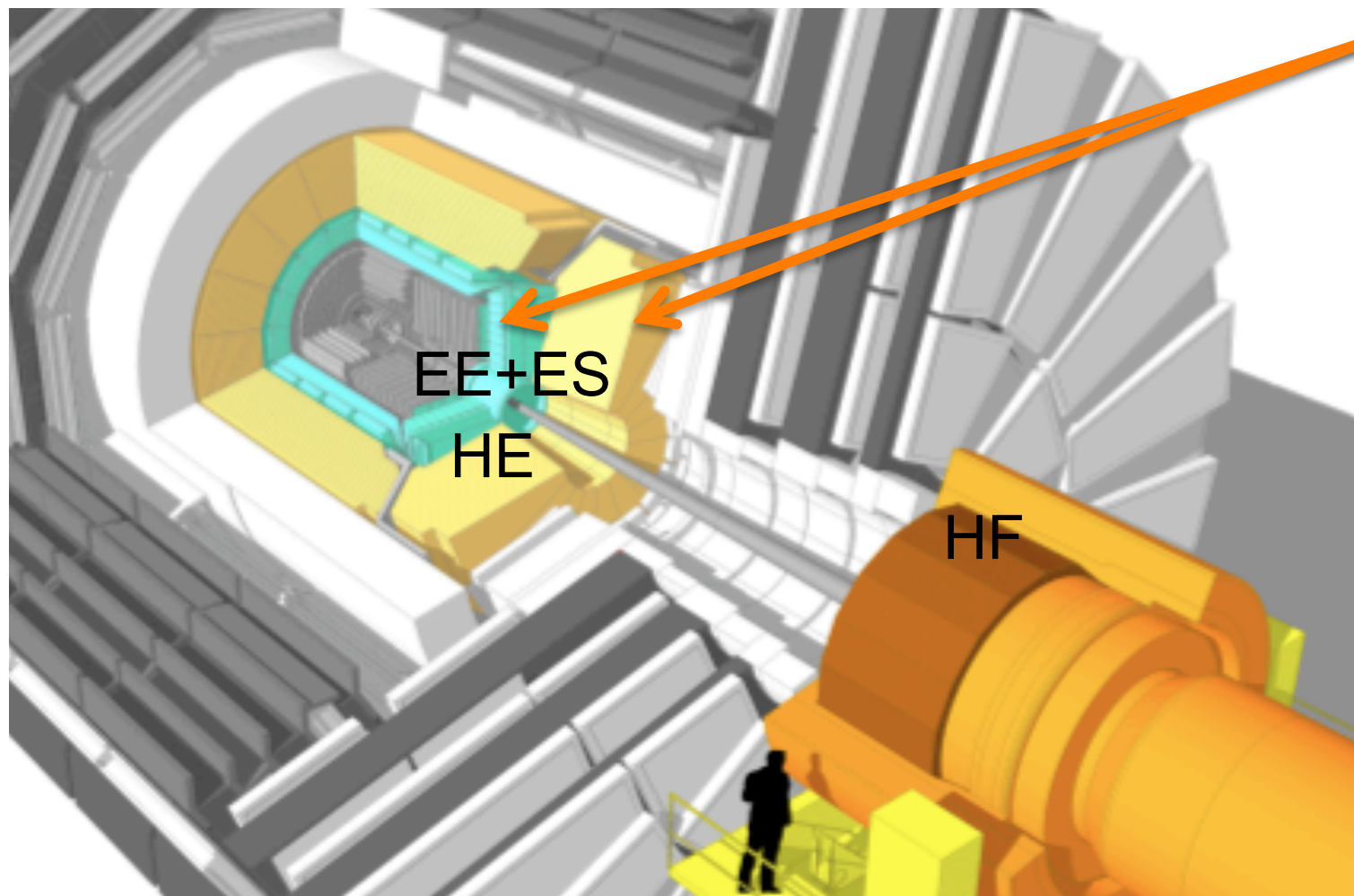
Significant gain in signal reconstruction efficiency:

H → 4μ	+41%
H → 2μ2e	+48%
H → 4e	+51%

Primary vertex resolution improved by ~1.5 - 2

Endcap calorimeters: longevity appraisal and upgrade plan

- *Substantial* performance degradation in the ECAL and HCAL endcaps
- *Moderate* damage in the ECAL and HCAL barrel
 - Increase of APD dark current in ECAL will require mitigation
- Moderate degradation in HF (operable throughout Phase II)



- Replacement/upgrade of both ECAL and HCAL endcaps in LS3
- Upgrade of the ECAL FE electronics: 40 MHz data stream (barrel)
- Mitigation of the APD current noise **needed**
 - FE with faster shaping time (also, improved timing, spike rejection)
 - Cooling of the barrel

ECAL: PbWO_4 crystals

HB/HE: Sci Tiles/WLS

HF: Quartz fibre Calo

High Granularity Calorimeter (HGCAL)

- High Granularity Calorimeter

- Fine depth segmentation

ECAL: ~33 cm, 25 X_0 , 1 λ

30 layers Si separated by lead/Cu

HCAL: ~66 cm, 3.5 λ

12 planes of Si separated by absorber

- 9 Mch & 660 m² Si

- Back HCAL as HE re-build 5 λ

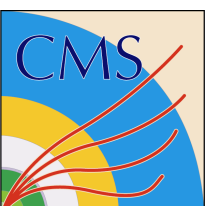
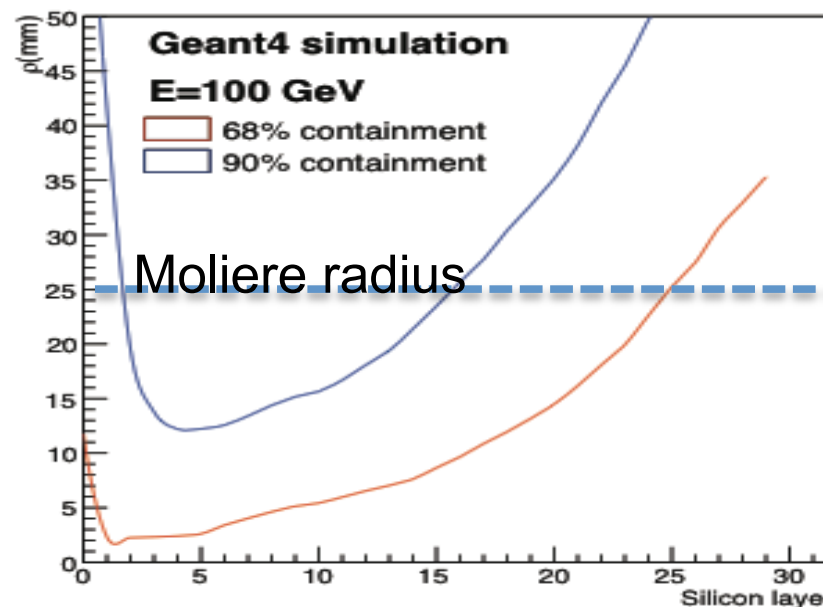
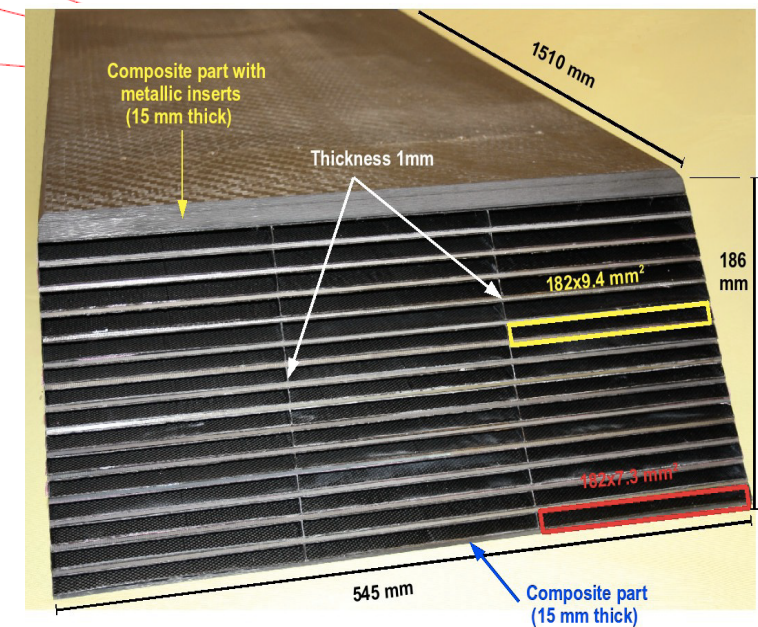
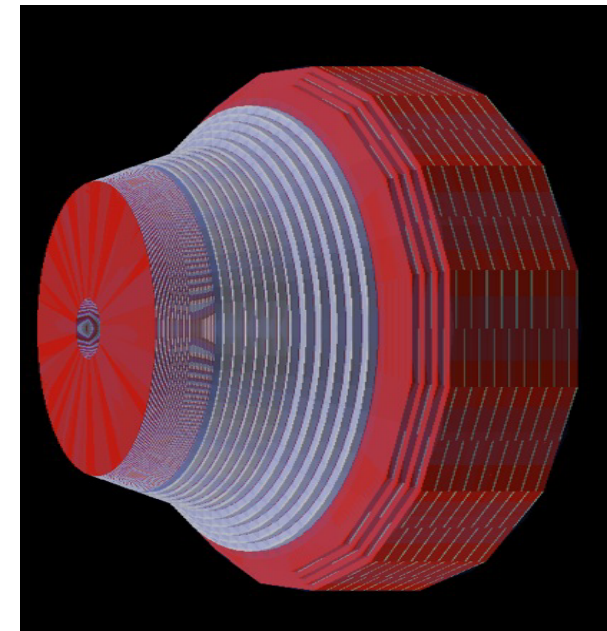
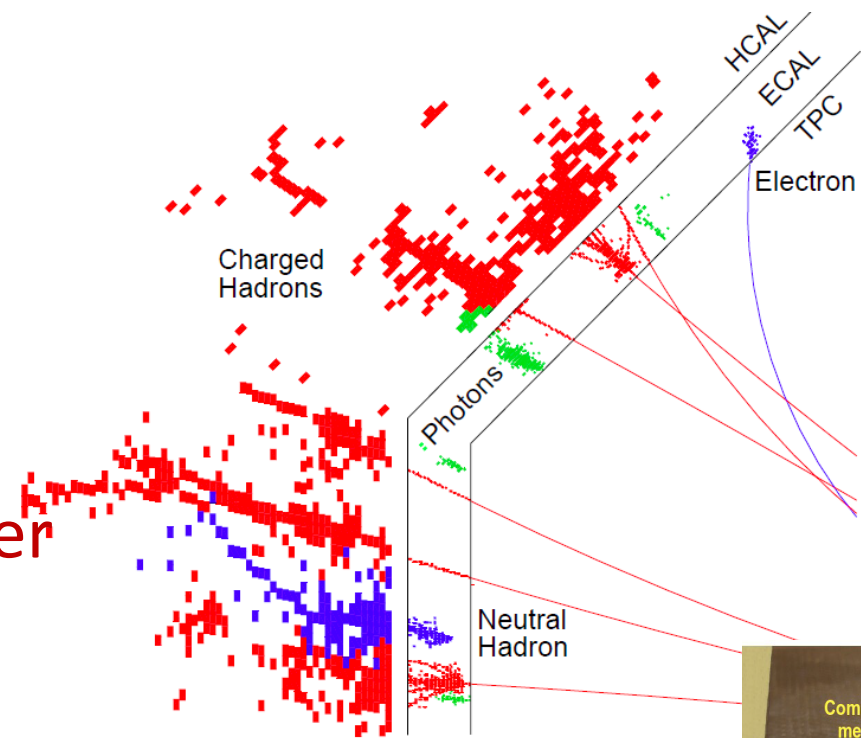
- With increased transverse granularity

- 3D measurement of the shower topology

- 25 mm Moliere radius (shower narrower before max)

– **Expected e/ γ resolution ~ 20%/sqrt(E) + \leq 1%**

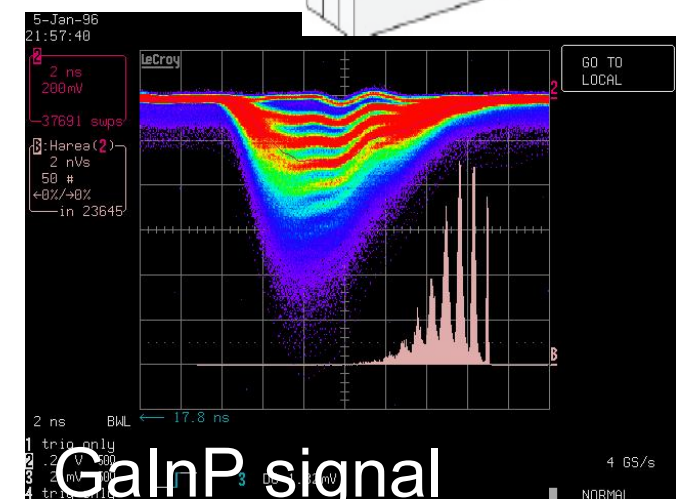
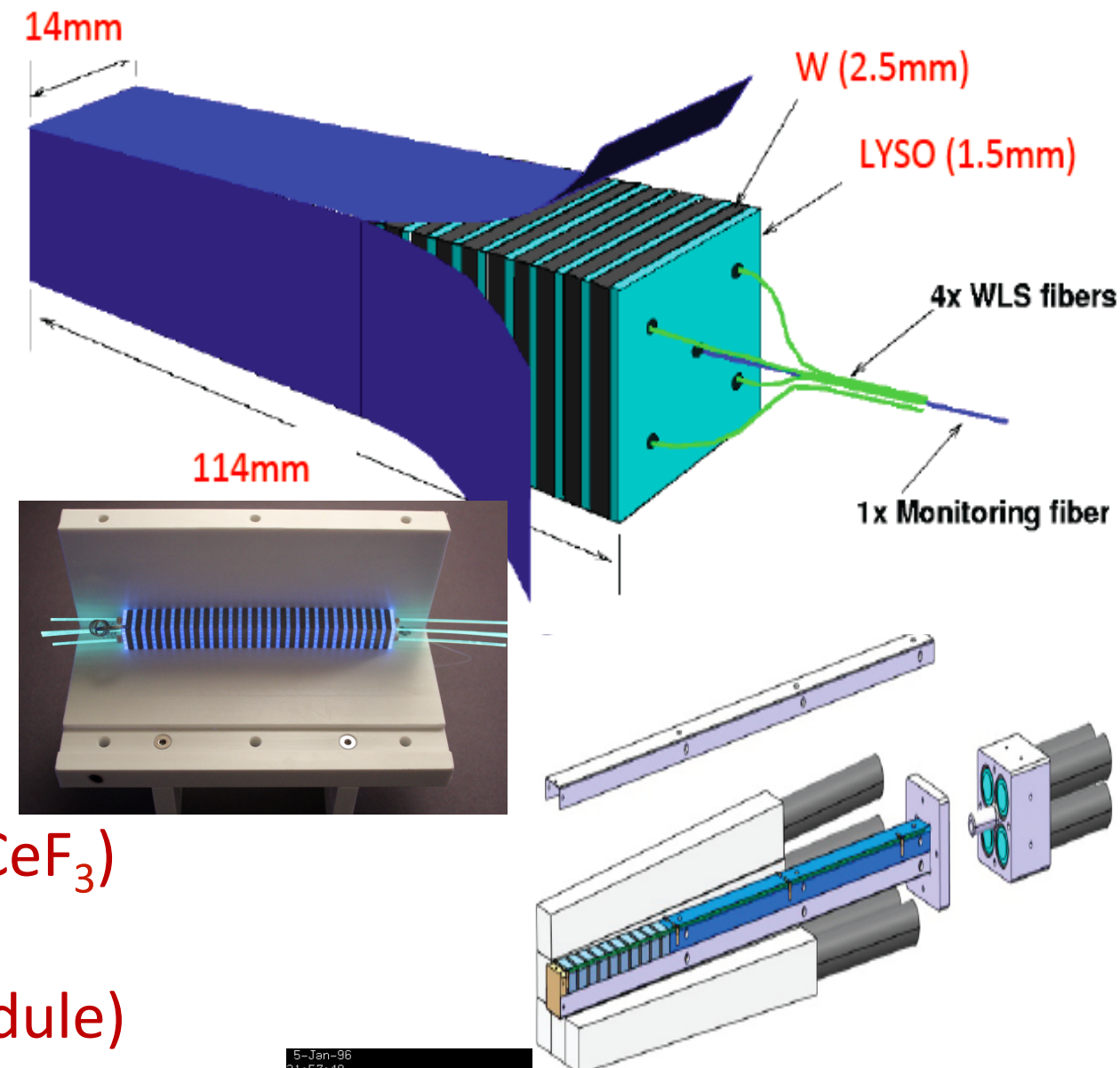
- Studies and R&D

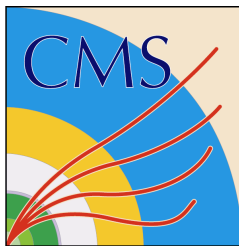


EE Shashlik – Test beam ongoing

○ EE Shashlik:

- W-absorber and Crystals LYSO (CeF₃ alternative) - 28 plates
 - Very compact (11 cm), small Moliere radius (14 mm) and fine granularity (14 mm²) to mitigate pile-up
 - high light yield for good e/γ **energy resolution ~ 10%/sqrt(E) + 1%**
- Readout with:
 - 4 WLS Capillaries (scintillating fibers CeF₃)
 - Calibration Fiber (1 per module)
 - GaInP(SiPM) Photosensors (4 per module)
- No depth segmentation but investigating:
 - Extraction of a signal near shower max with precise timing - WLS with scintillating dye on quartz core





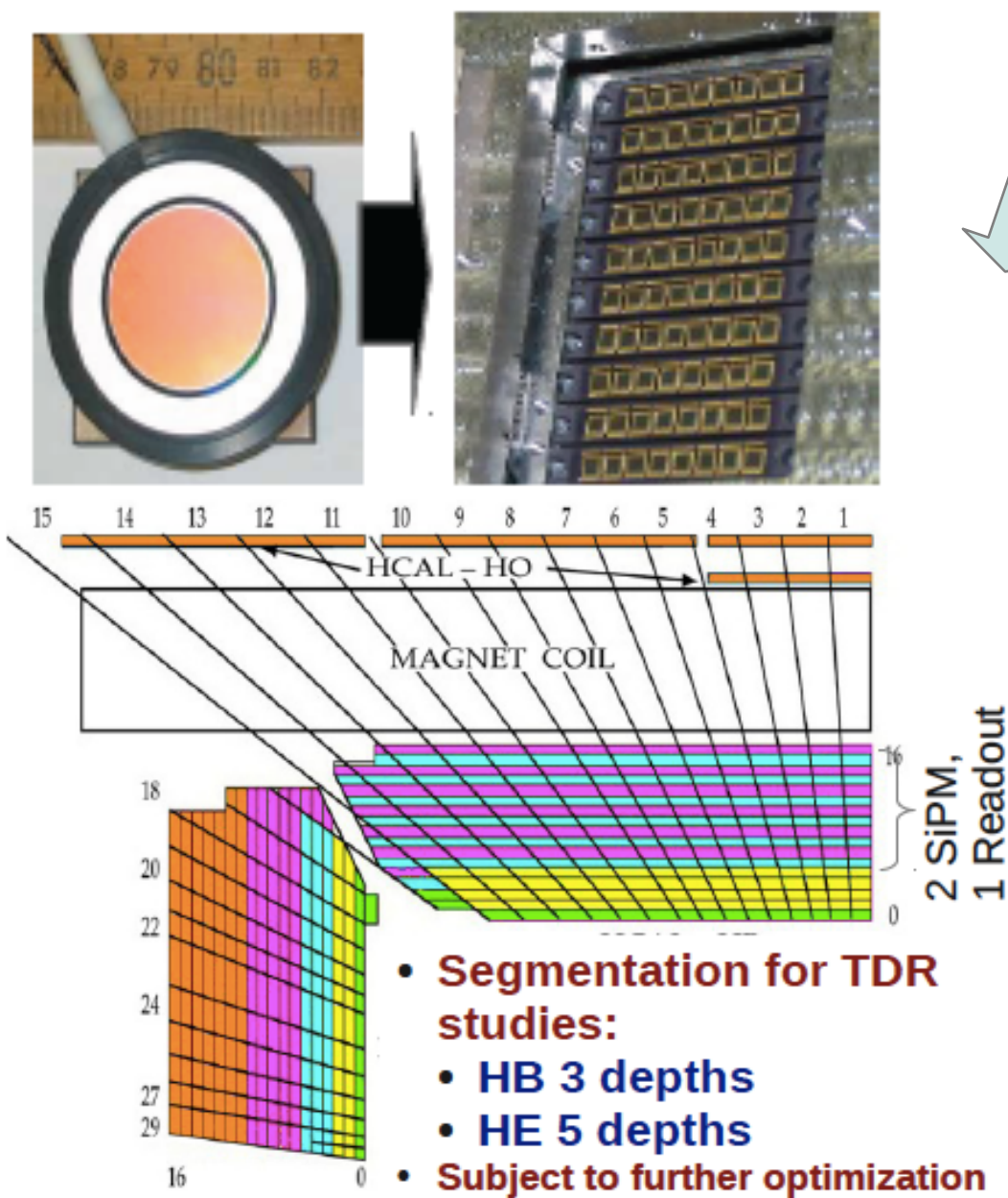
CMS HCAL Read-Out Upgrades

Installation during LS1(HO)/LS2(HB/HE)

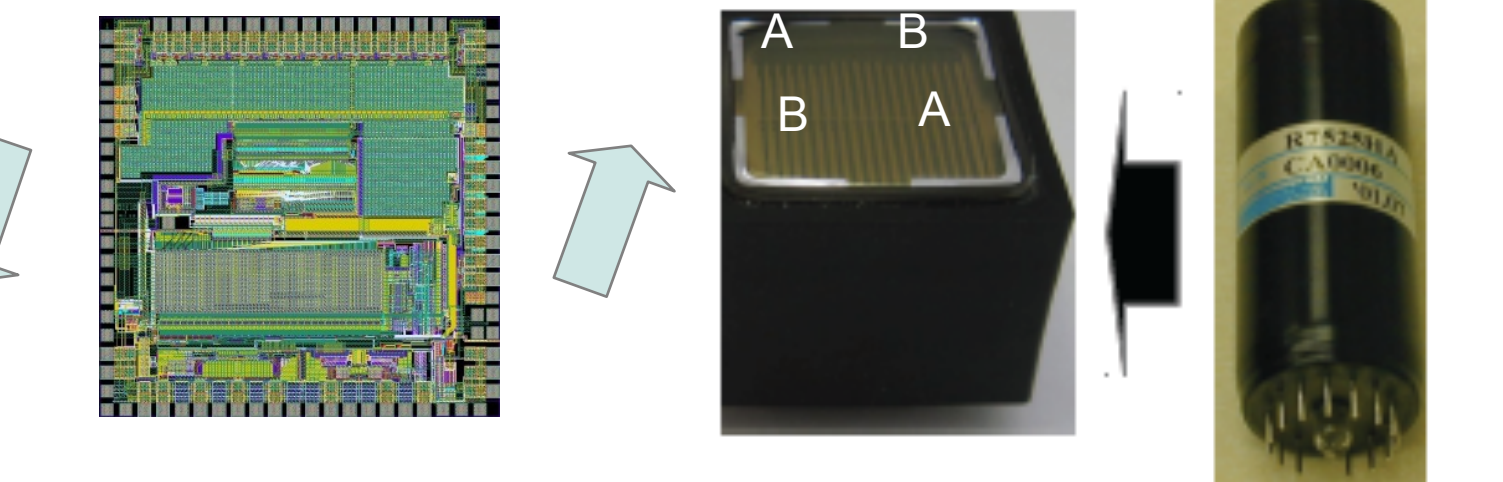
Installation during LS1

HB/HE/HO
From HPD to SiPM's

HF
From single to multi-anode PMT's

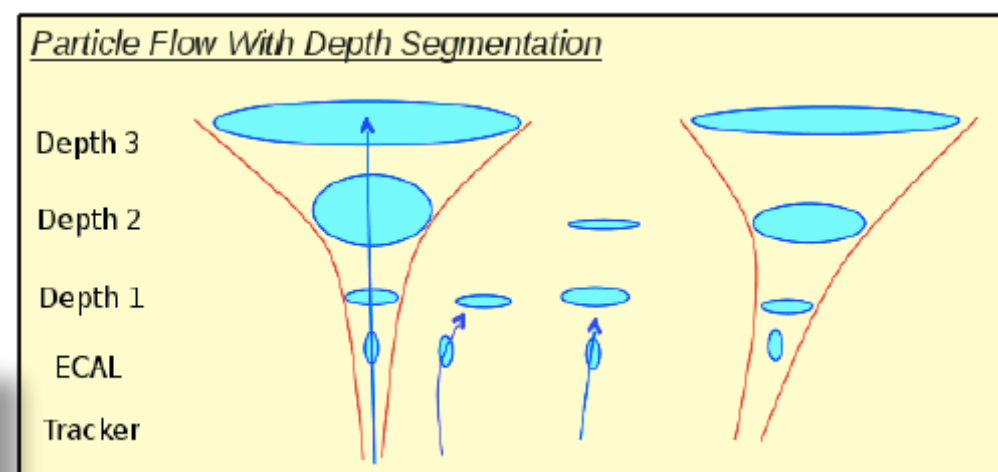


- **Segmentation for TDR studies:**
 - HB 3 depths
 - HE 5 depths
 - Subject to further optimization



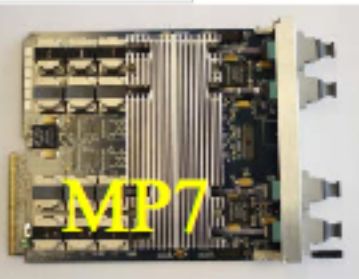
- Use SiPM's to increase HB/HE Depth Segmentation
- Improved PF Hadronic shower localization
- Provides effective tool for pile-up mitigation at high luminosity
- Mitigate radiation damage to scintillator & WLS fibers

Depth segmentation: mitigate high pileup



New hardware!
Limited number of boards.

Ambitious plan assume parallel running of a (part of) new system in 2015. Full replacement 2015/16 YEST



Global Trigger:

- more algorithms,
- flexibility

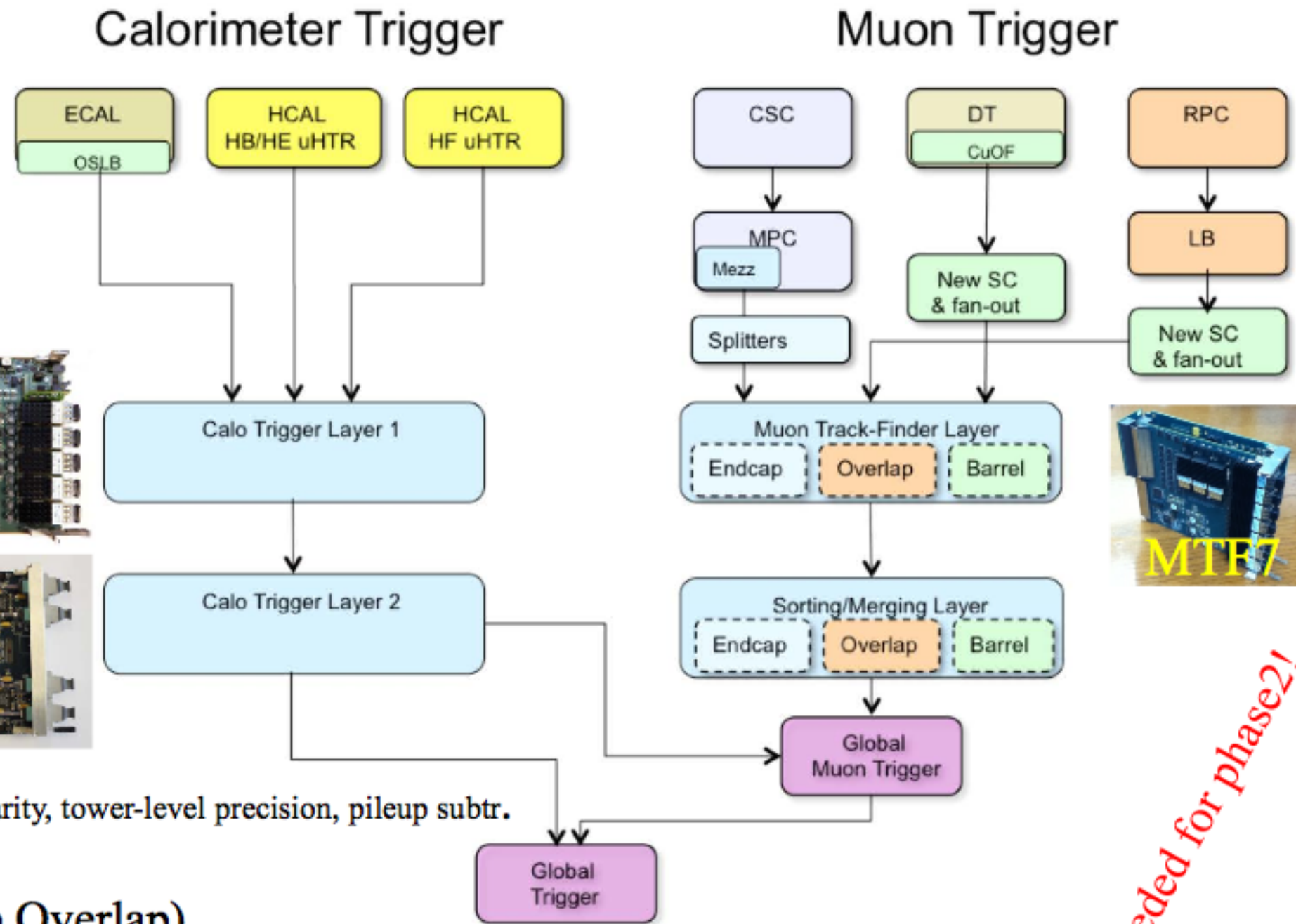
Calorimetry:

- improved algorithms, granularity, tower-level precision, pileup subtr.

Muons:

- 3 partitions (Barrel, Endcap, Overlap)
- explore the available information at early step of triggering.

Currently independent candidates from DTTF, CSCTF, PACT merged at GMT



More needed for phase2!



L1 Trigger upgrade

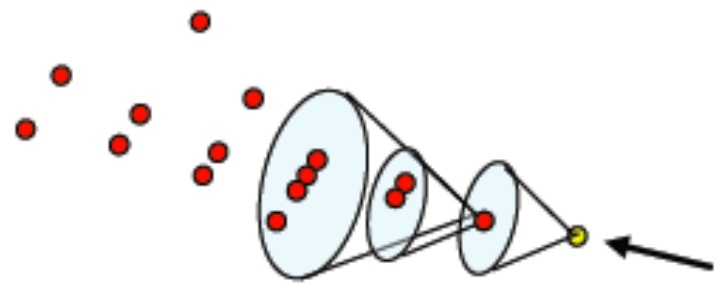
- **Level-1 trigger rate** limited to **1kHz**, 4 μ s latency by detector readout.
- Mitigate through improved:
 - **muon triggers**: improved μ p_T resolution w/ full information from 3 systems in track finding, more processing
 - **calorimeter triggers**: finer granularity, more processing means better $e/\gamma/\mu$ isolation & jet/ τ resolution w/ PU subtraction
- Increased system flexibility and algorithm sophistication
- Build/commission in parallel with current system – staged installation, will benefit already at start of Run 2

Larger FPGAs, finer granularity input, high speed optical links

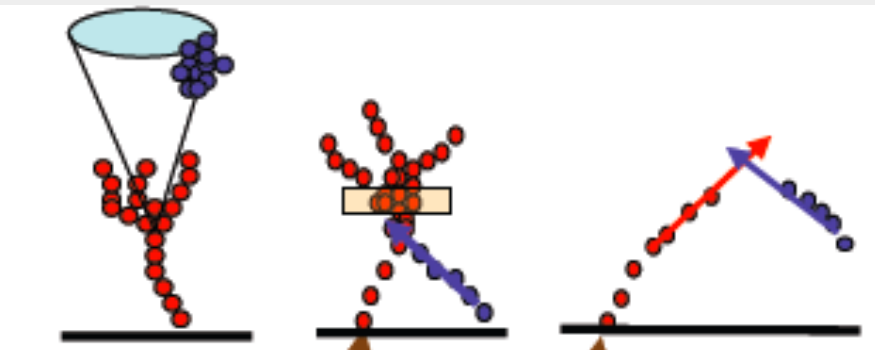
Trigger efficiency @ $2e34 \text{ cm}^{-2}\text{s}^{-1}$

Channel	Current	Upgrade
W(e ν),H(bb)	37.5%	71.5%
W($\mu\nu$),H(bb)	69.6%	97.9%
VBF H($\tau\tau(\mu\tau)$)	19.4%	48.4%
VBF H($\tau\tau(\epsilon\tau)$)	14.0%	39.0%
VBF H($\tau\tau(\tau\tau)$)	14.9%	50.1%
H(WW(ee $\nu\nu$))	74.2%	95.3%
H(WW($\mu\mu\nu\nu$))	89.3%	99.9%
H(WW(e $\mu\nu\nu$))	86.9%	99.3%
H(WW($\mu e\nu\nu$))	90.7%	99.7%

Mark Thomson



ConeClustering Algorithm

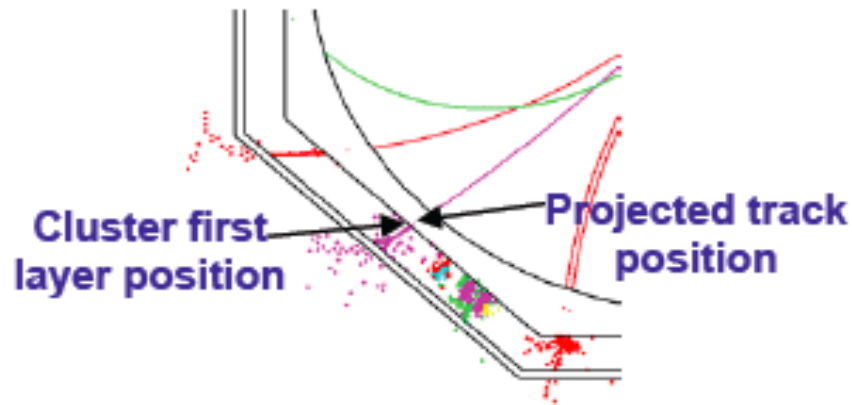


Cone associations

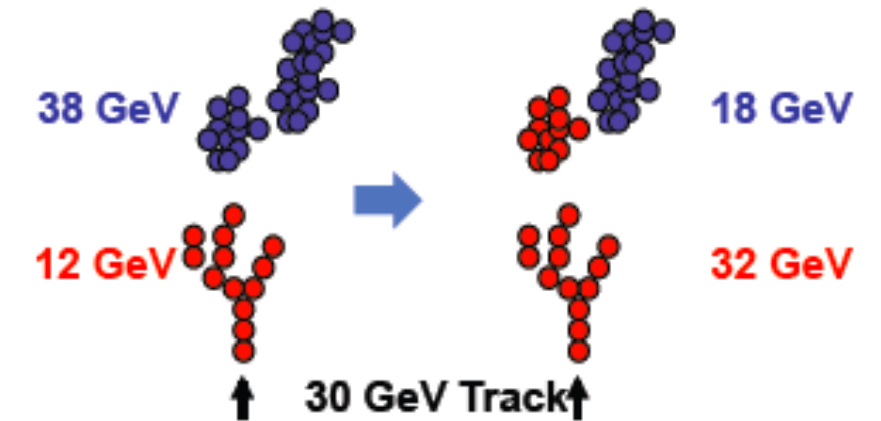
Back-scattered tracks

Looping tracks

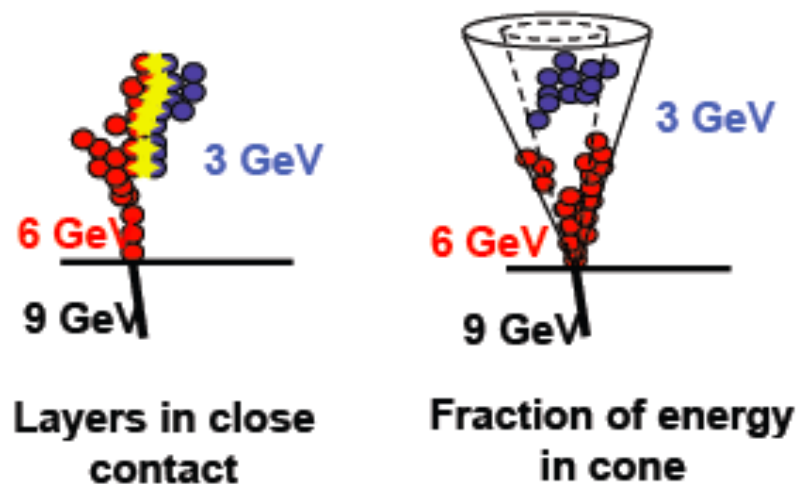
Topological Association Algorithms



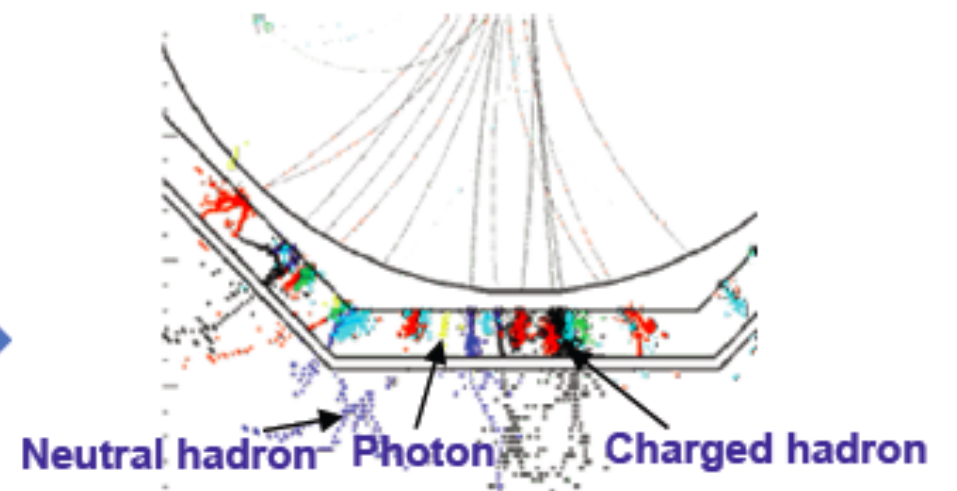
Track-Cluster Association Algorithms



Reclustering Algorithms



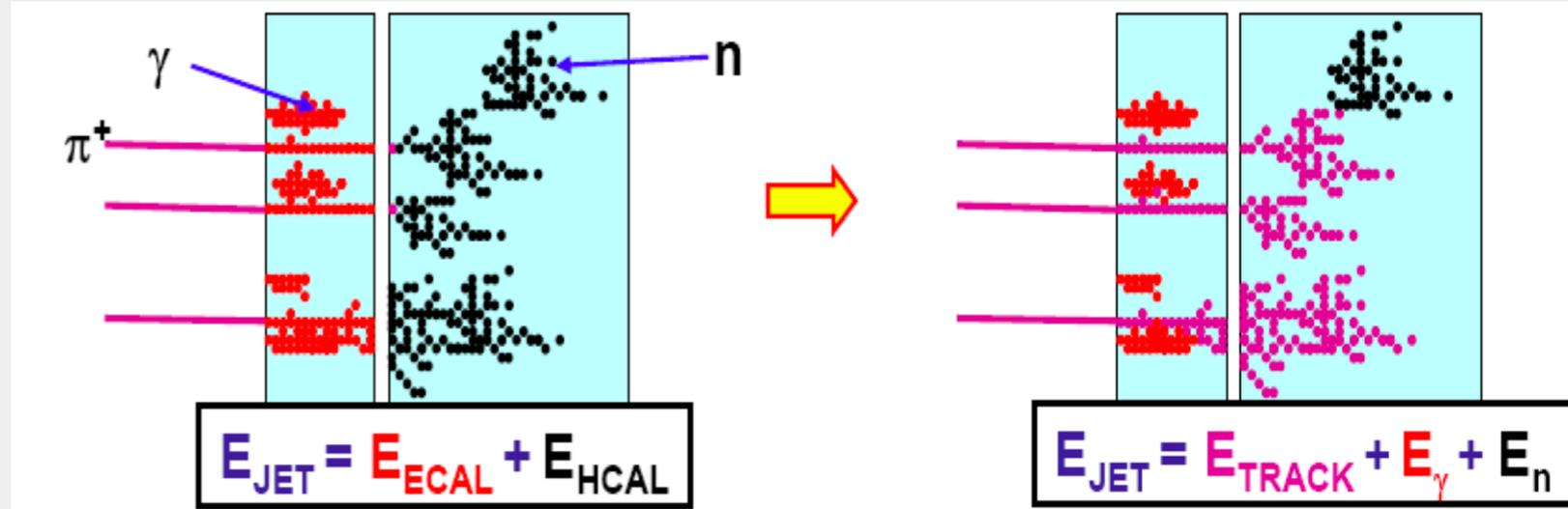
Fragment Removal Algorithms



PFO Construction Algorithms

Design detectors for Pflow

- ECAL and HCAL: inside solenoids
- Low mass tracker
- High granularity for imaging calorimetry
- It also require sophisticated software



HCAL

ECAL

Two proto-collaborations for ILC (ILD and SLD)

- ECAL: Highly segmented S_IW or Scintillator-W sampling calorimeters
 - Transverse segmentation: $\sim 5 \times 5 \text{ mm}^2$
 - ~ 30 longitudinal sampling layers
- HCAL: Highly segmented sampling calorimeters Steel or W absorber+ active material (RPC, GEM)
 - Transverse segmentation: $1 \times 1 \text{ cm}^2 - 3 \times 3 \text{ cm}^2$
 - ~ 50 Longitudinal sampling layers !

• *Aiming at*

$$\sigma_E / E < 3.5\%$$

The CMS Phase II Upgrades

New Tracker

- Radiation tolerant - high granularity - less material
- Tracks in hardware trigger (L1)
- Coverage up to $\eta \sim 4$

Muons

- Replace DT FE electronics
- Complete RPC coverage in forward region (new GEM/RPC technology)
- Investigate Muon-tagging up to $\eta \sim 4$

New Calorimeter EndCaps

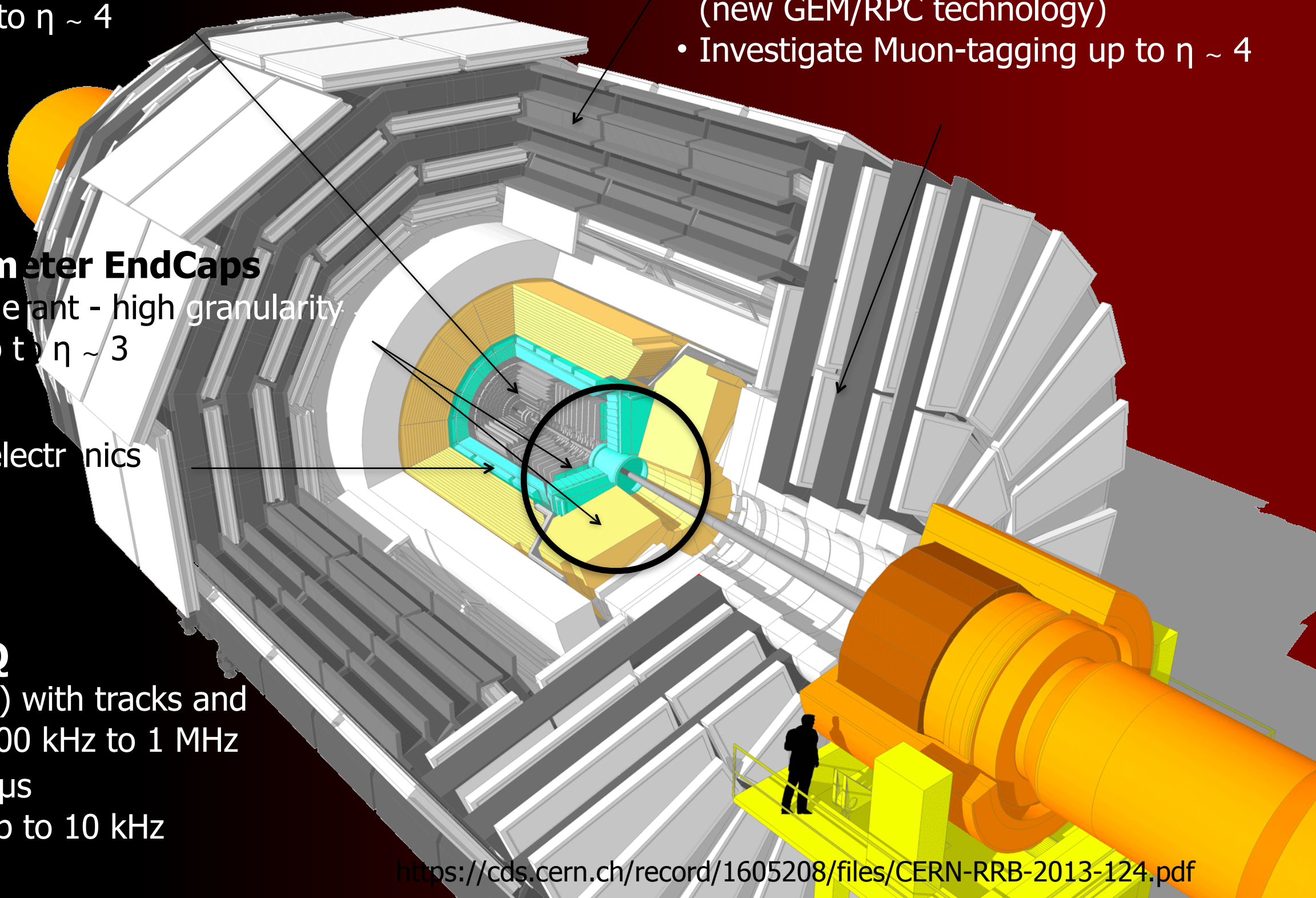
- Radiation tolerant - high granularity
- Coverage up to $\eta \sim 3$

Barrel ECAL

- Replace FE electronics

Trigger/DAQ

- L1 (hardware) with tracks and rate up ~ 500 kHz to 1 MHz
- Latency $\geq 10\mu\text{s}$
- HLT output up to 10 kHz





Why HGCAL?

- A dense, highly granular 3D sampling calorimeter provides
 - unprecedented topological information and shower tracking capability
- together with
 - energy resolution well matched to boosted kinematics of particles and jets in the End-Cap acceptance
- Aim to exploit these for feature extraction and precision calorimetry, both at L1 and offline, with Particle Flow reconstruction in the high occupancy environment of the HL-LHC



Why HGC?

- Leptons, electrons and photons, will remain a key physics signature for the HL-LHC
- Hadronic tau decays and jets will play a central role in much of the HL-LHC physics program
 - **VBF $H \rightarrow \tau\tau \Rightarrow$ precision Higgs**
 - **VBF $H \rightarrow$ Invisible \Rightarrow Dark Matter**
 - **VBS, EWSB, resonances etc**
 - **VBF SUSY \Rightarrow EWK SUSY sector, charginos, neutralinos**
 - **Require good MET resolution and clean tails, in presence of high p_T VBF jets in EndCap!**



Why HGC?

- **Tracking e/γ shower development as function of depth in order to**
 - **Unfold the effect of non-projective geometry**
 - **Apply PU subtraction & measure the energy of the electron shower using dynamic clustering**
 - **Layer-by-layer using knowledge of lateral and longitudinal EM shower shapes and longitudinal PU development**
 - **Update and new results see Pedro's talk**
 - **Use 3D shower development to further improve e/γ identification**
 - **Measure high energy electron/photon shower directions to a few mrad.**



Why HGC?

- **Tracking Jet shower development as function of depth in order to**
 - **Unfold the effect of non-projective geometry**
 - **Apply PU subtraction, identify and measure the energy of (VBF) Jets using narrow cones**
 - **Layer-by-layer using knowledge of lateral and longitudinal Jet shapes and longitudinal PU development**
 - **First results see Pedro's talk**
 - **Use 3D Jet development to discriminate against QCD jets "promoted" by PU**
 - **Provide L1 Jet trigger and improve PF Jet reconstruction**

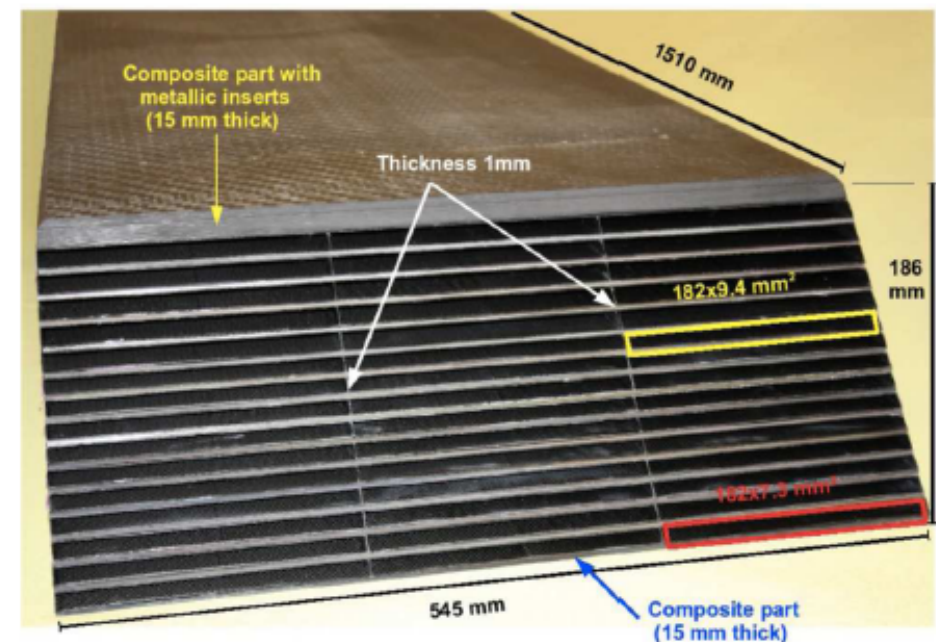
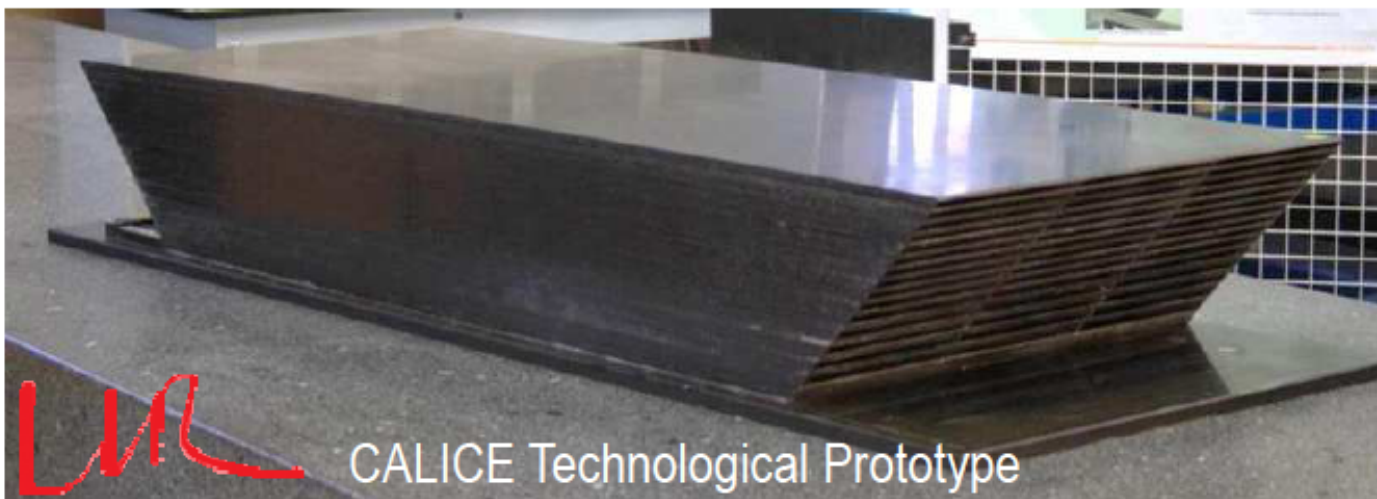
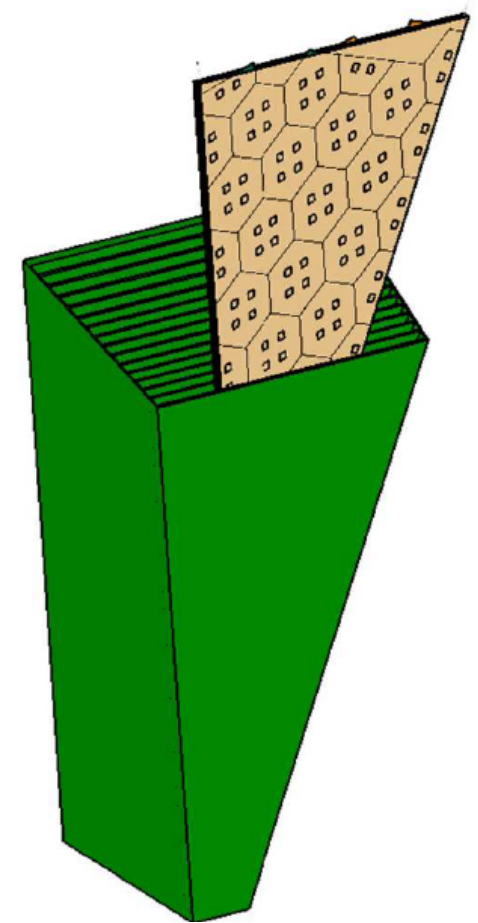
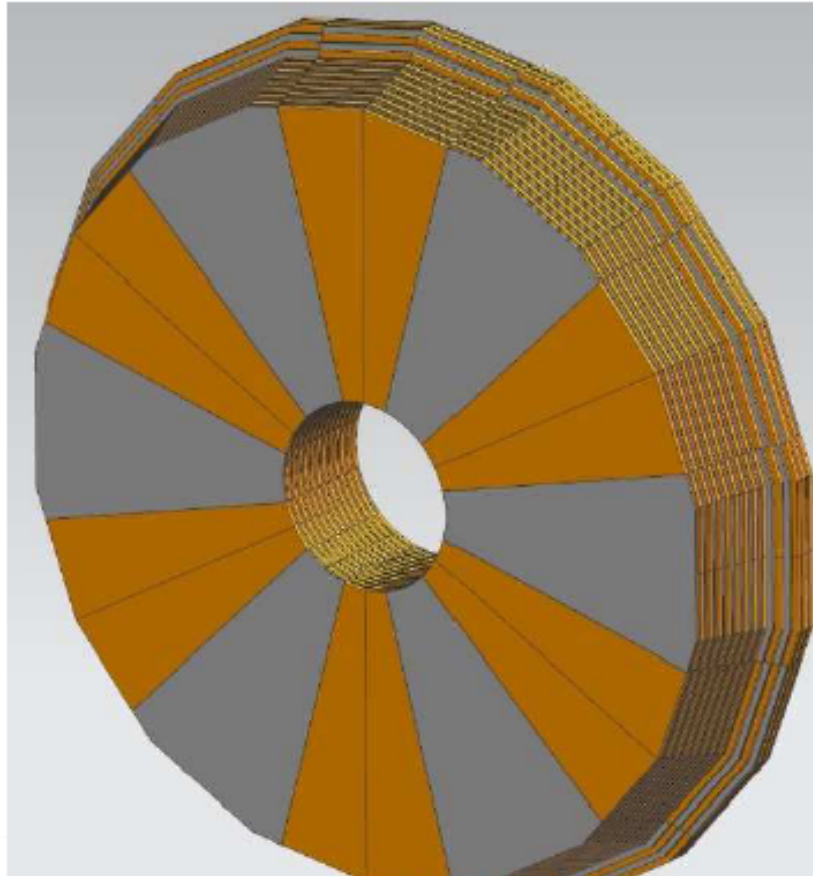
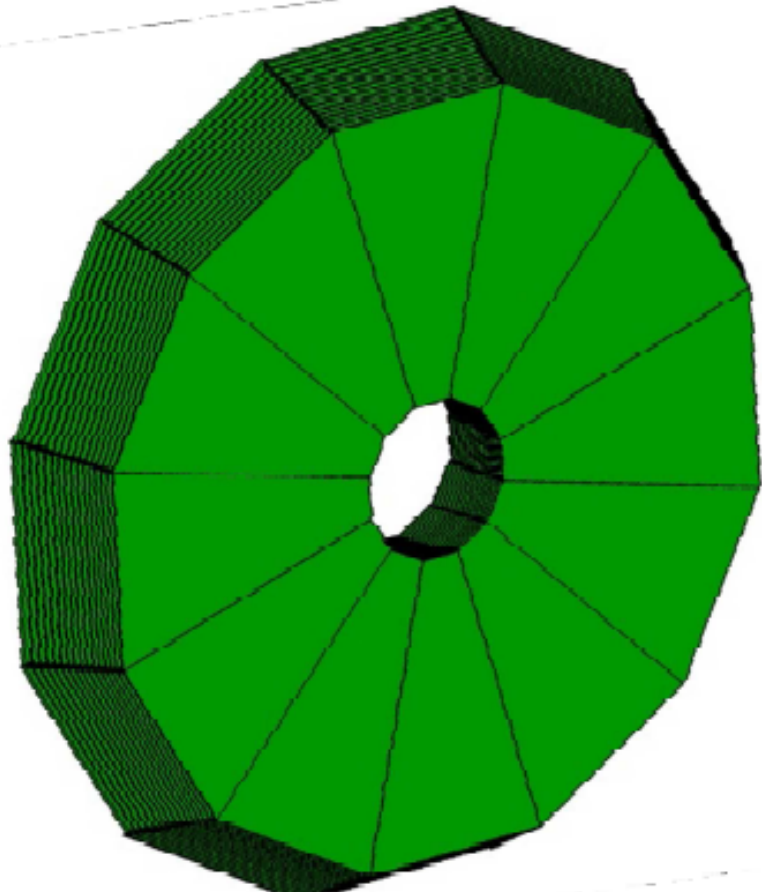


HGCAL Mechanical Design

- **Developed viable mechanical design, with independent Cassettes inserted into Alveolar support structures**
 - **Cassettes: Modules mounted on both sides of 6mm thick Cu plate, which integrates CO₂ capillary and cooling pipes**
 - **EE CF/W composite Alveolar structure based on CALICE design**
 - **Geometry adapted to integrate into CMS End-Cap, and mitigate effect of inhomogeneity at Cassette boundaries**
 - **FH Brass Alveolar structure based on HE**

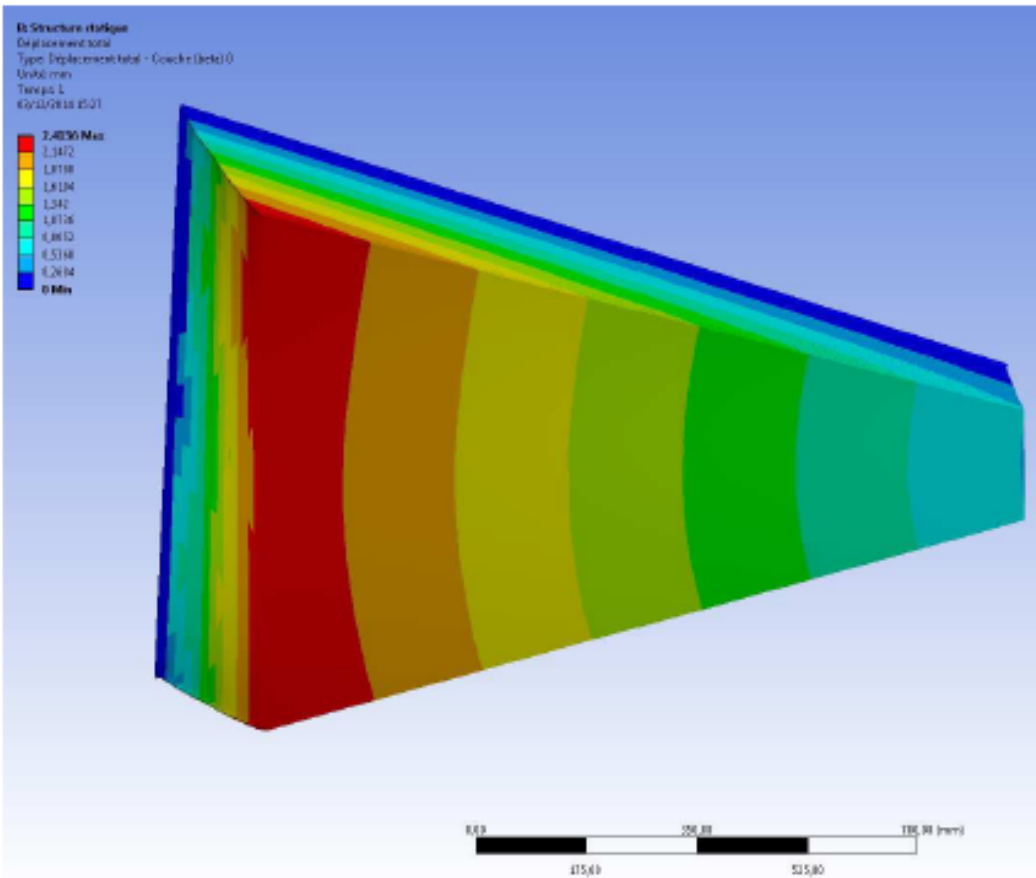


HGC Mechanical Design

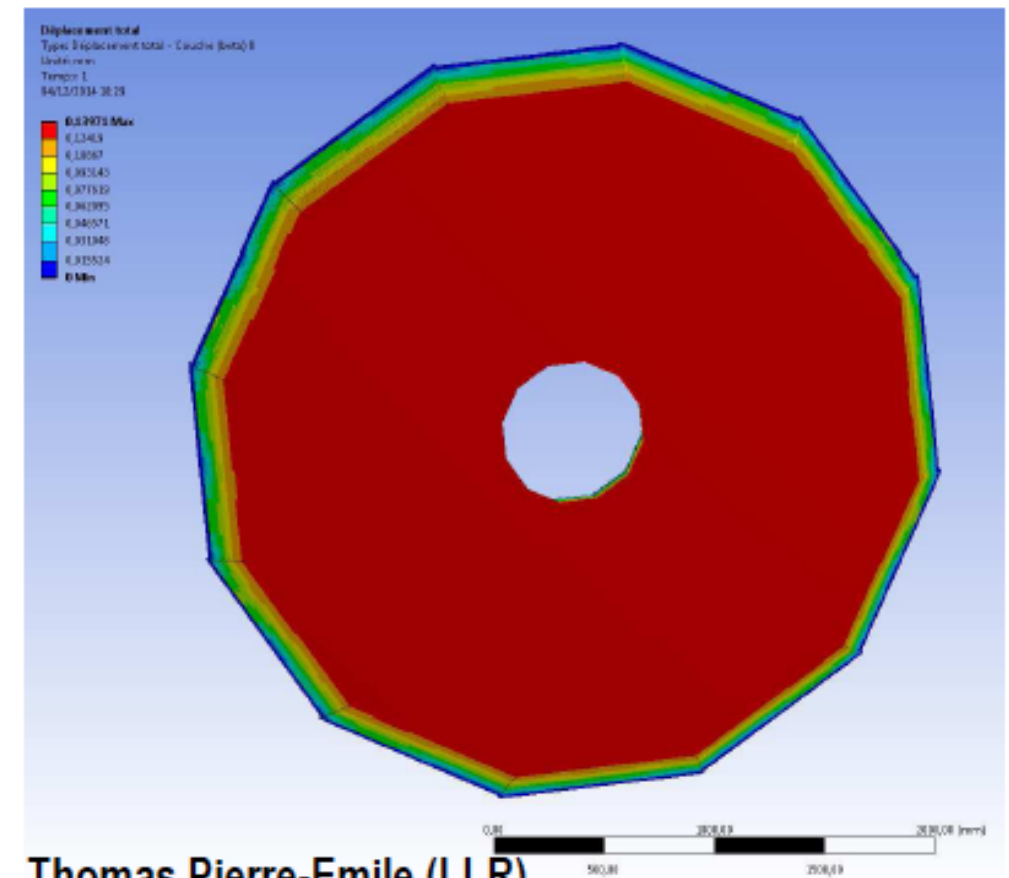


HGC Mechanical Design

Standalone wedge (at 270°)



Full "wheel"



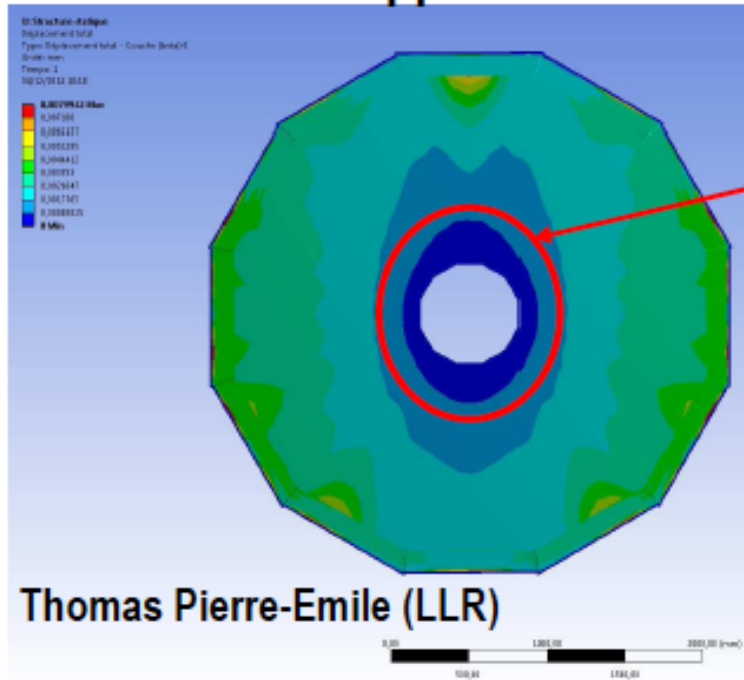
Thomas Pierre-Emile (LLR)

	Standalone (270°)	Full wheel
Displacement (max)	2.4 mm	0.14 mm
Failure criteria F (max)	~0.3	~ 0.10
Margin of Safety	85 %	210 %

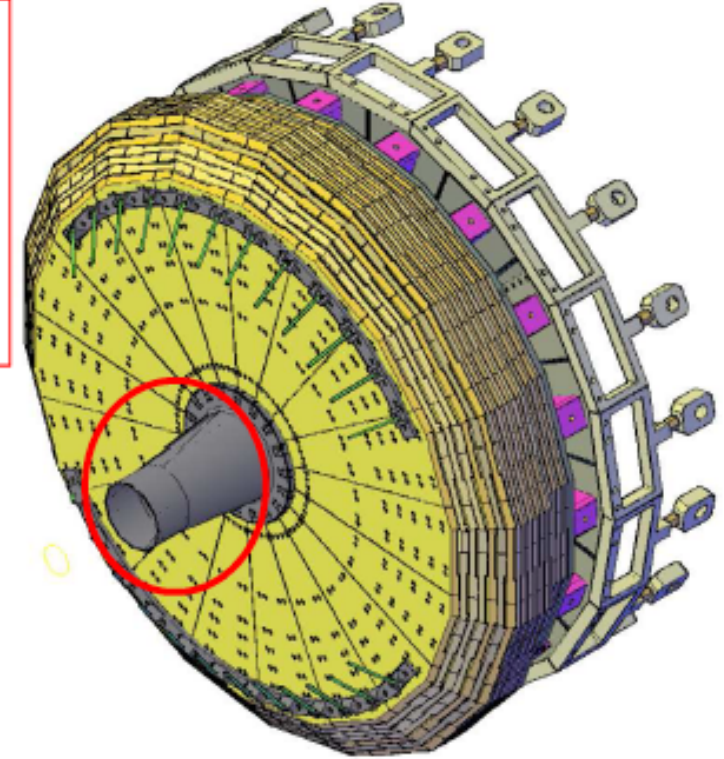
- **Failure occurs when failure criteria $F \geq 1$**
- Margin of Safety $\propto (1/\sqrt{F} - 1)$,
 - **200% is reasonable from engineering point of view**

HGC Mechanical Design

Full "wheel"
+ inner support cone



First look at:
Fix node on the edges to simulate an attachment to a infinitely rigid inner support cone (optimistic, for illustration)

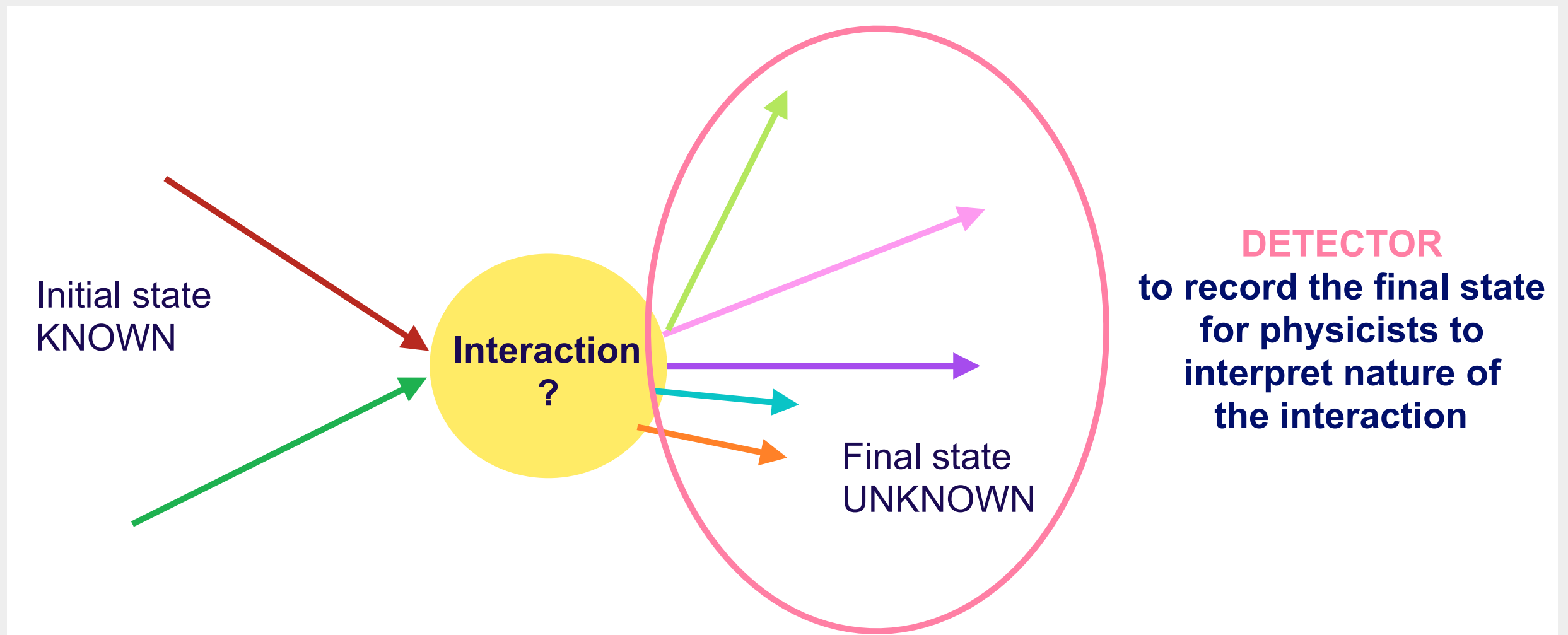


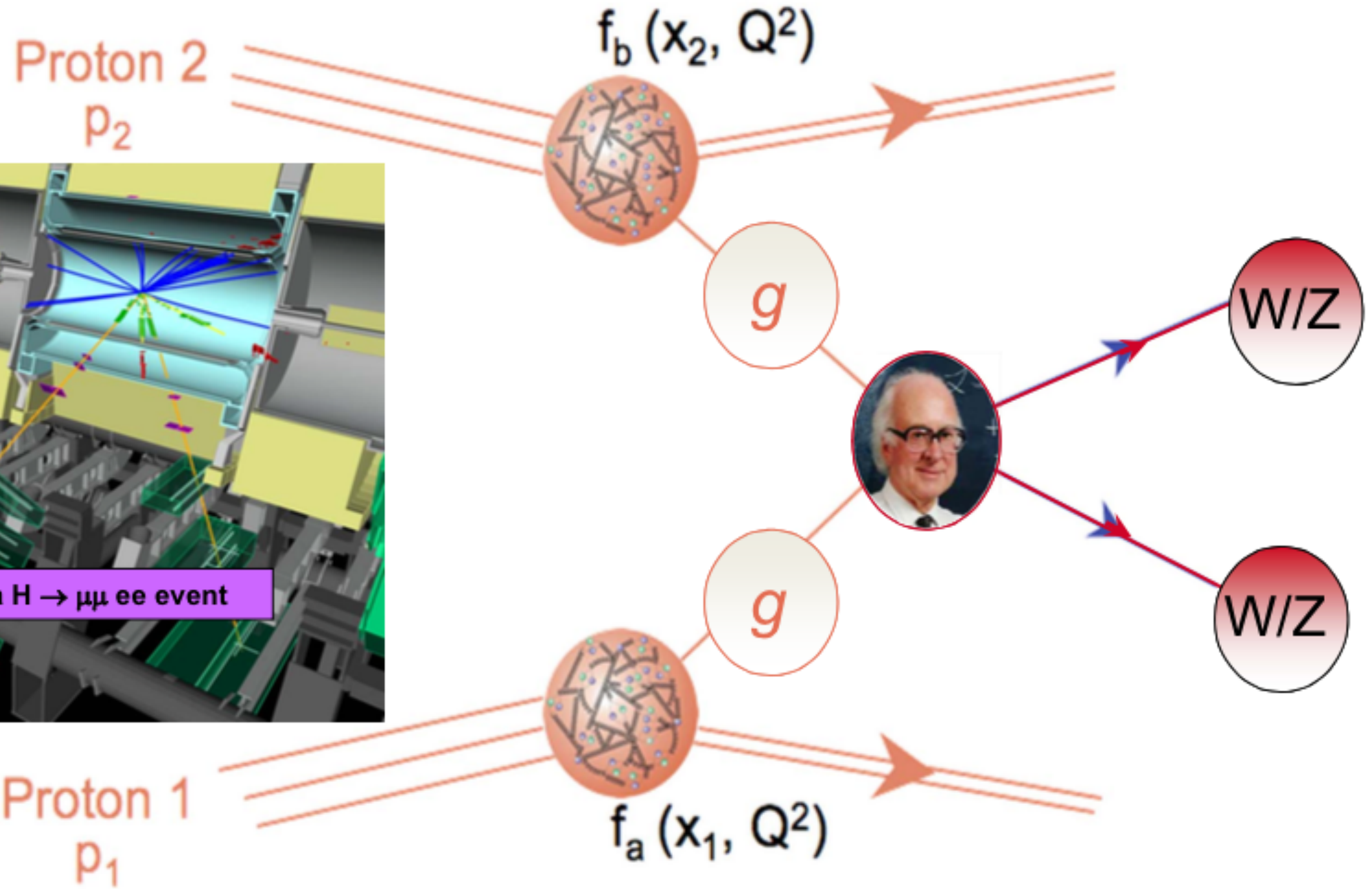
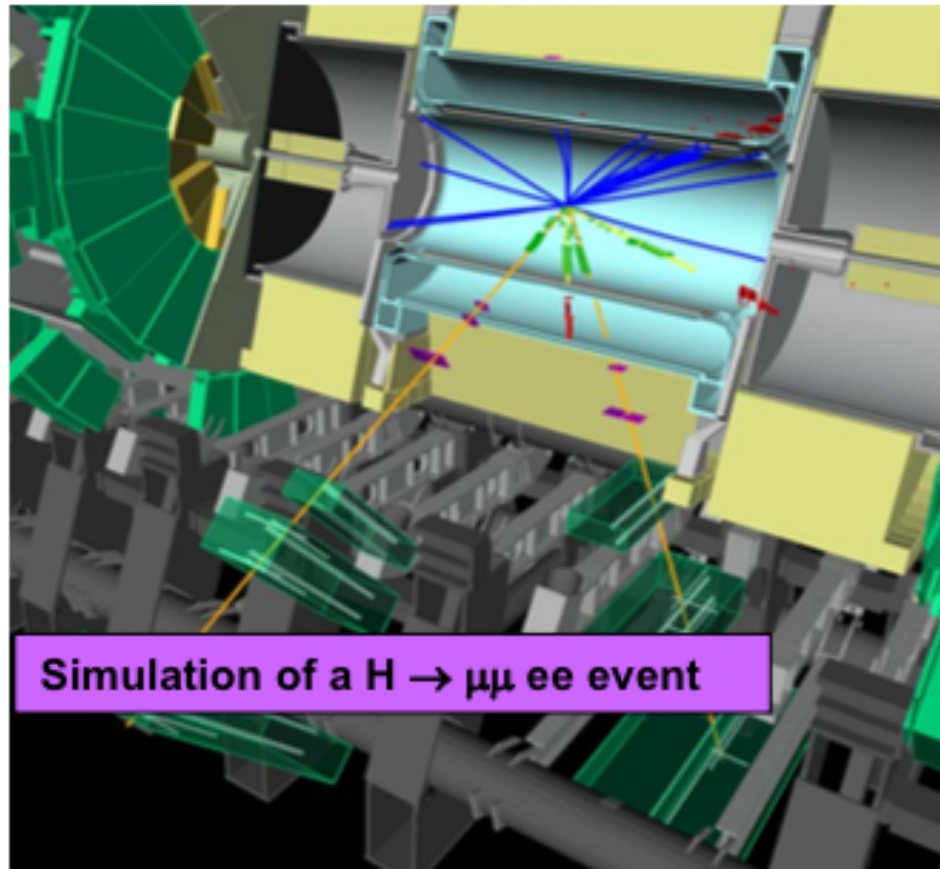
	Standalone (270°)	Full wheel	Full wheel + support cone
Displacement (max)	2.4 mm	0.14 mm	0.008 mm
Failure criteria F (max)	~0.3	~ 0.10	0.008
Margin of Safety	85 %	210 %	1000 % !

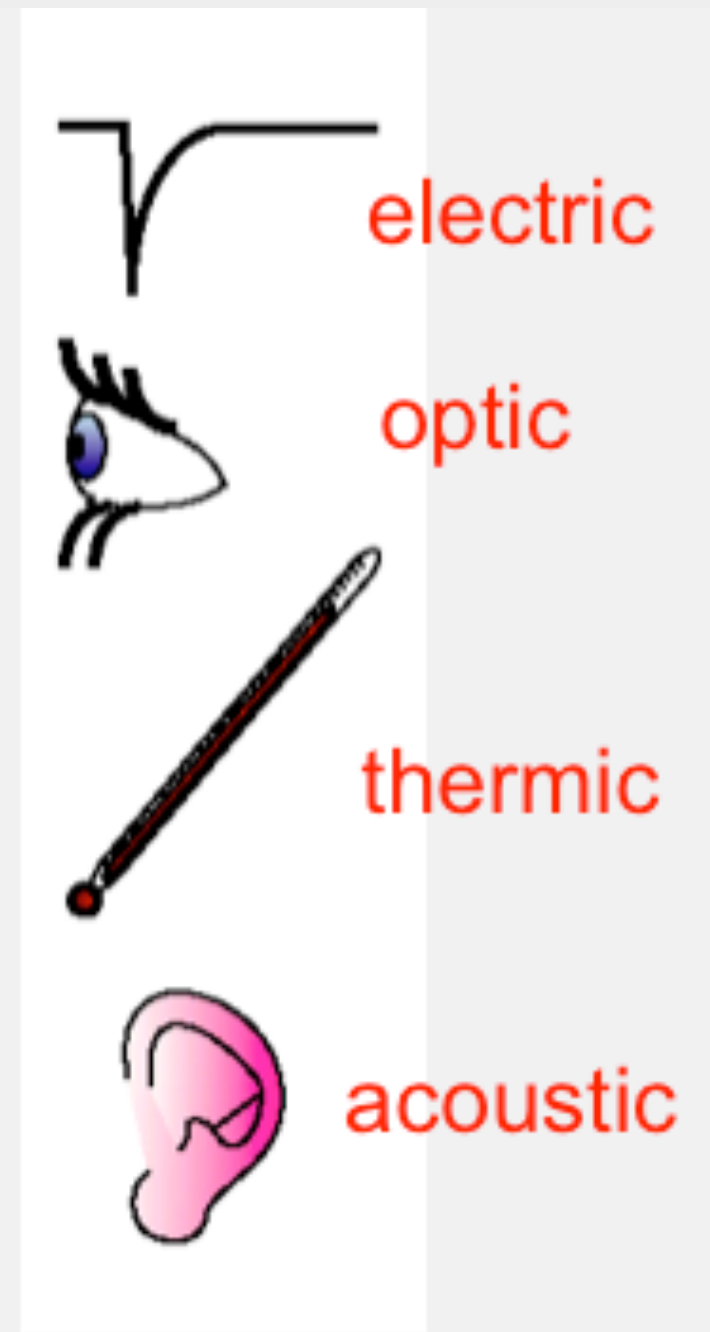
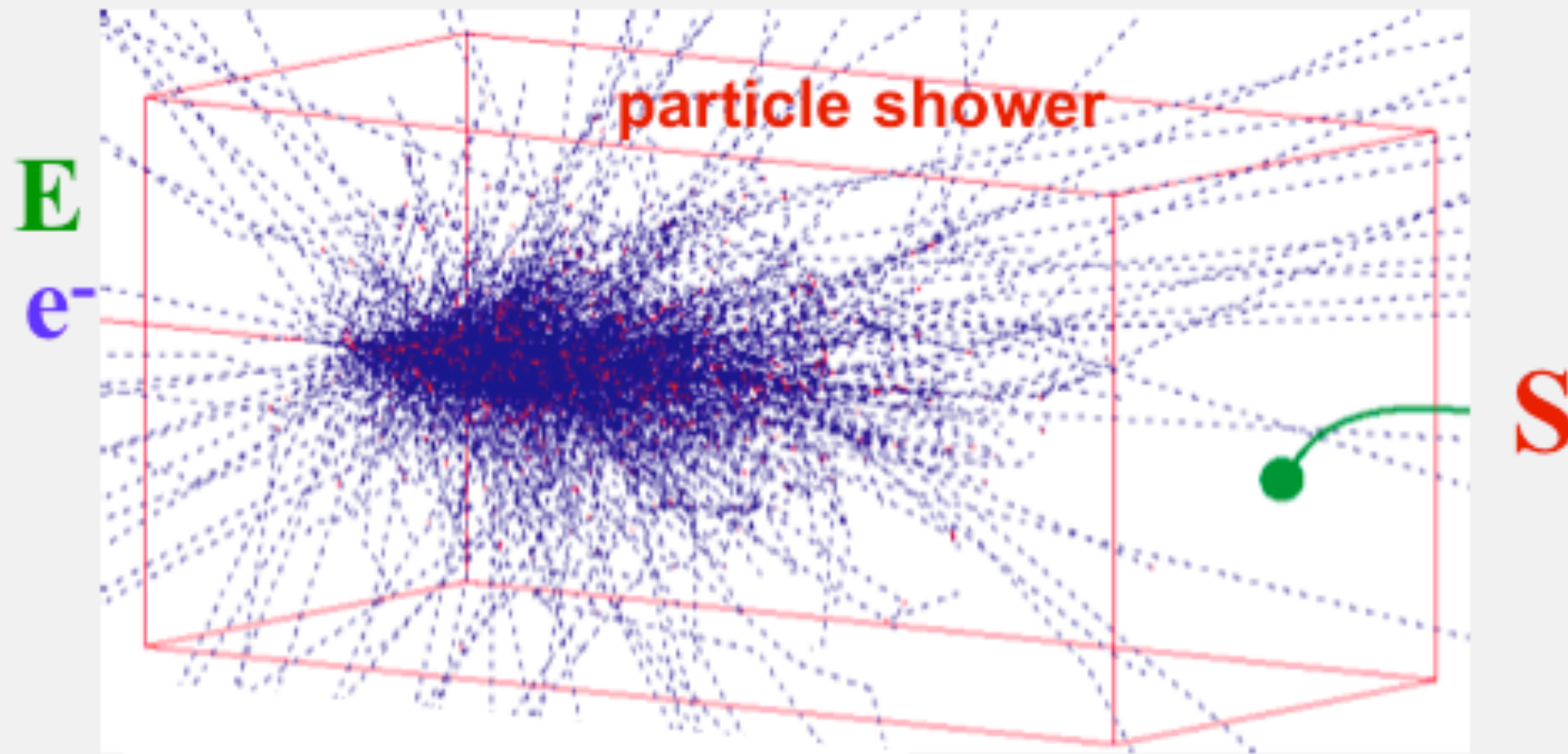
- **User of an inner support cone allows additional handle to better distribute the load.**
 - Would help reducing the side walls thickness
 - May lead to further design optimization and alternatives
- **All these studies have to be verified with destructive tests** on small samples or demonstrator (**on-going**)

WHY DO WE NEED PARTICLE DETECTORS ? *M*

- An astronomer uses a telescope
- A biologist uses a microscope
- We (a lot of us at least) use a camera to take a snapshot of reality
- Particle physicists invent, build and operate detectors to record the products of initial particles interactions:





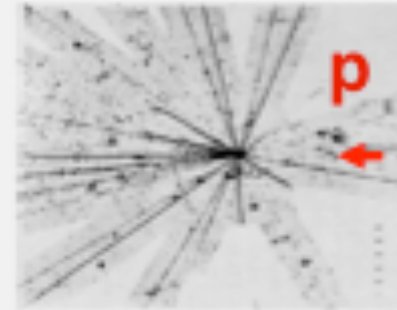


Converts energy **E** of incident particles
to detector response **S**:

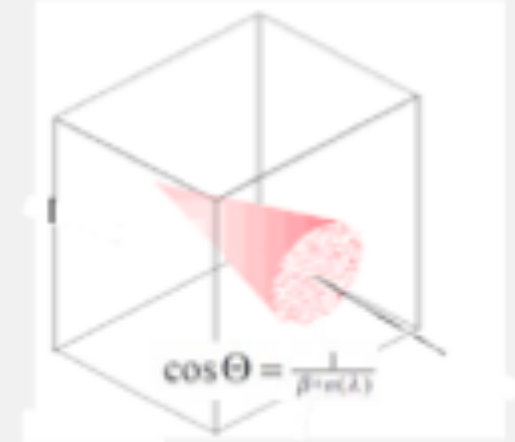
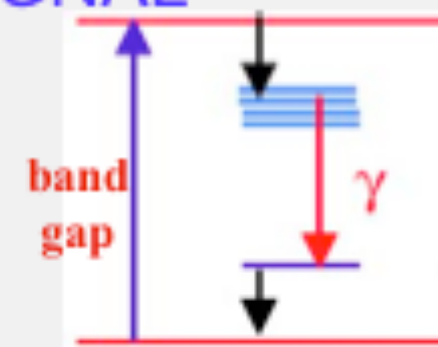
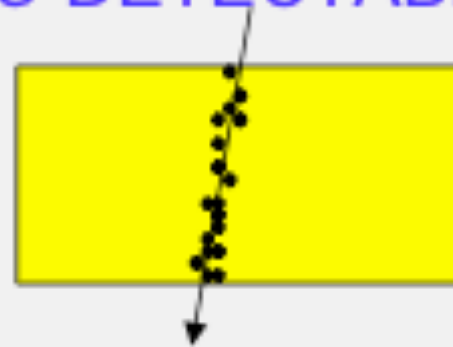
$$S \propto E$$

Calorimetry is a “destructive” method. Energy and particle get absorbed !

PARTICLE INTERACTION IN MATTER (depends on the impinging particle and on the kind of material)

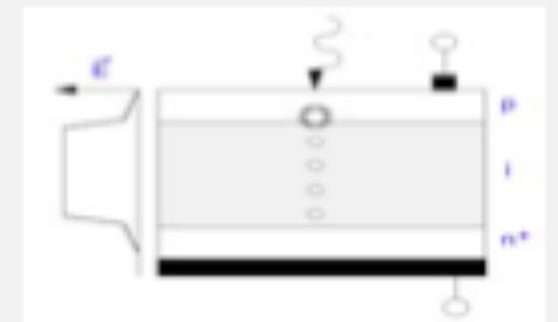
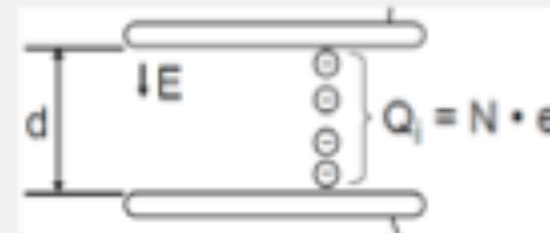
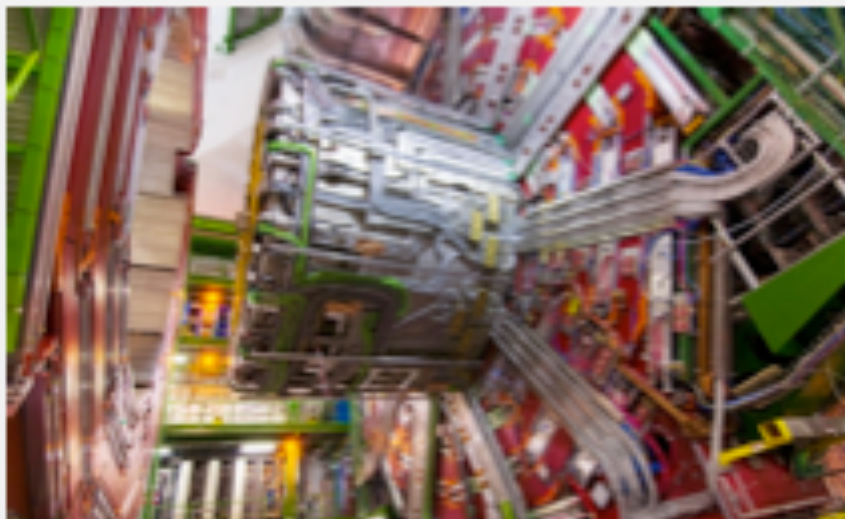


ENERGY LOSS TRANSFER TO DETECTABLE SIGNAL
(depends on the material)



SIGNAL COLLECTION (depends on signal, many techniques of collection)

BUILD A SYSTEM



Homogeneous calorimeters

Homogeneous calorimeters: Detector = absorber

- ⇒ good energy resolution
- ⇒ limited spatial resolution (particularly in longitudinal direction)
- ⇒ only used for electromagnetic calorimetry



Two main types:

1. Scintillators



Scintillator	Density [g/cm ³]	X ₀ [cm]	Light Yield γ/MeV (rel. yield*)	τ ₁ [ns]	λ ₁ [nm]	Rad. Dam. [Gy]	Comments
NaI (Tl)	3.67	2.59	4×10 ⁴	230	415	≥10	hygroscopic, fragile
CsI (Tl)	4.51	1.86	5×10 ⁴ (0.49)	1005	565	≥10	Slightly hygroscopic
CSI pure	4.51	1.86	4×10 ⁴ (0.04)	10 36	310 310	10 ³	Slightly hygroscopic
BaF ₂	4.87	2.03	10 ⁴ (0.13)	0.6 620	220 310	10 ⁵	
BGO	7.13	1.13	8×10 ³	300	480	10	
PbWO ₄	8.28	0.89	≈100	440 broad band 530 broad band		10 ⁴	light yield =f(T)

2. Cherenkov devices



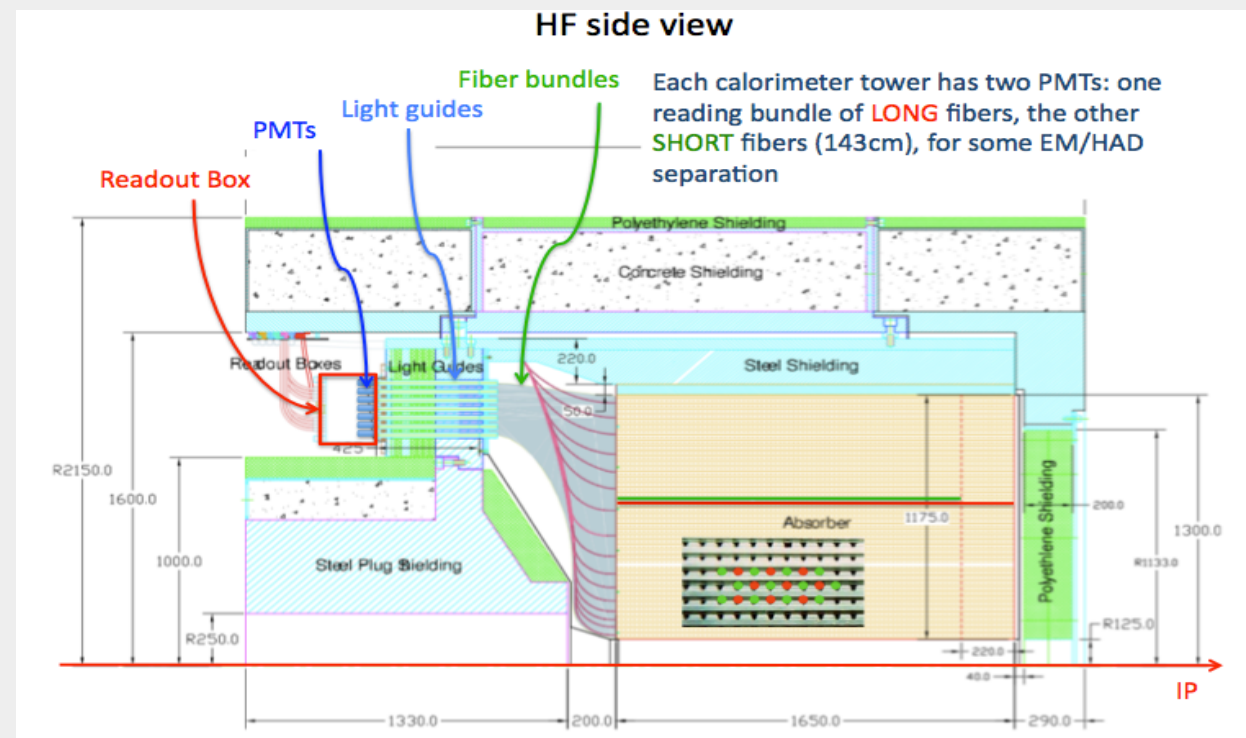
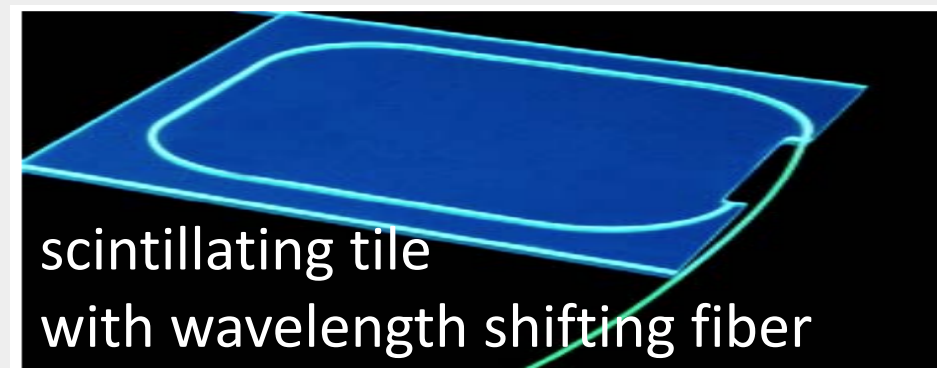
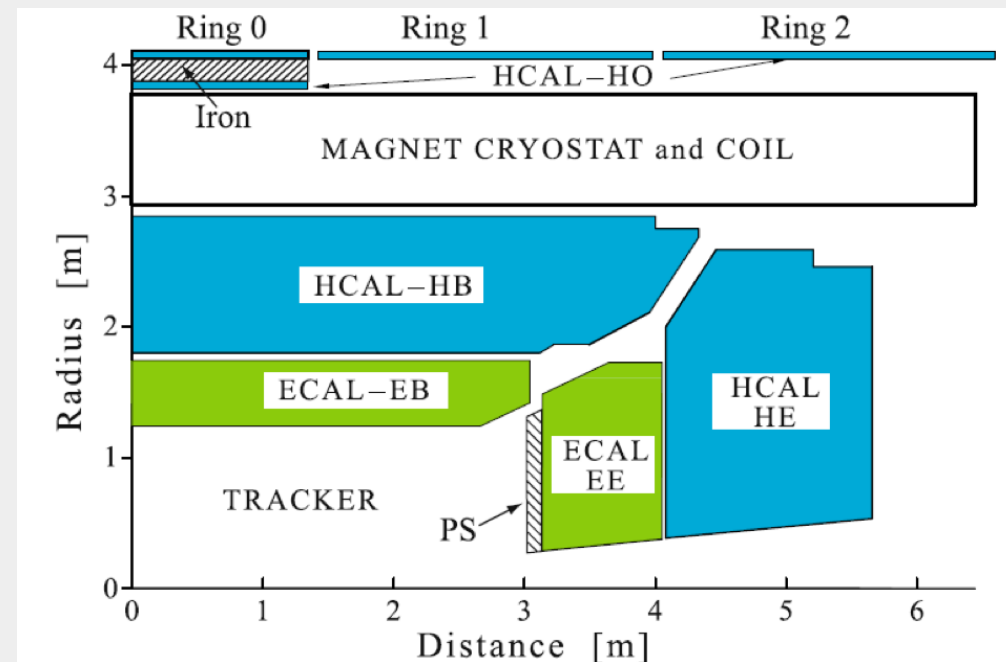
* Relative light yield: rel. to NaI(Tl) readout with PM (bialkali PC)

Material	Density [g/cm ³]	X ₀ [cm]	n	Light yield [p.e./GeV] (rel. p.e.*)	λ _{cut} [nm]	Rad. Dam. [Gy]	Comments
SF-5 Lead glass	4.08	2.54	1.67	600 (1.5×10 ⁻⁴)	350	10 ²	
SF-6 Lead glass	5.20	1.69	1.81	900 (2.3×10 ⁻⁴)	350	10 ²	
PbF ₂	7.66	0.95	1.82	2000 (5×10 ⁻⁴)		10 ³	Not available in quantity

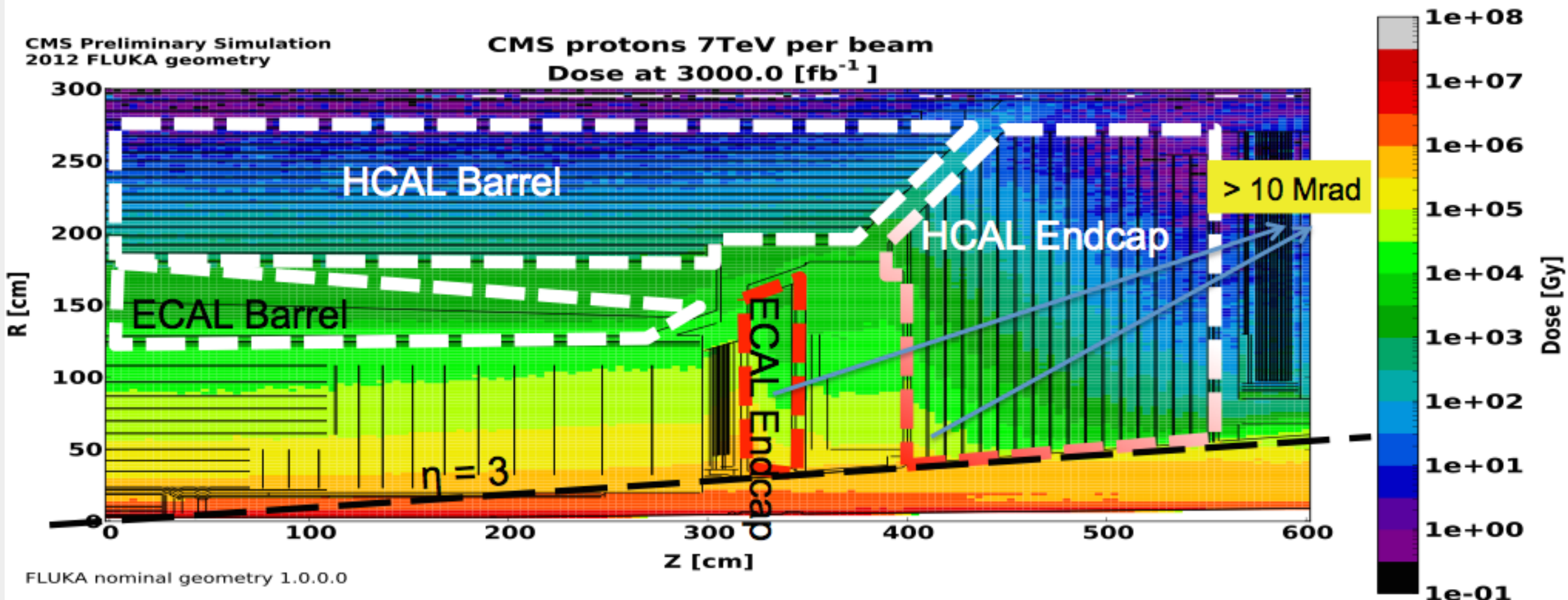
In both cases the signal consists of photons.

Readout via photomultiplier-diode/triode, APD, HPD

- **HCAL Barrel (HB) $0 < |\eta| < 1.3$ and Endcap (HE) $1.3 < |\eta| < 3$**
 - Sampling calorimeter, alternating layers of brass absorber and plastic scintillator tiles.
 - Hybrid photo-detector (HPD) readout
- **Outer (HO): Outside solenoid**
 - Tail catcher with scintillator layers
 - HPD readout
- **Forward (HF) at $|z|=11$ m: $2.9 < |\eta| < 5$**
 - Cherenkov light from scintillating quartz fibers in steel absorber
 - read out with conventional PMTs
- **Stability of photo-detector gains monitored using LED system**
- **Pedestals, and signal synchronization (timing) monitored using Laser data**



- Radiation six times higher than nominal LHC design
- $5(7)E34 \text{ Hz/cm}^2 \rightarrow \sim 140 (200) \text{ collisions/bunch crossing}$



Longevity studies and simulation for $300 \text{ fb}^{-1}/\text{y} \rightarrow 3000 \text{ fb}^{-1}$ total

Phase 2 Upgrades Strategy:

- Maintain performance at extreme $\langle \text{PU} \rangle$
- Sustain rates and radiation doses